Next generation stationary phases for high performance chelation ion chromatography

Thesis submitted for the degree of Doctor of Philosophy

Nicola McGillicuddy, B.Sc.

Under the supervision of

Prof. Brett Paull

Dr. Ekaterina Nesterenko

Dr. Brendan O'Connor

School of Chemical Sciences

Dublin City University

September 2013

Table of Contents

Declaration

I hereby certify that this material, which I now submit for assessment on the programme of study leading to the award of Doctor of Philosophy is entirely my own work, that I have exercised reasonable care to ensure that the work is original, and does not to the best of my knowledge breach any law of copyright, and has not been taken from the work of others save and to the extent that such work has been cited and acknowledged within the text of my work.

Signed: _____(Candidate) ID No.: _____

Date: _____

List of publications and conference presentations

Publications

1. **N. McGillicuddy**, E.P. Nesterenko, P.N. Nesterenko, P. Jones, B. Paull, "*Chelation ion chromatography of alkaline earth and transition metals a using monolithic silica column with bonded N-hydroxyethyliminodiacetic acid functional groups*", Journal of Chromatography A 1276 (2013) 102.

2. **N. McGillicuddy**, E.P. Nesterenko, P. Jones, D. Caldarola, B. Onida, A.T. Townsend, D.P. Mitev, P.N. Nesterenko and B. Paull, "*Direct determination of transition metals in mussel tissue digests using high-performance chelation ion chromatography with monolithic silica based chelating ion exchangers*", Analytical Methods 5 (2013) 2666.

List of poster presentations

1. **N. McGillicuddy**, E. Nesterenko, P. Nesterenko, B. Paull, International Symposium on Chromatography (ICS 2010), "*High performance chelation ion chromatography of lanthanides*", 12-16th September 2010, Valencia, Spain.

2. **N. McGillicuddy**, E. Nesterenko, P. Nesterenko, B. Paull, "*High performance chelation ion chromatography of lanthanides*", International Ion Chromatography Symposium (IICS 2010), 19-22nd September, Cincinnati, USA.

3. **N. McGillicuddy**, E. Nesterenko, P. Nesterenko, B. Paull, "*High performance Chelation Ion Chromatography of Lanthanides on Poly-IDA Polymeric and IDA-Silica Gel Chelating Ion Exchange columns*", Conference on Analytical Sciences (CASI 2011), 21-22nd February, Dublin City University, Dublin, Ireland.

4. **N. McGillicuddy**, E. Nesterenko, P. Nesterenko, B. Paull, "*Characterisation and application of a new iminodiacetic acid functionalised monolithic column for the simultaneous separation of alkaline earth, transition and heavy metal cations in complex environmental samples*", 11th Asia Pacific International Symposium on Microscale Separations and Analysis (APCE 2011), 27-30th November 2011, University of Hobart, Tasmania, Australia.

5. **N. McGillicuddy**, E. Nesterenko, P. Nesterenko, P. Jones, B. Paull, "*Characterisation of iminodiacetic acid modified silica monolithic stationary phase and its application for detection and quantification of selected metal cations in shellfish*", Analytical Research Forum (ARF 2012), 2-4th July 2012, Durham University, UK.

6. **N. McGillicuddy**, E. Nesterenko, P. Nesterenko, P. Jones, J.O. Omamogho, J.D. Glennon, B. Paull, "*Next generation silica based stationary phases for high performance chelation ion chromatography*", International Ion Chromatography Symposium (IICS 2012), 16 – 20th September 2012, Berlin.

7. **N. McGillicuddy**, E. Nesterenko, P. Nesterenko, J. Omamogho, J. Glennon, B. Paull, "*Chelation ion chromatography of alkaline earth, transition and lanthanide metal cations using a novel IDA-silica core-shell stationary phase*", 39th International Symposium on High-Performance-Liquid-Phase Separations and Related Techniques (HPLC 2013), 16-20th June 2013, Amsterdam, Netherlands.

List of oral presentations

1. **N. McGillicuddy**, E. Nesterenko, P. Nesterenko, P. Jones, J.O. Omamogho, J.D. Glennon, B. Paull, "*Next generation silica based stationary phases for high performance chelation ion chromatography*", International Ion Chromatography Symposium (IICS 2012), 16 – 20th September 2012, Berlin (invited speaker).

Abbreviations

β	Overall formation/stability constant
ΔG	Gibbs energy
ΔH	Enthalpy
ΔS	Entropy
2-D	Two dimensional
5-Br PADAP	2-(5-bromo-2-pyridylazo)-5-(diethylamino)phenol
AAS	Atomic absorption spectroscopy
AES	Atomic emission spectroscopy
AIDA	Acetyl-iminodiacetic acid
ANOVA	Analysis of variance
APAS	Aminophosphonate
AS	Autosampler
ATP	Adenosine triphosphate
CAS	Chromazurol S
o-CPC	*o*-cresolphthalein complexone
CR-CTC	Continuously regenerated-cation trap column
DC	Detector compartment
DP	Dual pump
DPA	Dipicolinic acid
DW	Distilled water
ECR	Eriochrome cyanine R
EDTA	Ethylenediamenetetraacetic acid
EG	Eluent generator
EP	European pharmacopoeia
HEIDA	*N*-hydroxyethyliminodiacetic acid
HEPMA	*N*-(2-hydroxyethyl)-*N*-(2-[phosphonomethyl)amino]acetic
HETP	Height equivalent to theoretical plate
HPCIC	High performance chelation ion chromatography
ICP-AES	Inductively coupled plasma - atomic emission spectroscopy
ICP-MS	Inductively coupled plasma - mass spectroscopy
IC	Ion chromatography

I.D.	Internal diameter
IEC	Ion exchange chromatography
IDPA	Iminodipropionic acid
IDA	Iminodiacetic acid
IMAC	Immobilised metal affinity chromatography
k'	Retention factor
$K^{'}$	Stepwise formation/stability constant
K_2EDTA	ethylenediamenetetraacetic acid dipotassium-salt dihydrate
Li-DS	Lithium dodecylsulfate
MSA	Methanesulfonic acid
MTB	Methylthymol blue
N	Efficiency
ODS	Octadecylsilyl
PAR	4-(2-pyridylazo) resorcinol
PCR	Post-column reaction
PCV	Pyrocatechol violet
PEEK	Polyetheretherketone
PGMA	Poly(glycidylmethacrylate) gel
pK_a	Acid dissociation constant at logarithmic scale
PMA	2-[(phosphonomethyl)amino]- acetic
PP	Phthalein purple
PS-DVB	Poly(styrene-divinylbenzene
RDM	Reagent delivery module
REE	Rare earth elements
RFIC-ER	Reagent free ion chromatography with eluent regeneration
RP	Reversed Phase
RP-LC	Reversed phase-liquid chromatography
SEM	Scanning electron microscopy
UHPLC	Ultrahigh-performance liquid chromatography
XO	Xylenol orange
ZnEDTA	Zinc ethylenediaminetetraacetate

List of Figures

Chapter 1

transition and heavy metal cations. Peaks: 1: 2.8 ppm Pb^{2+}, 2: 1.5 ppm Cu^{2+}, 3: 3.0 ppm Cd^{2+}, 4: 0.7 ppm Co^{2+}, 5: 0.9 ppm Mg^{2+}, 6: 1.25 ppm Ca^{2+}, 7: 1.75 ppm Sr^{2+}, and 8: 1.75 ppm Ba^{2+}. Eluent: 4 m*M* HNO_3/0.3 m*M* DPA, Flow rate: 0.8 mL/min, Injection volume: 20 µL, Detection: spectrophotometric at 540 nm after PCR with 0.2 m*M* ZnEDTA/0.12 m*M* PAR.

Fig. 3.9 (a) Effect of eluent cation (monovalent) upon retention of transition metal ions at concentration 0.165 *M*, at pH 2.0 (HNO_3). Flow rate: 0.8 mL/min, Column temperature: 25 °C, Injection volume: 20 µL, Detection: spectrophotometric at 510 nm after PCR with 0.15 m*M* PAR.

Fig. 3.9 (b) Effect of eluent cation (monovalent) upon retention of transition metal ions at concentration 0.165 *M*, at pH 2.5 (HNO_3). Chromatographic details as Fig. 3.9 (a).

Fig. 3.9 (c) Effect of eluent cation (monovalent) upon retention of transition metal ions at concentration 0.5 *M*, at pH 2.0 (HNO_3). Chromatographic details as Fig. 3.9 (a).

Fig. 3.9 (d) Effect of eluent cation (monovalent) upon retention of transition metal ions at concentration 0.5 *M*, at pH 2.5 (HNO_3). Chromatographic details as Fig. 3.9 (a).

Fig. 3.9 (e) Effect of eluent cation (divalent) upon retention of transition metal ions at concentration 0.165 *M*, at pH 2.0 (HNO_3). Chromatographic details as Fig. 3.9 (a).

Fig. 3.9 (f) Effect of eluent cation (divalent) upon retention of transition metal ions at concentration 0.165 *M*, at pH 2.5 (HNO_3). Chromatographic details as Fig. 3.9 (a).

Fig. 3.10 Effect of eluent flow rate (mL/min) on peak efficiency (HETP) for transition metal cations (Mn^{2+}, Cd^{2+}, Co^{2+} and Zn^{2+}). Eluent: 0.5 *M* KNO_3 eluent, pH 2.5, Column temperature: 25 °C, Flow rate: 0.6–1.8 mL/min, Injection volume: 20 µL, Detection: spectrophotometric at 510 nm after PCR with 0.15 m*M* PAR.

Fig. 3.11 Effect of eluent flow rate upon the separation of transition and heavy metal cations. Peaks: 1: 5 ppm Mn^{2+}, 2: 5 ppm Co^{2+}, 3: 5 ppm Cd^{2+},

Chapter 5

List of Tables

Chapter 4

Chapter 5

Acknowledgements

First and foremost I would like to thank Prof. Brett Paull for the chance to undertake this Ph.D. and the opportunity to travel to UTAS to carry out part of my research. The biggest thanks to Dr. Katya Nesterenko who has helped me so much over the last four years, and Dr. Brendan O'Connor for his guidance and advice.

Thanks to those who have given me invaluable advice and help throughout my Ph.D; Prof. Pavel Nesterenko, Dr. Damian Connolly, Dr. Phil Jones, Prof. Apryll Stalcup, Prof. Jeremy Glennon and Dr. Jesse Omamogho. Thanks to my fellow NCSR colleagues; Patrick, Amy, Sara, Sinead, Aine, Orla, Ali, Disha, Ruth, Mercedes, Dave, Lily, Ugis, Larisa, Aymen, and last but not least Gillian whose friendship is one of the best things to come out of my time in DCU.

Thanks to the staff and technicians in the school of chemistry and the NCSR, especially in the Umbrella Office for giving me much needed laughs, and the biggest thanks to Stephen Fuller who could not have been more helpful, and also (without much choice) took on the role of my agony uncle - without his help I'm certain I would still be trying to finish my labwork!

Thanks to all my wonderful friends who have given me such amazing support and have been understanding of my absenteeism - Sharon, Beca, Hazel, Cailin, Caoimhe, Faye, Rob, Wendy, Elmo, Elaine, my Biovail big sisters, Éadaoin, Jess, my roomie Aoife, Aimee and Christy. Thanks to all of the Rónin Crossfit sons and lady sons for keeping me (semi) sane, and for giving me a positive place to go when everywhere else seemed to be grey and cloudy. Thanks to Paul who always manages to cheer me up whether he says the right or the wrong thing! And the biggest thanks of all to Niamh, who I'll forever be grateful to for the advice, support and laughs over the last 4 years. I'm not sure I could have done it without you.

Thanks to all of the McGillicuddys – Nana, aunts, uncles and cousins, who have been so wonderful and helped me through my highs and lows in the last 4 years (and there have been a lot!). Most importantly, my family, who this thesis is dedicated to -

Mam, Suzie (the best cheerleader ever), Sarah and Nially, your help and support over the last 4 years has been unwavering, I don't have the words to express my thanks - I love you all so much.

"Happiness is neither virtue nor pleasure nor this thing nor that but simply growth, We are happy when we are growing"

William Butler Yeats

Abstract

This study was dedicated to the development and characterisation of novel stationary phases for the detection and separation of metal cations in high performance chelation ion chromatography (HPCIC). Standard ion exchange chromatography is often unsuitable for the analysis of metals in complex samples as the ion exchange sites can become swamped by the presence of alkali metal salts. Commonly used spectroscopic techniques can be costly and time consuming due to the requirement of sample dilution and/or preconcentration, which can affect sensitivity and limits of detection. Furthermore, many of these methods also require a large sample volume and are unable to tolerate even minute quantities of salts in complex matrices. HPCIC has proven to be a promising alternative to spectroscopic detection techniques and standard ion exchange chromatography, mainly due to the ease in which the selectivity for metal cations can be manipulated. Therefore, in the work presented herein, a number of stationary phases of different morphologies were fabricated and/or characterised for the determination of metal cations in HPCIC.

Firstly, polymeric and silica based columns functionalised with IDA were compared for their chromatographic behaviour for selected metal cations. A commercially available silica monolith column was covalently modified with *N*-hydroxyethyliminodiacetic (HEIDA) groups and successfully characterised for alkaline earth and selected transition and heavy metal cations, achieving peak efficiencies of 54,000, 60,000 and 64,000 *N*/m, for Zn^{2+}, Mn^{2+} and Cd^{2+}. The monolithic HEIDA-silica column and a *N*-(2-hydroxyethyl)-*N*-(2[phosphonomethyl)amino]acetic (HEPMA) modified silica monolith with alternative selectivity were applied to the development of a new HPCIC method for the quantitative determination of Mn^{2+}, Cd^{2+} and Zn^{2+} in mussel digest samples. Finally, a chelating HEIDA modified core-shell stationary phase was fabricated and characterised for a number of metal cations including rare earth elements. The stationary phase was fully characterised and showed peak efficiencies (>200,000 *N*/m) far exceeding those previously observed on any IDA-silica stationary phase. The work carried out proved HPCIC to be a convenient and efficient analytical method for the determination and separation of metal cations in complex samples, and a possible alternative to the aforementioned spectroscopic techniques.

1. Introduction

1.1 Principles of ion exchange chromatography

Ion exchange chromatography (IEC) is a form of chromatography whereby solute ions are retained by oppositely charged sites in the stationary phase by electrostatic force. Cation exchange chromatography retains positively charged cations because the stationary phase displays negatively charged functional groups, and anion exchange chromatography retains negatively charged anions using positively charged functional groups.

Separation of analytes in IEC is dependent on the exchange equilibrium of the analyte ions in solution between the stationary phase and the eluent [1]. Eluent and analyte ions compete for ion exchange sites on the stationary phase, where they are displaced. An eluent ion displaces, and is subsequently replaced by an analyte ion, as demonstrated in Eqn 1.1 [2]. The higher the affinity the analyte ions have for ion exchange sites, the longer they are retained on the stationary phase. Ion exchangers can be classified as strong ion exchangers, that retain their charge over the entire pH range, or weak ion exchangers, that only retain their charge across a narrow pH range.

$$Res^+ E^- + A^- = Res^+ A^- + E \qquad \text{Eqn 1.1}$$

where Res^+ denotes the ion exchange resin, E^- denotes the eluent ions and A^- denotes the analyte ions.

An example of a cation exchange reaction is illustrated employing a negatively charged COO^- functional group and can be expressed as:

$$nResCOO^-H^+ + M^{n+} \leftrightharpoons (ResCOO)nM + nH^+ \qquad \text{Eqn 1.2}$$

An example of an anion exchange reaction is illustrated employing a positively charged NR_3^+ functional group and can be expressed as:

$$nResNR_3^+OH^- + A^{n-} \leftrightharpoons (ResNR_3)nA + nOH^- \qquad \text{Eqn 1.3}$$

Selectivity of metal cations in IEC is dependent on a number of factors including the atomic weight of the metal ion, ionic hydration of metal ions in solution, and also by the charge of the metal. Generally di-valent ions are retained for longer than mono-valent ions, and tri-valent ions retained longer again. Other factors that can include selectivity are the type of ionic group bonded to the stationary phase, the nature of the eluent, and the size of both the ion exchange resin and the column. As discussed further in Section 1.4.5, the use of a complexing agent in the eluent can enhance separation selectivity and speed up the elution process through the formation of complexes with metal ions.

1.2 High performance chelation ion chromatography

1.2.1 Principles of high performance chelation ion chromatography

As discussed in Section 1.1, simple cation exchange chromatography is based on electrostatic interactions between metal cations and negatively charged functional groups within a cation exchange stationary phase [3]. In the case of standard IEC, selectivity is rather limited, and there is little scope for the variation of this selectivity for metal separations [4]. Furthermore, complex samples with high alkali salt concentrations can cause swamping of ion exchange sites, resulting in the so-called 'sample self-elution' effect, whereby reduced retention of target solutes occurs.

High performance chelation ion chromatography (HPCIC) is a form of ion exchange chromatography, based on the formation and subsequent dissociation of metal-ligand complexes (chelates) formed on the surface of the stationary phase [5]. In coordination chemistry, a ligand is an ion or molecule that binds to a central metal atom to form a coordination complex. Ligands (electron donating Lewis bases) can bind to metal ions (electron pair accepting Lewis acids) through more than one atom, such as ethylenediamine (bidentate), or adenosine triphosphate (ATP) (tetradentate). Multidentate ligands form more stable metal complexes than monodentate ligands. This is known as the "chelate effect", where multidentate ligands have greater entropy (ΔS) and lower enthalpy (ΔH) values. "Chelation" can therefore be defined as the formation of two or more spatially separate covalent binding events between a

single polydentate ligand (chelating agents) and a central metal ion [6]. The donor atoms of chelating ligands may be part of an acidic or basic functional group.

The separation of analytes is a result of the difference in the stability/formation constants (*K*') between metal-ligand complexes, which depends on the nature and selectivity of immobilised complexing or chelating ligands on the stationary phase. The dominant separation mechanism is stationary phase metal–ligand complexation, hence retention depends on the strength of the complexes formed, which can be controlled via eluent pH. Therefore, the main difference between HPCIC and standard IEC is the type of interactions between the metal cations and the stationary phase [5,7].

The key advantages that chelating phases provided over standard IEC phases are their insensitivity to complex matrices, and the control over selectivity that they exhibit [4]. For many common chelating ligands applied within HPCIC, the complexes formed with alkali metals on the surface of the stationary phases results in non-retention under acidic conditions, where alkaline earth metals are moderately retained and transition and rare-earth metals are strongly retained [8], resulting in further enhanced selectivity and ease of separation of metal ions [9-17].

When complex formation occurs on the surface of the stationary phase, there is restricted mobility of the immobilised ligand, which is not the case with solution complexation, where it is relatively easy for ligands to change conformation [3]. This restricted mobility results in a typical 1:1 stoichiometry of the surface complexes, with some exceptions. Stationary phases with relatively small chelating ligands can have a 2:1 ligand: metal ratio, such as 3-aminopropylsilica, which contains two aminopropyl groups that react with Cu^{2+} [18]. However, it is generally assumed that the stoichiometry of chelating ligand to metal ion would be 1:1, simplifying the equilibrium equations discussed in Section 1.2.2.

The stepwise interaction of a chelating ligand with a metal ion, in this case the popular chelating functionality iminodiacetic acid (IDA), is shown in Fig. 1.1. The initial formation (structure **I**) and completion (structure **II**) of ion pairs within the surface complexation are demonstrated. The arrangement is then converted from an

outer sphere to inner sphere (structure **III**), which is a result of the rate-determining process in the complex formation. The rate constant can vary, depending on the characteristics of the metal ion of interest, and can be increased by manipulating the ionic strength, acidity of the mobile phase and column temperature, where peak efficiency is improved as a result.

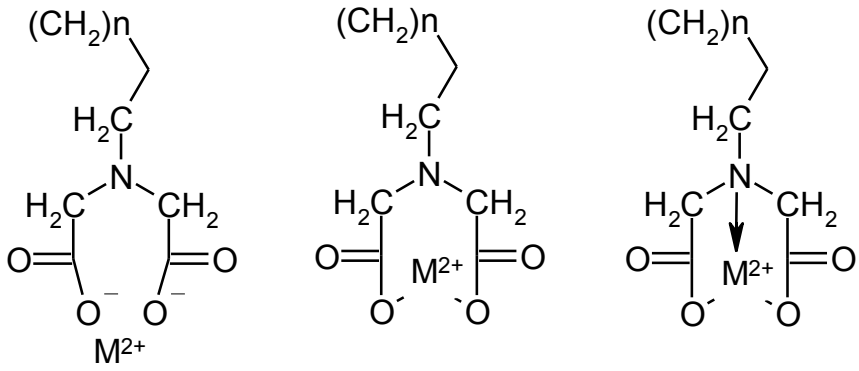

I II III

Fig. 1.1: The stepwise interaction of IDA functional groups with divalent metal cations [3].

1.2.2 Metal-ligand complexes

Metal-ligand complex reactions can be expressed in terms of the aforementioned equilibrium stability complexes. The equilibrium constant for a metal-ligand reaction is called the formation or stability constant, K_n [6]. For a given chelating ligand, the stepwise formation constant, which gives information on the relative concentrations of various metal species can be expressed as:

$$\mathrm{M} + \mathrm{L} \rightleftharpoons \mathrm{ML} \qquad K_1 = \frac{[\mathrm{ML}]}{[\mathrm{M}][\mathrm{L}]} \qquad \text{Eqn 1.4}$$

$$\mathrm{M} + \mathrm{L} \rightleftharpoons \mathrm{ML_2} \qquad K_2 = \frac{[\mathrm{ML_2}]}{[\mathrm{M}][\mathrm{L}]} \qquad \text{Eqn 1.5}$$

$$ML_{n-1} + L \rightleftharpoons ML_n \qquad K_n = \frac{[ML_n]}{[ML_{n-1}][L]} \qquad \text{Eqn 1.6}$$

where M denotes the metal ion, L denotes the ligand that reacts with the metal ion, and n is the maximum coordination number of the ML complex.

The overall (cumulative) formation constant, β_1, which gives information on all of the complexed species for a metal-ligand reaction can be expressed as:

$$M + L \rightleftharpoons ML \qquad \beta_1 = \frac{[ML]}{[M][L]} \qquad \text{Eqn 1.7}$$

For a metal ion that forms more than one complex with the complexing ligand L (multidentate), the overall formation constants, βn, can be expressed as:

$$M + nL \rightleftharpoons ML_n \qquad \beta_n = \frac{[ML_n]}{[M][L]^n} \qquad \text{Eqn 1.8}$$

Thus, the relationship between the overall (β_n) and stepwise (K_n) formation constants is:

$$\beta_n = K_1 K_2 \ldots\ldots K_n \qquad \text{Eqn 1.9}$$

The above formation constants are assumed to be at 0.1 *M* ionic strength, room temperature and constant pressure. A change in these conditions would lead to a change in metal/ligand species in solution, changing the overall stability constant. The conditional formation/stability constant, K_i, is the equilibrium constant for a formation of a complex under a particular set of conditions such as pH, ionic strength and secondary complexation, The conditional stability constant takes into account all of the species present. and can be expressed as:

$$K_i = \frac{[ML_i]}{[ML_{i-1}][L]} = \frac{K_i \gamma ML_{i-1} \gamma L}{\gamma ML_1} \qquad \text{Eqn 1.10}$$

The principle of conditional stability constants can be demonstrated using the popular chelating ligand ethylenediamenetetraacetic acid (EDTA), a compound that forms strong 1:1 complexes with many metal ions, bonding through four oxygen and two nitrogen atoms [6]. EDTA is a hexaprotic system, designated H_6Y^{2+}. It exists as one of five species in solution, dependent on pH. The greater the increase in pH acidity, the more protonated (and less stable) the EDTA species becomes. At pH 12, 98.5% of the EDTA present is in the form $EDTA^{4-}$ (Y^{4-}), compared to 52.1% present in the form H_3EDTA^-, at pH 2.3.

The formation constant for a metal-EDTA complex, K_f, in the species Y^{4-} can be expressed as follows:

$$M^{n+} + Y^{4-} \rightleftharpoons MY^{n-4} \qquad K_f = \frac{[MY^{n-4}]}{[M^{n+}][Y^{4-}]} \qquad \text{Eqn 1.11}$$

The conditional stability constant for a metal-EDTA complex, K_f, can therefore be expressed as follows:

$$K_f' = \alpha_{Y^{4-}} K_f \frac{[MY^{n-4}]}{[M^{n+}][EDTA]} \qquad \text{Eqn 1.12}$$

where [EDTA] is the total concentration of all EDTA species not bound to a metal ion and $\alpha_{Y^{4-}}$is the fraction of all free EDTA in the form Y^{4-} ($\frac{Y^{4-}}{[EDTA]}$). $K_f' = \alpha_{Y^{4-}} K_f$ describes the formation of MY^{n-4} at a particular pH. Using the conditional stability constant, it is possible to find $\alpha_{Y^{4-}}$and evaluate K_f' at a given pH.

1.2.3 Mixed mode mechanism

Like most other types of chromatography, HPCIC can display a mixed mode mechanism, as many chelating ligands, such as IDA, are also weak ion exchangers. Various studies have been carried out investigating mixed mode mechanisms in HPCIC [19-21]. The concentration of the background electrolyte has an effect on ion activity, and therefore the stability constants [22]. If ion exchange interactions

between the metal ion and negatively charged functional groups are not suppressed (i.e. in a low ionic strength eluent), then both cation exchange and chelation can occur at the surface.

If stability constants for surface complexes, β_1, are high enough for metal cations, then chelation may be the dominant retention mechanism even in the absence of high ionic strength eluents [23]. The retention of alkaline earth, transition and heavy metal ions in HPCIC with the use of a non-complexing eluent occurs through both repulsive and electrostatic forces, and coordination interactions between metal cations and the functional groups on the substrate surface, as the chelators are usually charged. An example of this is an IDA-silica stationary phase and the retention of transition metal cations. The retention order in a low concentration nitric acid eluent is $Mn^{2+} < Co^{2+} < Cd^{2+} < Zn^{2+} < Ni^{2+} < Pb^{2+} < Cu^{2+}$, which corresponds to the order of stability constants for the IDA-metal complexes formed. At high ionic strength eluents, this order of retention remains unchanged [24], meaning that chelation is the dominant retention mechanism at the surface for transition metal cations at log β_1 values higher than 4.72 (the effects of ionic strength and its effect on retention and selectivity is discussed in detail in Section 1.4.4).

Ion exchange has been proven to be the dominant mode of retention for alkaline earth metals in the pH range of 2 to 5, as complexation is not significant under such acid conditions [25]. Studies have shown that considerable retention of alkali and alkaline earth metal ions was possible through simple ion exchange interactions with the dissociated carboxylic acid groups of IDA (pK_{a1} = 1.76, pK_{a2} = 2.70) [20]. Therefore, on IDA-silica in weakly acidic conditions, the retention order corresponds to simple ion exchange (Fig. 1.2).

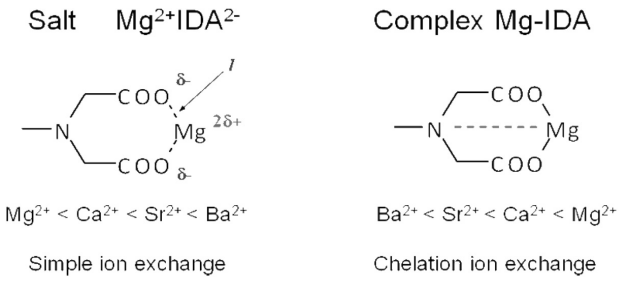

Fig. 1. 2: Comparison of ion exchange and chelation ability of IDA-silica [23].

Secondary or auxiliary equilibrium can also be present within the eluent with the addition of a complexing agent such as dipicolinic acid (DPA), which affects the retention and separation selectivity of metal ions. If a metal ion is added to the eluent, then competitive complexation between the metals in the chelating phase can be used to speed up the elution. The concentration of complexing agent added is typically similar to that of the immobilised ligand, with either a small concentration of strong complexing agents, or a larger concentration of weak complexing agents present. Ionic strength and complexation in the eluent are discussed further in Sections 1.4.4 and 1.4.5 respectively.

1.2.4 Overview of developments in high performance chelation ion chromatography

The formation of complexes were discovered by Alfred Werner in 1893 [26]. Lev Chugaev then discovered that chelates with five to six member rings are typically more stable complexes when considering different complex structures [19]. These innovations were the beginning of the exploitation of complexes in analytical chemistry. Jones and Schwedt [27] achieved the first efficient chelation separation of metal ions with complexation at the surface of the stationary phase, using polystyrene-divinylbenzene (PS-DVB) resins coated with hydrophobic chelating dyes. In this work the eluents used were high ionic strength, therefore any interference from simple ion exchange processes was suppressed, ensuring chelation was the dominant retention mechanism. Chelating columns were originally used for sample preconcentration, but have become an increasingly popular chromatographic method due to a number of advantages over simple IEC. There have been many developments in new materials with modified surfaces, improving metal-ligand interactions and allowing a greater knowledge of surface chemistry [4]. Several reviews on HPCIC and its application to the determination of trace metal ions have been published by Jones and Nesterenko, discussing the parameters that control the chelation sorption mechanism and give an excellent oversight of the applications to date of HPCIC [4,23].

1.3 Stationary phases for high performance chelation ion chromatography

1.3.1 Requirements

A major advantage of HPCIC is the large number of chelating ligands available, each with unique metal selectivity [28]. The choice of ligand to be bonded to the matrix surface depends on several criteria [5], namely:

1. Reversible adsorption. The metal ions should have sufficiently rapid association and dissociation kinetics, therefore the complexes formed should be kinetically labile. Lower conditional stability constants, such as di-valent metal ions have faster dissociation reactions.
2. Appropriate selectivity of functional groups. One of the main advantages of HPCIC is the number of widely available and varied chelating ligands available. Clearly the selection of functional group would depend on their selectivity towards the metal ion of interest.
3. Homogeneous distribution of functional groups on the surface. A 1:1 ratio of metal/chelating ligand interaction is ideal, as the kinetics of complexation are faster.
4. Surface structure. The surface structure should ideally consist of uniform monolayers of covalently bound or adsorbed ligands of thin polymer layers with grafted chelating functional groups. The matrix sorbent should also have good porosity.
5. High hydrolytic stability of the ligand. Separation of metal ions should ideally be carried out in acidic conditions, therefore stationary phases should be able to withstand such conditions.
6. Thermal stability of the ligand. The improved separation selectivity with increased column temperature has been well documented [28], therefore the column must be stable at high temperatures for prolonged periods of time.
7. Mechanical stability of the ligand. The stationary phase must be able to withstand long periods of high pressure, and not shrink or swell in the presence of mobile phases with high ionic strength.

1.3.2 Covalently bonded chelating ion exchangers

Covalently bound chelating ion exchangers are the most popular stationary phases in HPCIC. The functional groups are at the surface of the stationary phase only, where there is greater interaction with metal ions, and the kinetics of mass transfer is improved. As a result, separation efficiency is improved. Functional groups are present either on the surface as a monolayer of bonded ligands or within a covalently attached polymer layer [3], dependent on the immobilisation chemistry used. The polymer layer should be relatively thin in order to enhance the diffusion of metal ions. Most chelating ligands can be immobilised on either a silica or polymer surface with the relatively simple approach of oxirane chemistry [29]. Silica is typically used for the attachment of chelating groups due to the use of acid conditions to avoid hydrolysis of transition metals.

1.3.2.1 Polymer based chelating stationary phases

For many years, polymeric stationary phases covalently functionalised with chelating groups were the dominant phases used for both low and high pressure chromatography due to the idea that they provided better hydrolic stability over silica based functionalities [3]. In pioneering work, Fritz *et al.* investigated a range of PS-DVB based chelating adsorbents with various functional groups, including o-hydryoxymine [30], amide [31], hydroxamic acid [32,33], thioglycolic acids [34] and propylenediamenetetraacetic acid [35] for their suitability for stationary phases in HPCIC. PS-DVB can, however, present some problems, including the need for complex synthetic procedures and by-products forming as a result of the surface reactions. In addition, the surface can become contaminated by adsorption of neutral organic species from the sample matrix, reducing separation efficiency and selectivity. As a result of the aforementioned issues with PS-DVB, other more polar and hydrophilic organo-polymers, such as polymethacyrlates and poly(acrylonitrile-DVB) became increasingly popular as chelating ion exchangers.

The hydrophilic macroporous poly(glycidylmethacrylate) gel (PGMA) contains terminal glycidoxy groups which can covalently attach chelating ligands with reactive amino, thiol or hydroxyl groups. Suzuki *et al.* attached PGMA with various

chelating ligands, including 1-aminobenzyl-1,2-diaminopropane-*N,N,N',N'*-tetraacetic acid [36] and lysine-*N,N*-diacetic acid [37], and compared them for the separation of rare earth metals (REE) with a PS-DVB-IDA-bonded stationary phase [38]. IDA is one of the most popular and well characterised complexing ligands, as it has moderate selectivity for alkaline earth metals, and excellent selectivity fortransition and heavy metal ions [5,17,25]. IDA-metal complexes formed are relatively labile, which is an essential prerequisite for HPCIC in order to achieve reasonable peak efficiencies. Using a HNO_3 gradient, REE were separated on a 150 x 4.6 mm I.D. lysine-*N,N*-diacetic acid-bonded column in 22 minutes.

Barron *et al.* evaluated a poly-IDA functionalised polymeric stationary phase (Dionex Propac IMAC-10, 50 x 2.0 mm I.D.) [17], generally used for protein separation, for the separation of transition metals for HPCIC. This stationary phase is composed of long chain poly-iminodiacetic acid groups grafted to a hydrophilic layer surrounding a 10 μm polymeric bead, with a metal ion capacity of 80 μmol Cu^{2+} per column, or 40 μmol Cu^{2+}/g [34]. In this work the retention and selectivity of metal cations were evaluated; when compared with other IDA functionalised stationary phases the retention order was similar ($Mn^{2+} < Fe^{2+} < Co^{2+} < Zn^{2+} < Cd^{2+}$), with only the exception of Cd^{2+} forming less stable surface complex than Zn^{2+} (Fig. 1.3).

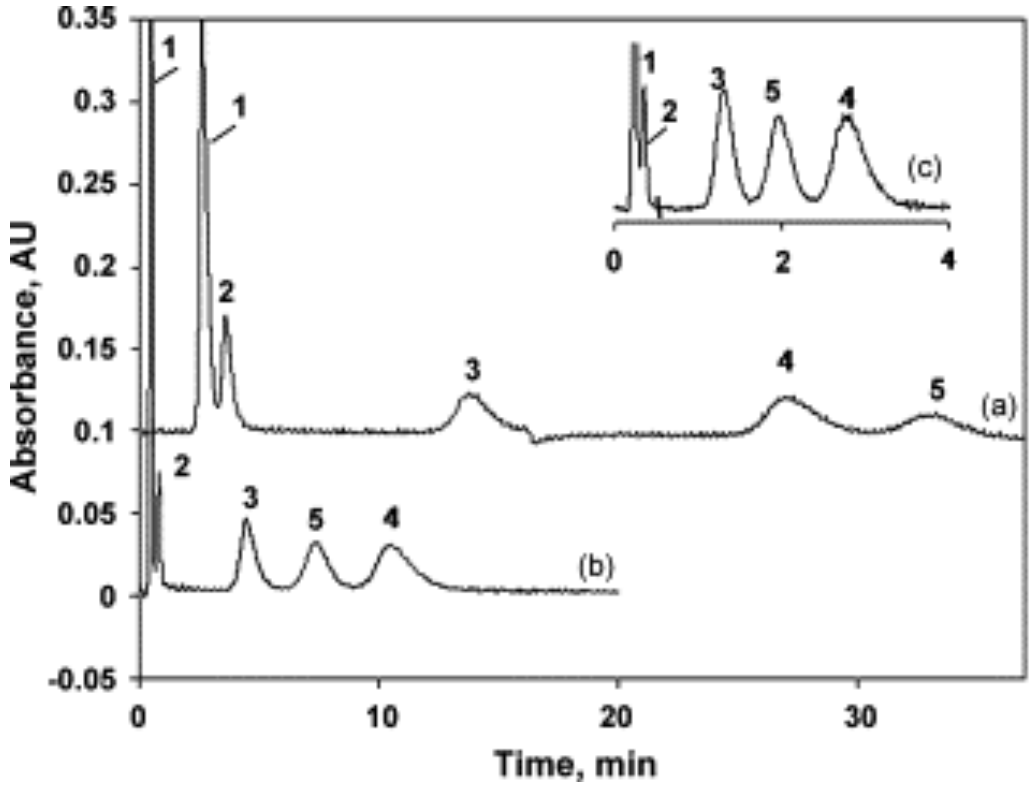

Fig. 1.3: Isocratic separations of transition metals on Propac IMAC-10 column. Eluents: (a) 0.25 m*M* HNO_3, (b) 0.25 m*M* HNO_3/7.5 m*M* KCl and (c) 0.55 m*M* HNO_3/7.5 m*M* KCl, Flow rate: 2.5 mL/min, Detection: spectrophotometric at 510 nm after PCR with 4-(2-pyridylazo) resorcinol (PAR). Elution order: 1: Mn^{2+}, 2: Fe^{2+}, 3: Co^{2+}, 4: Zn^{2+} and 5: Cd^{2+}. Signals offset by 0.1 AU in (a) and (b) for clarity [17].

The effect of flow rate, column temperature and ionic strength were evaluated, and it was shown that adjusting the ionic strength of the eluent could be used to change the retention order and therefore the selectivity of Cd^{2+} and Zn^{2+}.

Monolithic stationary phases have become increasingly popular for applications in ion chromatography, as they provide a good alternative to conventional particle packed columns. The main advantages are the good mass transfers and low column back pressure drop obtained when operating at normal mobile phase flow rates, and the convection based diffusion, which contributes to the maintenance of acceptable peak efficiencies when operating at elevated mobile phase flow rates [39]. The functions of monoliths are broad, and range from purification of proteins and DNA

[40] to separations of biomolecules [41], peptides [42] and nucleosides [43]. In the field of ion chromatography, the separation of anions with monolithic supports has been studied, however there has not been as much investigation into the separation of metal cations. Compared to particle packed columns, there are fewer types of monolithic stationary phase chemistries and supports due to their relative novelty [44]. The advantages of polymeric monoliths include their ease of preparation and the introduction of reactive groups during the preparation of the column, allowing functional group modification. The majority of commercially available monoliths are polymer based, and include polymethacrylate (PMA), PS-DVB and polyacrylamide [45]. Recently, Moyna *et al*. [46] applied a number of acetyl-iminodiacetic acid (AIDA) modified capillary monoliths of different lengths and ligand density to the separation of Mn^{2+}, Cd^{2+} and Cu^{2+}. These capillary housed polymer monoliths were functionalised with varying amounts of vinyl azylactone, followed by modification with IDA via epoxy groups. An increase in cation retention and resolution with the highest capacity columns was observed. In further work [47], the isocratic separation of Na, Mg^{2+}, Mn^{2+}, Co^{2+}, $Cd^{2+}$and Zn^{2+} was achieved on a 250 mm AIDA modified monolith. Peak efficiencies of up to 5,000 *N*/m were achieved.

This work highlighted how the method of attachment of a chelating ligand to the stationary phase can have an effect on separation selectivity, in this case IDA. The bonding chemistry used produced a hydroxyethyliminodiacetic acid (HEIDA) functionalised phase, therefore any further research work described in this thesis concerning IDA-bonded stationary phases will be referred to as HEIDA phases, but will remain IDA for this chapter.

1.3.2.2 Silica based chelating stationary phases

There is a mistaken belief that the hydrolytic stability of chelating silica based stationary phases is poor, which has often led to the use of polymeric chelating-adsorbents over their silica-based counterparts [30,48]. The advantages of chelating silica phases over chelating polymer phases include higher peak efficiencies and their resistance to shrinking or swelling in eluents containing high solvent concentrations or high ionic strength [45]. The higher efficiencies can be clearly seen

in Table 1.1 below [17], which compares a short polymer-IDA column to a bare IDA-silica and an IDA-silica monolith, albeit at different eluent conditions.

Table 1.1: Comparison of column efficiency (*N*/m) of different IDA-functionalised columns [17].

Metal	ProPac 10-IMAC, 10 μm, 50 × 2.0 mm I.D.[a]	IDA–silica, 5 μm, 100 × 4.0 mm I.D.[b]	Merck Chromolith IDA–silica, 100 × 4.6 mm I.D.[c]
Mn^{2+}	3,470	48,480	16,300
Fe^{2+}	7,780	–	–
Co^{2+}	4,500	22,510	27,530
Cd^{2+}	10,060	43,280	9,400
Zn^{2+}	10,420	37,720	16,450
Pb^{2+}	2,240[d]	16,200	18,930
Al^{3+}	1,200[e]	6,870[f]	–

Eluents: [a]0.25 m*M* HNO_3/10 m*M* KCl; [b]10 m*M* nitric acid; [c]10 m*M* HNO_3/0.2 *M* KCl; [d]15 m*M* HNO_3; [e]7.25 m*M* HNO_3/10 m*M* KCl; [f]30 m*M* HNO_3/0.5 *M* KCl.

Depending on the chemistry used, immobilising ligands onto silica can result in reactions between functional groups and reactive groups such as epoxy groups [29]. Following Weetalls revolutionary work on the preparation of porous glass substrates modified by 8-hydroxyquinoline [49], a number of different functional groups have been immobilised on silica surfaces. These include IDA [50] and α-amino acids [51] such as glutamic acid and lysine.

IDA has been bonded to various silica based stationary phases in recent years for HPCIC [28,52-54]. The first to employ IDA-silica for the separation of alkaline earth and transition metals were Bonn *et al*. [25], who synthesised a stationary phase by covalent binding of IDA to a porous silica support. Using various chelating eluents such as citric, tartaric and dipicolinic acids, the retention mechanisms of alkali, alkaline earth and transition metals were studied, which allowed the determination of

transition metal ions in complex matrices. IDA-bonded silica has been applied to the chromatographic separation of the lanthanide series, which also show a high affinity for cation exchangers and have high IDA-complex stability constants [13,17,55-59]. Nesterenko and Jones were the first to achieve an isocratic separation of the lanthanides on an IDA-silica stationary phase [13]. Using a dilute nitric acid eluent (16 m*M*), the combination of the addition of 0.5 *M* potassium nitrate to the eluent to increase the ionic strength, and increase in column temperature (65 °C) ensured that chelation was the dominant retention mechanism, and the isocratic separation of 14 lanthanide ions and yttrium was achieved in ~65 minutes (Fig. 1.4).

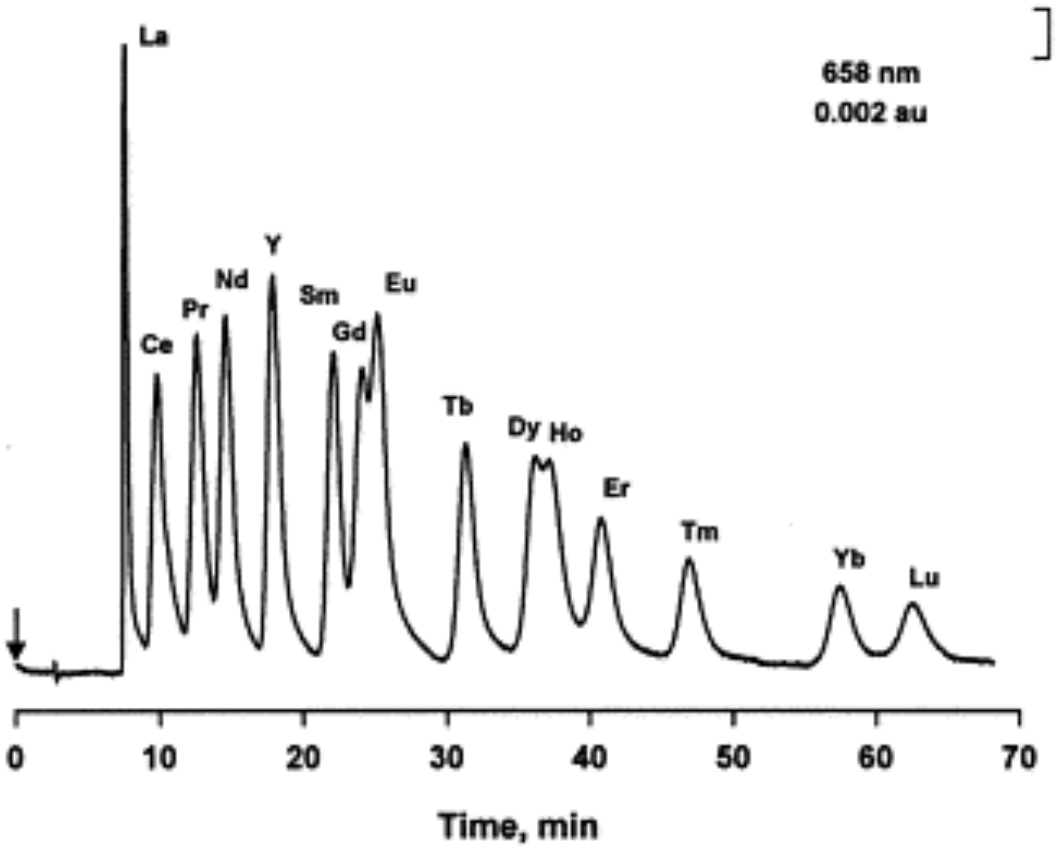

Fig. 1.4: Isocratic separation of standard mixture of 14 lanthanides and yttrium. Eluent: 16 m*M* HNO_3/ 0.5 *M* KNO_3, Flow rate: 1.0 mL/min, Column temperature: 65 °C, Sample volume: 20 µl, Analyte concentration: 4 ppm [13].

In later work [23] the selectivity of the lanthanides on IDA-silica was further exploited by optimising the eluent (0.025 *M* nitric acid with 0.75 *M* potassium nitrate) and increasing the column temperature to 75 °C, allowing for better separation selectivity and a run time of < 40 minutes (Fig. 1.5). This work proved IDA to be an effective complexing functionality for the separation of rare earth metal cations, as the elution order could be predicted due to the correspondence of the stability constants to the corresponding complexes. IDA-silica has also been applied to immobilised metal affinity chromatography (IMAC) [60]. Particles of different porosity were loaded with Fe^{3+} to yield IMAC stationary phases for phosphopeptide enrichment.

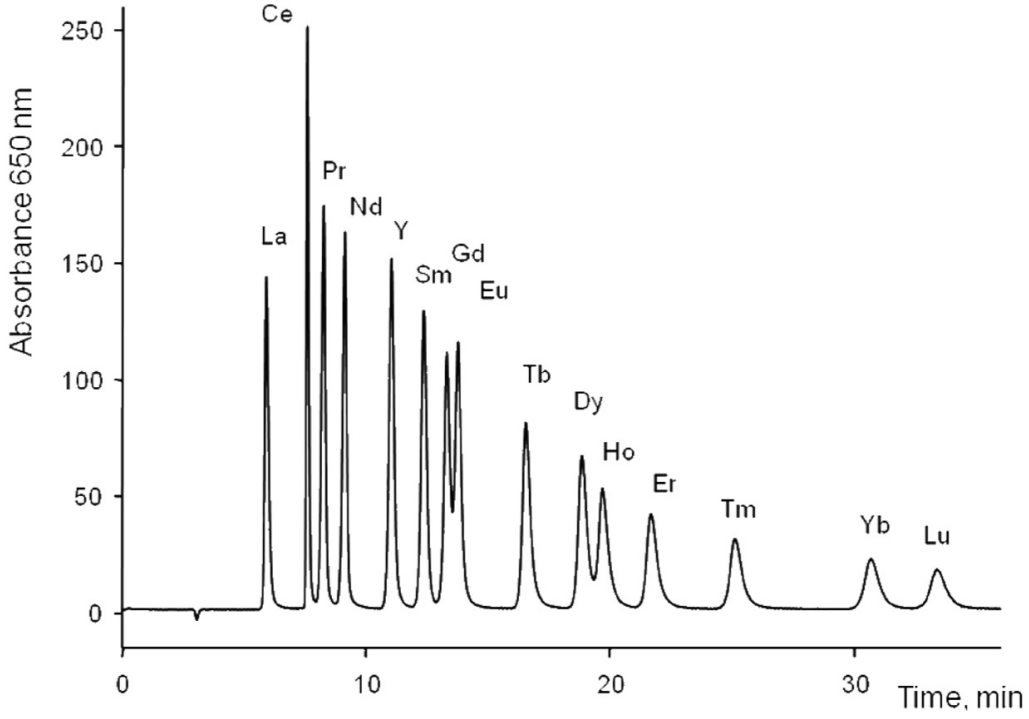

Fig. 1.5: Isocratic separation of standard mixture of 14 lanthanides and Y^{3+} on a 150 x 4.0 mm I.D., 5 µm IDA-silica column. Eluent: 25 m*M* HNO_3/0.75 *M* KNO_3, Flow rate, 1.0 mL/min; Column temperature: 75 °C, Sample volume: 20 µL, Sample concentration: 4 mg/L in 0.2% HNO_3, Detection: spectrophotometric at 650 nm after PCR with arsenazo III [23].

Aminophosphonate (APAS)-functionalised silica has been proved to be a particularly popular chelating stationary phase for the separation of alkaline earth, transition and heavy metal cations [48]. In this work, the kinetics of complexation was proven to be as good as that for IDA. Under acid conditions the selectivity coefficients were more closely spaced and therefore the separation of a number of metals was possible in less than 20 minutes and the high affinity for Mn^{2+} was demonstrated (Fig. 1.6).

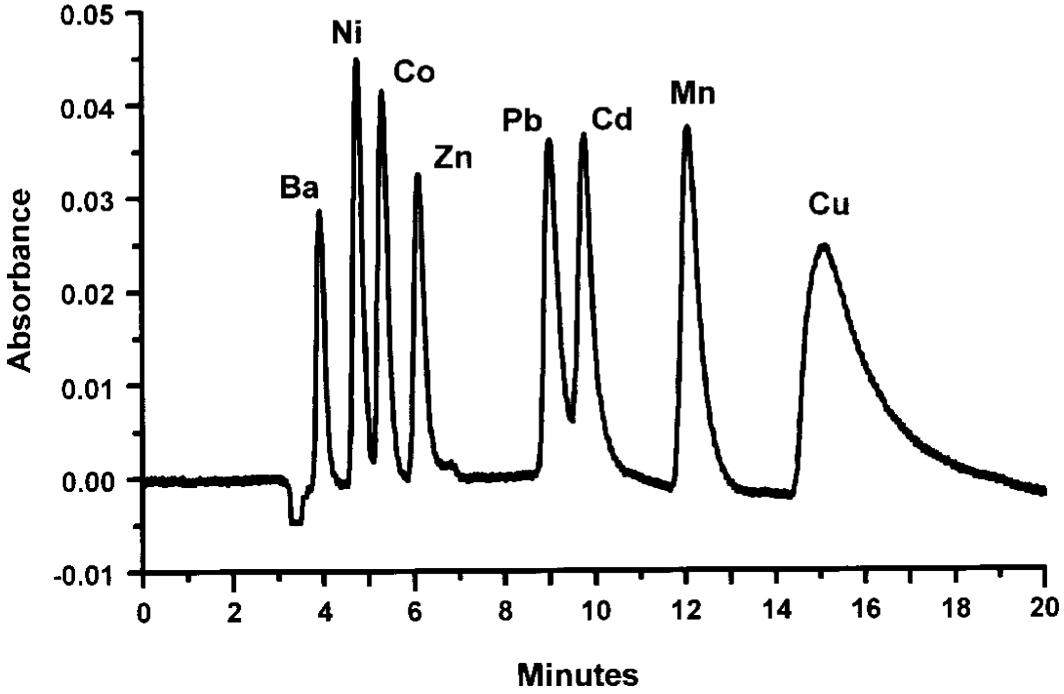

Fig. 1.6: Separation of 1.5 ppm Ba^{2+}, 1.0 ppm Ni^{2+}, 2.0 ppm Co^{2+}, 1.0 ppm Zn^{2+}, 5.0 ppm Pb^{2+}, 2.5 ppm Cd^{2+}, 1.5 ppm Mn^{2+} and 5.0 ppm Cu^{2+} on a 250 x 4.6 mm I.D., aminophosphonic acid-functionalised silica column. Eluent: 1 *M* KNO_3, 5 m*M* HNO_3 [47].

In further work [23], the more evenly spaced retention times required a nitric acid only eluent to separate 11 metal species in ~20 minutes as seen in Fig. 1.7. The broader peak observed for Cu^{2+} had previously been observed on IDA-silica columns.

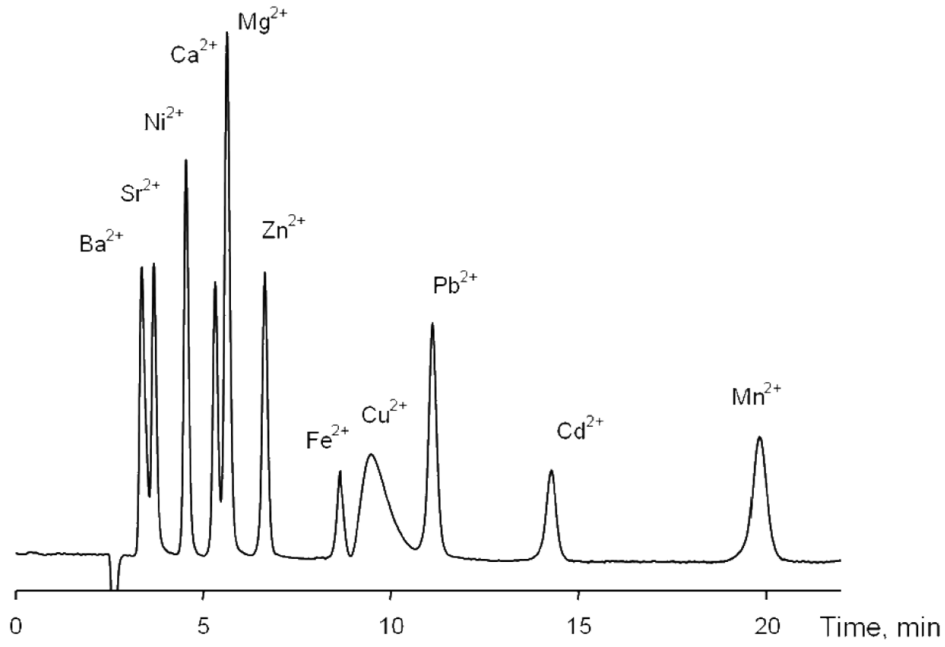

Fig. 1.7: Separation of model mixture of alkaline-earth and transition metal ions on APA-silica 150 x 4.0 mm I.D., 3 μm column. Eluent: 50 m*M* HNO_3/0.8 *M* KNO_3, Detection: spectrophotometric at 510 nm after PCR with PAR-ZnEDTA [23].

Silica-based monolithic stationary phases have received increasing attention in recent years, particularly in reversed-phase liquid chromatography (RP-LC), due to the excellent efficiencies they provide [45]. However, they have also been applied in other types of chromatography, for example, the separation of alkaline and transition metals on a bare porous silica monolith was achieved using solvent enhanced chromatography [61]. In earlier work on bare silica supports [62], retention was due to weak ion exchange interactions, which should become stronger with increased organic solvent content due to a lower number of water molecules associated with the ion. Following on from this, the effect upon cation retention of mobile phase ionic strength, pH and organic content was evaluated using solvent-based acetate buffered eluents. An optimised separation of Mn^{2+}, Cd^{2+}, Co^{2+}, Cu^{2+} and Ni^{2+} in under 4 minutes was obtained using an eluent composed of 80% acetonitrile/10.3 m*M* ammonium acetate, pH 4.6 with spectrometric detection at 510 nm after post-column reaction (PCR) with PAR. The eluent composition and ionic strength was shown to have an influence on both peak shape and stability, and the separation of Ba^{2+} and Sr^{2+} was achieved in 6 minutes without peak splitting.

Xu *et al.* were the first to apply silica monoliths to the detection and separation of H^+ and metal ions [63-65]. Using a monolithic reversed-phase (RP) octadecylsilyl (ODS) silica gel column modified with lithium dodecylsulfate (Li-DS), they developed a method for the separation of Na^+, NH_4^+, K^+ and H^+ in rainwater [63]. This was achieved using an acidic LiCl eluent with conductivity detection. In further work, Xu *et al.* separated H^+ from mono- and di-valent metal cations (Na^+, NH_4^+, K^+, Mg^{2+} and Ca^{2+}) in under 2 minutes with conductivity detection, using a ethylenediamenetetraacetic acid (EDTA) dipotassium-salt dihydrate (K_2EDTA) as eluent [64]. This method was applied to the determination of acidity of rainwater and deionised water. Continuing from this work, the separation of H^+ from Mg^{2+} and Ca^{2+}, the ionic compounds found in acid rain, was determined using the Li-DS monolithic stationary phase [64,65]. This was achieved in 4 minutes using 2 m*M* ethylenediamene, 0.1 m*M* Li-DS as eluent. Compared to standard particle-packed ion chromatography (IC) columns, the main advantage of using silica-based monoliths in this case was the high speed of analysis. IC columns previously applied to the determination of acidity required 12-30 minutes for the separation of H^+ from monovalent cations [66,67].

In other work, a novel zwitterionic lysine-bonded silica monolithic stationary phase was evaluated for anion and cation selectivity [68]. A 100 x 4.6 mm I.D. column was covalently modified "in-situ" with lysine (2,6 diaminohexanoic acid) groups, and due to its zwitterionic nature, the column possessed anion and cation exchange capacity. Analysis of alkali and alkaline earth metals was carried out using a 3 m*M* HNO_3 eluent with suppressed conductivity detection, however very little selectivity and retention was observed and co-elution occurred. Separation of transition metal cations was successful and using a 3 m*M* KCl eluent with spectrometric detection after PCR, the separation of Mn^{2+}, Cd^{2+}, Co^{2+} and Zn^{2+} in under 10 minutes was achieved (see Fig. 1.8), with Pb^{2+} more strongly retained on the column (> 30 mins). Eluent pH was varied to manipulate selectivity, and the strong pH dependence of the column was observed, particularly for Zn^{2+} and Pb^{2+}. In further work, the lysine-bonded column also showed excellent selectivity for the separation of inorganic anions, and by varying the eluent composition and pH, a separation of nitrate, bromate, bromide, nitrate, iodide and thiocyanate was achieved [69].

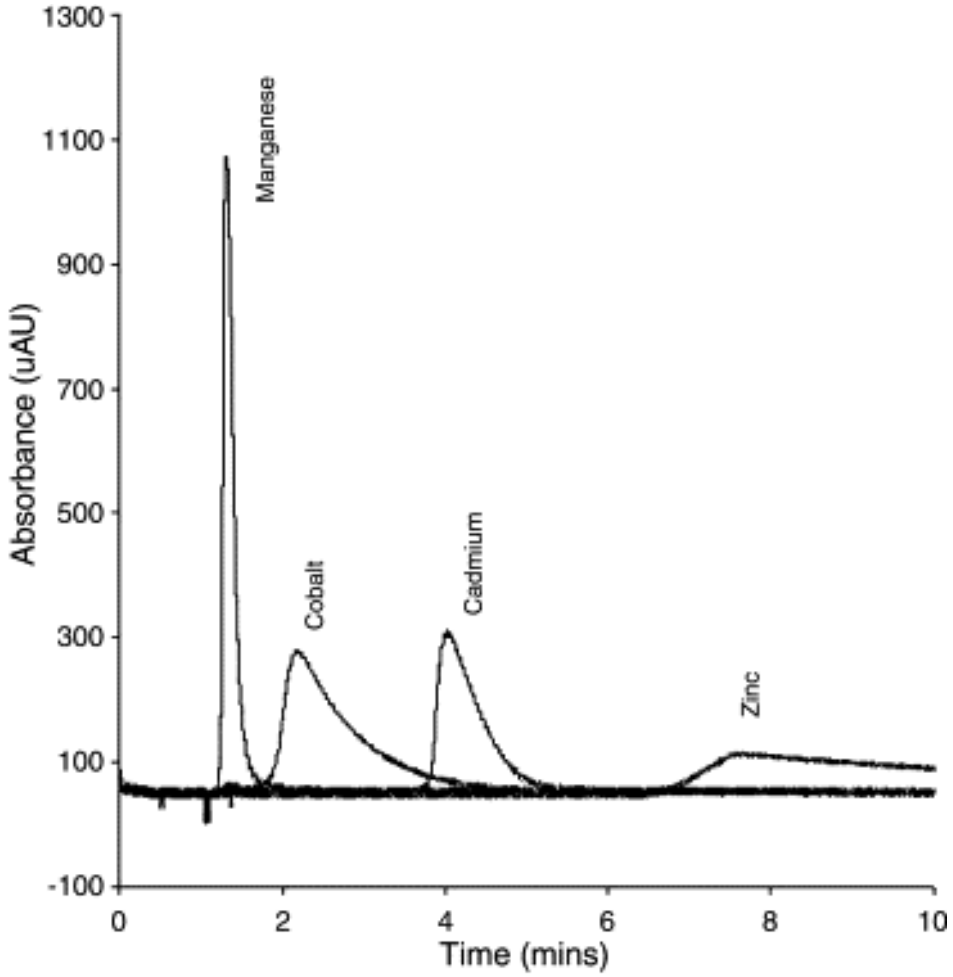

Fig. 1.8: Overlay of Mn^{2+}, Co^{2+}, Cd^{2+} and Zn^{2+} chromatograms obtained on a lysine modified monolith. Eluent: 3 m*M* KCl, pH 4.5; Flow rate: 2.0 mL/min; Detection: spectrophotometric at 495 nm after post-column reaction with PAR [68].

IDA has also been used for the preparation of silica monoliths. Sugrue *et al.* covalently attached IDA groups to a 100 x 4.6 mm I.D. commercially available PEEK lined bare monolithic silica column and investigated the selectivity of alkaline earth metals compared to an IDA-silica particle packed column [70]. The selectivity and efficiencies observed on the two phases were very similar, with slightly higher retention of Ca^{2+} on the monolithic phase, due to the higher eluent pH employed. In further work [45], the IDA-monolith was applied to the separation of Mn^{2+}, Cd^{2+}, Co^{2+}, Zn^{2+} and Pb^{2+} (Fig. 1.9), and showed better efficiencies when compared to a particle packed column.

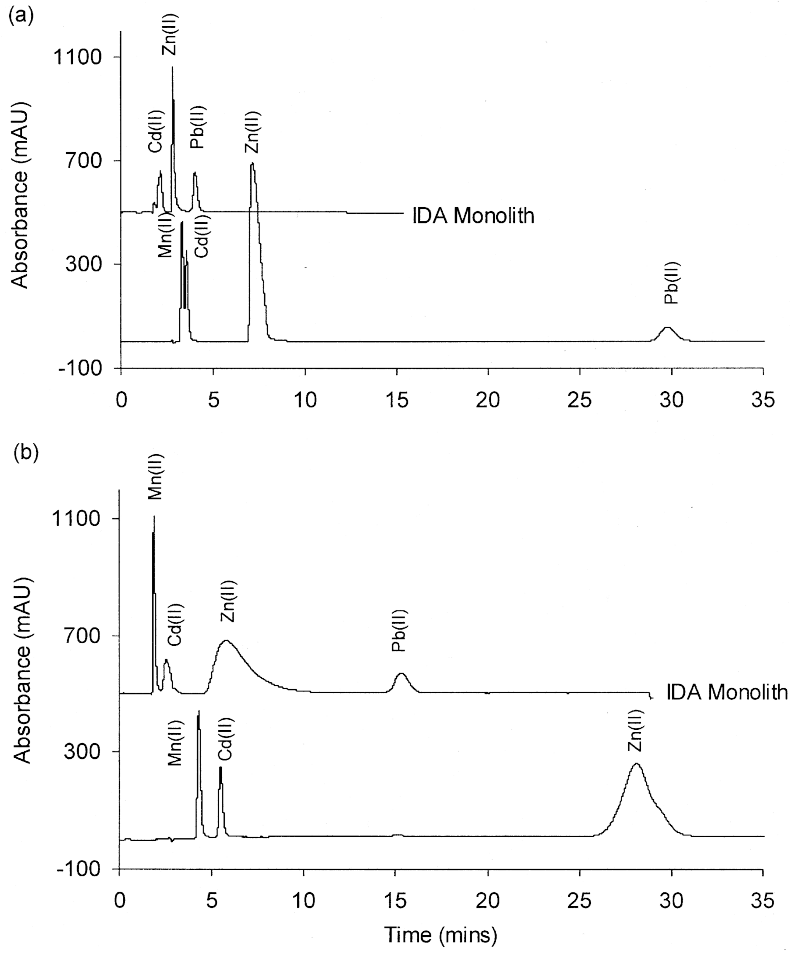

Fig. 1.9: Comparison of column capacity and selectivity for Mn^{2+}, Cd^{2+}, Zn^{2+}, and Pb^{2+} on IDA-silica monolith and IDA-silica gel columns; (a) Eluent: 0.2 *M* KCl, pH 2.0, (b) Eluent: 0.2 *M* KCl, pH 2.5, Detection: spectrophotometric after post-column reaction with PAR [45].

1.3.3 Dynamically modified and impregnated stationary phases

During the preparation of chelating stationary phases, unwanted secondary interactions can occur [3]. In addition, the chemistry used to bind the ligand to the stationary phase support can be unpredictable, and change the selectivity of the ligand. A simpler alternative to covalent attachment of ligands is to either impregnate or dynamically modify the stationary phase. The selectivity of both methods is based on the conditional stability constants of the chelates formed, and eluent pH mainly controls the elution of metal ions.

1.3.3.1 Impregnated (pre-coated) chelating stationary phases

Semi-permanent impregnating is carried out by "pre-coating" the stationary phase with the ligand. The stationary phase is generally coated with the ligand, followed by conditioning with a range of aqueous solutions of varying pH [71]. The separation of metal ions is based on the differences in stability constants, and can be controlled by changing the eluent pH. Metallochromic ligands can be used to pre-coat the stationary phase [72]. One of the first instances of the use of an impregnating chelating phase was the modification of a reversed-phase column with *N-n*-dodecyliminodiacetic acid [73] for the separation of alkaline earth metal ions in a high ionic strength sample. Ca^{2+}, Mg^{2+}, Sr^{2+} and Ba^{2+} were successfully separated in under 8 minutes using a mobile phase with dilute tartaric acid.

Jones and Schwedt [27] employed a single column (PS-DVB), coated with chromazurol S (CAS) for the preconcentration and separation of di- and trivalent metal cations. A number of alkaline earth and transition metals were separated using a pH step gradient method. In further work, impregnated polymer resins were successfully applied to the analysis of trace metals in various samples [74-77]. Paull *et al*. used a xylenol orange (XO) impregnated resin for the combined preconcentration and separation of Zn^{2+}, Pb^{2+}, Ni^{2+} and Cu^{2+} in coastal seawater [74]. Prior to this, XO was most commonly used as a metal ion indicator in complexiметric titrations, and has also been used as a post-column reagent for the lanthanides [78]. A structurally similar ligand which has been applied to the pre-coating of chelating stationary phases is methylthymol blue (MTB), which complexes through one of two IDA groups. Jones *et al.* [76] applied a PS-DVB based column impregnated with MTB to the separation of (in order of elution) Ba^{2+}, Sr^{2+}, Mg^{2+} and Ca^{2+} in under 20 minutes. The elution order, which differed from standard ion exchange, allowed the separation of Ba^{2+} and Sr^{2+} in samples containing large amounts of Mg and Ca.

One disadvantage of impregnating the stationary phase support is that "bleeding" of the ligand from the column can occur when the ionic strength of the eluent is changed. This can result in reduced capacity over extended periods of time. In

addition, separation efficiencies are not as high as covalently bound chelating stationary phases [72].

1.3.3.2 Dynamic modification

Dynamic modification includes the ligand through the mobile phase during the chromatography. With dynamic coating, the ligand is present in the eluent, and can also act as a complexing agent to control selectivity. This process is extremely complex due to the presence of the ligand in the mobile and stationary phase. However, similar retention characteristics compared to pre-impregnated phases is observed. There is an increased column capacity that leads to improved separation efficiency, and a different selectivity due to the competing equilibria from the mobile phase. In addition, often with dynamically modified phases direct visible detection is possible and there is no need for post-column reaction.

The same ligands applied to pre-coating columns can be applied here, namely phthalein purple (PP), MTB and XO. Paull *et al*. [79] used a PS-DVB reversed-phase column together with a mobile phase containing PP for the detection and separation of alkaline earth metals. Dynamic modification of stationary phases with chelating ligands has also been used for the detection and separation of transition and heavy metal ions [7], selected lanthanide ions [71] and U^{6+} [80]. Shaw *et al.* [7] investigated the behaviour of transition metals lanthanides, Al^{3+} and UO_2^{2+} on a 7 μm PS-DVB packed column with a 4-chlorodipicolinic acid mobile phase, where the dependence of the retention factor upon mobile phase pH was observed. The complexation between the metal ions and the ligand adsorbed on the resin was influenced heavily by the decrease in dynamic loading with increase in pH. Possible reversed-phase interactions between metal-chlorodipicolinic acid complexes and the hydrophobic PS-DVB stationary phase may have occurred. A separation of Mn^{2+}, Co^{2+}, Ni^{2+}, Zn^{2+}, Cu^{2+}, Pb^{2+} and Cd^{2+} in a water sample (Fig. 1.10) was successfully achieved in under 20 minutes using a 0.25 m*M* chlorodipicolinic acid, 1 *M* potassium nitrate, pH 2.2 eluent.

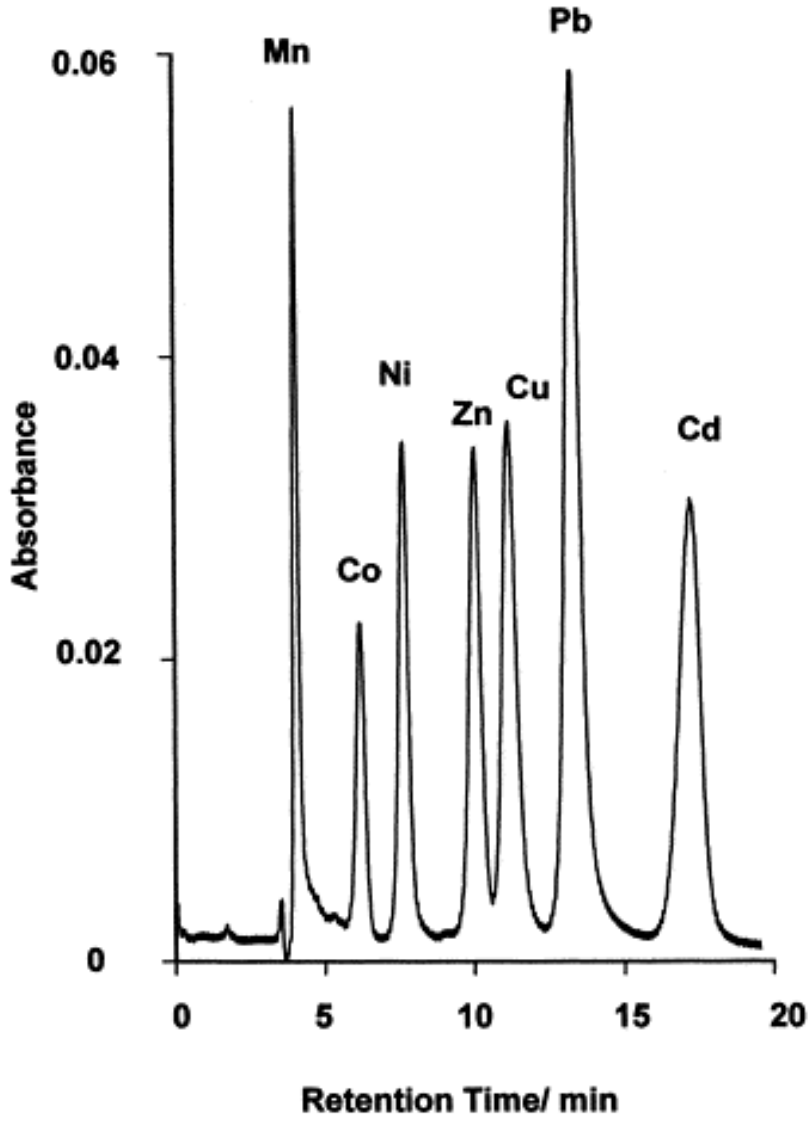

Fig. 1.10: Separation of metal cations on a 300 × 4.6 mm I.D. PRP-1 7 μm PS–DVB column. Analyte concentration: Mn^{2+}: 0.5 mg/L, Co^{2+}: 0.5 mg/L, Ni^{2+}: 0.5 mg/L, Zn^{2+}: 2 mg/L, Cu^{2+}: 1 mg/L, Pb^{2+}: 10 mg/L and Cd^{2+}: 20 mg/L, Eluent: 1 *M* potassium nitrate, 0.25 m*M* chlorodipicolinic acid and 6.25 m*M* nitric acid (pH 2.2). Detection: spectrophotometric at 520 nm after post-column reaction with PAR [7].

1.4 Mobile phase factors affecting the retention of metal ions in high performance chelation ion chromatography

There are a number of different mobile phase parameters that can affect elution in HPCIC, where the primary function of the mobile phase is to ensure a chelation dominant retention mechanism. Various parameters including eluent pH, eluent composition, the addition of a complexing agent to the eluent and column temperature can all disrupt the hydration sphere of a metal cation, thus increasing rate constants and improve the peak efficiency. These parameters may be adjusted to manipulate the selectivity and retention of metal cations

1.4.1 Eluent pH

As discussed in Section 1.2.6, most chelating functional groups are weakly acidic or basic, therefore the conditional stability constants of the metal complexes formed are pH dependent. An increase or decrease in eluent pH will lead to the dissociation or protonation of these functional groups [19]. Dissociation of acidic groups on the surface of the stationary phases results in a strong increase of the stability constants of complexes on the surface, therefore increased retention of metal cations is usually observed with increased eluent pH [81]. However, at the same time, dissociation of weak acid functional groups of the stationary phase results in an increase of ion exchange capacity, which is dependent on dissociation constant. Usually for isocratic elution, eluent pH is adjusted so that the retention factors of metal cations would be in the range of 10-15 (Section 1.2.3). As a result, the stability constants of complexes formed are rather low and it can be assumed that metal cation retention would be the result of two retention mechanisms: chelation and ion exchange. Therefore a decrease in retention is observed with decreased eluent pH. Generally, in low ionic strength eluents between pH values of 2 and 5, ion exchange will be the dominant mechanism and as a result alkaline earth metals will show an increase in retention. Ion exchange capacity will also be increased by the dissociation of weak acid groups, dependent on acid dissociation constant, K_a, values.

1.4.2 Column temperature

The effect of temperature in standard ion exchange chromatography is relatively small [53], compared to HPCIC where the temperature affect upon retention is generally much more profound. In HPCIC retention is dominated by complex formation, that can either occur as an exothermic or endothermic process, dependent upon the nature of the ligand and metal ions involved. For a given chromatographic system, retention dependence upon temperature can be described by van't Hoff equation:

$$\ln k = \frac{\Delta H^\circ}{RT} + \frac{\Delta S^\circ}{R} + \ln \varphi \qquad \text{Eqn 1.13}$$

where ΔH° and ΔS° are sorption enthalpy and entropy, respectively, and φ is the phase volume ratio [24]. In a system based upon pure ion exchange, the dependence of ln k on temperature should be linear, and for negative values of enthalpy ($-\Delta H$), in the case of an exothermic process, retention should decrease with an increase in column temperature. In the case of chelation, ΔH values are typically much greater than for ion exchange, and as mentioned, can be either exothermic or endothermic. Additionally, true chelation is associated with high entropy values, and as such the change of Gibbs energy (ΔG) with an increase in temperature would be negative, leading to an increase in the associated equilibrium constant. With thermodynamic processes dominating chelation based retention, metal ions retained predominantly via (stationary phase) chelation/complexation should exhibit increasing retention with increasing column temperature.

Various studies have been carried out investigating the effects of column temperature on the retention and separation selectivity of metal cations. Chong *et al.* [82] have demonstrated that the separation time for cations can be reduced by 60% with the use of elevated column temperatures in ion chromatography. This is due to decreased viscosity and therefore decreased backpressure at higher increased temperature. Hatsis and Lucy [83] observed the decrease in retention of metal ions with increased temperature on a CS12A carboxyated/phosphonated cation exchange column, showing that metal ions belonging to the same group showed similar selectivity, but behaved differently to those in other groups. A number of studies have been carried out to observe the effect of temperature on alkaline earth metals [20,53,84,85] and

transition and lanthanide metals [28,45,85-87], with various chelating ion exchangers. The effect of temperature upon efficiency and resolution on selected alkaline earth and transition metals is demonstrated in Fig. 1.11, where Mg^{2+}, Ca^{2+}, Mn^{2+} and Cd^{2+} were separated on an itaconic acid functionalised chelating column at 19, 40 and 50 ^{o}C [81].

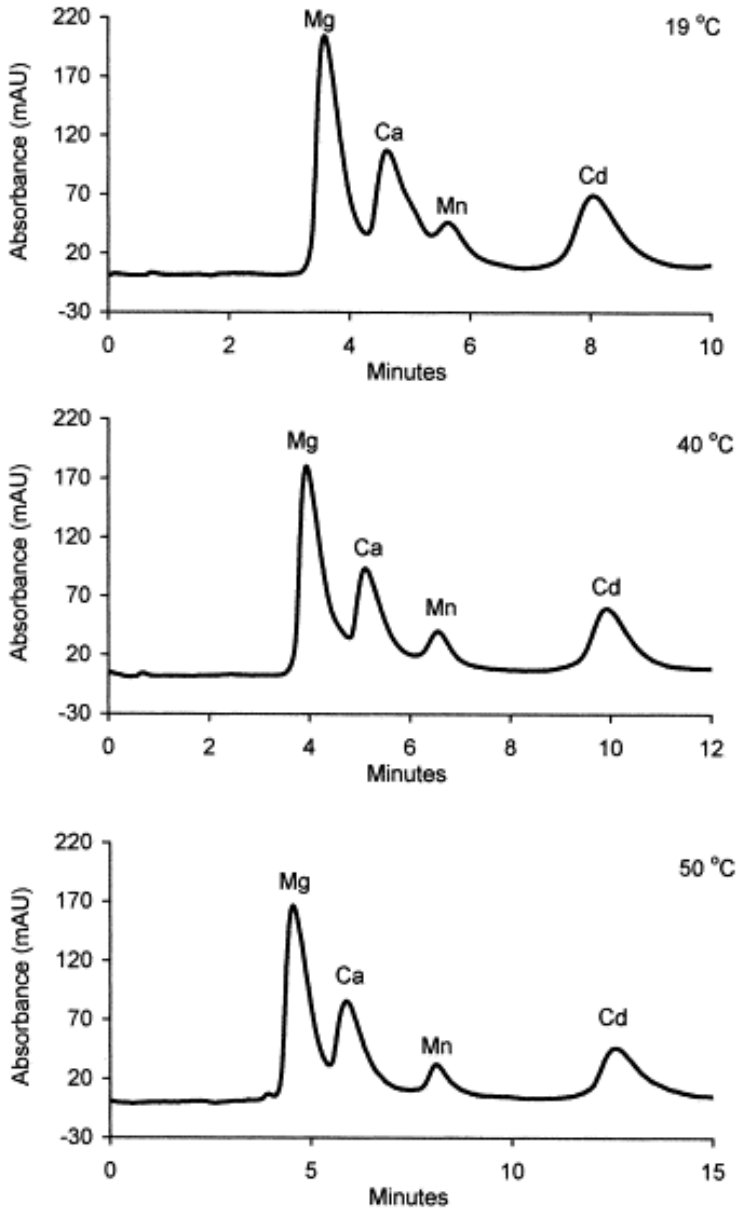

Fig. 1.11: Chromatograms showing the resolution of Mg^{2+}, Ca^{2+}, Mn^{2+} and Cd^{2+} at 19, 40 and 50 °C. Eluent: 20 m*M* KCl, pH 3.5, Standard composition: Mg^{2+}: 5 mg/L, Ca^{2+}: 2 mg/L, Cd^{2+} and Mn^{2+}: 0.2 mg/L, Detection: spectrophotometric after PCR with PAR [81].

The improvement in separation efficiency at increased temperatures is clearly seen. Cd^{2+}, which retained more strongly at elevated temperatures, retained the same peak width at all temperatures.

Kolpachnikova *et al.* [86] studied the effect of temperature on glutamic acid (Glu-silica), diaminohexanoic acid (Lys-silica) and IDA (IDA-silica) modified silica gel columns for alkali and alkaline earth metal ions. Paull and Bashir [53] have previously shown that in chelation dominant chromatography where high ionic strength eluent was used, the retention of alkali, alkaline earth and selected transition metals is increased at higher temperatures. The effect of temperature upon the retention of metal ions on sufonated and mono-, di-, and aminocarboxylated cation exchange columns was investigated over the range 19 – 65 ^{o}C, with a significant effect on the retention between mono- and divalent metal cations. Alkali metals demonstrated exothermic behaviour, where transition metals showed endothermic behaviour. The behaviour of alkaline earth metals was not clearly defined, however strongly endothermic behaviour was observed on certain eluents. In some cases, a dual retention mechanism of both ion exchange and chelation occurred, and temperature could be used to manipulate retention process at certain eluents.

Nesterenko and Jones examined the effect of column temperature on the lanthanides and yttrium [13]. Various effects were observed with increased temperature, namely increase in retention times of metal ions, improvement of peak shapes and changed in separation selectivity. The dependence of the retention of lanthanides as a function of temperature was determined (see Fig. 1.12), where the resultant van't Hoff plot demonstrates an improvement in selectivity. The effect of increased temperature was more significant for Y^{3+}, allowing the manipulation of its retention, thus enhancing selectivity and the separation of a number of REE.

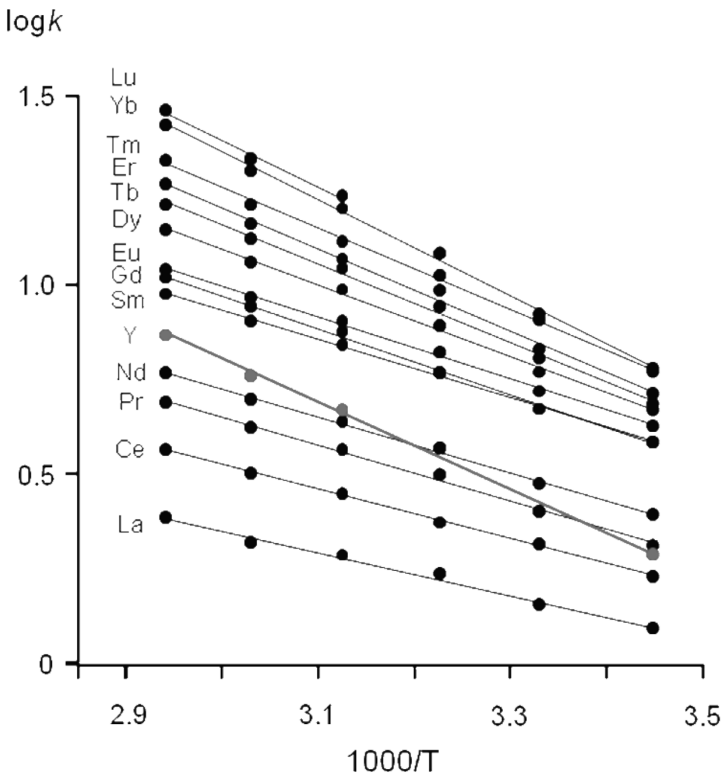

Fig. 1.12: Effect of column temperature on the retention of REE on IDA-silica column. Eluent: 13.6 m*M* HNO_3/0.5 *M* KNO_3 [13].

1.4.3 Organic solvents

Polar water-miscible organic solvents such as methanol, acetonitrile and ethanol are often added to mobile phases in HPCIC, which can affect retention on bonded phases (coated or impregnated phases may bleed and lose capacity) due to changes involving the dissociation and protonation of functional groups. The conformational mobility of chelating groups attached to hydrophobic matrices may be improved with the addition of organic solvent additives, thus changing their accessibility for cation interaction [88]. The addition of solvents causes the dielectric constant of the eluent to change, and secondary equilibria in the chromatographic system are affected [4]. These include solvation of metal ions and the solubility of metal complexes in the eluent. In early work on this subject, the effect of the concentration of methanol in the eluent was studied, showing the increase of complex stability with increased methanol concentration [89]. Another study investigated the retention of metal

cations on an amino acid-type chelating column [87] with 5-20% acetonitrile or isopropanol in the eluent. Different temperatures were examined, and only Cu^{2+} displayed a change in retention behaviour. One advantage was an improvement in peak shape, however investigation would be needed to draw more comprehensive conclusions. The use of a large amount of organic solvent in the mobile phase may have an effect on separation selectivity, as observed on an IDA-silica column [54]. Table 1.2 shows how the elution order and column efficiency are both changed with a change in mobile phase methanol concentration [3].

Table 1.2: The effect of the concentration of mobile phase methanol on the separation selectivity and efficiency of IDA-silica (150 x 4.0 mm I.D.) column. Mobile phase: 2.5 m*M* dipicolinic acid/5 m*M* HCl, Flow rate: 0.8 mL/min [3].

Methanol content (%)	Retention time (min)			Theoretical plates (*N*)		
	Fe^{2+}	Fe^{3+}	Cu^{2+}	Fe^{2+}	Fe^{3+}	Cu^{2+}
20	3.35	4.44	3.88	712	1090	1540
40	3.74	5.23	4.94	1698	899	2040
60	4.31	8.57	9.04	2227	659	1933

1.4.4 Ionic strength

As discussed in Section 1.2.3, the use of an eluent of lower ionic strength, mixed mode mechanisms can occur (both ion exchange and chelation), as many chelating ligands, such as IDA, are also weak ion exchangers. The addition of a high level concentration of electrolytes to the eluent in order to increase ionic strength would suppress electrostatic interactions between negatively charged carboxylic groups in chelating functional groups and cations in the eluent [19]. Nitrate, chloride or perchlorate alkali metal salt eluents are most commonly used for this purpose, as they do not form complexes and do not precipitate with the metal cations. The concentration of the background electrolyte has an effect on ion activity and therefore the stability constants [22]. An increase in ionic strength increases the ratio of chelation-to-ion exchange, therefore if the concentration of salt is increased, ion

exchange would become less significant. The ideal ionic strength of the eluent for HPCIC is between 0.5 and 1.0 *M*, which corresponds to the concentration of 0.5 to 1.0 *M* of a monovalent salt.

Bashir and Paull [19] investigated the effect of the use of high ionic strength eluents on the retention mechanism of alkaline earth metals. Varying concentrations of KNO_3 eluents were employed to observe any changes in the order of elution of alkaline earth metals, which had previously been determined to be $Mg^{2+} < Ca^{2+} < Sr^{2+} < Ba^{2+}$, using ion exchange eluent conditions [20], and also using weak carboxylic acid cation exchange resins [2]. At 0.1 *M* KNO_3, ion exchange was clearly the dominant retention mechanism, with the selectivity matching that of typical ion exchange conditions. The effect of increased KNO_3 is clearly seen in Fig 1.13, in particular with regards to Ba^{2+}, which changes from last eluting cation at a mixed mode retention mechanism using 0.1 *M* KNO_3 (A), to first eluting at a complexation dominant retention mechanism using 1.5 *M* KNO_3 (F).

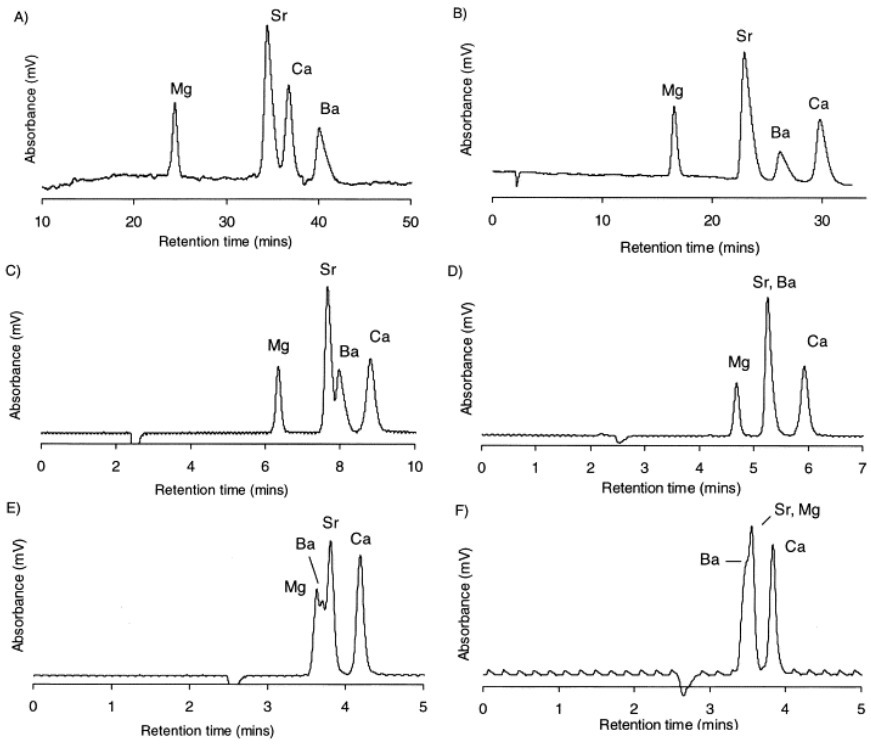

Fig. 1.13: Separations of alkaline earth metal ions using the IDA-silica column with (A) 0.1 *M*, (B) 0.2 *M*, (C) 0.3 *M*, (D) 0.5 *M*, (E) 1.0 *M* and (F) 1.5 *M* KNO_3 eluent. Other conditions: eluent pH 4.2 (HNO_3) [19].

In further work [28], the retention of alkaline earth and transition metal ions on an IDA-silica column was evaluated with various eluents employed (0.5 and 1.0 *M* KNO_3, $NaNO_3$, KCl and NaCl), between the pH range 2 to 3. As expected, ion exchange interactions were suppressed using these eluents, and alkaline earth metal cation were not retained. This work highlighted how ion exchange mechanisms can be suppressed by the use of a high ionic strength eluent, and how eluent pH and ionic strength can be used to exploit the retention mechanism.

The nature of the salt eluent can also have an effect on retention [28]. Fig. 1.14 demonstrates the effect of the use of a KNO_3 and NaCl eluent, both concentrations 0.5 *M*, pH 2.0, on the retention and selectivity of metal cations. The difference in retention is clearly seen, particularly on Cd^{2+} where there is a noticeable decrease in retention with the use of NaCl in the eluent.

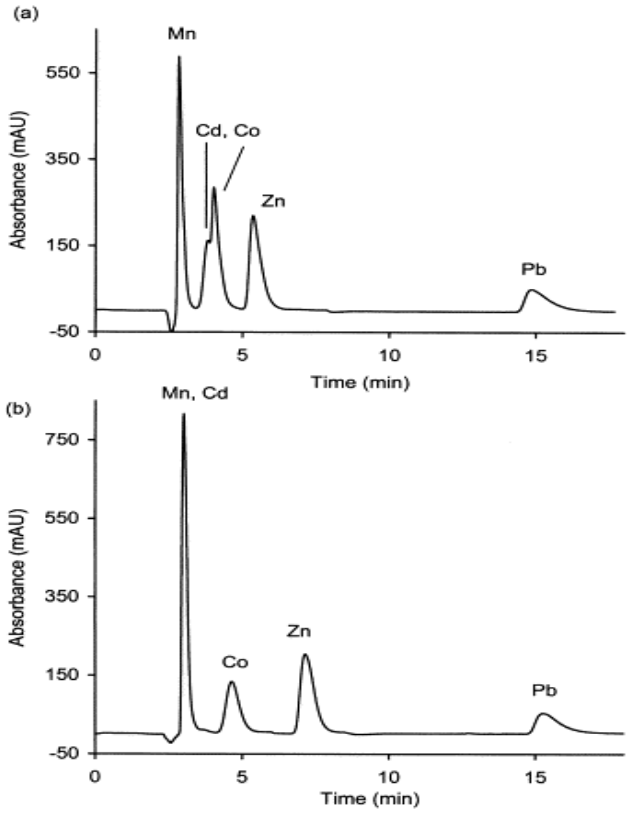

Fig. 1.14: Chromatogram showing (a) the separation of Mg^{2+}, Co^{2+}, Cd^{2+}, Zn^{2+} and Pb^{2+} using a 0.5 *M* KNO_3 eluent, pH 2.0 and (b) the separation of Mg^{2+}, Co^{2+}, Cd^{2+} Zn^{2+} and Pb^{2+} using a 0.5 *M* NaCl eluent, pH 2.0, Standard concentration: 1 mg/L for Mg^{2+}, Co^{2+}, Cd^{2+} Zn^{2+}, and 5 mg/L for Pb^{2+} [28].

1.4.5 Complexing agents in the eluent for competitive chelation

The addition of a complexing agent to the eluent can greatly enhance separation and selectivity. This technique has previously been used to regulate separation speed of transition metals in simple cation exchange chromatography [90,91], where the charge of the cations is decreased proportionally to the corresponding conditional stability constants. In HPCIC the effects are greater, due to competitive complexation that occurs between metal complexes in both the eluent and the surface of the stationary phase [23]. The selectivity obtained with di- and tri-protic organic acids depends on their metal-ligand formation constants, dissociation constants and mobile phase pH [3]. Organic acids with acidic carboxylic groups are used as complexing agents as they typically do not form insoluble products with metal ions, and show different selectivity to the immobilised ligands on the surface of the stationary phase.

Jones and Nesterenko have recently taken a novel approach to predict the selectivity of common metal ions with the addition of various complexing agents to the eluent, by plotting the stability constants of the complexing agents against those of IDA-metal complexes [8]. In this work, the effect of a number of complexing agents on the retention times and retention orders of some common metals on an IDA-silica stationary phase, as shown in Table 1.3. The values for the strongly retained metals, Pb^{2+}, Cu^{2+} and Fe^{3+} particularly high, with Fe^{3+} presenting the biggest issue in terms of prolonged retention times.

The effect of the addition of dipicolinic acid, iminodiacetic acid and sulfosalicylic acid on the retention and separation on seven metal cations using a Diasorb IDA column was compared, with a difference in selectivity observed between the various complexing agents in the mobile phase. These results are shown chromatographically in Fig. 1.15. Dipicolinic acid was shown to have the greatest complexing ability under acidic conditions, and is particularly effective for controlling the retention of Pb^{2+}, where picolinic acid demonstrated a higher selectivity for Cu^{2+}. Other popular complexing agents in HPCIC include EDTA [56], 8-hydroxyquinoline, dicarboxylic acid [92] and oxalic acid [93].

Table 1.3: The effect of addition of different complexing agents on retention (minutes) of metal ions on a Diasorb IDA column [8].

Metal	100 m*M* oxalic acid	Eluent: 15 m*M* HNO_3/0.5 *M* KNO_3 with different complexing additives					
		No complexing agent	1 m*M* 5-sulfosalicylic acid	0.5 m*M* dipicolinic acid	2 m*M* iminodiacetic acid	2 m*M* picolinic acid	4 m*M* picolinic acid
Mn^{2+}	4.08	3.65	3.62	3.61	3.66	3.65	3.63
Co^{2+}	4.29	4.58	4.42	4.37	4.62	4.53	4.43
Cd^{2+}	4.81	5.28	4.57	4.65	5.30	5.35	5.25
Zn^{2+}	4.92	6.13	5.77	5.38	6.23	6.05	5.77
Pb^{2+}	6.34	23.28	20.92	5.07	23.83	24.13	22.18
Ni^{2+}	5.08	No peak	~17.0	14.60	No peak	~10.0	~8.0
Cu^{2+}	24.9	No peak	No peak	17.13	No peak	39.10	19.63
Fe^{3+}	12.01	No peak	No peak	58.20	No peak	No peak	No peak

Note: “No peak” means strongly retained.

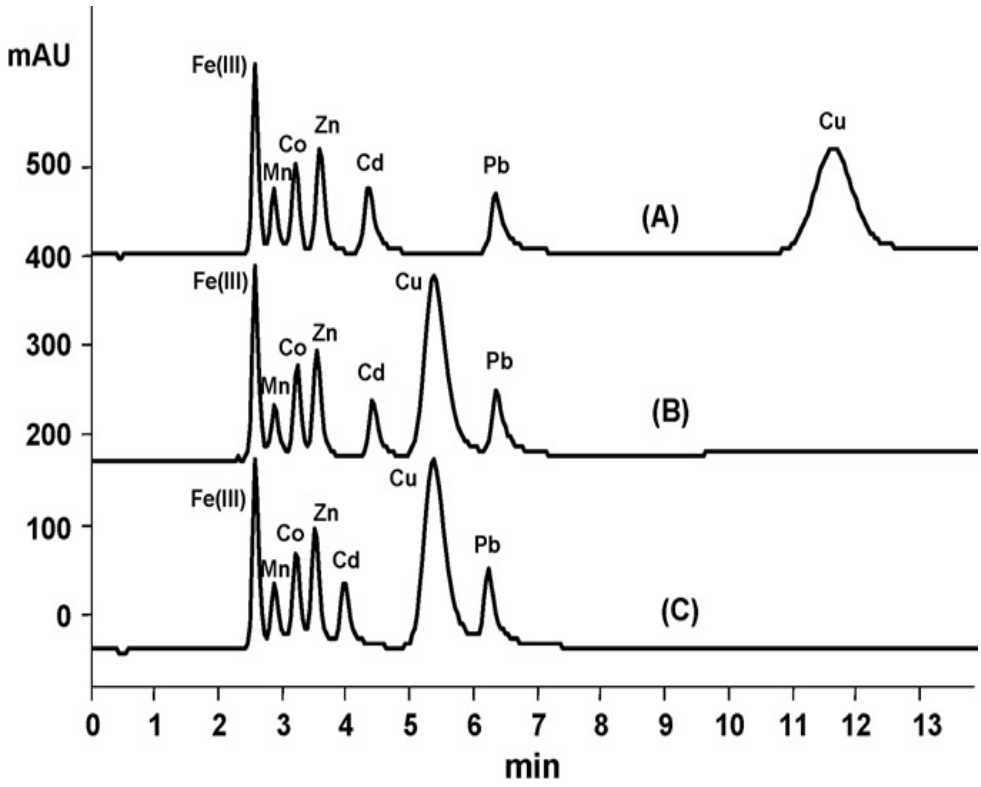

Fig. 1.15: Comparison of a seven metal separations using multicomponent eluents with a 150 mm IDA-silica column. Eluent: (A) 25 m*M* oxalic acid containing 0.5 *M* potassium nitrate, (B) 25 m*M* oxalic acid containing 0.5 *M* potassium nitrate and 2 m*M* picolinic acid, (C) 25 m*M* oxalic acid containing 0.5 *M* potassium nitrate, 2 m*M* picolinic acid and 20 m*M* potassium chloride. All eluents were adjusted to pH 2.40 [8].

1.5 Detection

1.5.1 Post-column reaction for spectrophotometric detection of metal ions

Detection in HPCIC can be problematic, as unlike with gas chromatography, the mobile phase is not inert, and metal species cannot be easily exploited by techniques such as UV-visible absorption [7]. Alkali and alkaline earth metals can be detected by suppressed conductivity detection [94,95]. However, this technique is unsuitable for all other metal species as high ionic strength eluents commonly used for HPCIC cannot be used, and hydrolysis and precipitation can occur. One approach that can be employed is post-column reaction, of which a number of reviews detailing its development have been published [96,97].

PCR is used for non- or weakly absorbing analytes, to achieve the lowest possible limit of detection. A reagent is mixed with column effluent at a T or Y junction, which then reacts with the eluted analytes, and a species with a higher molar coefficient is formed. The delivery system can be either a pneumatic or mechanical pump, preferably made of PEEK as metal parts can cause contamination. There are a number of commercially available PCR delivery systems available [98], which are typically equipped with a peristaltic pump, mixing tee and knitted reactor coil.

1.5.2 Post-column reagents

The choice of post-column reagent depends on the analyte of interest. The reagent of choice has a number of requirements, most importantly it must be water soluble, fast reacting and produce complexes with high molar absorptivities [3]. Fritz *et al.* [99] investigated a wide number of post-column reagents and found that 4-(2-pyridylazo) resorcinol (PAR) reacts with a wide number of metals (> 40), and produces complexes with high molar absorptivities. As a result, PAR is one of the most commonly used PCR reagents, particularly for use with transition metals [15]. However, much of the literature between research groups regarding PAR is contradictory and inaccurate [100]. Furthermore, its sensitivity for alkaline earth metal cations is poor; therefore for the analysis of these metals the addition of zinc ethylenediaminetetraacetate (ZnEDTA) can be used, resulting in enhanced detection due to a displacement reaction between ZnEDTA and the metal ions [7]. Other popular post-column reagents include arsenazo I and III for lanthanides [7], phthalein purple for alkaline earth metals [45], 5-Br-PADAP for transition metals [15] and pyrocatechol violet (PCV) for Al^{3+} [7]. A study was carried out highlighting the differences between detection using PAR and 5-Br-PADAP as post-column reagents [15]. Fig. 1.16 below shows the increased sensitivity for Cu^{2+}, Cd^{2+}, Zn^{2+} and Mn^{2+} with the use of 5-Br-PADAP, and the drastic decrease in sensitivity for Ni^{2+}, Fe^{3+} and Pb^{2+}.

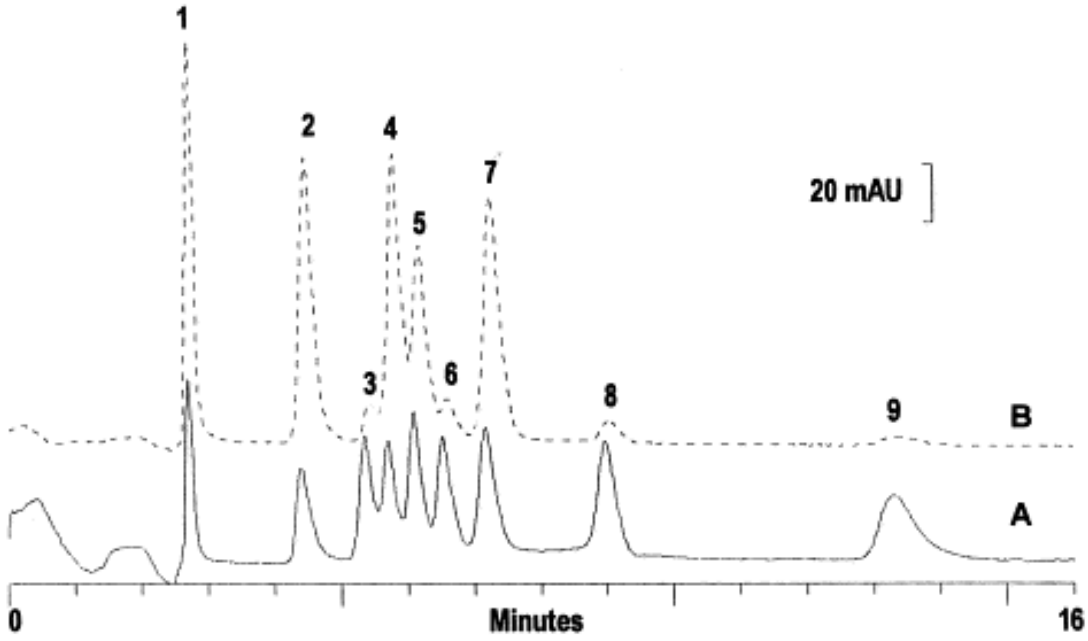

Fig. 1.16: Chromatogram of a standard solution of transition and heavy metals. Eluent: 28 m*M* Oxalic acid/45 m*M* NaCl/265 m*M* $NaNO_3$/40 m*M* HCl, Flow rate: 0.6 mL/min, Post-column reagent: (a) PAR, (b) 5-Br-PADAP, Peaks: 1: 50 µg/L Cu^{2+}, 2: 100 µg/L Cd^{2+}, 3: 50 µg/L Ni^{2+}, 4: 50 µg/L Zn^{2+}, 5: 50 µg/L Co^{2+}, 6: 100 µg/L Fe^{2+}, 7: 50 µg/L Mn^{2+}, 8: 50 µg/L Fe^{3+}, 9: 500 µg/L Pb^{2+} [15].

1.5.3 Noise reduction

Due to the requirement for the determination of metal ions at a very low level, there has been a large amount of work regarding developing methods to reduce baseline noise and drift [23]. This is difficult to achieve as high noise levels are usually present when using detectors with other equipment, particularly a PCR system where the eluents and/or reagents have different absorbances. A number of noise reduction methods have been developed to overcome this problem and reduce signal to noise ratio, such as software and electronic methods. A noise suppression system has been developed using a multiple wavelength approach, where the signals from a multiple wavelength detector are processed, removing the pump noise electronically, with no effect on peak width or symmetry.

1.6 Applications

1.6.1 Application of high performance chelation ion chromatography for the determination of metals in complex samples

HPCIC can be used for a wide variety of applications due to the advantages it provides over standard ion exchange chromatography. These applications include speciation of metals and trace analysis of metals, where both preconcentration and separation can be simultaneously carried out on a chelating column. Due to its insensitivity in samples of high ionic strength such as seawater and brine, HPCIC has received increasing attention in recent years in particular for the determination of trace metals in complex samples [9-12,14-16,101] due its superior selectivity that the selection of chelating ligand gives for a specific group of metals. HPCIC can also be applied to the analysis of biological tissues and fluids, where ion exchange methods are not suitable due to interference from charged biomolecules [3]

For many years, the preferred analytical method to quantify metal ions for these applications has been spectroscopic methods such as a atomic absorption spectroscopy (AAS), atomic emission spectroscopy (AES), inductively-coupled plasma - atomic emission spectroscopy ICP-AES) and inductively-coupled plasma-mass spectroscopy (ICP-MS), which require significant sample dilution, resulting in insufficient sensitivity [102]. Many of these methods also require a large sample volume (≥ 10mL), and furthermore cannot tolerate even minute quantities of salts in matrices such as saline samples. Due to the excellent selectivity that it provides, which can be easily manipulated for the targeted metal ions, HPCIC has proven to be a promising alternative to the aforementioned spectroscopic detection techniques. The low cost and simplicity of HPCIC are also noteworthy advantages. In addition, where analysis must be carried out in the field, the physical dimensions of the instrumentation are important, and many spectroscopic methods are unsuitable. There are a number of publications detailing the applications of HPCIC [102], which highlight its superiority over other popular analytical methods and its ability to cope with samples containing a high level of salt.

Polymer based chelating resins have been used for the analysis of high ionic strength environmental samples such as brines, mineral waters, and seawaters [3], and have been widely used for trace metal concentration and extraction in both environmental and industrial applications [103,104]. A dynamically modified approach was used to determine six transition and heavy metals in a water sample using a PS-DVB column modified with 4-chlorodipicolinic acid (Fig. 1.17) [7]. The use of dynamically modified stationary phases has also been applied for the determination of metals in complex matrices [74].

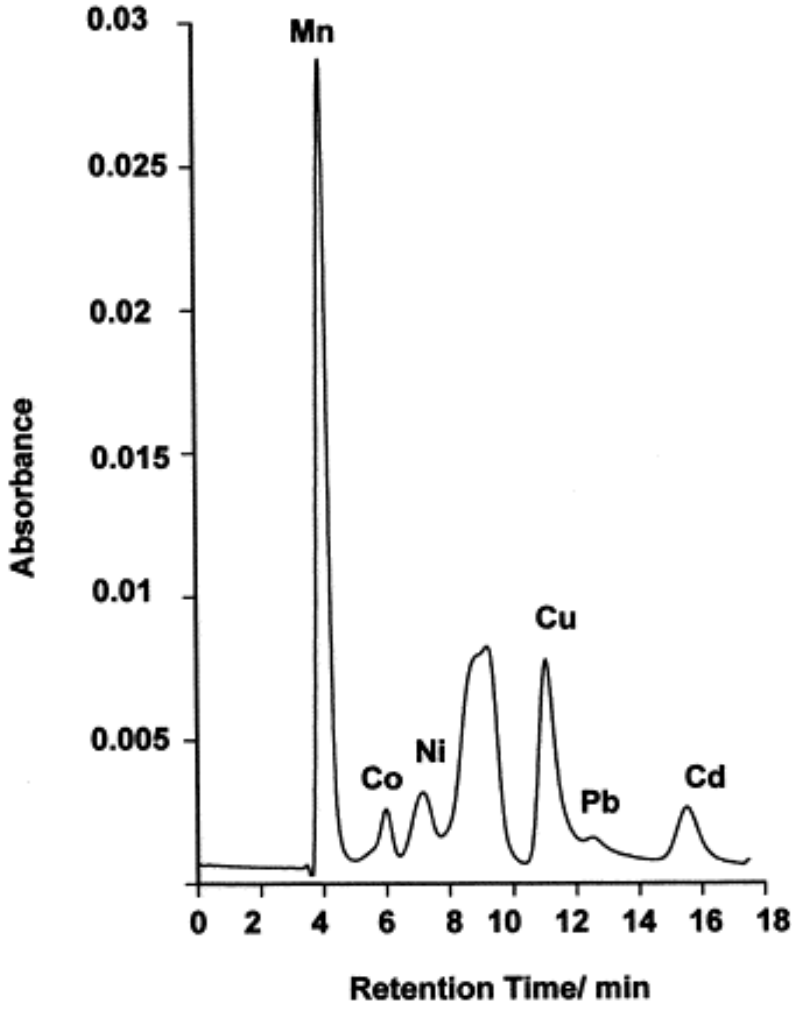

Fig. 1.17: Chromatogram of transition and heavy metal ions in the certified soft water sample TMDA 54.2. Column: 300 × 4.6 mm I.D. PRP-1 7 μm PS–DVB. Eluent: 1 *M* potassium nitrate, 6 m*M* nitric acid and 0.25 m*M* chlorodipicolinic acid. Detection: spectrophotometric at 520 nm after PCR with PAR [7].

High performance chelation ion chromatography has been applied extensively to the simultaneous preconcentration and separation of complex samples. Siriraks *et al*. [12] introduced the use of an on-line chelating IDA mini-column for the separation of transition and heavy metals from alkali and alkaline earth ions. A number of columns were investigated, one of which was a highly crosslinked macroporous PS-DVB iminodiacetate resin. Various pumps, switching valves and eluents were employed to preconcentrate targeted ions and remove interference prior to analysis. The method was then applied to complex samples such as estuarine and seawaters, and oyster tissue. This approach was also applied to the determination of Cu^{2+}, Ni^{2+}, Zn^{2+}, Co^{2+} and Mn^{2+} in seawater [105], Cd^{2+} and Pb^{2+} in seawater [106], Cd^{2+}, Co^{2+}, Cu^{2+}, Fe^{2+}, Mn^{2+}, Ni^{2+} and Zn^{2+} in coral skeletons [9], river and mineral waters [107] and sewage waste waters [15].

Murgia *et al.* [10] determined trace transition metals at low detection limits in environmental samples in 15 minutes using a bi-functional quaternary ammonium-sulfonate chelating column. The developed method utilised a 250 x 4.0 mm I.D. IonPac CS5A column and was applied to the determination of Fe^{3+}, Mn^{2+}, Cu^{2+}, Cd^{2+}, Co^{2+}, Zn^{2+} and Ni^{2+} in polluted soil and water samples. This method allowed direct injection of the soil sample. Also employing a bi-functional chelating stationary phase, a number of transition and heavy metals were determined in biological samples [108]. Using a 50 x 4.0 mm I.D. column packed with styrene-based macroporous 12% cross-linked iminodiacetate-functionalised chelating resin, interfering components such as anions and alkali and alkaline earth metals were preconcentrated, and Pb^{2+}, Cu^{2+}, Cd^{2+}, Co^{2+} and Ni^{2+} were successfully separated.

A number of silica based chelating ligands have also been used for the preconcentration of metals [109,110]. Silica bonded IDA has been applied to various analysis of complex samples in HPCIC. Nesterenko and Jones applied an IDA-silica stationary phase to the analysis of trace metals in complex samples on a single chelating column [24]. Using an IDA-bonded Diasorb silica column, (250 x 4.0 mm I.D.), Mn^{2+}, Co^{2+}, Cd^{2+}, Zn^{2+}, Ni^{2+} and Cu^{2+} were preconcentrated and separated from highly saline water using a gradient elution scheme. Aluminium, which has known toxicological effects, was determined in an environmental sample at different pH values [11], using a 200 x 4.0 mm I.D. IDA-silica column. Varying post-column

reagents were investigated, and eriochrome cyanine R (ECR) was selected due the good sensitivity and efficiency it provided (see Fig. 1.18). Speciation capabilities were also reported, demonstrating different selectivity towards non-labile aluminium species.

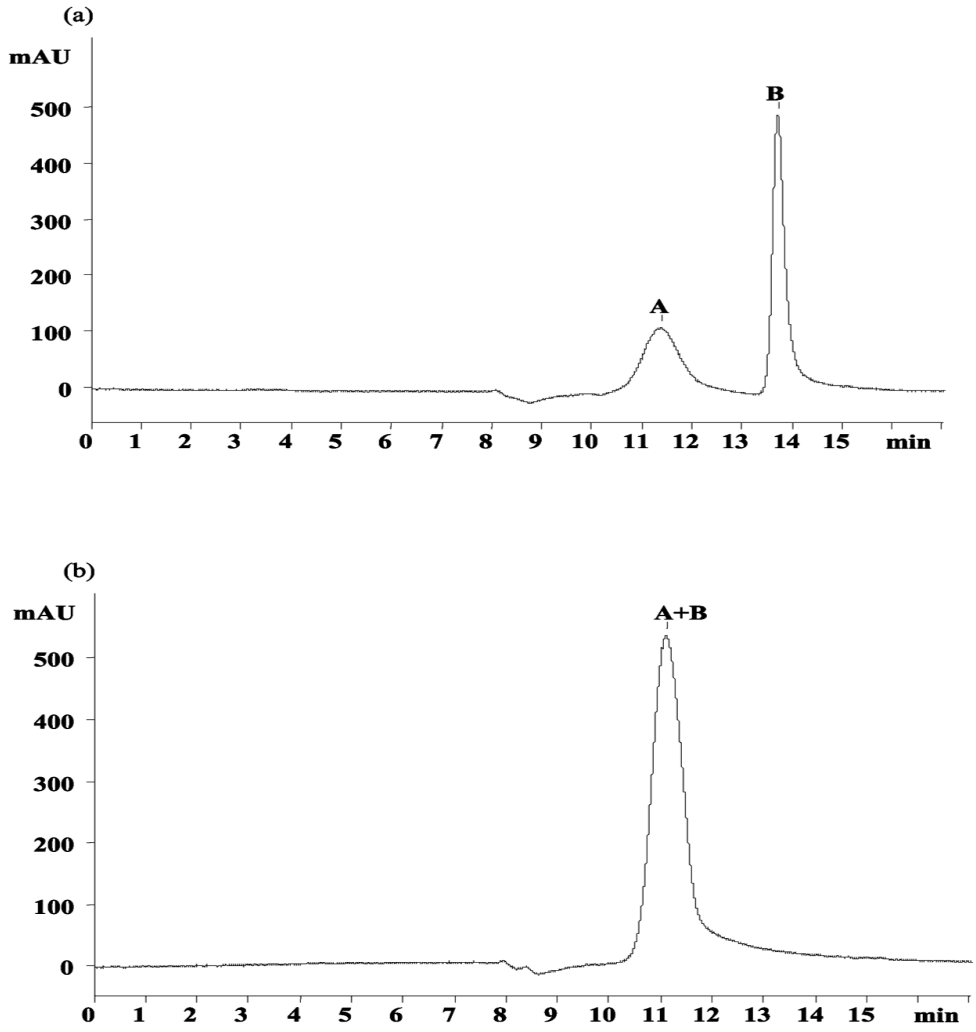

Fig. 1.18: Chromatogram of mill whitewater at pH 4.8 (a) and pH 1.0 (b) on a 200 x 4.0 mm I.D. IDA-silica column using optimised ECR-system (20 µL sample loop). Eluent: 0.25 *M* KCl/40 m*M* HNO_3; Flow rate: 0.3 mL/min; Column temperature: 71 ^{o}C. A + B = Aluminium [11].

Recently Dias *et al.* developed an isocratic separation method on an IDA-silica column for the determination of trace transition metals in fuel ethanol [54]. Optimising the chromatographic method for the effect of DPA concentration, HCl concentration, methanol concentration and column temperature allowed for the separation of 9 metals in ~30 minutes, as seen in Fig. 1.19.

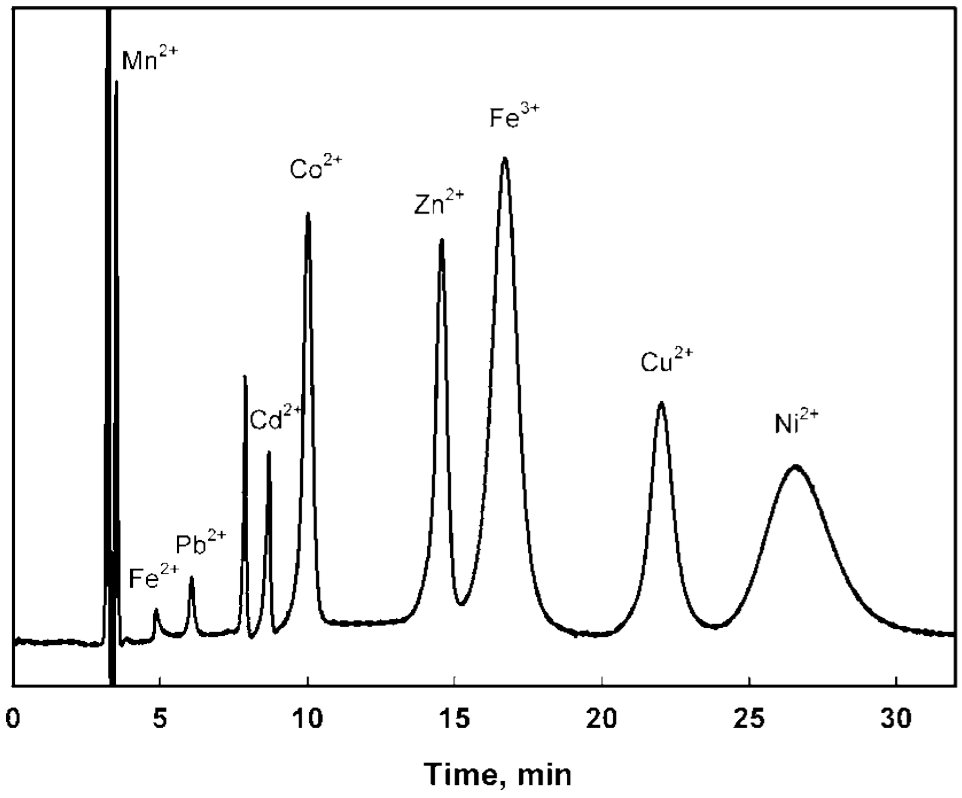

Fig. 1.19: Chromatogram of nine metals under optimised conditions. Eluent: 2.5 m*M* DPA, 10 m*M* HCl and 60% MeOH, Flow rate: 0.5 mL/min. Column temperature: 40 ^{o}C, PCR reagent flow rate at 0.82 mL/min. Multielement standard solution with standard concentrations: 0.25 mg/L Mn^{2+}, 3 mg/L Fe^{2+}, 2 mg/L Pb^{2+}, 1 mg/L Cd^{2+}, 1 mg/L Co^{2+}, 1 mg/L Zn^{2+}, 1 mg/L Fe^{3+}, 2 mg/L Cu^{2+}, 5 mg/L Ni^{2+} [54].

1.7 Project aims

The aim of this project was to develop and characterise novel chelating stationary phases for the determination of metal cations for HPCIC, and explore the possibility of these phases for the analysis of complex samples, providing a more efficient and cheaper analytical method than commonly used spectroscopic techniques. Firstly, polymer and silica based columns with IDA functionalities would be examined, and the possibility of a reagent free system for HPCIC explored. The aim was also to investigate various chelating ligands, column morphologies and detection methods. The stationary phases included silica monoliths, which were modified with both HEIDA and *N*-(2-hydroxyethyl)-*N*-(2-[phosphonomethyl)amino]acetic (HEPMA) acid, and an HEIDA modified core-shell column. Chromatographic behaviour of metal ions on each stationary phase including retention, selectivity and efficiency was examined. Following characterisation of the each stationary phase, the separation of a number of metal ions could be achieved, depending on the selectivity of each particular column.

References

[1] H. Small, Ion Chromatography, ed D. Hercules, Plenum Press, N.Y (1989).

[2] P.R. Haddad, P.E. Jackson, Ion Chromatography: Principles and Applications, Elsevier, Amsterdam (1990).

[3] B. Paull, P.N. Nesterenko, P. Jones, High Performance Chelation Ion Chromatography, RSC Chromatography Monographs, Royal Society of Chemistry Publishing, Cambridge, UK (2011).

[4] P. Jones, P.N. Nesterenko, Journal of Chromatography A 789 (1997) 413.

[5] P.N. Nesterenko, O.A. Shpigun, Russian Journal of Coordination Chemistry 28 (2002) 726.

[6] D.C. Harris, Quantitative Chemical Analysis, W. H. Freeman, N.Y (2010).

[7] M.J.M. Shaw, P.P. Jones, P.N.P. Nesterenko, Journal of Chromatography A 953 (2002) 141.

[8] P. Jones, P.N. Nesterenko, Journal of Chromatography A 1213 (2008) 5.

[9] W. Shotyk, I. Immenhauser-Potthast, Journal of Chromatography A 706 (1995) 167.

[10] S.M. Murgia, R. Selvaggi, A. Poletti, Environmental Monitoring and Assessment 174 (2011) 313.

[11] J. Tria, P.R. Haddad, P.N. Nesterenko, Journal of Separation Science 31 (2008) 2231.

[12] A. Siriraks, H.M. Kingston, J.M. Riviello, Analytical Chemistry 62 (1990) 1185.

[13] P.N. Nesterenko, P. Jones, Journal of Chromatography A 804 (1998) 223.

[14] R.M.C. Sutton, S.J. Hill, P. Jones, Journal of Chromatography A 789 (1997) 389.

[15] N. Cardellicchio, S. Cavalli, P. Ragone, J.M. Riviello, Journal of Chromatography A 847 (1999) 251.

[16] J.-C. Hsu, C.-H. Chang, C.Y. Liu, Analytical and Bioanalytical Chemistry 362 (1998) 514.

[17] L. Barron, M. O'Toole, D. Diamond, P.N. Nesterenko, B. Paull, Journal of Chromatography A 1213 (2008) 31.

[18] Y. Kholin, V. Zaitsev, Pure and Applied Chemistry 80 (2008) 1561.

[19] W. Bashir, B. Paull, Journal of Chromatography A 907 (2001) 191.

[20] M.G. Kolpachnikova, N.A. Penner, P.N. Nesterenko, Journal of Chromatography A 826 (1998) 15.

[21] A.I. Elefterov, M.G. Kolpachnikova, P.N. Nesterenko, O.A. Shpigun, Journal of Chromatography A 769 (1997) 179.

[22] A.R. Timerbaev, G.K. Bonn, Journal of Chromatography A 640 (1993) 195.

[23] P.N. Nesterenko, P. Jones, Journal of Separation Science 30 (2007) 1773.

[24] P.N. Nesterenko, P. Jones, Journal of Chromatography A 770 (1997) 129.

[25] G. Bonn, S. Reiffenstuhl, P. Jandik, Journal of Chromatography A 499 (1990) 669.

[26] A. Werner, Zeitschrift für Anorganische und Allgemeine Chemie 3 (1893) 267.

[27] P. Jones, G. Schwedt, Journal of Chromatography A 482 (1989) 325.

[28] W. Bashir, B. Paull, Journal of Chromatography A 942 (2002) 73.

[29] S.H. Chang, K.M. Gooding, F.E. Regnier, Journal of Chromatography A 120 (1976) 321.

[30] J.N. King, J.S. Fritz, Journal of Chromatography A 153 (1978) 507.

[31] C. Pohllandt, J.S. Fritz, Journal of Chromatography A 176 (1979) 189.

[32] R.J. Phillips, J.S. Fritz, Analytica Chimica Acta 139 (1982) 237.

[33] R.J. Phillips, J.S. Fritz, Analytica Chimica Acta 121 (1980) 225.

[34] R.J. Phillips, J.S. Fritz, Analytical Chemistry 50 (1978) 1504.

[35] E.M. Moyers, J.S. Fritz, Analytical Chemistry 49 (1977) 418.

[36] H. Kumagai, T. Yokoyama, T.M. Suzuki, T. Suzuki, Analyst 124 (1999) 1595.

[37] Y. Inoue, H. Kumagai, Y. Shimomura, T. Yokoyama, T.M. Suzuki, Analytical Chemistry 68 (1996) 1517.

[38] H. Kumagai, Y. Inoue, T. Yokoyama, T.M. Suzuki, T. Suzuki, Analytical Chemistry 70 (1998) 4070.

[39] J. Scancar, R. Milacic, Trends in Analytical Chemistry 28 (2009) 9.

[40] A. Jungbauer, R. Hahn, Journal of Chromatography A 1184 (2008) 62.

[41] M. Barut, A. Podgornik, L. Urbas, B. Gabor, P. Brne, J. Vidic, S. Plevcak, A. Strancar, Journal of Separation Science 31 (2008) 1867.

[42] E.G. Vlakh, G.A. Platonova, G.P. Vlasov, C. Kasper, A. Tappe, G. Kretzmer, T.B. Tennikova, Journal of Chromatography A 992 (2003) 109.

[43] T. Ikegami, H. Fujita, K. Horie, K. Hosoya, N. Tanaka, Analytical and Bioanalytical Chemistry 386 (2006) 578.

[44] F. Svec, T.B. Tennikova, Z. Deyl, Journal of Chromatography Library, Elsevier 67 (2003) 395.

[45] E. Sugrue, P. Nesterenko, B. Paull, Journal of Separation Science 27 (2004) 921.

[46] Á. Moyna, D. Connolly, E. Nesterenko, P.N. Nesterenko, B. Paull, Journal of Chromatography A 1249 (2012) 155.

[47] Á. Moyna, D. Connolly, E. Nesterenko, P.N. Nesterenko, B. Paull, Analytical and Bioanalytical Chemistry 405 (2012) 2207.

[48] P.N. Nesterenko, M.J. Shaw, S.J. Hill, P. Jones, Microchemical Journal 62 (1999) 58.

[49] H.H. Weetall, Biochimica et Biophysica Acta 212 (1970) 1.

[50] F.B. Anspach, Journal of Chromatography A 676 (1994) 249.

[51] G. Gübitz, S. Mihellyes, Chromatographia 19 (1984) 257.

[52] W. Bashir, B. Paull, Journal of Chromatography A 910 (2001) 301.

[53] B.B. Paull, W.W. Bashir, Analyst 128 (2003) 335.

[54] J.C. Dias, L.T. Kubota, P.N. Nesterenko, G.W. Dicinoski, P.R. Haddad, Analytical Methods 2 (2010) 1565.

[55] P.N. Nesterenko, P. Jones, Analytical Communications 34 (1997) 7.

[56] G.J. Sevenich, J.S. Fritz, Analytical Chemistry 55 (1983) 12.

[57] S. Elchuk, R.M. Cassidy, Analytical Chemistry 51 (1979) 1434.

[58] C.H. Knight, R.M. Cassidy, B.M. Recoskie, L.W. Green, Analytical Chemistry 56 (1984) 474.

[59] T.A. Walker, Journal of Liquid Chromatography 16 (1993) 1573.

[60] L. Trojer, G. Stecher, I. Feuerstein, S. Lubbad, G.K. Bonn, Journal of Chromatography A 1079 (2005) 197.

[61] P.N. Nesterenko, A.V. Ivanov, N.A. Galeva, Journal of Analytical Chemistry 52 (1997) 736.

[62] P.N. Nesterenko, M.J. Shaw, S.J. Hill, P. Jones, Microchemical Journal 62 (1999) 12.

[63] Q. Xu, K. Tanaka, M. Mori, M.I. Helaleh, H. Toada, W. Hu, K. Hasebe, Chromatographia 57 (2003) 19.

[64] Q. Xu, K. Tanaka, M. Mori, M.I.H. Helaleh, W. Hu, K. Hasebe, H. Toada,

Journal of Chromatography A 997 (2003) 183.

[65] Q. Xu, M. Mori, K. Tanaka, M. Ikedo, W. Hu, Journal of Chromatography A 1026 (2004) 191.

[66] W. Hu, A. Iles, K. Hasebe, H. Matsukami, S. Cao, K. Tanaka, Analytical and Bioanalytical Chemistry 370 (2001) 48.

[67] W. Hu, K. Hasebe, A. Iles, K. Tanaka, Analyst 126 (2001) 821.

[68] E. Sugrue, P.N. Nesterenko, B. Paull, Journal of Chromatography A 1075 (2005) 9.

[69] E. Sugrue, P. Nesterenko, B. Paull, Analytica Chimica Acta 553 (2005) 9.

[70] E. Sugrue, P. Nesterenko, B. Paull, Analyst 128 (2003) 417.

[71] B. Paull, P. Nesterenko, P.R. Haddad, Analytica Chimica Acta 375 (1998) 117.

[72] B. Paull, P.R. Haddad, Trends in Analytical Chemistry 18 (1999) 107.

[73] S. Yamazaki, H. Omori, C.E. Oh, Journal of High Resolution Chromatography & Chromatography Communications 9 (1986) 765.

[74] B. Paull, M. Foulkes, P. Jones, Analyst 119 (1994) 937.

[75] B. Paull, M. Foulkes, P. Jones, Analytical Proceedings including Analytical Communications 31 (1994) 209.

[76] P. Jones, M. Foulkes, B. Paull, Journal of Chromatography A 673 (1994) 173.

[77] O.J. Challenger, S.J. Hill, P. Jones, Journal of Chromatography A 639 (1993) 197.

[78] A. Hrdlička, J. Havel, M. Valiente, Journal of High Resolution Chromatography 15 (1992) 423.

[79] B. Paull, M. Clow, P.R. Haddad, Journal of Chromatography A 804 (1998) 95.

[80] M.J. Shaw, S.J. Hill, P. Jones, P.N. Nesterenko, Chromatographia 51 (2000) 695.

[81] W.W. Bashir, E.E. Tyrrell, O.O. Feeney, B.B. Paull, Journal of Chromatography A 964 (2002) 113.

[82] J. Chong, P. Hatsis, C.A. Lucy, Journal of Chromatography A 997 (2003) 161.

[83] P. Hatsis, C.A. Lucy, Analyst 126 (2001) 2113.

[84] M.A. Rey, C.A. Pohl, Journal of Chromatography A 739 (1996) 87.

[85] M.J. Shaw, P.N. Nesterenko, G.W. Dicinoski, P.R. Haddad, Journal of Chromatography A 997 (2003) 3.

[86] M.G. Kolpachnikova, N.A. Penner, P.N.Nesterenko, Journal of Chromatography A 826 (1998) 15.

[87] A.I. Elefterov, M.G. Kolpachnikova, P.N. Nesterenko, O.A. Shpigun, Journal of Chromatography A 769 (1997) 179.

[88] M.A. Kraus, A. Patchornik, Journal of Polymer Science: Macromolecular Reviews 15 (1980) 55.

[89] T.B. Field, W. McBryde, Canadian Journal of Chemistry 59 (1981) 555.

[90] G. J Sevenich, J.S. Fritz, Journal of Chromatography A 371 (1986) 361.

[91] P. Janoš, Journal of Chromatography A 699 (1995) 1.

[92] E.E. Santoyo, S.S. Santoyo-Gutiérrez, S.P.S. Verma, Journal of Chromatography A 884 (2000) 229.

[93] P. Nesterenko, P. Jones, Journal of Liquid Chromatography & Related Technologies 19 (1996) 1033.

[94] W.W. Buchberger, P.R. Haddad, Journal of Chromatography A 789 (1997) 67.

[95] W.W. Buchberger, Trends in Analytical Chemistry 20 (2001) 296.

[96] P.K. Dasgupta, Journal of Chromatographic Science 27 (1989) 422.

[97] I.S. Krull, Chromatography and Separation Chemistry: Recent Advances in New and Potentially Novel Detectors in High-Performance Liquid Chromatography and Flow Injection Analysis, Chapter 9, American Chemical Society, Washington, DC (2009) 137.

[98] R. Weinberger, R.A. Femia, Journal of Chromatography Library, Elsevier (1988) 395.

[99] J.S. Fritz, J.N. Story, Analytical Chemistry 46 (1974) 825.

[100] J. Dugay, A. Jardy, M. Doury-Berthod, Analusis 23 (1995) 196.

[101] C.Y. Liu, N. Lee, T.H. Wang, Analytica Chimica Acta 337 (1997) 173.

[102] M.J.M. Shaw, P.R.P. Haddad, Environment International 30 (2004) 29.

[103] V.D. Kopylova, Solvent Extraction and Ion Exchange 16 (1998) 267.

[104] S.K. Sahni, J. Reedijk, Coordination Chemistry Reviews 59 (1984) 1.

[105] R. Caprioli, S. Torcini, Journal of Chromatography A 640 (1993) 365.

[106] N. Cardellicchio, S. Cavalli, J.M. Riviello, Journal of Chromatography A 640 (1993) 207.

[107] S. Motellier, H. Pitsch, Journal of Chromatography A 739 (1996) 119.

[108] H. Lu, X. Yin, S. Mou, J.M. Riviello, Journal of Liquid Chromatography & Related Technologies 23 (2000) 2033.

[109] J.F. Biernat, P. Konieczka, B.J. Tarbet, J.S. Bradshaw, R.M. Izatt, Separation & Purification Reviews 23 (1994) 77.

[110] P.K. Jal, S. Patel, B.K. Mishra, Talanta 62 (2004) 1005.

2. The separation of metal cations using iminodiacetic acid functionalised silica and polymer chelating stationary phases and electrolytically generated eluent

Abstract

Silica based chelating stationary phases have become increasingly popular in recent years, in some regards disproving the idea that the previously dominant polymeric chelating phases display better hydrolytic stability. This is especially true of iminodiacetic acid (IDA) modified silica phases, as this class of chelating ion exchanger has been well characterised and proved to demonstrate excellent selectivity towards metal cations. Here, the selectivity of IDA bonded polymer and silica based stationary phases (poly-IDA and HEIDA-silica) has been evaluated and compared using high performance chelation ion chromatography for a number of metal cations. The retention of a range of alkali, alkaline earth, transition and lanthanide metals was observed, and a number of gradient methods were developed in order to achieve the simultaneous separation of a range of cations. For the first time, electrolytically generated methanesulfonic acid (MSA) as an eluent was utilised in conjunction with chelating stationary phases. Suppressed conductivity detection was used to detect a number of the selected lanthanides with further detection carried out by UV-Vis detection after post-column reaction (PCR). A clear difference in selectivity was observed between the two columns, suggesting that the method of attachment of the ligand has a significant effect. The efficiency of the columns was also compared, where *N*/m values obtained for the HEIDA-silica phase far exceeded those for the poly-IDA phase. Finally, although a reagent free chelation chromatography system was successfully applied to HPCIC, it was inferior to the routinely used method of PCR.

Aims

The overall aim of this work presented herein was to compare the selectivity, retention and efficiency of silica-HEIDA and poly-IDA stationary phases, employing reagent-free ion chromatography for the determination of selected alkali, alkaline earth, transition and lanthanide metal cations.

2.1 Introduction

2.1.1 Overview of high performance chelation ion chromatography

High performance chelation ion chromatography is an increasingly popular chromatographic approach for the separation and detection of metal cations due to the selectivity it provides over other popular methods such as standard ion exchange chromatography. Its ability to handle high ionic strength samples is also advantageous over common spectroscopic methods such as ICP-AES and AAS, which often require significant sample preconcentration and/or dilution [1]. As discussed in Sections 1.3.2.1 and 1.3.2.2, the negatively charged chelating ligand IDA (see Fig. 2.1 (a)) is a popular and well-characterised ligand used for the determination of metal cations in HPCIC due to the unique selectivity it provides, particularly towards transition metals [2].

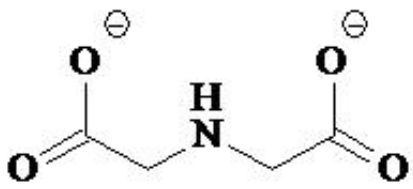

Fig. 2.1 (a) Structure of iminodiacetic acid.

Iminodiacetic acid, which is also a weak cation exchanger, displays sufficiently fast kinetics of complexation with metal ions to provide relatively good separation efficiencies [3] and has been used with a number of polymer and silica based stationary phases for the determination of metal cations.

However, recently [4,5] it was shown that the approach used for the introduction of IDA moieties on the surface significantly affects selectivity. It was also shown that the final functionality, obtained via epoxysilane chemistry is not simply IDA, but indeed hydroxyethyliminodiacetic acid (HEIDA), the structure of which is shown in Fig. 2.1 (b).

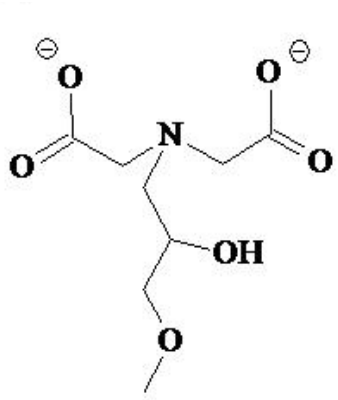

Fig. 2.1 (b) Structure of hydroxyethyliminodiacetic acid.

2.1.2 Electrolytically regenerated eluent for ion chromatography

"Reagent-free" ion chromatography with eluent regeneration (RFIC-ER) is a popular technique for anion and cation analysis [6]. It provides many advantages over standard IC, including reduced labour time and eluent waste, improved reliability and reproducibility of the eluent concentration, and because of the closed loop, the system remains equilibrated.

Eluent generation is a process whereby a precisely controlled current is applied to electrodes positioned within an ion exchange membrane, with electrolysis of water occurs as a result. Hydroxide (for cations) and hydronium (for anions) ions are generated at the cathode and anode respectively. The species does not recombine into

water due to the ion exchange membrane, and the eluent (in this case MSA for the detection of cations) is formed when a counter ion migrates across the membrane. Eluent concentration can be varied by changing the current applied to the electrodes. Electrolytically generated MSA is commonly used for the separation of cations [7]. Suppressed eluent is passed through an analyte trap column after detection, removing any remaining ions, and is then returned to the suppressor to be re-used for the electrolytical generation of eluent [6]. This effluent is passed through a catalytic column to recombine H_2 and O_2 gases, and water is formed and returns to the eluent reservoir. The use of an analyte trap column helps the removal of all cationic contaminants in the eluent, and provides very low baseline drift during gradient separations. Fig. 2.2 demonstrates a typical eluent generation system.

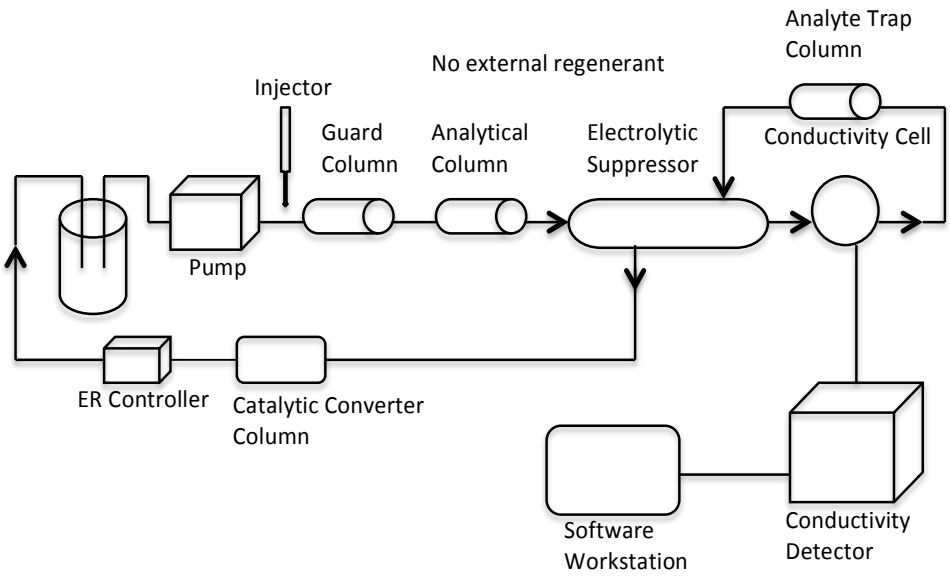

Fig. 2.2: Schematic of a typical eluent regeneration system.

2.1.3 Suppressed conductivity detection

As discussed in Section 1.6.1, detection of metal ions using HPCIC is typically carried out with the use of PCR, where weakly absorbing analytes are converted into coloured complexes and the monitoring wavelength is in the visible region [8]. The detection of alkali and alkaline earth metals are one exception, where suppressed conductivity is a possible method of detection as hydrolysis and precipitation does not present a problem in the way it does for many other non absorbing cations [9,10]. Suppressed conductivity detection works by reducing background conductivity of the eluent, by converting the analyte to its free acid/hydroxide form, and increasing the sensitivity of the ion (Fig. 2.3).

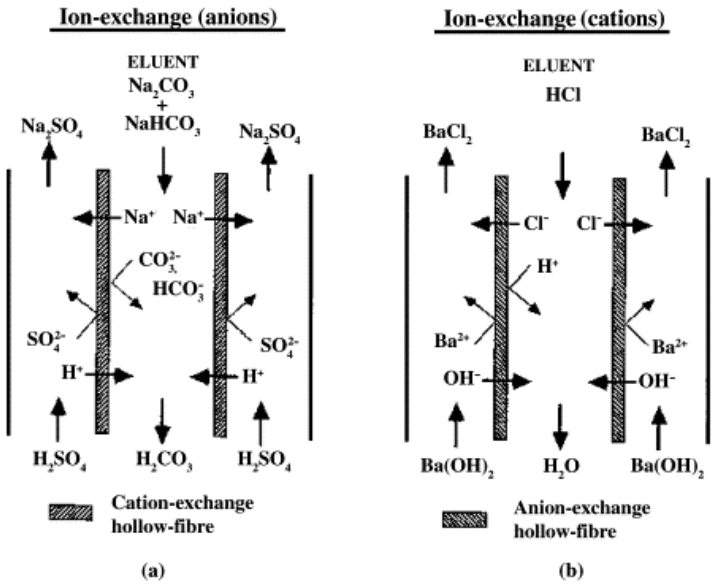

Fig. 2.3: Schematic diagram of suppressed conductivity detection for anion and cations [11].

Suppressed conductivity detection is generally not a popular method of detection for the more strongly retained ions such as transition and rare earth metals in HPCIC, as it does not permit the use of eluents with high ionic strength. In recent years, the determination of lanthanides in various samples has received increasing attention, since they not only commonly occur in nature (except for promethium), but have also been widely used in various areas such as material science, medical diagnostics, or in nuclear reactors, leading to their increased presence in the environment. To date, the use of electrolytically generated eluent with suppressed conductivity for the

determination of transition and lanthanide metal cations for HPCIC has not been achieved. Using an electrolytically generated eluent would remove the need for the presence of high ionic strength salts in the eluent. In the work presented herein, the selectivity of IDA functionalised columns (silica and polymer based), using electrolytically generated MSA as eluent with both suppressed conductivity detection and PCR, was studied and compared. The columns were then used to determine selected alkali, alkaline earth, transition and lanthanide metal cations.

2.2 Experimental

2.2.1 Instrumentation

For all chromatographic separations, a Dionex ICS-3000 chromatography system (Sunnyvale, CA, USA) was used. Chromeleon 6.8 software was employed for all data acquisition and analysis. This chromatographic system was comprised of a DP (dual pump) for delivery of eluent, EG (eluent generator) for delivery of electrolytically generated MSA, DC (detector compartment) and AS (autosampler). The system included a PEEK sample loop of desired sample injection volume (μL). For 2-D separations, a switching valve was used with the sample loop to "cut" a fraction of the sample and transfer it from the first dimension to the second. For the use of electrolytically generated MSA as eluent, a Dionex conductivity detector cell and Continuously Regenerated Cation Trap Column (CR-CTC) were used. For suppressed conductivity detection of metal cations, a Cation Self-Regenerating Suppressor (CSRS 300 (4 mm)) was used. Where this mode of detection was not sufficient, spectrophotometric detection with a VWD UV-Vis dual wavelength detector at 650 nm with post-column reagent arsenazo III was employed. For spectrophotometric detection of metal cations, post-column reagent (PCR) module Dionex Reagent Delivery Module (RDM) Model RDM-1 (Dionex, Sunnyvale, CA, USA) with a T-piece and mixing coil was used for the delivery of the reagent at the desired flow rate. A high purity nitrogen generator, available on site, was used to supply nitrogen to the RDM.

2.2.2 Reagents

Analytical or higher grade reagents and ultra pure water from a Millipore Milli-Q Water system (Millipore, Bedford, MA, USA) were used for the preparation of all solutions. The MSA cartridge for eluent generation was obtained from Dionex (Sunnyvale, CA, USA). Post-column reagent arsenazo III and acetic acid were purchased from Sigma Aldrich (Dublin, Ireland). For cationic analytes, the chloride or nitrate salts of each metal cation were supplied by Sigma Aldrich (Dublin, Ireland) (Na^{2+}, Cs^{2+}, K^{2+}, Li^{2+}, Ca^{2+}, Sr^{2+}, Mg^{2+}, Ag^{2+}, NH_4^+) and BDH (Poole, UK) (Ba^{2+}, Mn^{2+}, Co^{2+}, Cd^{2+}, Zn^{2+}, Ni^{2+}), and prepared in acidified (5% (v/v)) Milli-Q water with concentrations 100 m*M*. 1.00 g/L rare earth element standards (La^{3+}, Y^{3+}, Ce^{3+}, Pr^{3+}, Nd^{3+}, Tm^{3+}, Er^{3+}, Ho^{3+}, Gd^{3+}, Dy^{3+}, Tb^{3+}, Yb^{3+}, Sm^{3+}, Eu^{3+} and Lu^{3+}) were obtained from Johnson Mattey (Karlsruhe, Germany) and were diluted to working concentrations. All working metal cation standard solutions were prepared from stock standard solutions in acidified (5% (v/v)) Milli-Q water on the day of use unless stated otherwise, and stored in polypropylene bottles.

2.2.3 Chromatographic columns

For the comparison of polymeric and silica based IDA stationary phases, two columns were used. A 150 x 4.0 mm I.D., 5 μm silica Nucleosil 100-5 column of surface area 350 m^2/g (Machery-Nagel, Germany) which was covalently functionalised with *N*-hydroxyethyliminodiacetic acid groups (further referred to as HEIDA-silica), and a commercially available Dionex Propac IMAC, 250 x 4.6 mm I.D., nonporous column packed with 10 μm poly-IDA beads (Sunnyvale, CA, USA) were used (further referred to as poly-IDA as labeled by Dionex [12]). The metal ion capacity of the ProPac IMAC resin is about 80 μmol Cu^{2+} per 250 × 4.0 mm I.D. column [12]. This column is typically used for the separation of proteins for IMAC, and the selectivity and retention of transition metals on a short (50 x 2.0 mm I.D.) ProPac column has been investigated by Barron *et al* [2].

For the 2-D cation separation, the aforementioned HEIDA-silica column was used on the first dimension to separate the rare earth metals La^{3+} and Y^{+}, and a Dionex IonPac CS12A (50 x 4.0 mm I.D., 8 μm) medium-capacity, carboxylate-functionalised cation-exchange column (Sunnyvale, CA, USA) which is commonly used for the separation of selected mono- and divalent metal cations was used on the second dimension for the separation of alkali metal cations Na^{+} and K^{+}.

2.3 Results and discussion

2.3.1 Separation of metal cations on HEIDA-silica and Poly-IDA stationary phases with electrolytically generated methanesulfonic acid and suppressed conductivity detection

For a number of years, polymeric stationary phases covalently functionalised with chelating groups have been explored for both low and high pressure chelation chromatography [13,14]. Silica based chelating stationary phases have also become increasingly popular in recent years [3,15] due to common advantages over polymer phases (highlighted in Section 1.3.2.2), including higher peak efficiencies, and resistance to shrinking or swelling in eluents containing high solvent concentrations or high ionic strength [16]. Thus, it would seem interesting to compare IDA based chelation ion exchangers prepared from either silica or polymer substrates, to evaluate which would be more suitable for the analysis of particular groups of metal cations.

Herein, the separation and detection of metal cations on chelating stationary phases using electrolytically generated MSA as eluent, of which there has been no reported instance to date, has been studied. To evaluate the differences in retention and selectivity between the Poly-IDA and a HEIDA-silica stationary phase, the retention of various metal cations was studied on both columns at different concentrations of MSA. The concentration of electrolytically generated MSA was varied, but all other chromatographic conditions (flow rate, column temperature, injection volume) were kept constant.

The stability constants for IDA-metal complexes with alkaline earth and transition metals are not excessively high (Table 2.1), meaning relatively weak eluents can be used for the separation of these groups of metals.

Table 2.1: Stability constants of complexes of alkaline earth and transition earth metal cations with IDA (25 °C, ionic strength 0.1).

Cation	$\log \beta_1$ Iminodiacetic acid
Ba^{3+}	5.88
Sr^{3+}	6.18
Ca^{3+}	6.44
Mg^{3+}	6.50
Mn^{3+}	6.64
Cd^{3+}	6.68
Co^{3+}	6.73
Zn^{3+}	6.78

2.3.1.1 Alkali, alkaline earth and transition metal cations

With regard to the separation of alkali metals, there was no retention on the Poly-IDA phase, even at low (1 m*M*) concentrations of MSA (Fig. 2.4), whereas on the HEIDA-silica phase, very weak retention was observed, although full resolution of Li^+ and Na^+ could not be achieved (Fig. 2.5). For the alkaline earth metals, on the Poly-IDA column, Mg^{2+}, Ca^{2+} and Ba^{2+} were successfully separated in under 8 minutes at low MSA concentration (1 m*M*) (Fig. 2.6). On the HEIDA-silica column at a concentration of 5 m*M* MSA resolution of Mg^{2+}, Ca^{2+} and Ba^{2+} was achieved. However, peak fronting occurred (Fig. 2.7). Poor retention of alkali and alkaline-earth metal cations on the Poly-IDA column under what are clearly predominantly ion-exchange conditions using only an acidic eluent was due to the much lower ion-exchange capacity of the Poly-IDA column, compared to HEIDA-silica (80 μmol Cu^{2+} per 250 × 4.0 mm I.D. column compared to 450 μmol Zn^{2+} per 250 × 4.0 mm

I.D. column [8]. Neither phase provided the resolution of Ca^{2+} and Sr^{2+}, even at lower eluent concentrations due to the similar complexes that the two metals form with IDA, resulting from the similar stability constants (2.23 for Sr^{2+} and 2.60 for Ca^{2+}, albeit with ionic strength 0.1 [8]).

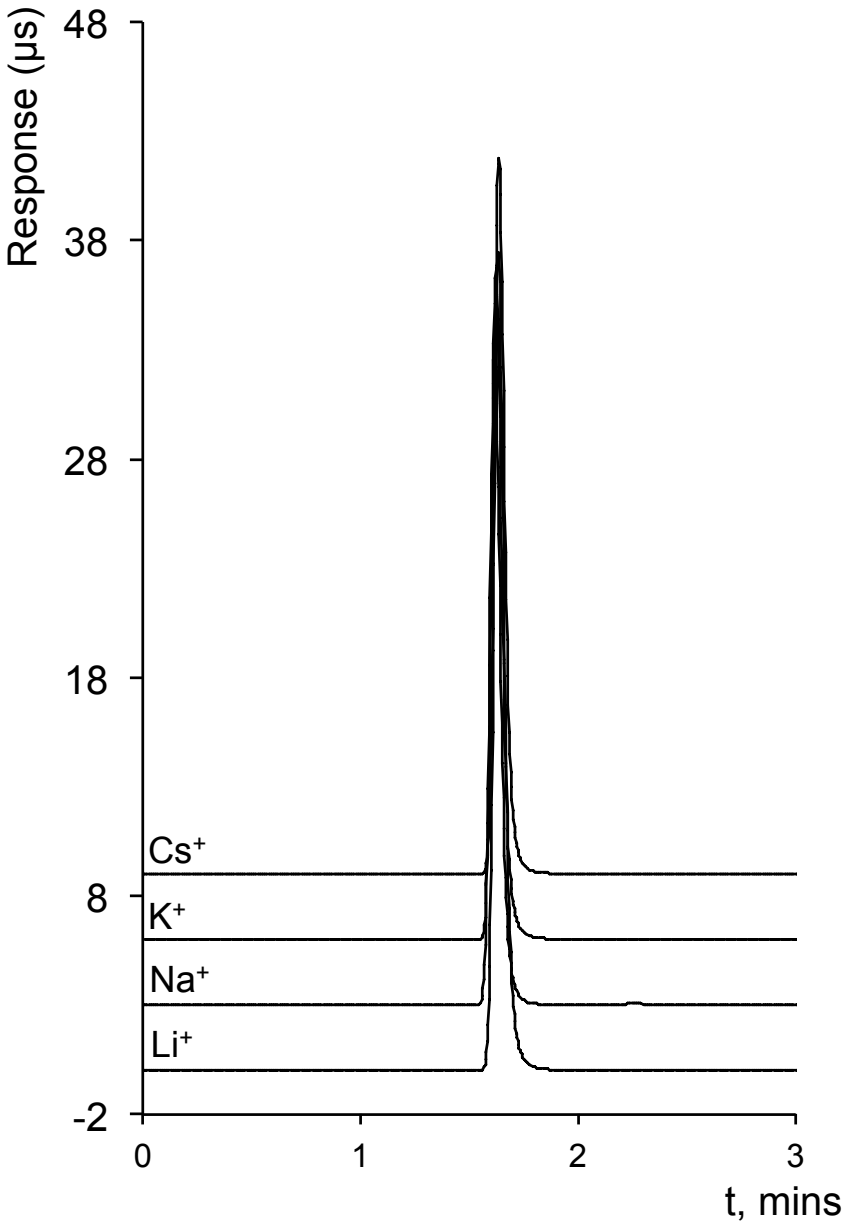

Fig. 2.4: Chromatographic overlay of 1 m*M* Li^+, Na^+, K^+ and Cs^+ on Poly-IDA column. Eluent: 1 m*M* electrolytically generated MSA with DW, Flow rate: 1.0 mL/min, Column temperature: 25 ^oC, Injection volume: 20 µL. Method of detection: suppressed conductivity.

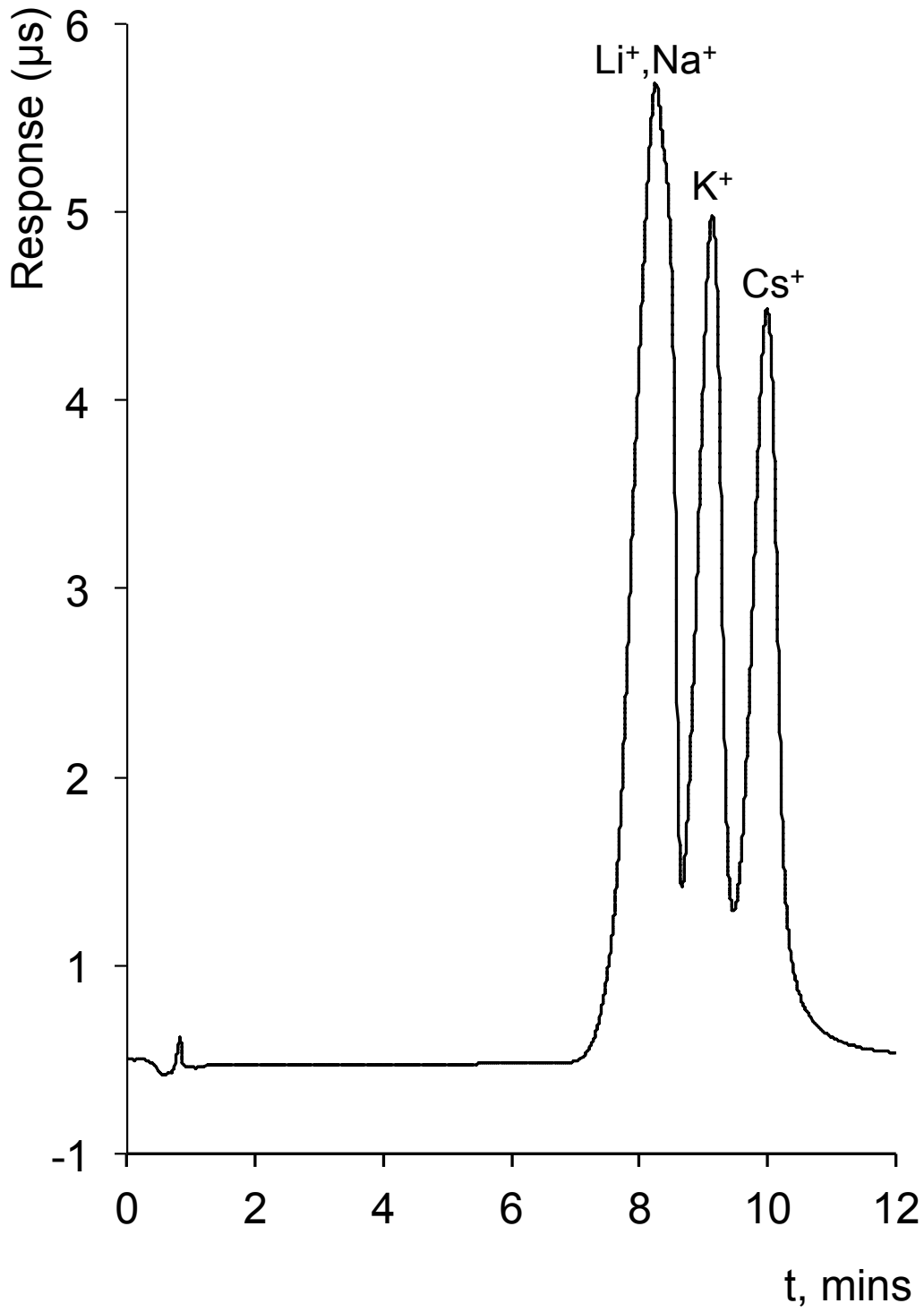

Fig. 2.5: Isocratic separation of 1 m*M* Li^+, Na^+, K^+ and Cs^+ on HEIDA-silica column. Eluent: 1 m*M* electrolytically generated MSA with DW, Flow rate: 1.0 mL/min, Column temperature: 25 ^oC, Injection volume: 20 µL. Method of detection: suppressed conductivity.

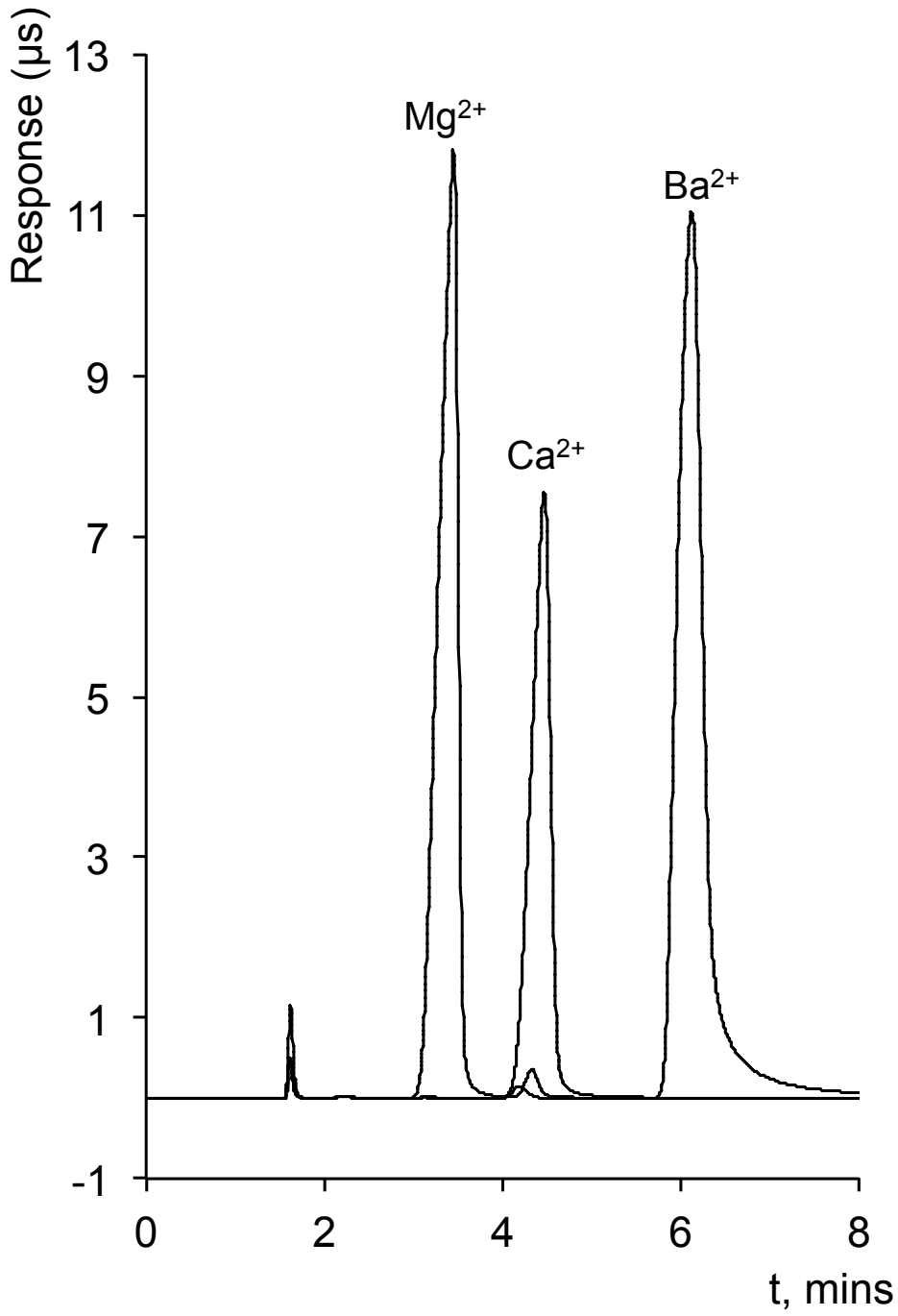

Fig. 2.6: Isocratic separation of 1 m*M* Mg^{2+}, Ca^{2+}, and Ba^{2+} on Poly-IDA column. Eluent: 1 m*M* electrolytically generated MSA with DW, Flow rate: 1.0 mL/min, Column temperature: 25 ^{o}C, Injection volume: 20 µL. Method of detection: suppressed conductivity.

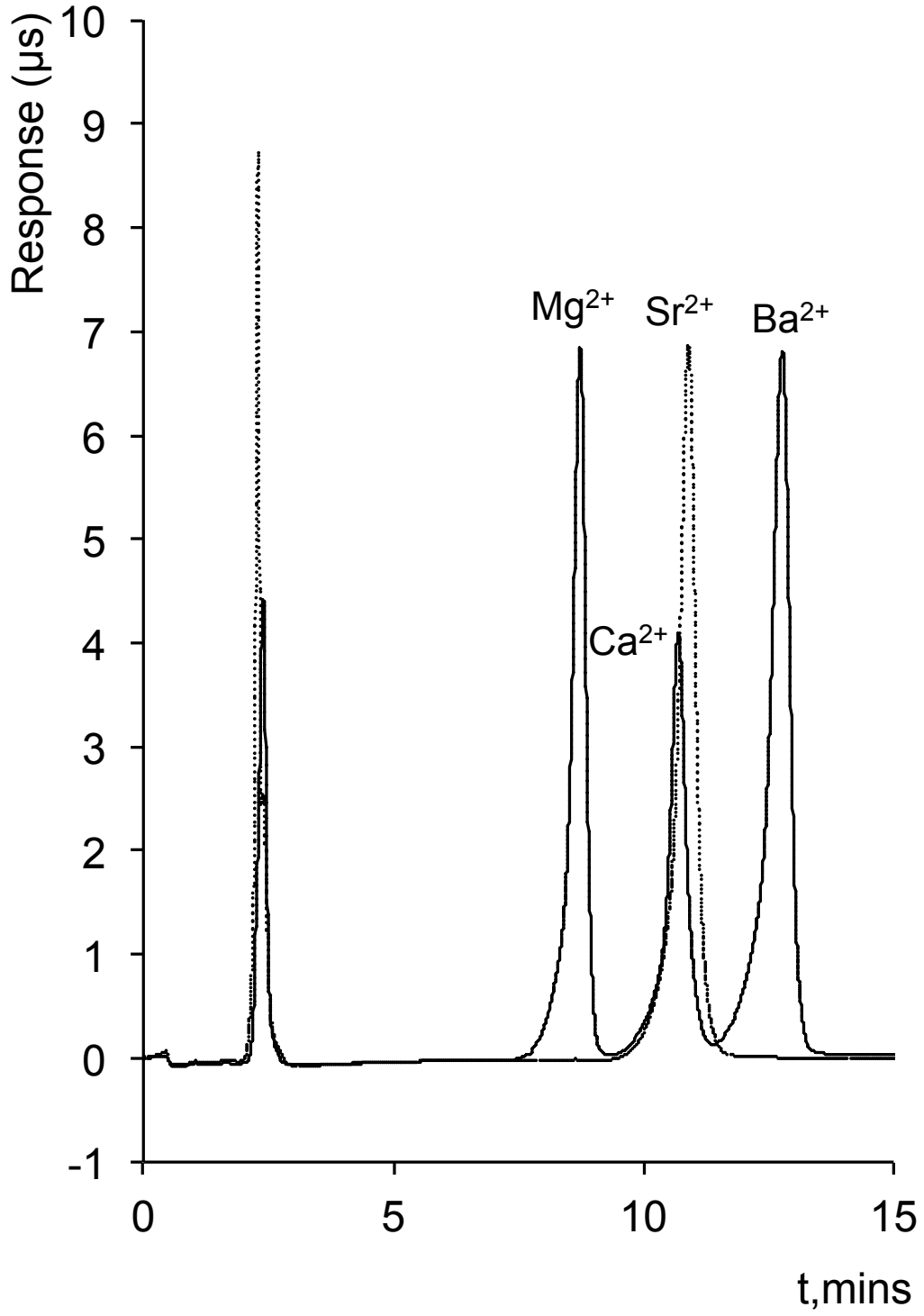

Fig. 2.7: Isocratic separation of 1 m*M* Mg^{2+}, Ca^{2+} and Ba^{2+} on HEIDA-silica column. Eluent: 5 m*M* electrolytically generated MSA with DW, Flow rate: 1.0 mL/min, Column temperature: 25 ^{o}C, Injection volume: 20 µL. Method of detection: suppressed conductivity.

The study of the retention of transition metal cations was carried out with 10 m*M* MSA as eluent. Mn^{2+}, Co^{2+}, Cd^{2+} and Zn^{2+} were all separated in under 6 minutes on the Poly-IDA column (Fig. 2.8), on the HEIDA-silica stationary phase separation was achieved in ~20 minutes, and Cd^{2+} and Zn^{2+} could not be resolved (Fig. 2.9). At lower concentrations of MSA (≤ 7 m*M*) resolution was possible. However, poor peak shape and excessively long run times were observed as a result.

The retention data for alkali, alkaline earth and transition metal cations on both stationary phases is shown in Figs. 2.10 and 2.11, where retention is plotted vs eluent concentration (*M*). It is clear from these plots that different retention mechanisms are responsible for the retention of different groups of metal cations. Alkali metals show very little increase in retention, alkaline earth metals show little to moderate retention, and transition metals show moderate to strong retention on the phases (note: due to excessively long run times, data for transition metal plots on the HEIDA-silica column was not recorded). This suggests that the more strongly retained transition metals have a dual mechanism of standard cation exchange and chelation, which one would expect in a non-suppressed (where a weak ionic strength eluent results in the non-suppression of electrostatic interactions) elution system (the suppression of ion-exchange interactions is discussed further in detail in Section 3.3.1). The slopes obtained for the metals further prove this theory (Table 2.2). The more strongly retained the metal, the higher the slope, and closer to the absolute charge of the metal cation. The retention of Mn^{2+} was significantly different to that observed for the other transition metals, likely due to the similar stability constant that it has for IDA-complexes to alkaline earth metals. However, the slope was higher which suggests that some degree of chelation was responsible for retention.

The clear difference between retention on the Poly-IDA and HEIDA-silica columns is also observed. The slopes for the Poly-IDA column are lower, suggesting a lower degree of chelation due to the absence of an OH group in close proximity to IDA on the polymeric stationary phase. Clearly the method of attachment of IDA groups has a significant effect on the retention of metal cations.

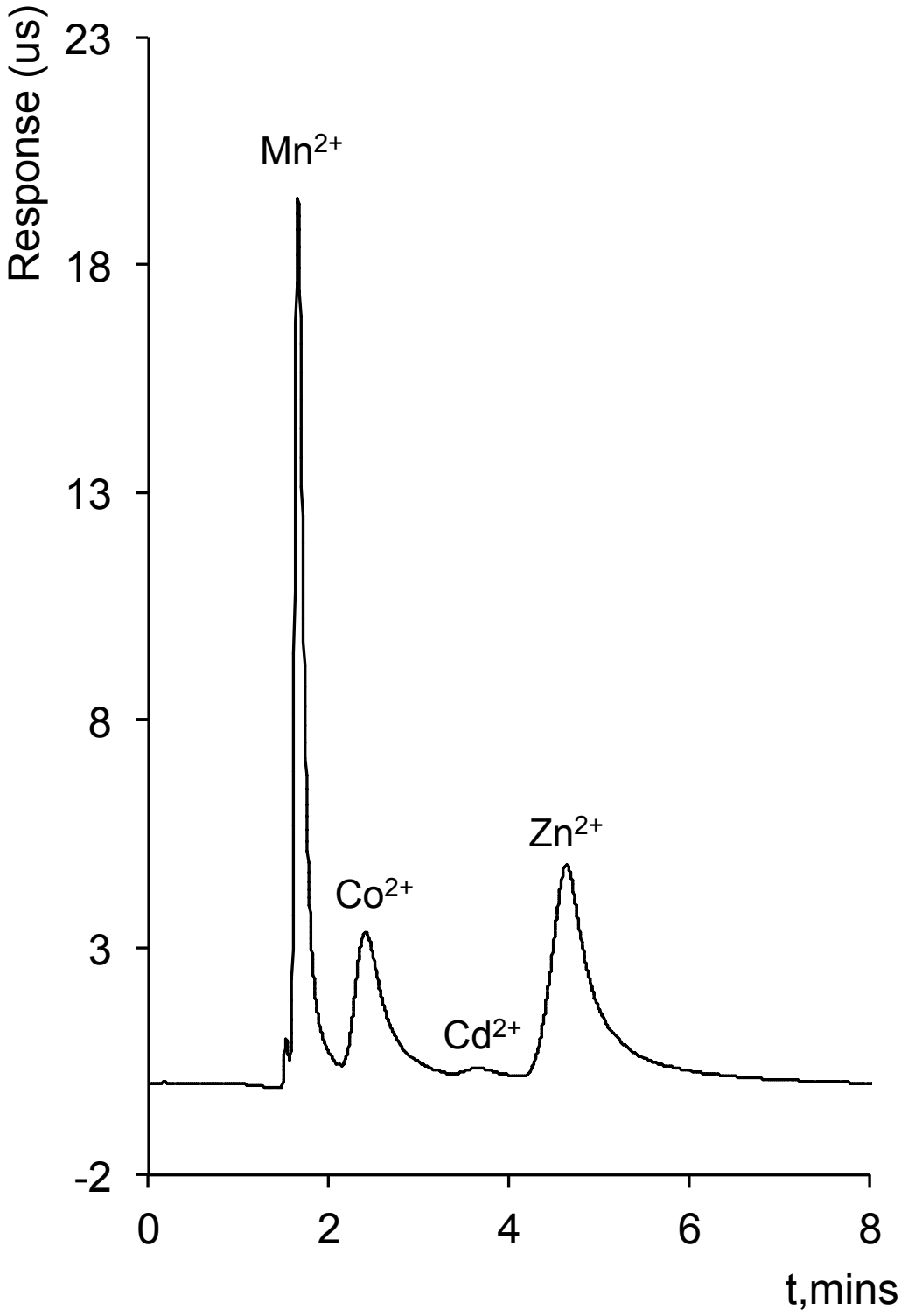

Fig. 2.8: Isocratic separation of 1 m*M* Mn^{2+}, Co^{2+}, Cd^{2+} and Zn^{2+} on Poly-IDA column. Eluent: 5 m*M* electrolytically generated MSA with DW, Flow rate: 1.0 mL/min, Column temperature: 25 ^{o}C, Injection volume: 20 µL. Method of detection: suppressed conductivity.

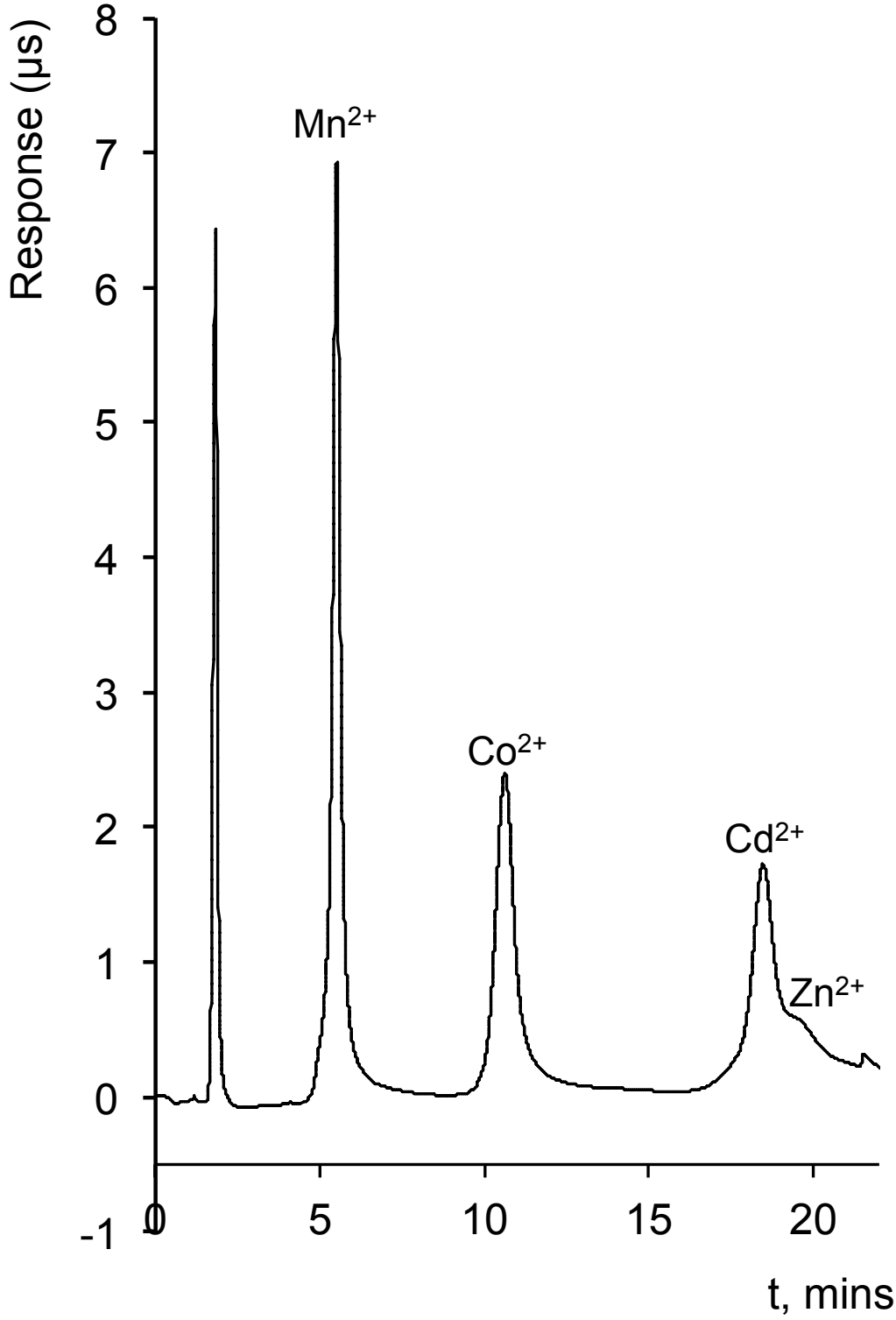

Fig. 2.9: Isocratic separation of 1 m*M* Mn^{2+}, Cd^{2+} and Co^{2+} on HEIDA-silica column. Eluent: 10 m*M* electrolytically generated MSA with DW, Flow rate: 1.0 mL/min, Column temperature: 25 ^{o}C, Injection volume: 20 µL. Method of detection: suppressed conductivity.

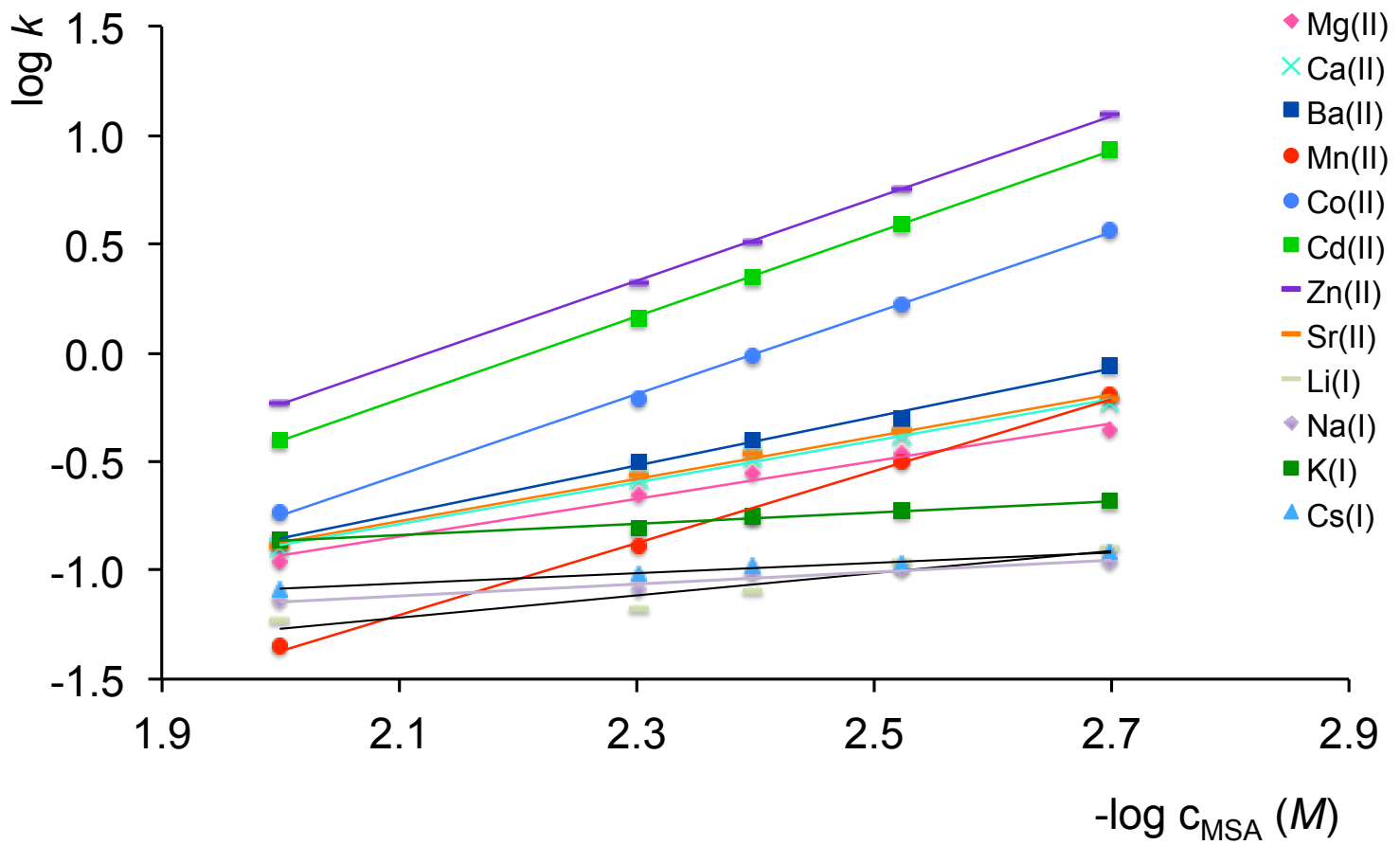

Fig. 2.10: Effect of MSA eluent concentration on metal cations on Poly-IDA column. Eluent: electrolytically generated MSA with DW, Flow rate: 1.0 mL/min, Column temperature: 25 ^{o}C, Injection volume: 20 µL, Analyte concentration: 1 m*M*, Method of detection: suppressed conductivity detection.

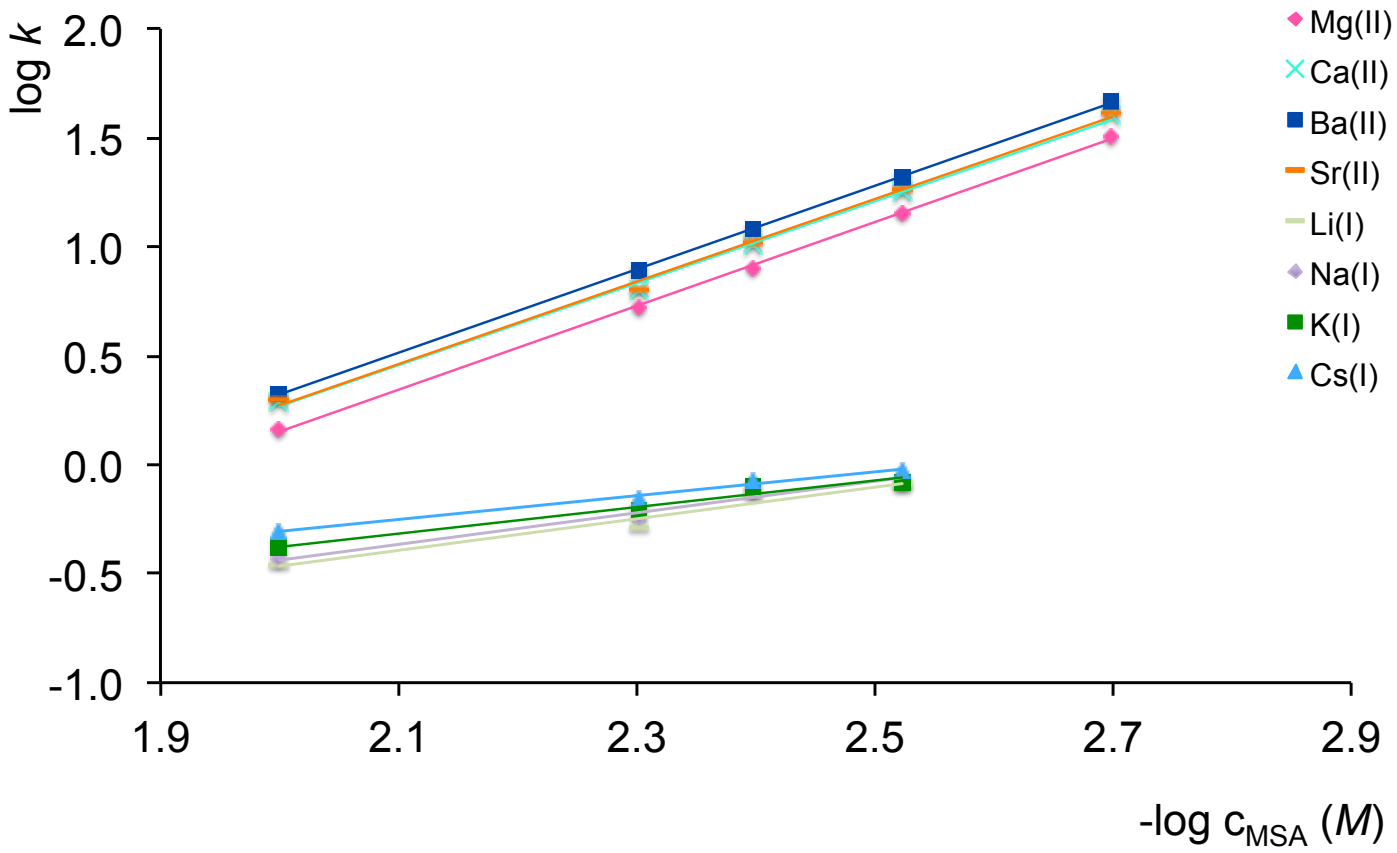

Fig. 2.11: Effect of MSA eluent concentration on metal cations on a HEIDA-silica column. Eluent: electrolytically generated MSA with DW, Flow rate: 1.0 mL/min, Column temperature: 25 ^{o}C, Injection volume: 20 µL, Analyte concentration: 1 m*M*, Method of detection: suppressed conductivity detection.

Table 2.2: Slope of effect of MSA concentration on lanthanides on Poly-IDA and HEIDA-silica columns.

Cation	Poly-IDA	HEIDA-silica
Li^{+}	0.512	0.725
Na^{+}	0.275	0.724
K^{+}	0.258	0.610
Cs^{+}	0.237	0.546
Mg^{2+}	0.868	1.923
Ca^{2+}	0.959	1.880
Sr^{2+}	0.971	1.893
Ba^{2+}	1.118	1.915
Mn^{2+}	1.655	N/A
Co^{2+}	1.862	N/A
Cd^{2+}	1.905	N/A
Zn^{2+}	1.892	N/A

2.3.1.2 Suppressed conductivity detection for the separation of lanthanides

HPCIC is one of the most successful approaches for the determination of lanthanides, employing various chelating stationary phases of which IDA bonded silica is one of the most popular [17-19]. Lanthanide metal cations show a high affinity for cation exchangers, and have high IDA-metal complex stability constants (see Table 2.3), resulting in greater retention than di-valent metal cations.

Table 2.3: Stability constants of complexes of rare earth metal cations with iminodiacetic acid.

Cation	$\log \beta_1$ Iminodiacetic acid
La^{3+}	5.88
Ce^{3+}	6.18
Pr^{3+}	6.44
Nd^{3+}	6.50
Sm^{3+}	6.64
Gd^{3+}	6.68
Eu^{3+}	6.73
Tb^{3+}	6.78
Dy^{3+}	6.88
Ho^{3+}	6.97
Er^{3+}	7.09
Tm^{3+}	7.22
Yb^{3+}	7.42
Lu^{3+}	7.61

Prior to work carried out by Nesterenko and Jones who successfully employed a silica IDA column (250 x 4.0 mm I.D.) for the isocratic separation of a number of lanthanides, few isocratic methods had been successfully employed [20-23], with the separation of only eight or nine lanthanides achieved, mainly in gradient mode. This is due to the large difference in ionic radii of the trivalent lanthanides, and the resulting change in ion-exchange selectivity [19]. Furthermore, the determination of lanthanides using polymeric stationary phases, which incorporate bonded IDA functionalities, has received little attention to date.

The isocratic separation of lanthanides with PCR as a detection method for HPCIC has been previously documented [19]. However, this is not the case with suppressed conductivity detection, where detection of more strongly retained di- and tri-valent metal cations (transition and rare earth metals) is notoriously difficult due to the possible occurrence of precipitation [8]. Eliminating the need for PCR would result in a less costly and time-consuming method for cation analysis. Therefore, one of the aims of this work was to investigate the possibility of suppressed conductivity detection as a detection method for the determination of lanthanides and yttrium in HPCIC and evaluate the chromatographic behaviour of the Poly-IDA and HEIDA-silica columns under these conditions.

All chromatographic conditions were identical on both stationary phases. A reasonably high MSA eluent concentration (20 m*M*) was chosen in order to elute the analytes in a reasonable run time. The column temperature was kept relatively low (30 ^{o}C) in order to resolve Y^{3+} from La^{3+} and Ce^{3+}. The separation of La^{3+}, Y^{3+}, Ce^{3+}, Pr^{3+}, Nd^{3+}, Tm^{3+} and Eu^{3+} was successfully achieved on both columns, and the chromatograms are shown in Figs. 2.12 and 2.13. Table 2.4 illustrates the chromatographic data for the separations. There is a significant difference between the efficiency values reported for the rare earth metal cations at identical conditions. All analytes showed at least a 5-fold higher *N*/m values on the HEIDA-silica column. There is also greater resolution of all peaks compared to the Poly-IDA column, however the run time is excessively long at ~84 minutes.

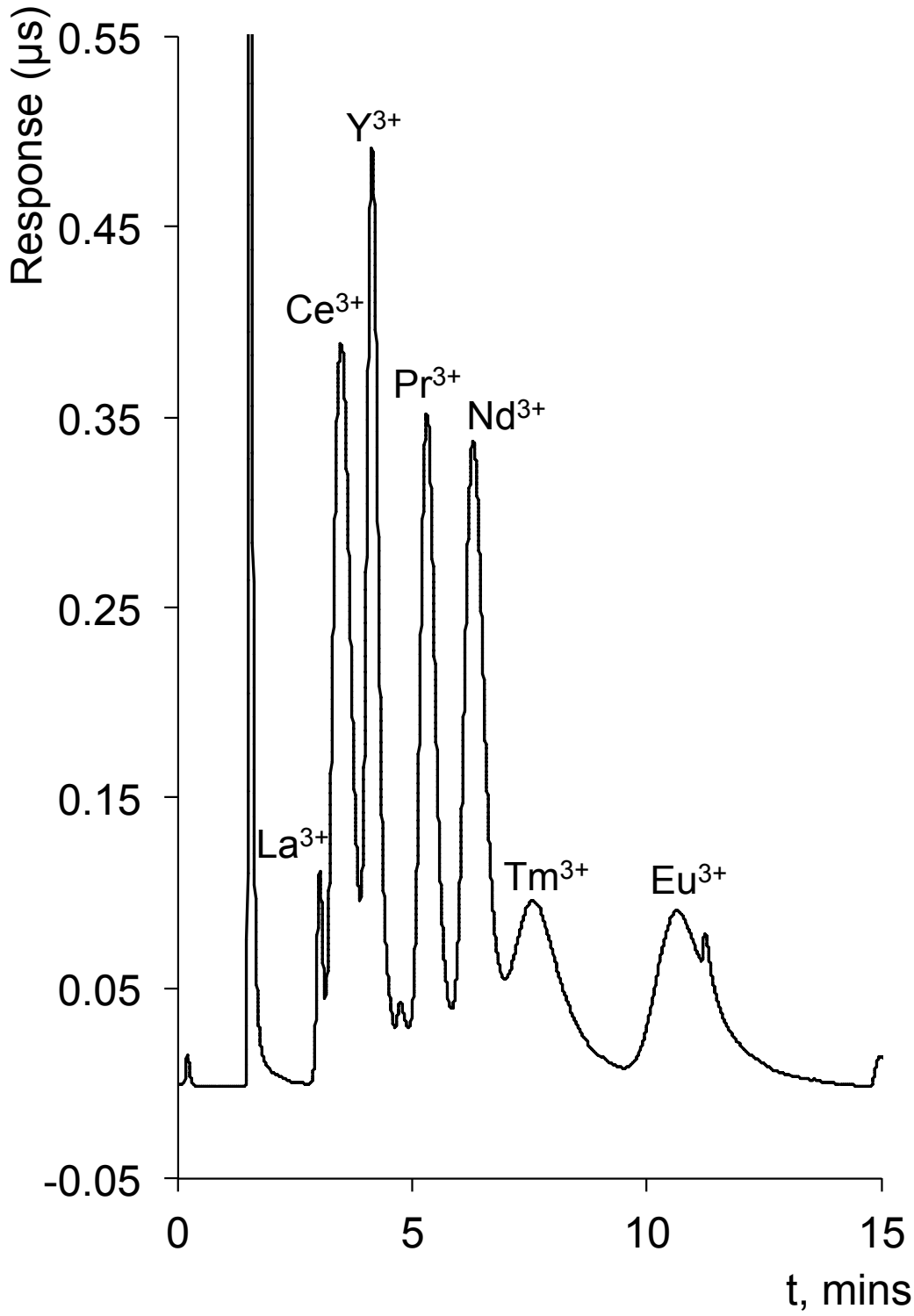

Fig. 2.12: Isocratic separation of lanthanides on Poly-IDA column. Eluent: 20 m*M* electrolytically generated MSA with DW, Flow rate: 1.0 mL/min, Column temperature: 30 ^{o}C, Injection volume: 25 µL, Analyte concentration: 5 ppm, Method of detection: suppressed conductivity.

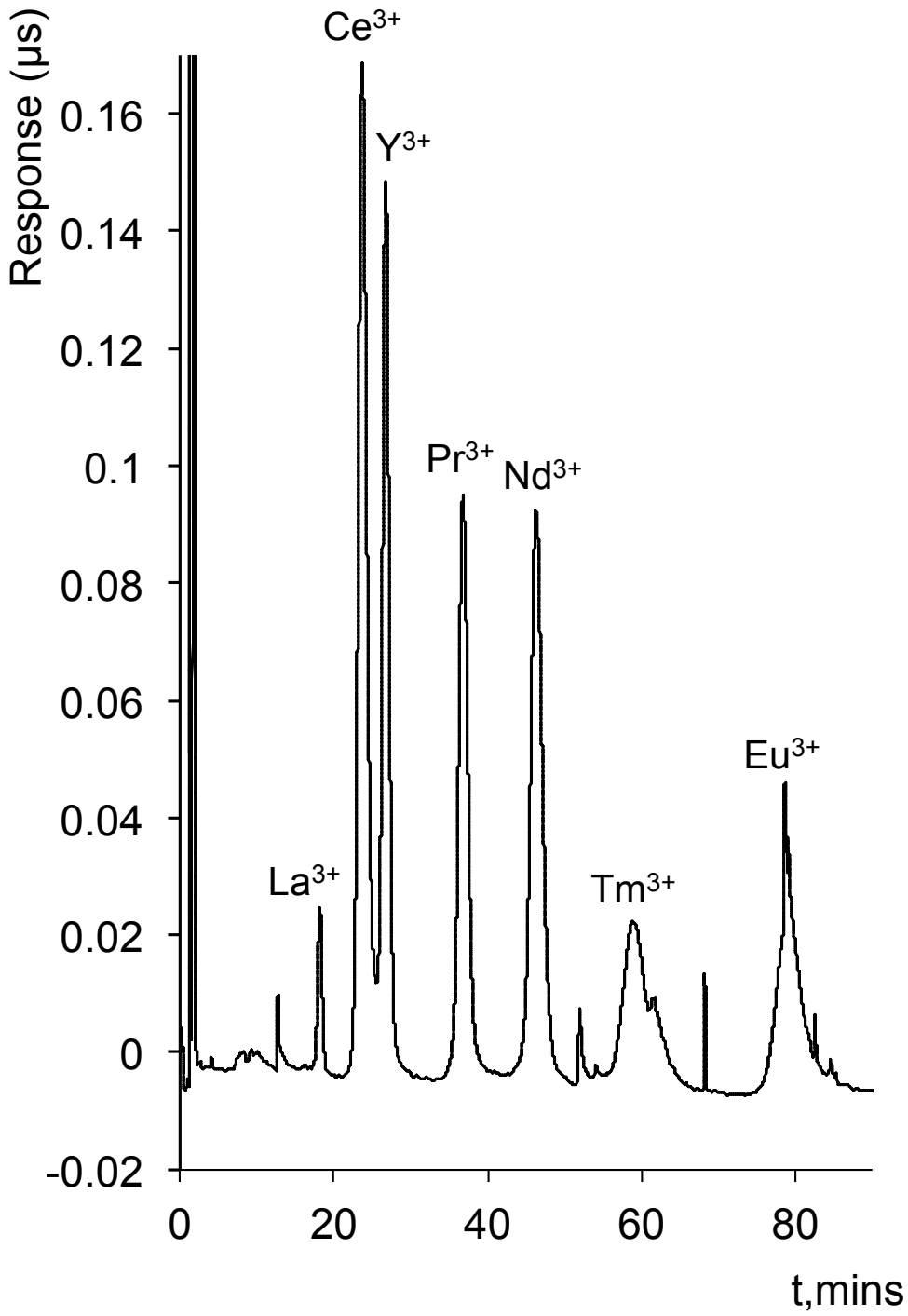

Fig. 2.13: Isocratic separation of lanthanides on HEIDA-silica column. Eluent: 20 m*M* electrolytically generated MSA with DW, Flow rate: 1.0 mL/min, Column temperature: 30 ^{o}C, Injection volume: 25 µL, Analyte concentration: 5 ppm, Method of detection: suppressed conductivity.

Table 2.4: Chromatographic data for isocratic separation of lanthanides on Poly-IDA and HEIDA-silica stationary phases.

Cation (5ppm)	Efficiency (*N*/m)		*k*'		Resolution	
	Poly-IDA	HEIDA-silica	Poly-IDA	HEIDA-silica	Poly-IDA	HEIDA-silica
La^{3+}	9,000	35,000	1.00	12.60	0.93	3.60
Y^{3+}	1,500	14,000	1.30	16.72	1.11	1.69
Ce^{3+}	5,100	31,000	1.73	19.01	2.23	5.28
Pr^{3+}	5,200	29,000	2.51	26.49	1.47	3.81
Nd^{3+}	4,500	29,000	3.16	33.61	1.17	3.18
Tm^{3+}	1,800	14,000	4.00	43.08	1.75	5.18
Eu^{3+}	1,600	14,000	6.03	57.82	N/A	N/A

2.3.2 Effect of temperature on retention and efficiency of selected cations

As discussed in Section 1.4.2, adjusting the column temperature can be used to increase retention of analytes and manipulate selectivity in HPCIC. The effect of temperature on HEIDA-silica stationary phases has been documented by Nesterenko and Jones [19]. Here, a brief study on the effect of elevated column temperature on selected lanthanide and yytrium metal cations was evaluated on the IDA-poymer column using suppressed conductivity detection. The experiment was repeated on HEIDA-silica for La^{3+}, Ce^{3+} and Y^{3+} for direct comparison.

Fig. 2.14 shows a van't Hoff plot for the Poly-IDA stationary phase. The resulting plot displays a similar trend to those observed on the HEIDA-silica column (see Fig. 2.15), where retention increases at elevated temperatures, indicating a chelation dominant retention mechanism.

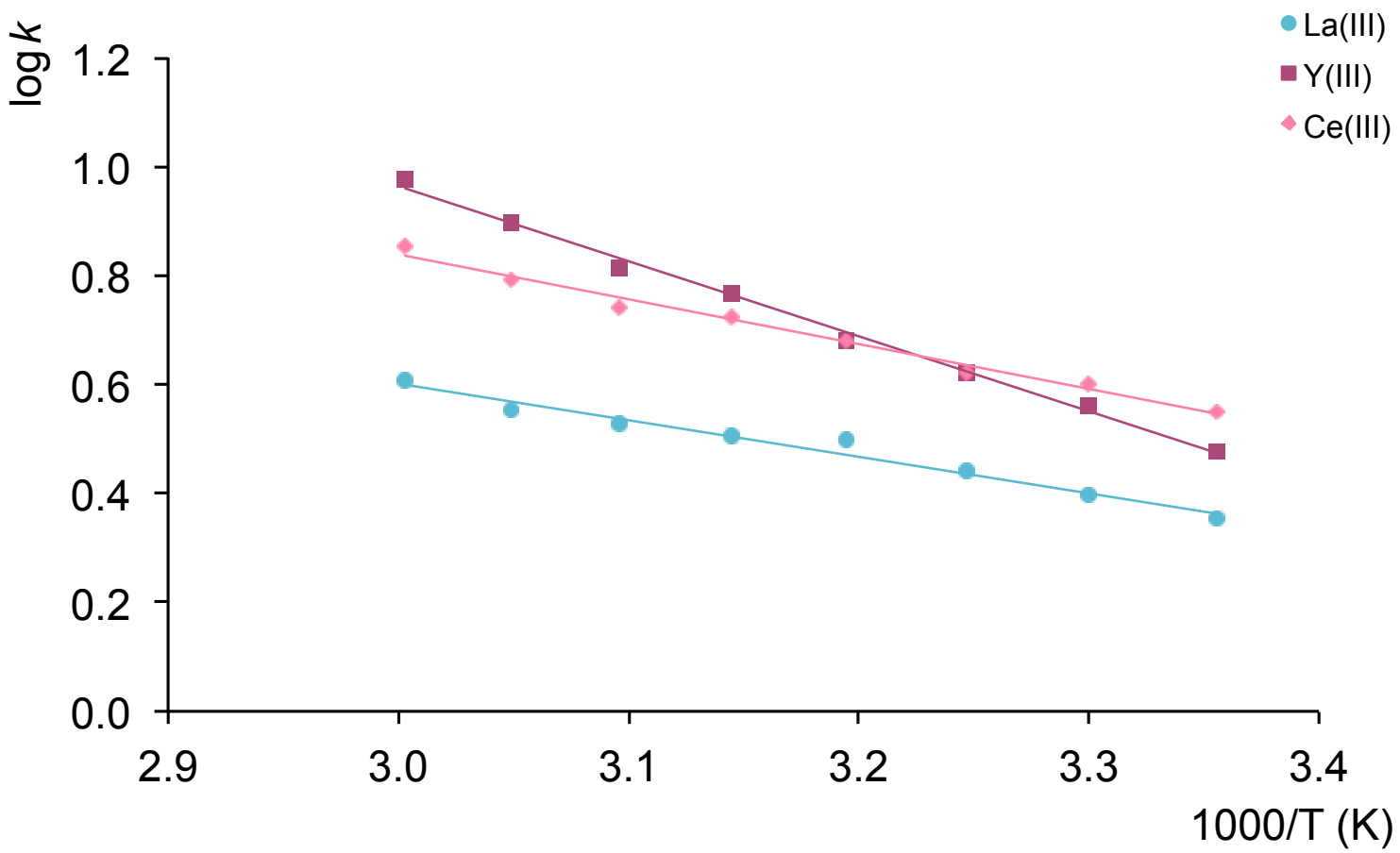

Fig. 2.14: Effect of column temperature on retention of La^{3+}, Y^{3+} and Ce^{3+} on HEIDA-silica column. Eluent: 20 m*M* electrolytically generated MSA with DW, Flow rate: 1.0 mL/min, Injection volume: 20 µL, Analyte concentration: 50 ppm, Method of detection: suppressed conductivity.

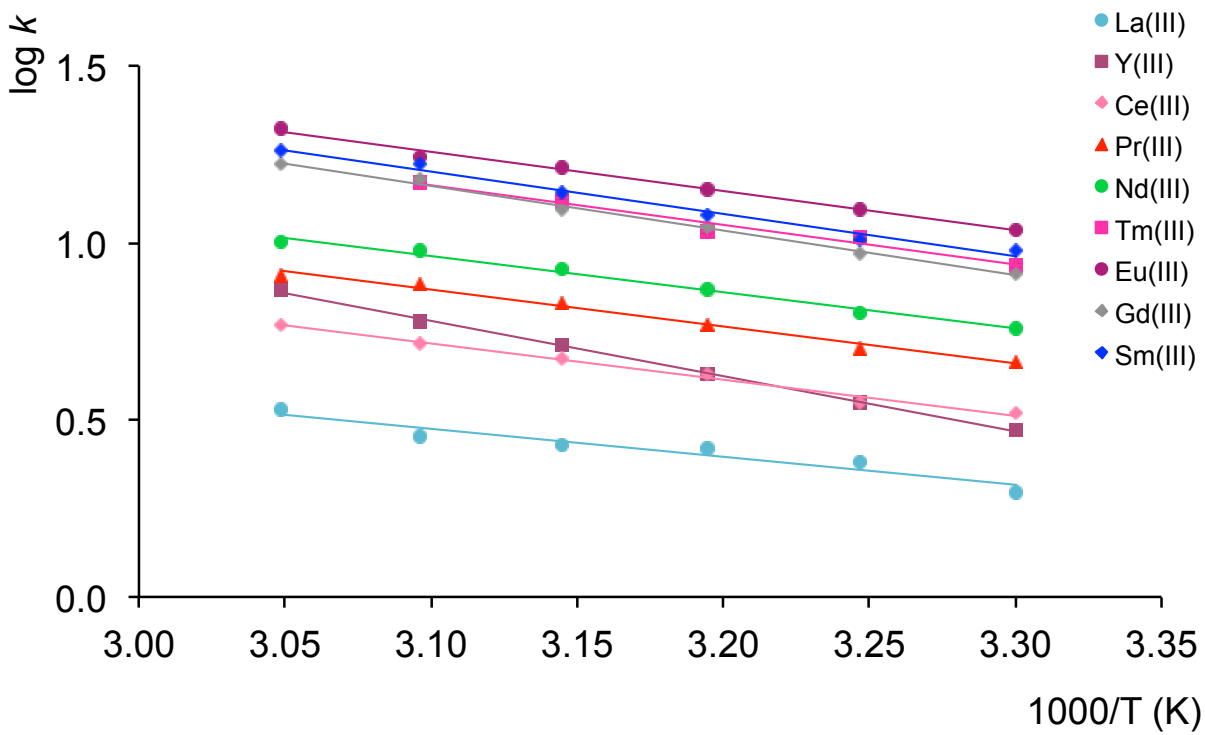

Fig. 2.15: Effect of column temperature on retention of rare earth metal cations on Poly-IDA column. Eluent: 20 m*M* electrolytically generated MSA with DW, Flow rate: 1.0 mL/min, Injection volume: 20 µL, Analyte concentration: 50 ppm, Method of detection: suppressed conductivity.

The slopes determined for La^{3+}, Ce^{3+} and Y^{3+} from Figs. 2.14 and 2.15 were 2.92, 3.89 and 5.61, respectively, for the Poly-IDA column and 2.62, 3.31 and 5.10, respectively, for the HEIDA-silica column. Therefore, it is clear that the two stationary phases exhibit retention by the same mehanism. As previously observed on a silica-IDA stationary phase [19], the effect of elevated column temperature on Y^{3+} is greater than for the lanthanide metal cations on both columns (note the higher slope values compared to La^{3+} and Ce^{3+}).

On the Poly-IDA column the slopes increased with increasing retention. The exceptions were Y^{3+}, which can display different behaviour to the lanthanides, and Gd^{3+} (slope 5.06), which would be expected to be similar or less than the later eluting Eu^{3+} (slope 4.68) due to the similar stability constants. The difference between behaviour of Gd^{3+} and Eu^{3+} further suggests that the rate of complexation of the two analytes may be different in a non ion exchange suppressed retention system, than in a chelation dominant system.

The effect of column temperature upon efficiency was also evaluated over the range 30 to 60 °C for La^{3+}. Fig. 2.16 shows there is an increase in efficiency on both columns, however the effect on the HEIDA-silica column (43% increase in *N*/m) is higher than that observed on the Poly-IDA phase (34% increase in *N*/m), which suggests that the higher column temperature on HEIDA-silica has a greater influence on the chelation effect (see later Section 3.3.3 for a detailed explanation into the effect of increased column temperature on chelating stationary phases).

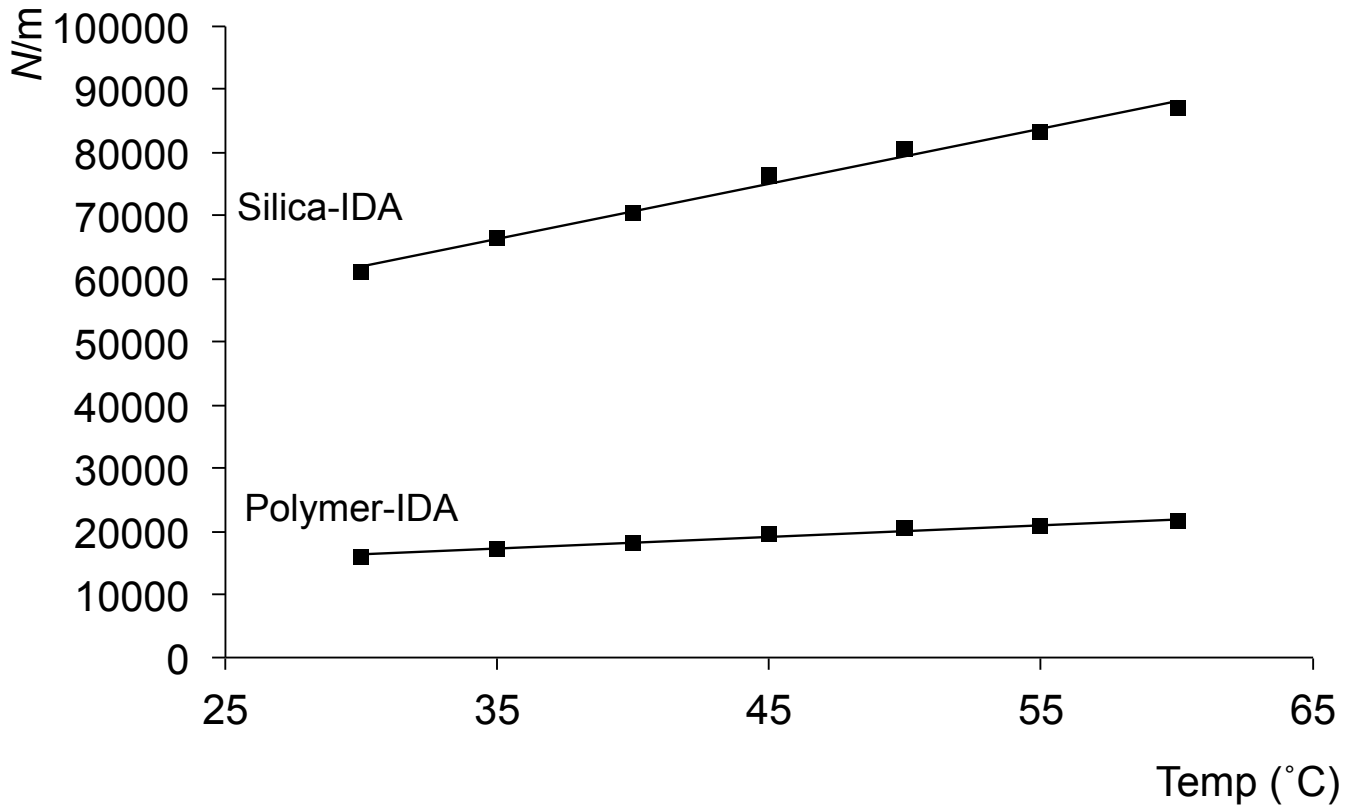

Fig. 2.16: Effect of column temperature on efficiency of La^{3+} on Poly-IDA and HEIDA-silica column. Eluent: 20 m*M* electrolytically generated MSA with DW, Flow rate: 1.0 mL/min, Injection volume: 25 µL, Analyte concentration: 50 ppm, Method of detection: suppressed conductivity.

2.3.3 Gradient separations

It was clear that in order to separate a number of metals belonging to different groups in a convenient timeframe, an eluent gradient method was required. As a result of the difference in stability constants of different IDA-metal complexes (see Tables 2.1 and 2.3), in order to successfully achieve the separation of a mixture of mono-, di- and tri-valent cations under identical isocratic conditions, an excessive run time would occur.

It is well documented that altering the eluent concentration can change separation selectivity and retention of an isocratic separation, whereas with gradient separations the steepness of the ramp is changed [24]. Therefore, using electrolytically generated MSA as eluent with suppressed conductivity detection, various gradient separation methods were carried out on both the Poly-IDA and HEIDA-silica columns in order to achieve maximum selectivity of a number of metal cations. The Poly-IDA phase was successfully utilized with a MSA gradient for the separation of transition and lanthanide metal cations (3.5 to 10 m*M)* MSA (Fig. 2.17). However, under these conditions it was not possible to resolve any alkaline earth metals, which all eluted in the void volume.

Due to the better selectivity that the HEIDA-silica phase showed towards alkaline earth metals it was possible to separate a number of alkaline earth, transition and lanthanide metal cations, using a gradient method of 8 to 19 m*M* MSA (Fig. 2.18). However, it was still not possible to resolve any alkali metals using such eluent concentrations.

Due to the absence of an alkali metal salt such as nitrate, chloride or perchlorate in the eluent to provide sufficient ionic strength to suppress any electrostatic interactions [25], it was likely that a dual retention mechanism of ion-exchange and chelation took place, thus the lanthanide metal cations showed poorer peak shape and lower efficiencies than those for transition metals on both columns, and as the eluent was not of high ionic strength, the peak shape worsened.

Although electrolytically generated MSA as eluent with suppressed conductivity was successfully applied to the determination of metals in HPCIC, after a number of

injections precipitation of the more strongly retained cations did indeed occur. A further drawback to the use of this detection method was peak noise, which was not eliminated and caused interference, particularly with the more strongly retained lanthanides. Therefore, it is very clear that spectrophotometric detection with PCR remains the most suitable method of detection for HPCIC. However, the detection of lanthanides in HPCIC using electrolytically generated MSA as eluent with chelating stationary phases is a significant achievement which has not previously been accomplished.

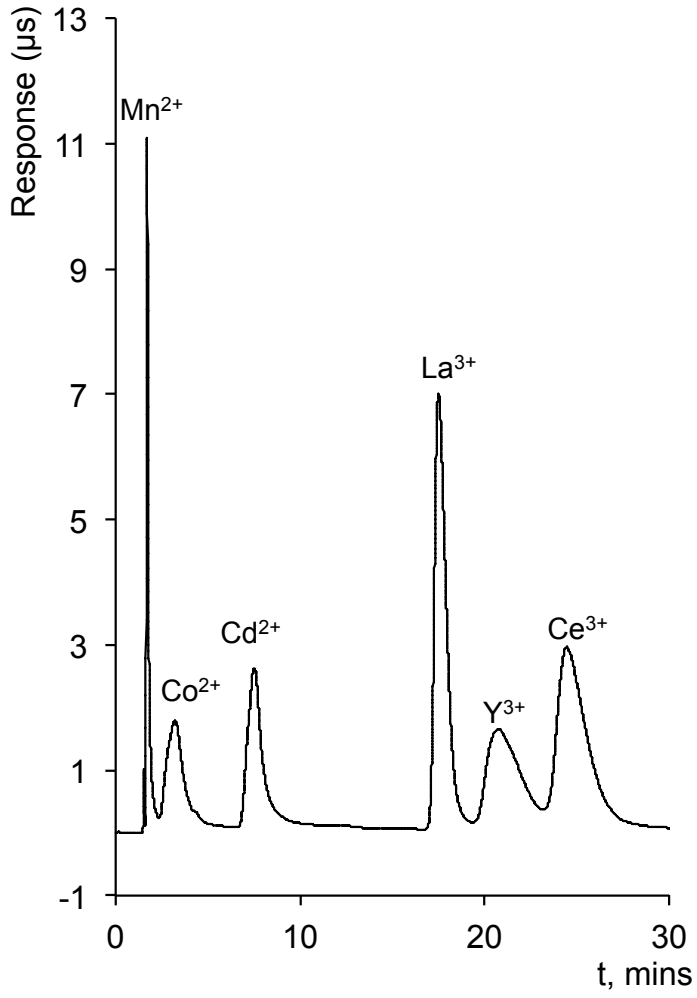

Fig. 2.17: Gradient separation of transition and lanthanide metal cations on Poly-IDA column. Eluent: Electrolytically generated MSA with DW, Flow rate: 0.8 mL/min, Column temperature: 25 ^{o}C, Injection volume: 20 µL, Analyte concentration: 1 m*M*. Method of detection: suppressed conductivity.

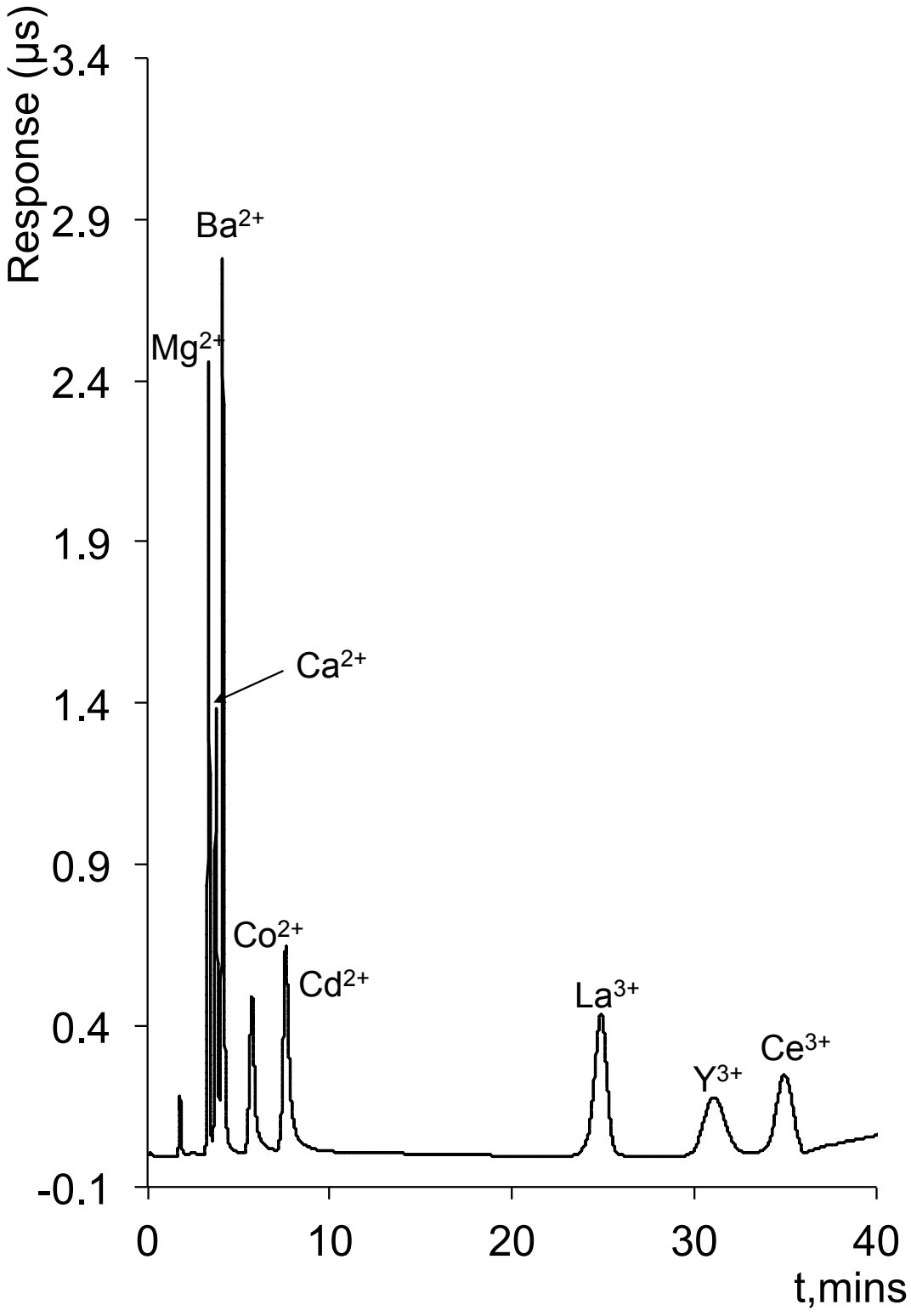

Fig. 2.18: Gradient separation of alkaline earth, transition and lanthanide metal cations on HEIDA-silica column. Eluent: Electrolytically generated MSA with DW, Flow rate: 1.0 mL/min, Column temperature: 25 ^{o}C, Injection volume: 20 µL, Analyte concentration: 1 m*M*. Method of detection: suppressed conductivity.

2.3.4 Effect of methanesulfonic acid eluent concentration on the retention of lanthanides using post-column reaction

In order to achieve direct and accurate comparison of the HEIDA-silica and Poly-IDA, the effect of concentration of electrolytically generated MSA on the retention and selectivity of metal ions was evaluated. From the work carried out in Section 2.3.1, it was clear that suppressed conductivity detection is a more suitable method for determination of alkali and alkaline earth metals than the more strongly retained di- and tri-valent metal cations due to the formation of metal hydroxide and oxide precipitates. Thus, while suppressed conductivity detection indeed proved a possible detection method for lanthanides (see Section 2.3.1.2), here PCR was employed to enhance detection. As previously discussed in Section 1.6, the detection of metal species often proves difficult in IC due to their chemical characteristics, therefore spectrophotometric detection was employed with the post-column reagent arsenazo III, which is a well known post-column reagent for the detection of rare earth metals [8].

The effect of MSA eluent concentration was evaluated on both IDA-functionalised columns, and a logarithmic relationship between the eluent concentration and retention factor (*k*') was plotted. As shown in Figs. 2.19 and 2.20, retention time for all lanthanides decreased as the MSA concentration in the eluent was increased. All analytes were greater retained for longer on the HEIDA-silica column as expected, but the slopes were smaller than for the Poly-IDA column. However as Table 2.5 demonstrates, the more strongly retained the analyte, the smaller the difference in slopes between stationary phases becomes.

The order of elution of lanthanides and yttrium deviates from the order of stability constants of complexes of rare earth metal cations with iminodiacetic acid (Table 2.3). The ionic radii of the lanthanides decrease from La^{3+} to Lu^{3+}, but because of their high affinity for ligands such as IDA, it is expected that chelation will be responsible for retention. The chelation effect is greater for the more strongly retained lanthanides, therefore it would be expected that the affinity of IDA groups is reduced from Lu^{3+} to La^{3+}. Here, the earliest eluting cations La^{3+}, Y^{3+}, Ce^{3+}, Pr^{3+} and

Nd^{3+} eluted in the expected order, however the later eluting, heavier lanthanides do not, strongly indicating that a mixed retention mode of chelating and ion-exchange is present, even at higher concentrations of MSA. The greatest deviations from the expected elution order are Sm^{3+}, which normally elutes directly after Nd^{3+} but in this case the retention is far greater, and Eu^{3+}, which due to their similar stability constants, often co-elutes with Gd^{3+}. Here, Eu^{3+} elutes either lastly or second to last. Thus, the ratio of simple cation exchange and chelation mechanisms varies between analytes.

Table 2.5: Slope of effect of MSA concentration on lanthanides on Poly-IDA and HEIDA-silica columns.

Cation	Poly-IDA	HEIDA-silica
La^{3+}	2.929	2.554
Y^{3+}	3.057	2.412
Ce^{3+}	2.876	2.641
Pr^{3+}	2.918	2.777
Nd^{3+}	3.000	2.617
Tm^{3+}	3.064	2.671
Er^{3+}	3.088	2.555
Ho^{3+}	3.139	2.670
Gd^{3+}	3.086	2.675
Dy^{3+}	3.091	2.603
Tb^{3+}	3.024	2.693
Yb^{3+}	2.977	2.718
Sm^{3+}	2.999	2.656
Eu^{3+}	3.063	2.726
Lu^{3+}	2.978	2.715

The order of elution changes slightly at different concentrations. Table 2.6 contains the order of elution of lanthanides at 15 and 25 m*M* MSA on both HEIDA-silica and Poly-IDA columns. On the Poly-IDA column the order of retention stays the same at

both MSA concentrations with the exception of Dy^{3+} and Tb^{3+}. On the HEIDA-silica there is a greater change to the order of elution, with most analytes eluting after Nd^{3+} showing a greater chance, although minimal. There is also a slight difference in the order of elution between stationary phases. As seen in Table 2.6, there are some differences between phases at both concentrations, with the later eluting analytes showing a larger change, possibly due to the degree of chelation becoming greater at higher eluent strength.

Table 2.6: Order of elution of lanthanide metal cations on Poly-IDA and HEIDA-silica columns.

Order of Elution	Poly-IDA		HEIDA-silica	
	Concentration MSA (m*M*)			
	15	25	15	25
1	La^{3+}	La^{3+}	La^{3+}	La^{3+}
2	Y^{3+}	Y^{3+}	Y^{3+}	Y^{3+}
3	Ce^{3+}	Ce^{3+}	Ce^{3+}	Ce^{3+}
4	Pr^{3+}	Pr^{3+}	Pr^{3+}	Pr^{3+}
5	Nd^{3+}	Nd^{3+}	Nd^{3+}	Nd^{3+}
6	Tm^{3+}	Tm^{3+}	Tm^{3+}	Er^{3+}
7	Er^{3+}	Er^{3+}	Er^{3+}	Ho^{3+}
8	Ho^{3+}	Ho^{3+}	Ho^{3+}	Tm^{3+}
9	Gd^{3+}	Gd^{3+}	Dy^{3+}	Dy^{3+}
10	Dy^{3+}	Tb^{3+}	Gd^{3+}	Gd^{3+}
11	Tb^{3+}	Dy^{3+}	Tb^{3+}	Tb^{3+}
12	Yb^{3+}	Yb^{3+}	Yb^{3+}	Yb^{3+}
13	Sm^{3+}	Sm^{3+}	Lu^{3+}	Sm^{3+}
14	Eu^{3+}	Eu^{3+}	Sm^{3+}	Lu^{3+}
15	Lu^{3+}	Lu^{3+}	Eu^{3+}	Eu^{3+}

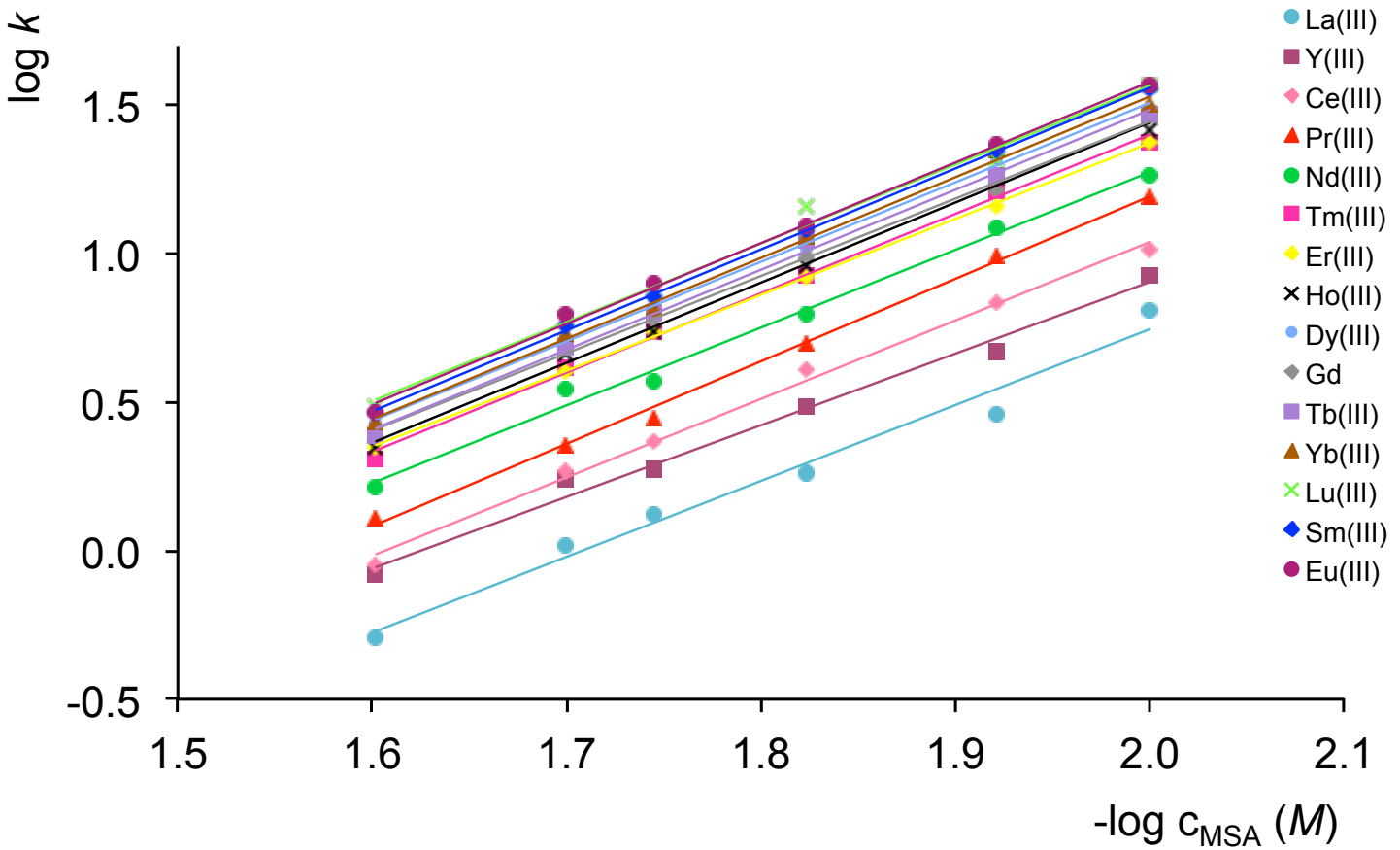

Fig. 2.19: Effect of MSA eluent concentration on rare earth metal cations on Poly-IDA column. Eluent: electrolytically generated MSA with DW, Flow rate: 1.0 mL/min, Column temperature: 25 ^{o}C, Injection volume: 20 µL, Analyte concentration: 10 ppm, Method of detection: spectrophotometric at 650 nm after PCR with 1.5 x 10^{-4} *M* arsenazo III at 0.3 mL/min.

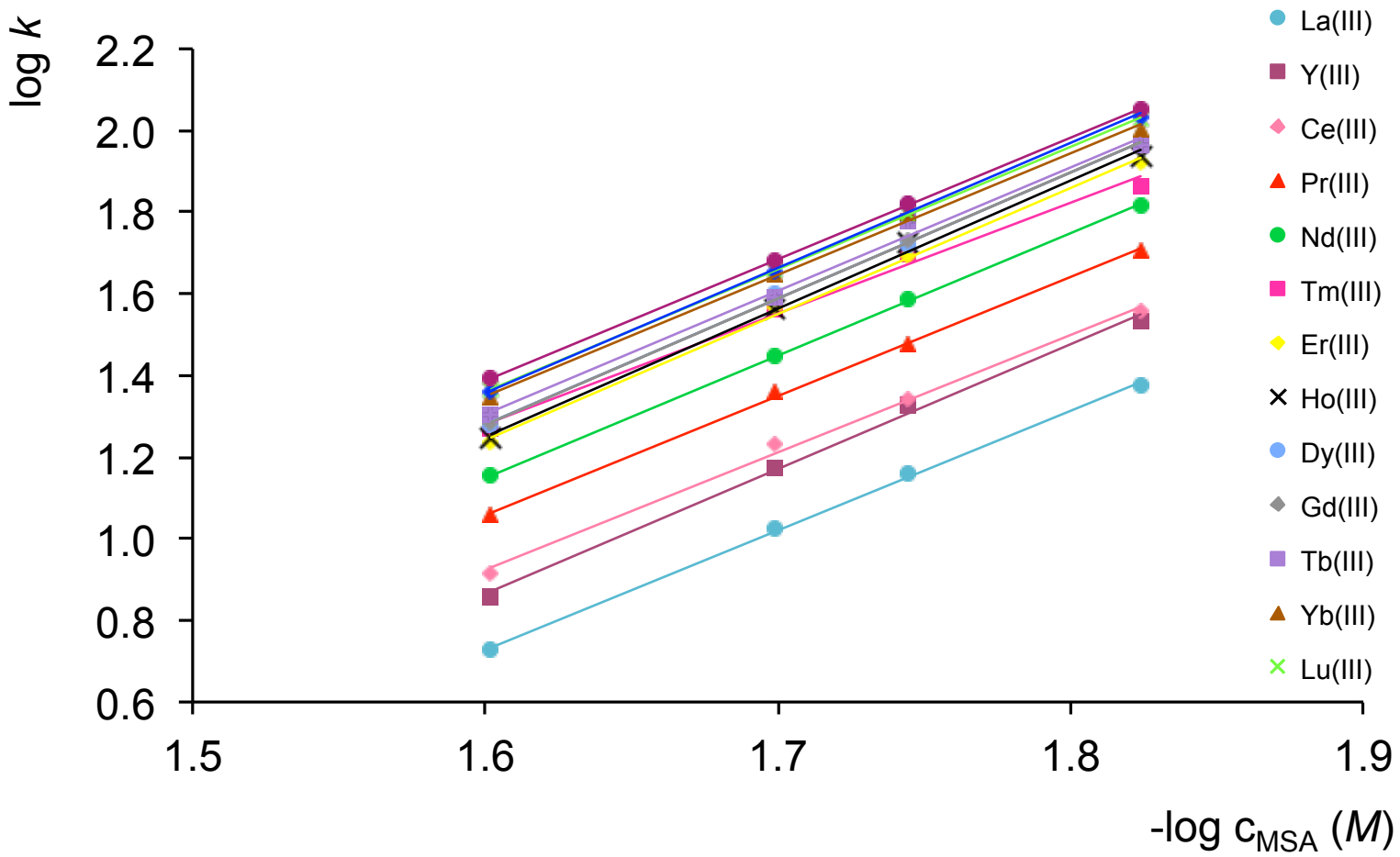

Fig. 2.20: Effect of MSA eluent concentration on rare earth metal cations on HEIDA-silica column. Eluent: electrolytically generated MSA with DW, Flow rate: 1.0 mL/min, Injection volume: 20 µL, Analyte concentration: 10 ppm, Method of detection: spectrophotometric at 650 nmafter PCR with 1.5 x 10^{-4} *M* arsenazo III at 0.3 mL/min.

2.3.5 Two-dimensional chromatography for the separation of selected cations

Often a one-dimensional separation does not provide adequate resolution of complex samples [26]. In these instances, two dimensional (2-D) chromatography can be applied, employing two different stationary phases with different selectivities. The choice of columns is clearly important, to ensure there is good orthogonality between the two stationary phases [27]. 2-D chromatography is generally either comprehensive mode, where the entire first dimension eluent is transferred into the second dimension [28], or "heart-cut" mode, where the fraction of interest is transferred from the first dimension to the second dimension. Comprehensive mode is typically used for the analysis of complex matrices containing large biomolecules. However, this mode requires the second dimension method to be fast enough to accommodate the first dimension sampling rate, which can compromise resolution. This is not a concern in heart-cut mode, therefore methods can be longer, and gradient elution can be employed.

Here, a brief investigation into the use of a chelating stationary phase for the 2-D test separation of metal cations was performed. Fig. 2.21 illustrates the set-up of the chromatography system setup used. Using the "heart-cut" approach, the sample was injected onto one column and passed through to the UV detector, after which fraction collection occurs. This fraction is then passed through the second column to the suppressed conductivity detector. Thus, a complex sample could be analysed utilising two different stationary phases with different detection methods.

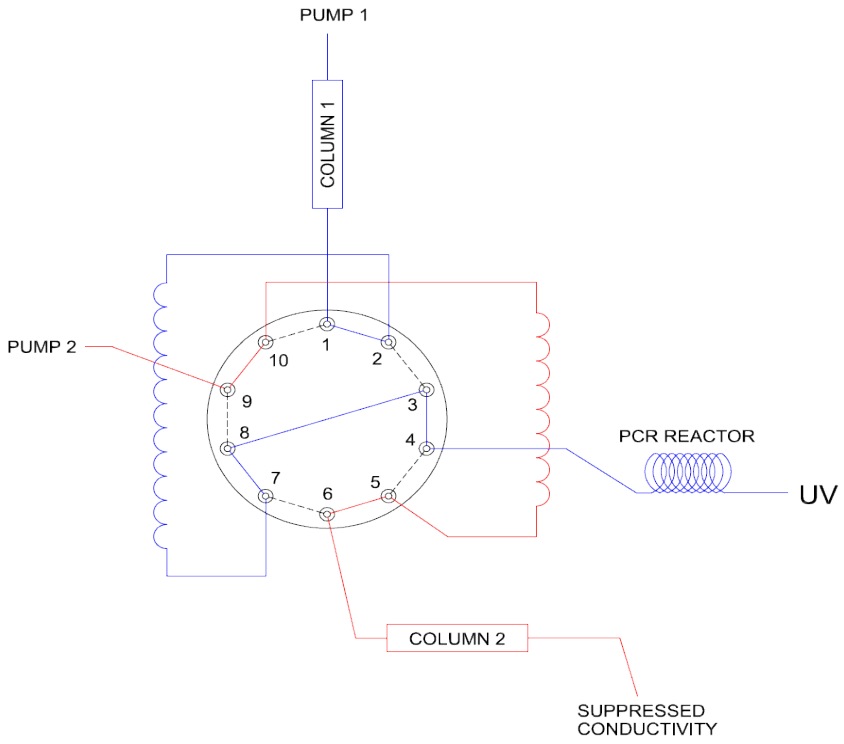

Fig. 2.21: Schematic of 2-D chromatography system with UV and suppressed conductivity detection.

Following earlier characterisation, the HEIDA-silica column was employed on the 1st dimension for the separation of La^{3+} and Y^{3+}, due to the superior efficiencies that the silica column demonstrated, using a gradient method with fraction collection (see Table 2.7) PCR with arsenazo III was chosen as the detection method. On the 2nd dimension, a commercially available cation-exchange column was employed with suppressed conductivity detection. The Dionex CS12A is a carboxylate-functionalised cation-exchange column typically used for the fast separation of selected alkali and alkaline earth metals and ammonium, typically using a MSA eluent [29]. Following a brief investigation into column selectivity (Fig. 2.22), a gradient method was selected (Table 2.8). Figs. 2.23 and 2.24 show the resulting chromatograms, where a 2-D separation was successfully achieved. This shows that chelating stationary phases are a suitable choice for the 2-D separation of a mixture of metal cations, though further optimisation is

clearly required to reduce the overall run time. Furthermore, under the optimum conditions, the separation of a wide range of alkali, alkaline earth, transition and lathanide metal cations is a possibility.

Table 2.7: Gradient method for 1st dimension separation on HEIDA-silica column.

Time (min)	MSA conc (m*M*)
0-5	5
5-6	5 - 20
6-30	20
30 - 40	5

Fraction collection at 3.4 mins for 0.2 min.

Table 2.8: Gradient method for 2nd dimension separation on Dionex CS12A Ionpac column.

Time (min)	MSA conc (m*M*)
0-3	5
3-10	9
10-13	9
13-30	5

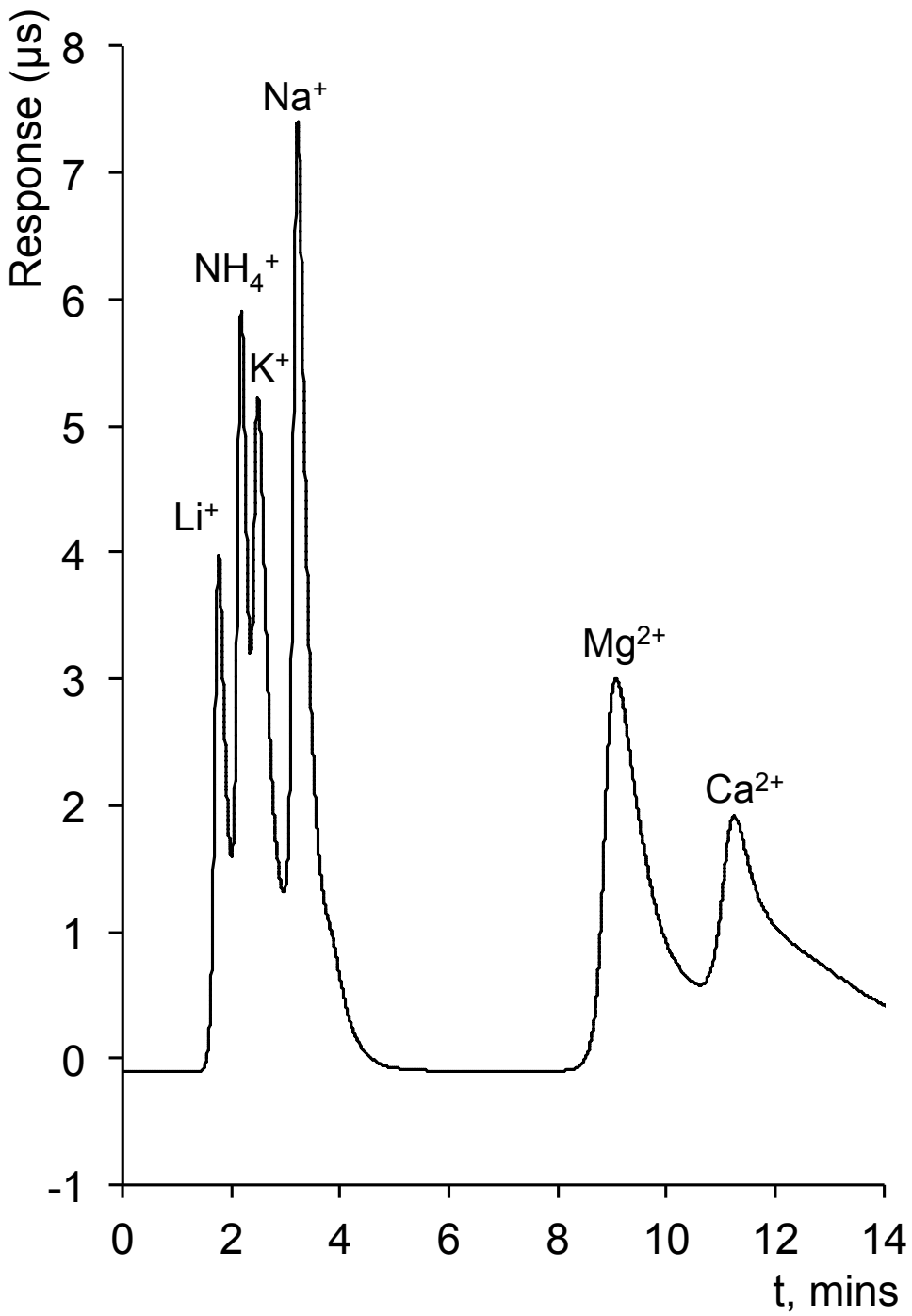

Fig. 2.22: Gradient separation of metal cations on Dionex CS12A IonPac column. Eluent: Electrolytically generated MSA with DW, Flow rate: 0.8 mL/min, Column temperature: 30 ^{o}C, Injection volume: 10 µL, Analyte concentration: 5 ppm, Method of detection: suppressed conductivity.

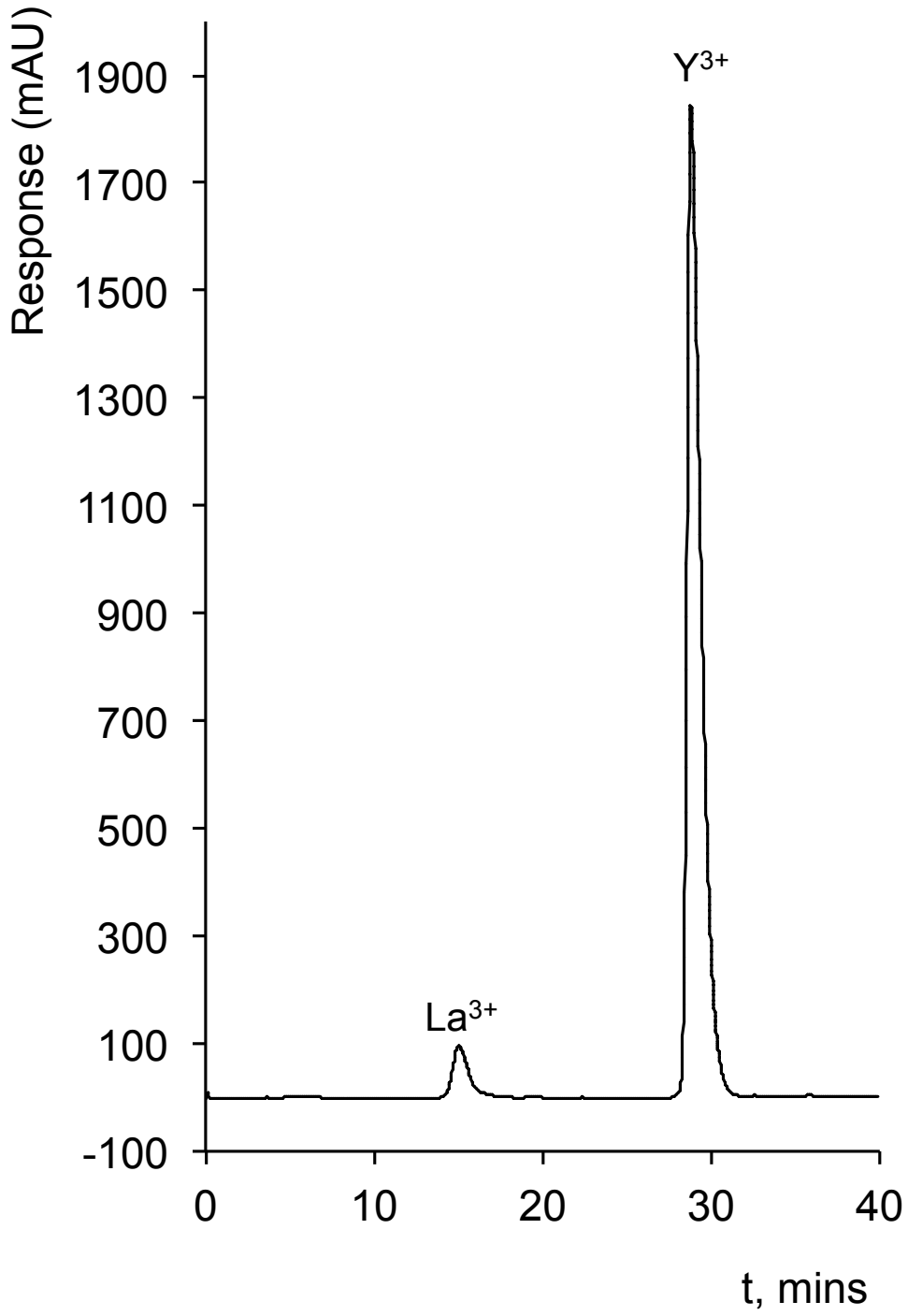

Fig. 2.23: 1st dimension gradient separation of 50 ppm La^{3+} and Y^{+} on HEIDA-silica 150 x 4.0 mm I.D. column. Eluent: Electrolytically generated MSA with DW, Flow rate: 0.7 mL/min, Column temperature: 30 ^{o}C, Injection volume: 25 μL, Method of detection: spectrophotometric at 650 nm after PCR with 1.5 x 10^{-4} *M* arsenazo III.

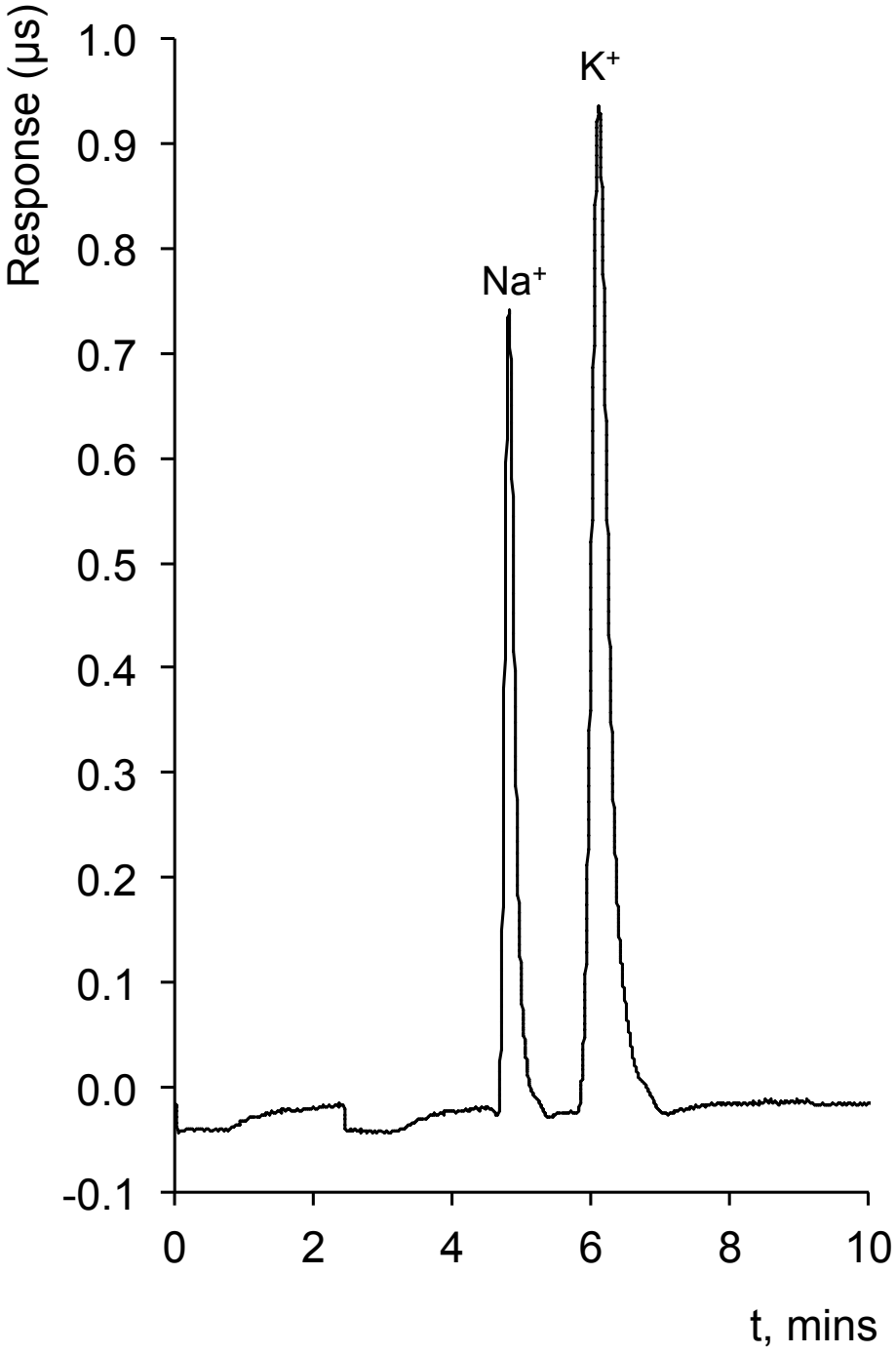

Fig. 2.24: 2nd dimension isocratic separation of 5 ppm Na^+ and K^+ on Dionex CS12A (50 x 4.0 mm I.D., 8 µm) column. Eluent: 5 m*M* electrolytically generated MSA with DW, Flow rate: 1.0 mL/min, Column temperature: 30 ^oC, Injection volume: 25 µL, Method of detection: suppressed conductivity.

2.4 Conclusions

HEIDA-silica and Poly-IDA chelating stationary phases were evaluated and compared for the detection and separation of alkali, alkaline earth, transition and rare earth metal cations using electrolytically generated MSA as eluent. The Poly-IDA column showed no selectivity for alkali metals, moderate selectivity for alkaline earth metals, and a strong affinity for transition and lanthanide metals. The HEIDA-silica column showed moderate affinity towards alkali metals, and alkaline earth, transition and lanthanide metal cations showed increasing retention respectively. The order of retention of the metal cations was consistent with their respective metal-IDA complex stability constants. Both isocratic and gradient separation methods were developed in order to improve the separation of a number of cations of different groups.

Using electrolytically generated MSA as eluent with suppressed conductivity detection, a number of lanthanides and yttrium were successfully separated in less than 15 minutes on the Poly-IDA column, which is the first reported incidence of this type of separation on a polymeric chelating column. It was shown that for the same separation under identical conditions, the HEIDA-silica column achieved significantly higher efficiency values, although the run time was considerably longer (~85 minutes). The effect of column temperature was carried out, with behaviour typical of a chelation retention mechanism observed on both columns.

Suppressed conductivity detection was determined to be a possible technique for the determination of metal cations. However, as prolonged use led to precipitation of the more strongly retained cations, detection with PCR proved a superior method of detection. The effects of MSA concentration on the lanthanides were studied using PCR, showing. The HEIDA-silica column, which provided superior efficiencies, was then employed to a 2-D separation of alkali metals on one dimension. Due to the excellent efficiencies they provided, the remainder of stationary phases investigated were silica based.

References

[1] C.-Y. Liu, N.-M. Lee, T.-H. Wang, Analytica Chimica Acta 337 (1997) 173.

[2] L. Barron, M. O'Toole, D. Diamond, P.N. Nesterenko, B. Paull, Journal of Chromatography A 1213 (2008) 31.

[3] W. Bashir, B. Paull, Journal of Chromatography A 942 (2002) 73.

[4] Á. Moyna, D. Connolly, E. Nesterenko, P.N. Nesterenko, B. Paull, Analytical and Bioanalytical Chemistry 405 (2012) 2207.

[5] Á. Moyna, D. Connolly, E. Nesterenko, P.N. Nesterenko, B. Paull, Journal of Chromatography A 1249 (2012) 155.

[6] http://www.dionex-france.com/library/literature/data_sheets/DS_FRIC_ER_IC_19Mar08_LPN2022_02.pdf.

[7] N. Karu, G.W. Dicinoski, M. Hanna-Brown, K. Srinivasan, C.A. Pohl, P.R. Haddad, Journal of Chromatography A 1233 (2012) 71.

[8] B. Paull, P.N. Nesterenko, P. Jones, High Performance Chelation Ion Chromatography, RSC Chromatography Monographs, Royal Society of Chemistry Publishing, Cambridge, UK (2011).

[9] W.W. Buchberger, P.R. Haddad, Journal of Chromatography A 789 (1997) 67.

[10] W.W. Buchberger, Trends in Analytical Chemistry 20 (2001) 296.

[11] P.R. Haddad, P.E. Jackson, M.J. Shaw, Journal of Chromatography A 1000 (2003) 725.

[12] http://www.dionex.com/en-us/products/columns/bio/protein/propac-imac/lp-73375.html.

[13] P.N. Nesterenko, M.J. Shaw, S.J. Hill, P. Jones, Microchem Journal 62 (1999) 58.

[14] J.N. King, J.S. Fritz, Journal of Chromatography A 153 (1978) 507.

[15] J.C. Dias, L.T. Kubota, P.N. Nesterenko, G.W. Dicinoski, P.R. Haddad, Analytical Methods 2 (2010) 1565.

[16] E. Sugrue, P. Nesterenko, B. Paull, Journal of Separation Science 27 (2004) 921.

[17] P.N. Nesterenko, P. Jones, Journal of Separation Science 30 (2007) 1773.

[18] P.N. Nesterenko, P. Jones, Analytical Communications 34 (1997) 7.

[19] P.N. Nesterenko, P. Jones, Journal of Chromatography A 804 (1998) 223.

[20] G.J. Sevenich, J.S. Fritz, Analytical Chemistry 55 (1983) 12.

[21] S. Elchuk, R.M. Cassidy, Analytical Chemistry 51 (1979) 1434.

[22] C.H. Knight, R.M. Cassidy, B.M. Recoskie, L.W. Green, Analytical Chemistry 56 (1984) 474.

[23] T.A. Walker, Journal of Liquid Chromatography 16 (1993) 1573.

[24] E. Tyrrell, R.A. Shellie, E.F. Hilder, C.A. Pohl, P.R. Haddad, Journal of Chromatography A 1216 (2009) 8512.

[25] A.R. Timerbaev, G.K. Bonn, Journal of Chromatography A 640 (1993) 195.

[26] P. Dugo, F. Cacciola, T. Kumm, G. Dugo, L. Mondello, Journal of Chromatography A 1184 (2008) 353.

[27] P. Jandera, Journal of Separation Science 29 (2006) 1763.

[28] K. Zhang, Y. Li, M. Tsang, N.P. Chetwyn, Journal of Separation Science (2013) In Press, DOI: 10.1002/jssc.201300493.

[29] J. Chong, P. Hatsis, C.A. Lucy, Journal of Chromatography A 997 (2003) 161.

3. Chelation ion chromatography of alkaline earth and transition metals using a monolithic silica column with bonded N-hydroxyethyliminodiacetic acid functional groups

Abstract

HPCIC has become an increasingly popular analytical method for the determination of metal cations in complex samples in recent years. Chelation exchange stationary phases offer a completely different selectivity relative to ion exchange materials based upon the formation of stable metal complexes with a bonded ligand such as HEIDA. Such stationary phases are particularly selective for transition and heavy metals, and selectivity control can be achieved both by eluent pH and by the use of high ionic strength eluents to suppress any competing retention mechanisms based upon cation exchange. In addition, chelating exchange phases are less sensitive to samples of high ionic strength. These advantages mean that routinely used spectroscopic methods such as AAS, AES and ICP-AES, which are both costly and time consuming, would no longer be necessary.

Therefore, a commercially available porous silica monolithic column (Onyx Monolithic Si, 100 × 4.6 mm I.D.) had previously been 'in-column' covalently functionalised with 2-HEIDA groups, and applied to the determination of selected alkaline earth and transition metal cations. Poor peak shapes and efficiencies suggested that an improved modification procedure was necessary to achieve homogeneous distribution of HEIDA groups. Therefore, an improved procedure was developed, and the silica monolith was applied simultaneous and rapid separation of alkaline earth and transition metal ions, using HPCIC. The baseline separation of various common transition, heavy metal ions and the four alkaline earth metal ions was achieved in under 14 min with a flow rate of just 0.8 mL/min. Significant effects from variation of eluent nature, concentration and temperature upon selectivity and retention were demonstrated with the new monolithic silica chelating phase. Under optimised conditions (0.165 *M* $LiNO_3$ eluent, pH 2.5), peak efficiencies of 54,000, 60,000 and 64,000 *N*/m, for Zn^{2+}, Mn^{2+} and Cd^{2+}, respectively, were recorded, which are higher than those observed on packed IDA-silica stationary phases.

Aims

The aim of this work was to improve the modification procedure of a monolithic silica phase with IDA based chelating functional groups and subsequently characterise selectivity and efficiency of the prepared stationary phase towards selected alkaline earth, transition and heavy metal cations. The effects of various parameters on retention and selectivity including eluent pH, complexing eluent, column temperature, eluent selectivity and flow rate were to be then investigated.

3.1 Introduction

Silica gel based stationary phases with bonded IDA groups have received considerable attention in recent years [1-7], both for the separation of metal ions in HPCIC, and more recently for separation of biomolecules in IMAC [8,9]. The use of monolithic substrates to support IDA groups is also a relatively recent development, although most attention has focused upon polymeric monoliths, which although suitable for larger biomolecule separations in IMAC mode [10-12], provide only limited potential at this stage for separation of metal ions in HPCIC applications [13,14]. In contrast, relatively little attention has been paid to silica monoliths with bonded IDA based groups.

Monolithic silica stationary phases offer several advantages over particle packed beds. Due to the monolith morphology (Fig. 3.1), i.e. the presence of large flow-through pores, these stationary phases are characterised by their relatively low column pressure drop, even whilst operating at higher than normal mobile phase flow rates.

In addition, monolithic phases provide what is described as ‘convection based diffusion’, which results in maintenance of a smaller C-term when applied under such elevated mobile phase flow conditions, helping to maintain peak efficiency [16]. At the same time, the presence of mesopores within the monolithic skeleton provides the developed surface area required for chromatography of small molecules, a primary reason for the popularity of monolithic silica columns for reversed-phase separations. When compared to polymer based monolithic phases, it is fair to conclude that silica monoliths provide a more uniform and reproducible skeleton, with greater surface area, and higher peak

efficiencies for small molecules and ions [17].

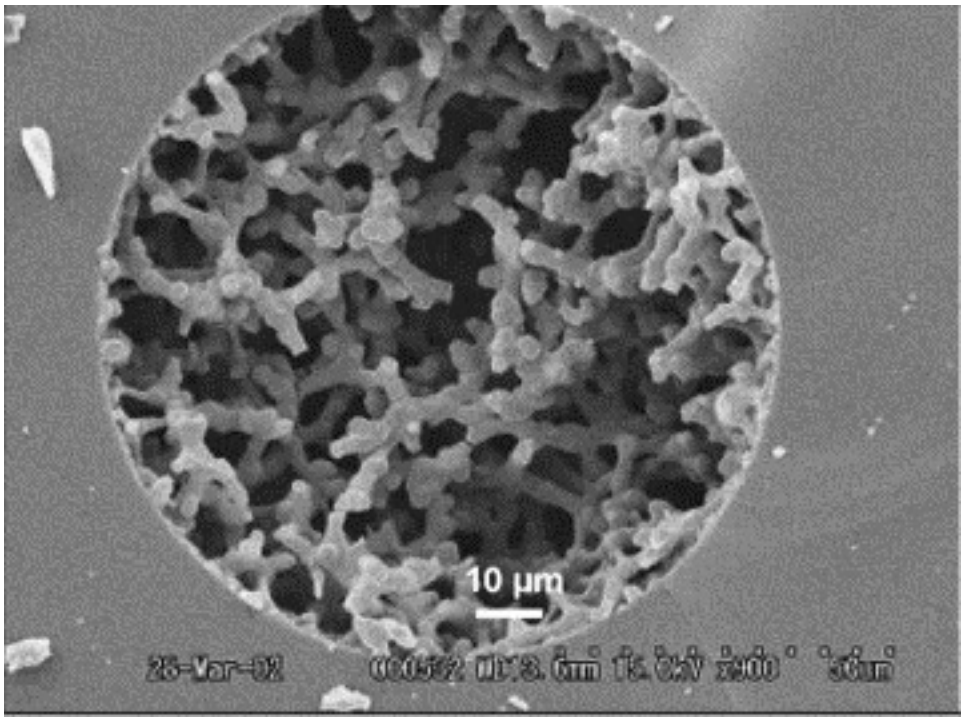

Fig. 3.1: Scanning electron microscopy (SEM) image from the cross section of a monolithic silica capillary column [15].

Sugrue *et al.* [18,19] were the first to report upon a silica monolith covalently modified "in column" with bonded IDA based ligands. In preliminary work [18], alkaline earth metals were rapidly separated on the modified monolithic phase, with Ca^{2+} and Mg^{2+} determined at low mg/L levels in saline samples. The selectivity and capacity of the column were compared with a particle packed silica stationary phase, where selectivity was found to be the same. In further work [19], this stationary phase was fully characterised for selectivity towards alkaline earth metal and selected transition metal ions. However, in this work Sugrue *et al*. were only able to demonstrate the isocratic baseline separation of four transition and heavy metals, namely Mn^{2+}, Cd^{2+}, Zn^{2+} and Pb^{2+}, in that order. In addition, the modified monolith exhibited extremely poor peak shape for Zn^{2+}, indicating secondary retention and possible interactions with the supporting silica matrix. Subsequent elemental analysis along the length of the column identified that the IDA based groups were heterogeneously distributed, resulting in free

silica surface and silanol groups, particularly in the second half of the column. Indeed, the work clearly highlighted the need for further investigations to provide enhanced surface coverage of IDA containing groups, and attention to their homogenous longitudinal distribution.

Therefore, in the work presented in this chapter, a much improved modification procedure has been applied, which resulted in a more homogenous distribution of the bonded IDA based groups. The bonding chemistry applied produces a HEIDA functionalised phase, which delivers greater capacity, as demonstrated through the separation of a considerably larger number of metals, with greatly improved peak shape and efficiency. A detailed study of the selectivity and performance of the new HEIDA modified monolithic phase is presented, with the effects of eluent (both nature and ionic strength), pH, column temperature, flow rate, and addition of eluent complexing agent upon the resultant selectivity assessed and discussed.

3.2 Experimental

3.2.1 Instrumentation

For the chromatographic studies and column characterisation, two chromatographic systems were used. Firstly, a Waters 2695 HPLC system with dual wavelength absorbance detector, Model 2487 (Waters, Milford, MA, USA) was used to determine the capacity of the column. Empower 3 software (Waters, Milford, MA, USA) was used for data acquisition with this chromatographic system. Secondly, for ion chromatographic separations, a Metrohm IC system was used, comprised of a Model 844 Compact IC, Model 830 IC Interface (Metrohm, Herisau, Switzerland), and coupled to a Shimadzu UV/Vis detector, model SPD-10AV (Shimadzu, Kyoto, Japan). The system included a 20 µL polyetheretherketone (PEEK) manual sample loop. Post-column reaction detection was performed using 4-(2-pyridylazo)-resorcinol (PAR) as the post-column reagent (PCR), delivered by peristaltic post-column pump (within Metrohm 844 Compact IC). The wavelength used was 510 nm, or 540 nm where stated. ICNet 2.3 SR4 software (Metrohm, Herisau, Switzerland) was used for data acquisition and processing of chromatograms.

3.2.2 Reagents

Analytical or higher grade reagents and Milli-Q water (Millipore, Bedford, MA, USA) were used for the preparation of all solutions. Copper sulphate and potassium chloride used for determination of column capacity were sourced from Sigma Aldrich (St. Louis, MO, USA). Nitric acid eluents were prepared from 70% nitric acid (Chem Supply, Australia). Metal salts for eluent preparation were from BDH Ltd. (Poole, UK) (including sodium nitrate, potassium nitrate, and strontium carbonate), VWR AnalaR Normapur (Australia) (barium nitrate and ammonium nitrate), or JT Baker (Netherlands) (lithium carbonate). Strontium and lithium carbonate salts were titrated with 5 *M* HNO_3 to generate desired strontium and lithium nitrate eluents, respectively. Post-column reagent PAR was purchased from Kodak (Rochester, NY, USA). Ammonium hydroxide (28%) for the preparation of the PCR reagent was supplied by Fluka (Glossop, UK). Dipicolinic acid (DPA) (as pyridine-2,6-dicarboxylic acid, 99%) was obtained from Sigma–Aldrich (Sydney, Australia). Spectrosol atomic absorption standard solutions containing Ca^{2+}, Sr^{2+}, Mg^{2+}, Ba^{2+}, Mn^{2+}, Co^{2+}, Cd^{2+}, Zn^{2+}, Pb^{2+}, Cu^{2+} and Fe^{3+}, with concentrations 1.00 g/L were purchased from BDH Chemicals (Poole, UK). Metal standard solutions were prepared from stock standards in acidified Milli-Q water, and stored in polypropylene bottles. Working standards were prepared on each day of use unless stated otherwise. All eluents were filtered before use through 0.22 μm nylon membrane filters and degassed using sonication.

3.2.3 Detection

The PCR solution used for the detection of transition metal ions for comparison was composed of 0.15 m*M* PAR, 2.0 *M* NH_4OH, pH 10.5 [20]. For separations involving both alkaline earth metals and transition/heavy metals, the PCR solution was modified through the addition of 0.2 m*M* ZnEDTA, to enable detection of the alkaline earth metal ions via ligand exchange with Zn^{2+} [21].

3.2.4 Modification of silica monolith

A 100 × 4.6 mm I.D. bare silica monolithic column (Onyx Monolithic Si), was purchased from Phenomenex (Cheshire, UK). According to the manufacturer, the silica monolith had a surface area of 300 m^2/g, equal to a total surface area of monolithic silica within the column of approximately 240 m^2. This silica exhibits a bimodal porous structure, comprised of macro-pores of 2 mm diameter and mesopores of 13 nm. The surface of the silica monolith was first activated by passing distilled water (DW) through the column for 24 h at 60 °C. Typical surface silanol density for silica dioxide is 4.6 silanol groups per 1 nm^2, approximately half of which are sterically able to react with bulky trimethoxy-anchor groups [22]. Following surface activation, 80 mL of an aqueous solution of approximately 20-fold excess of 3-glycidoxypropyltrimethoxysilane and 60-fold excess of IDA to relatively available silanols was recycled through the column to modify the monolithic silica with the resulting *N*-hydroxyethyliminodiacetic acid groups. The column was then flushed with the modification solution once more in the reverse direction, from outlet to inlet. This procedure was repeated twice more, once in each direction. The reagent mixture was recycled at 0.5 mL/min for a total of 20 h. Following modification, the column was then washed with 0.01 *M* nitric acid for 1 h to remove the residual reagent. Equilibration was performed with a nitric acid eluent overnight before initial use.

3.2.5 Determination of column capacity and efficiency

The column was washed for 1 h with 10 m*M* dipicolinic acid solution, pH 4.15 to remove any metal ion contaminants from the column, followed by 1 *M* KCl solution for 1 h to remove DPA, and finally deionised water for 1 h to remove any excess salt. The column was saturated with 20 m*M* $CuSO_4$ solution at a flow rate of 1.0 mL/min until breakthrough, as determined using UV absorbance detection at 210 nm. The resultant column capacity was found to be 134 µmol/column. This can be compared to the capacity of the original silica monolith, which was determined in the same way prior to modification, and was found to be ~75 µmol/column. Efficiency data was calculated using the standard USP formula, $N = 5.54\ (t/W_{h/2})^2$. No correction for extra column band

broadening due to post-column reaction tubing was included within the calculation.

3.2.6 Speciation diagrams

Speciation plots were constructed using Medusa and Hydra free software for chemical equilibrium calculations developed by Puigdomenech [23]. Stability constants (log β, 0.1 *M* ionic strength) used to construct speciation plots were as follows for Ca^{2+} and Cu^{2+} containing complexes; CaDPA = 4.36; CuDPA = 9.1; $Ca(DPA)_2$ = 7.4; $Cu(DPA)_2$ = 16.4; $CuHDPA^{-}$ = 11.1; CaHEIDA = 4.69; CuHEIDA = 11.75. Values for protonated ligands and minor complexes not present in acid solution were omitted for clarity. Values were sourced from NIST [24].

3.3 Results and discussion

Recently, the substantial contribution of bonding chemistry on metal selectivity of IDA-containing chelating phases has been reported [13,14,22]. These observations have highlighted how important linker or bonding chemistry is when considering the chelating properties and selectivity of the modified phase.

The retention behaviour of alkaline-earth metals on a monolithic silica column partially modified with IDA groups has been previously documented [19]. In this particular type of stationary phase, the IDA molecules were attached to the silica surface via a 3-glycidoxypropyl linker group, providing substitution of a proton at the nitrogen atom in IDA with an *N*-hydroxyethyl radical. As a result, the properties of this stationary phase should be more related to the complexing properties of *N*-hydroxyethyliminodiacetic acid than simple IDA.

With the above clarification in mind, it was clear that it was necessary to evaluate the chromatographic performance of a fully functionalised HEIDA monolith, for both alkaline earth and transition metals. Therefore in an attempt to characterise this column, and demonstrate unique column selectivity and obtain maximum possible efficiency, a number of different operational and eluent parameters were investigated as follows.

3.3.1 Eluent pH (HNO_3)

Eluent pH has a drastic effect upon retention of both alkaline earth and transition metal cations on IDA modified phases, as pH governs the conditional stability constants (K') describing the formation of the metal-IDA complexes. Using dilute HNO_3 only eluents, ranging from 2 to 10 m*M*, selectivity and retention of alkaline earth and selected transition metal ions was recorded. For this set of experiments both flow rate and column temperature were kept constant (0.8 mL/min and 25 °C, respectively).

As expected, the relationship between the retention (log k) and HNO_3 concentration (log C_{HNO3}) was determined to be linear over the range 6.0–10.0 m*M* HNO_3, (with slopes ranging from −2.21 to −2.25 for transition metal ions, and from −2.38 to −2.49 for alkaline earth metals and Mn^{2+}), although slight but reproducible deviation from this correlation was seen at the lowest HNO_3 concentration (Fig. 3.2).

The elution order, which remained constant within the limited pH window, was $Mg^{2+} < Sr^{2+} \leq Ca^{2+} < Mn^{2+} < Ba^{2+} < Co^{2+} < Cd^{2+} < Zn^{2+} \ll Pb^{2+} \ll Cu^{2+}$. The contribution to retention/selectivity for the above cations from both simple ion exchange and complexation (mixed mode) is clear from the above elution order for the alkaline earth cations. That is, neither mode is particularly dominant, with Ba^{2+} being controlled mainly by ion exchange (very large ion exchange selectivity coefficient) and Ca^{2+} eluting after Sr^{2+}, showing some complexation effect (Fig. 3.5(a)).

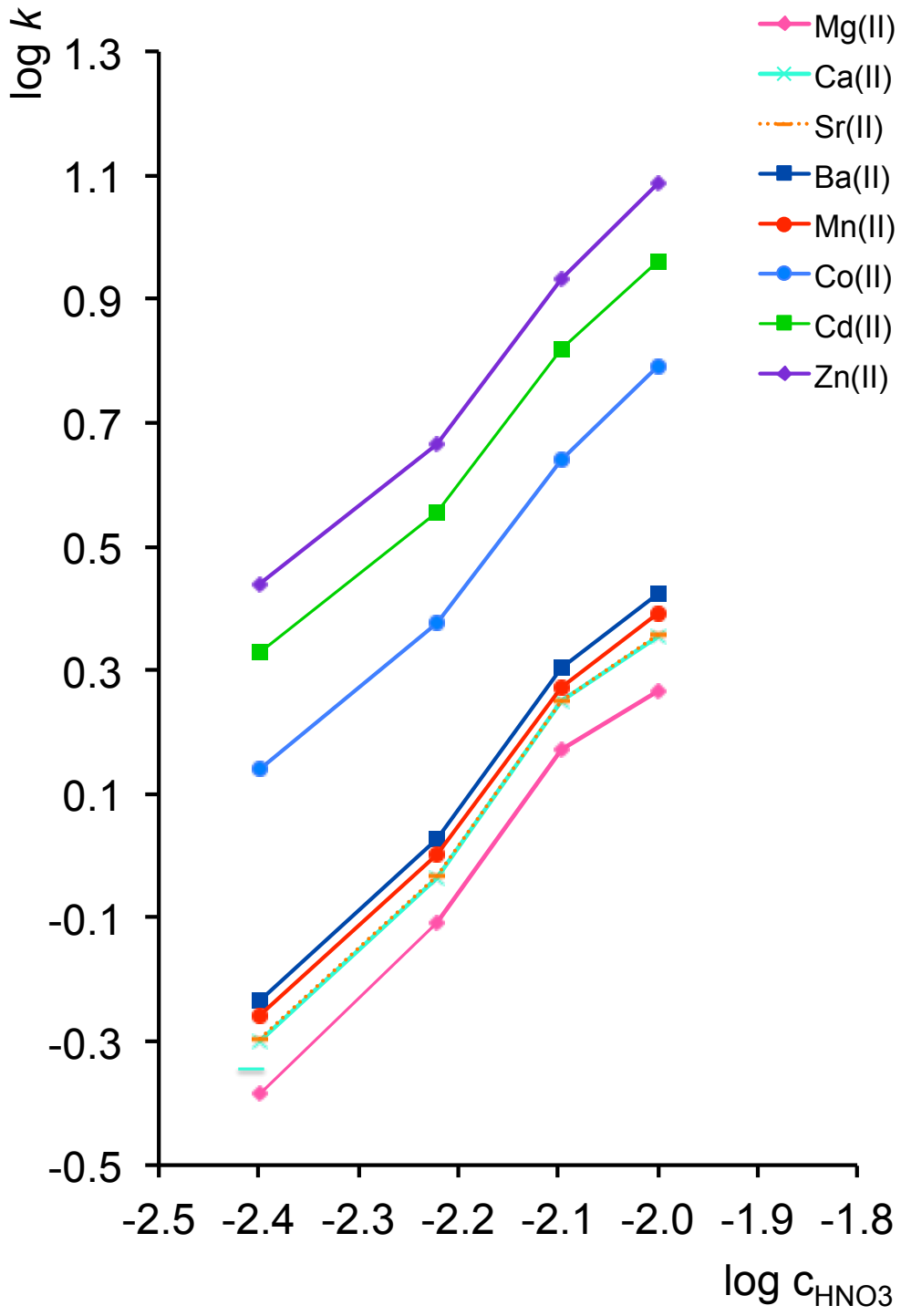

Fig. 3.2: Effect of HNO_3 concentration on retention of alkaline earth, transition and heavy metal cations. Eluent: 4–10 m*M* HNO_3, Flow rate: 0.8 mL/min, Column temperature: 25 ° C, Injection volume: 20 µL, Detection: spectrophotometric at 510 nm after PCR with 0.15 m*M* PAR, or 540 nm after PCR with 0.2 m*M* ZnEDTA/0.12 m*M*

PAR.

Thus it can be seen that the elution order somewhere between that shown on simple sulfonated cation is exchange resins ($Mg^{2+} > Ca^{2+} > Sr^{2+} > Ba^{2+}$) and the complete reverse order, assuming pure chelation, with regard to the known stability constants for these cations with HEIDA in solution, which increase in order $Ba^{2+} < Sr^{2+} < Ca^{2+} < Mg^{2+}$ [25]. For the transition metal ions, the selectivity shown was as expected, with increasing retention corresponding to increasing stability constants, and thus indicating complex formation is playing the major role in retention, confirming that the stationary phase has indeed been modified with HEIDA and exhibits typical selectivity.

3.3.2 Complexing eluents

As the underlying selectivity of chelating phases used within HPCIC is governed primarily by the differences in stability constants between the metal ion and the immobilised chelating ligand, the ability to separate large numbers of metal ions isocratically on such phases is limited, due to the large differences in stability constants for otherwise similarly charged cations, e.g. for IDA (ML) complexes, $I = 0.1$, 25 °C, β_1 = 1.67 (Ba^{2+}), 2.98 (Mg^{2+}), 5.71 (Cd^{2+}), 7.36 (Pb^{2+}) and 10.56 (Cu^{2+}) [21]. Therefore, to reduce such large selectivity differences and allow rapid isocratic separations in HPCIC, it is usual to add a complexing ligand to the eluent, whose effect upon retention will be opposite to that of the stationary phase. In this case competitive complexation occurs between the metal ions and ligands in both the eluent and upon the surface of the stationary phase. Nesterenko and coworkers [25] have previously taken a novel approach to predict the selectivity of common metal ions on similarly modified IDA-silica gel, following the addition of various complexing agents to the eluent, via plotting the stability constants of the complexing agents against those of IDA-metal complexes. Nesterenko and Jones demonstrated the strong effect of DPA on the retention and selectivity of metal cations, in particular Pb^{2+} and Cu^{2+}. Therefore, in this current study, low concentrations of DPA (range 0.1–0.5 m*M*) were added to a 4 m*M* HNO_3 eluent and retention data gathered. The effect of DPA concentration on retention factors for various metal cations is shown in Fig. 3.3.

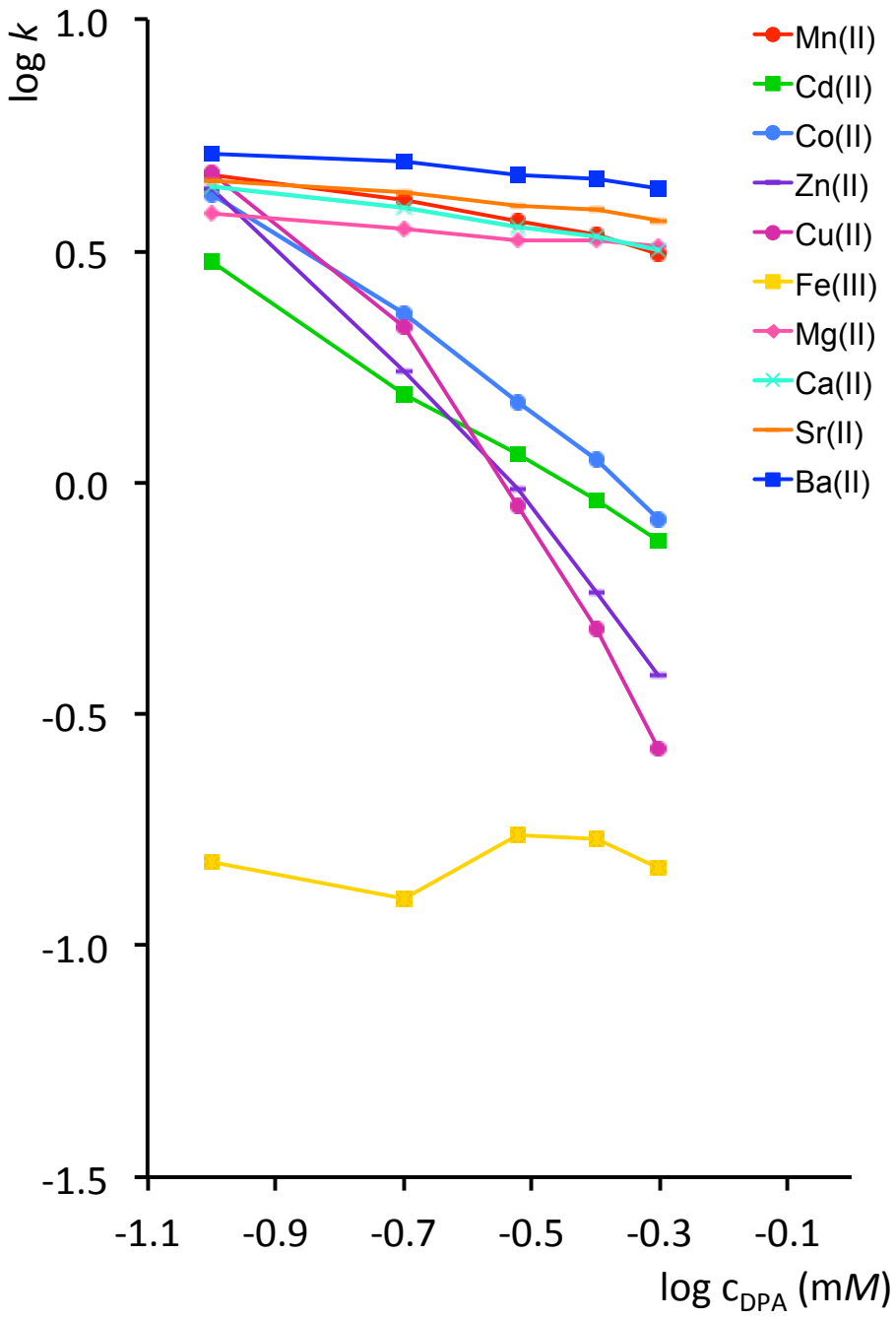

Fig. 3.3: Effect of concentration of dipicolinic acid (DPA, m*M*) on retention of alkaline earth, transition and heavy metal cations. Eluent: 4 m*M* HNO_3 and 0.1 – 0.5 m*M* DPA, Flow rate: 0.8 mL/min, Column temperature: 25 °C, Injection volume: 20 µL, Detection: spectrophotometric at 510 nm after PCR with 0.15 m*M* PAR, or 540 nm after PCR with 0.2 m*M* ZnEDTA/0.12 m*M* PAR.

From the data shown it can be seen that the use of DPA as a complexing agent produces a significant change in system selectivity for various metal cations as compared to stationary phase only complexation. Retention decreased dramatically for transition metal cations in comparison to alkaline earth metals, with the exception of Mn^{2+}, which was less affected over the concentration range, continuing to co-elute within the isolated grouping of alkaline earth metal ions. Compared with the retention data for stationary phase complexation (Fig. 3.2), the inclusion of DPA within the eluent provides a complete reversal in overall elution order for the two distinct sets of metal ions (alkaline earths and transition metal ions), providing a very elegant means for cross-confirmation of peak identity, where required. The slopes in this instance would correlate very closely to the stability constants of each cation with the eluent ligand, e.g. for DPA (ML) complexes, β_1 = 3.44 (Ba^{2+}), 4.36 (Ca^{2+}), 5.01 (Mn^{2+}), 6.36 (Co^{2+}, Cd^{2+}), 8.70 (Cu^{2+}), and 10.91 (Fe^{3+}) [21]. In the case of Fe^{3+}, the metal was completely unretained across the conditions shown, forming a stable negatively charged 1:2 DPA complex (ML_2^-), which would be completely excluded from the negatively charged stationary phase.

With the addition of a competing complexing ligand within the eluent, the effect upon overall selectivity of eluent pH is less predictable than shown above (Section 3.3.1). To demonstrate this, and to illustrate the drastic effect upon observed selectivity eluent pH would play within a mechanism based upon competitive complexation, the concentration of HNO_3 was adjusted between 2 and 10 m*M*, within a 4 m*M* KNO_3/0.3 m*M* DPA containing eluent. The dramatic results can be seen in Fig. 3.4. From the trends shown a number of clear conclusions can be made.

Firstly, for alkaline earth metal ions and Mn^{2+}, whilst there may be only a small amount of eluent phase complexation, it is still sufficient to dominate stationary phase complexation, thus ensuring that retention is primarily cation exchange based for this group of cations. Therefore, retention decreases with increasing eluent acidity (increasing concentration of competing cation [H_3O^+]), and increased protonation of the bonded HEIDA (for free HEIDA, pK_a^1 = 1.60; pK_a^2 = 2.20 [26]).

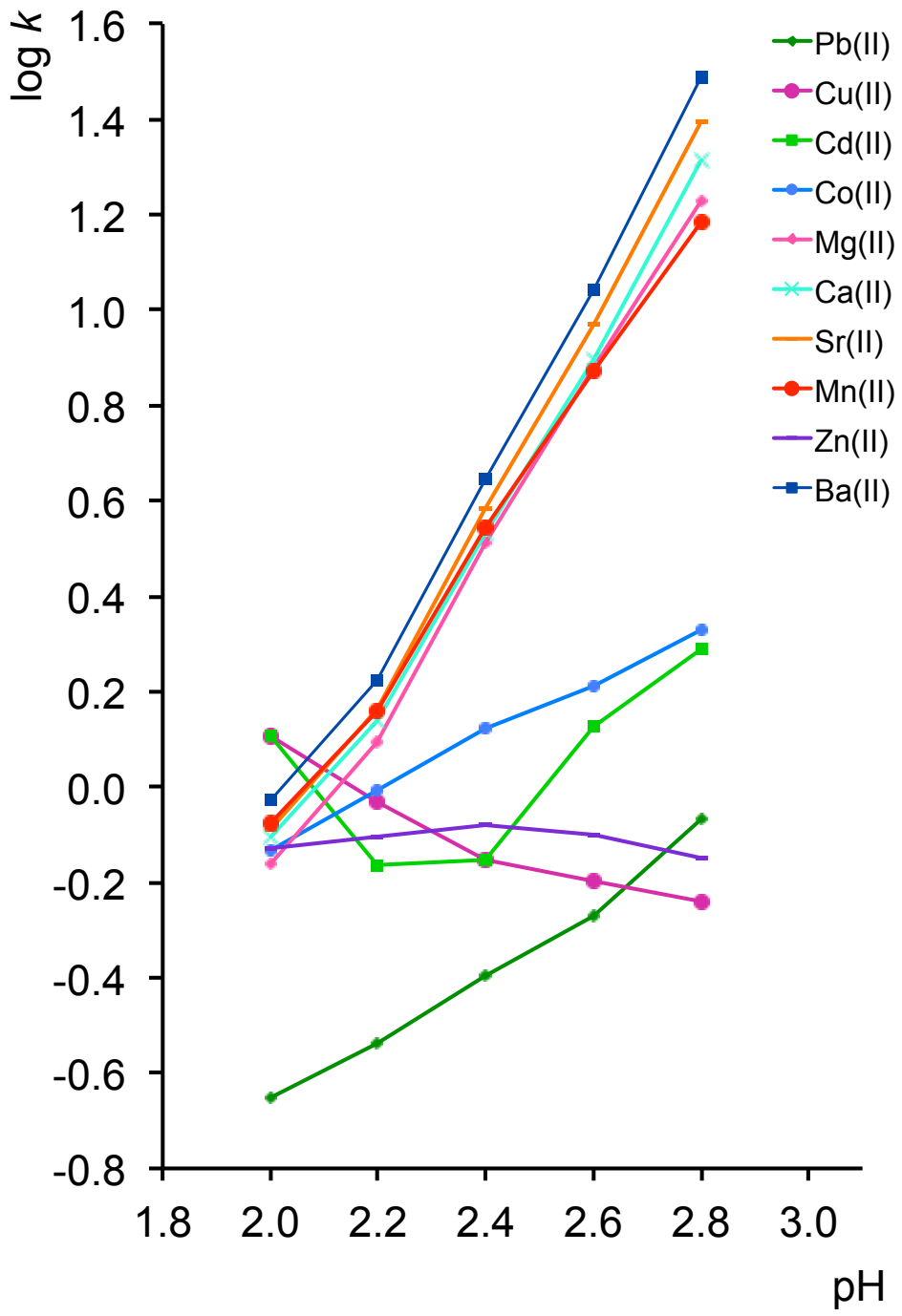

Fig. 3.4: Effect of eluent pH on retention of alkaline earth, transition and heavy metal cations. Eluent: 4 m*M* HNO_3/0.3 m*M* DPA and 2.0–10.0 m*M* HNO_3, Flow rate: 0.8 mL/min, Column temperature: 25 °C, Injection volume: 20 µL, Detection: spectrophotometric at 510 nm after PCR with 0.15 m*M* PAR, or 540 nm after PCR with 0.2 m*M* ZnEDTA/0.12 m*M* PAR.

Secondly, a number of transition metal ions show a significant increase in retention as eluent pH is increased, namely Pb^{2+} and Co^{2+}, this being similar to that seen without DPA (Section 3.3.1), thus suggesting the dominance of stationary phase complexation, although some eluent phase complexation is also having an effect upon the observed slope. The retention data for Cd^{2+}, Zn^{2+} and Cu^{2+} are all quite unusual, with Zn^{2+} showing only minimal dependence, suggesting the strength of both stationary phase and eluent phase complexation is well matched, with Cu^{2+} uniquely exhibiting a very clear decrease in retention as the eluent pH was increased, indicating the dominance of eluent Cu–DPA complexation. The trend for Cd^{2+} was unusual, initially showing a decrease in retention, but generally showing an increase similar to that seen with Co^{2+}.

To investigate these effects further, speciation curves were constructed for Ca^{2+} and Cu^{2+} ions with HEIDA (100 m*M*), the closest solution phase analogue to the immobilised ligand [22], in the presence of DPA (0.3 m*M*). Fig. 3.5 (a) and (b) shows these speciation data for the two metal ions, and clearly support the retention data in Fig. 3.4. Under the pH conditions investigated Ca^{2+} remains predominantly uncomplexed, with DPA complexation not becoming significant until pH 3.0 and upwards. However, the Ca^{2+} speciation plots also show some minimal HEIDA complexation under these acidic conditions. For Cu^{2+} ions the speciation curves are significantly different, with Cu^{2+} being strongly complexed with either DPA or HEIDA across the pH range shown. It should be pointed out that the MHEIDA plots represent the proportion of metal complexed on the monolith substrate and the $M(DPA)_x$ plots represent the proportion of metal complexed in the eluent. Interestingly, within this dual complexing system, HEIDA shows dominance over the pH range 1.3–2.2, which explains clearly the increase in retention of Cu^{2+} below pH 2.2 shown in Fig. 3.4. Above this pH, the formation of the negatively charged ML_2^{2-} complex rapidly becomes dominant over stationary phase complexation, resulting in the significant reduction in retention, from being most retained, to eluting first, over the eluent conditions shown.

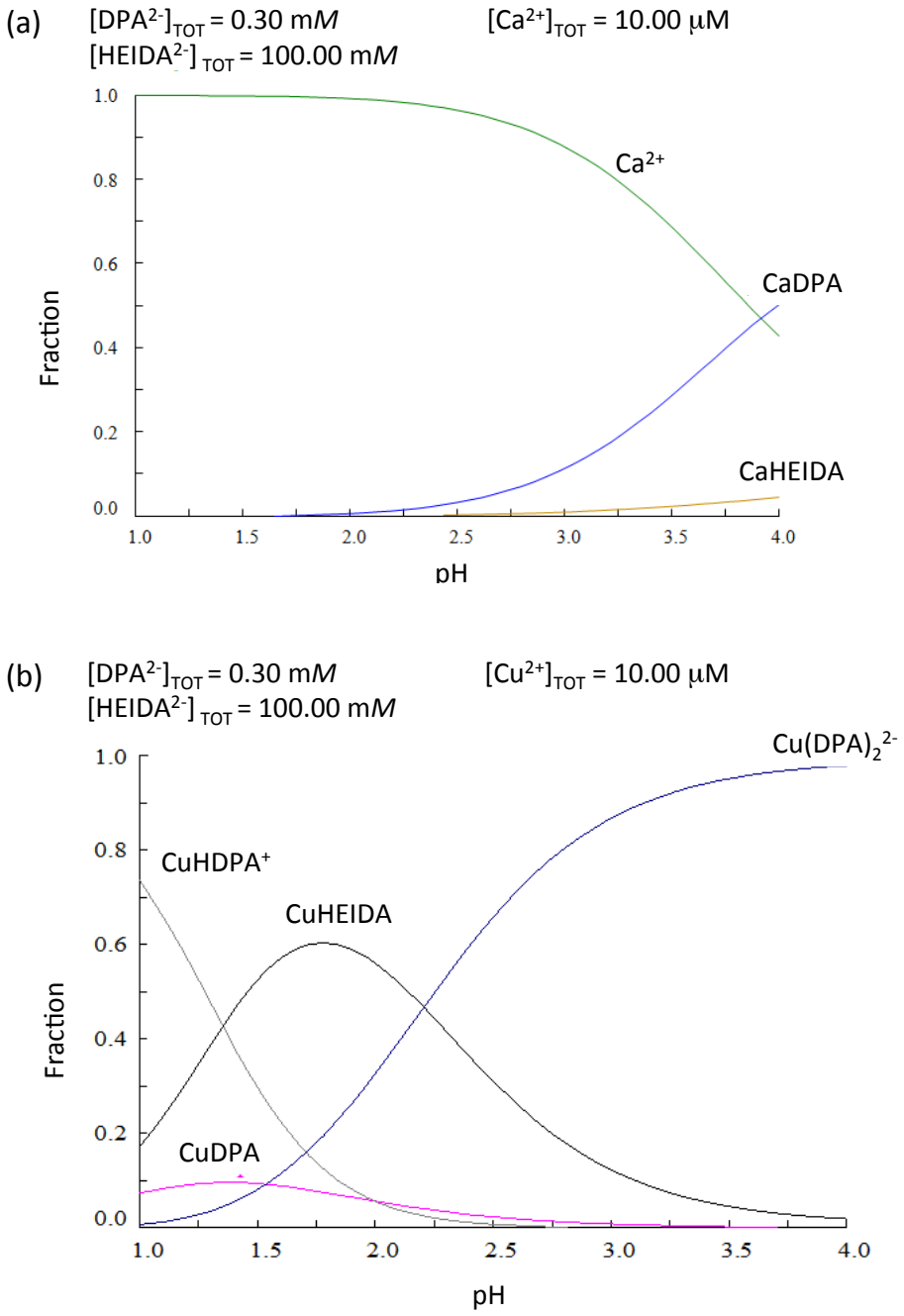

Fig. 3.5: (a) Speciation diagram for Ca^{2+} in the presence of 0.3 m*M* DPA and 100 m*M* N-hydroxyethyliminodiacetic acid (HEIDA). (b) Speciation diagram for Cu^{2+} in the presence of 0.3 m*M* DPA and 100 m*M* HEIDA.

Overall the versatility of the system for control of selectivity is clear from Figs. 3.2 to 3.5, as several very different elution orders can be obtained across a relatively small pH window. These selectivity changes are illustrated within the following selectivity matrix (Fig. 3.6).

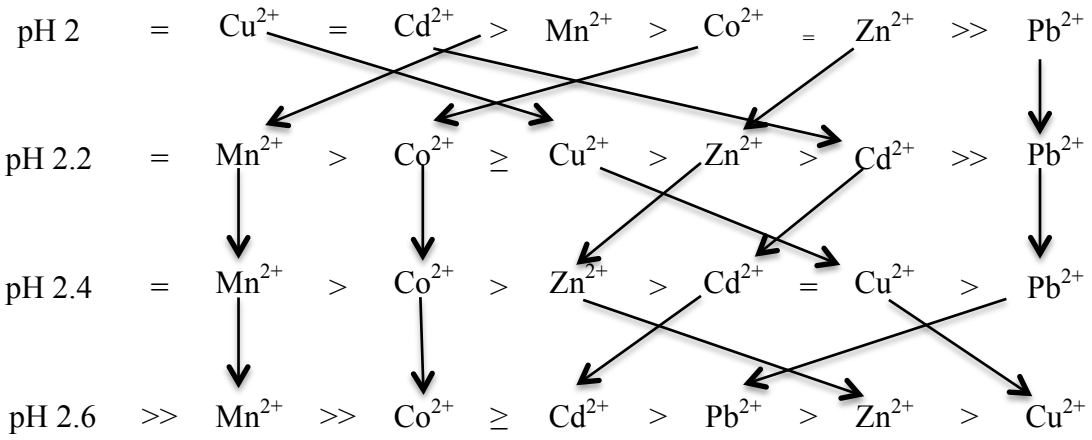

Fig 3.6: Selectivity matrix of metal cations Mn^{2+}, Co^{2+} Cd^{2+} and Zn^{2+} at varying pH values.

3.3.3 Effect of column temperature

The effects of temperature in chelation ion chromatography have been discussed in detail in Chapter 1. A van't Hoff plot for alkaline earth and transition metal ions on the HEIDA-silica monolith was constructed (Fig 3.7). The eluent (pH 2.4) in this instance includes DPA, albeit at a low concentration (0.3 m*M*). Therefore, the observed slopes potentially reflect retention involving both stationary and mobile phase complexation. Metal ions were chromatographed at increasing temperatures over the range 25–60 °C. The resultant van't Hoff plot very clearly shows three very different responses. Firstly, the plots show how an increase in temperature had very little effect on retention of alkaline earth metals and Mn^{2+} (slopes for Ca^{2+}, Mg^{2+} and Mn^{2+} = −0.103, −0.050 and −0.128, respectively), with a slight decrease seen in the retention of Sr^{2+} and Ba^{2+} (slopes = 0.017 and 0.083, respectively).

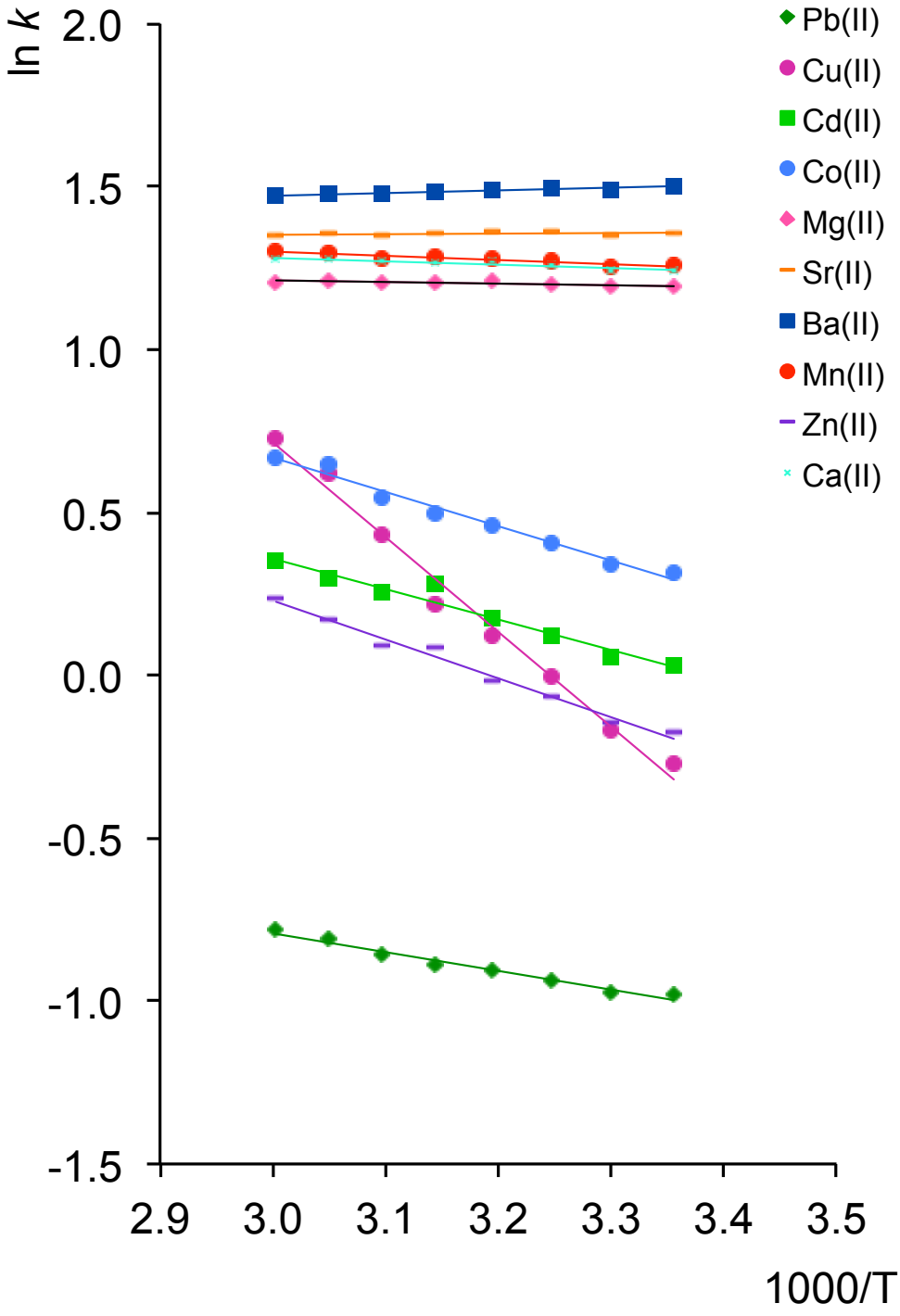

Fig. 3.7: Effect of column temperature (25–60 °C) on retention of alkaline earth, transition and heavy metal cations. Eluent: 4 m*M* HNO_3/0.3 m*M* DPA, Flow rate: 0.8 mL/min, Injection volume: 20 µL, Detection: spectrophotometric at 540 nm after PCR with 0.2 m*M* ZnEDTA/0.12 m*M* PAR.

Secondly, the dependences exhibited by Co^{2+}, Cd^{2+}, Zn^{2+} and Pb^{2+} were all very similar (slopes = −1.052, −0.933, −1.192 and −0.575, respectively), all showing a moderate increase in retention with temperature. Finally, the data clearly shows the unique behaviour of Cu^{2+} within this system (slope = −2.909), which exhibited a much greater increase in retention in response to temperature, resulting in a complete change in elution order amongst this core group of transition metal ions. Fig. 3.5 suggests that under the conditions tested (pH 2.4), stationary phase complexation should still be significant for Cu^{2+}, and that increased temperature would appear to favour stationary phase complexation over eluent DPA complexation. How this data looks chromatographically can be seen in Fig. 3.8, where Cu^{2+} shows a greater shift in retention relative to the other analytes, eluting prior to Cd^{2+} at 25 °C and after Cd^{2+} at > 45 °C.

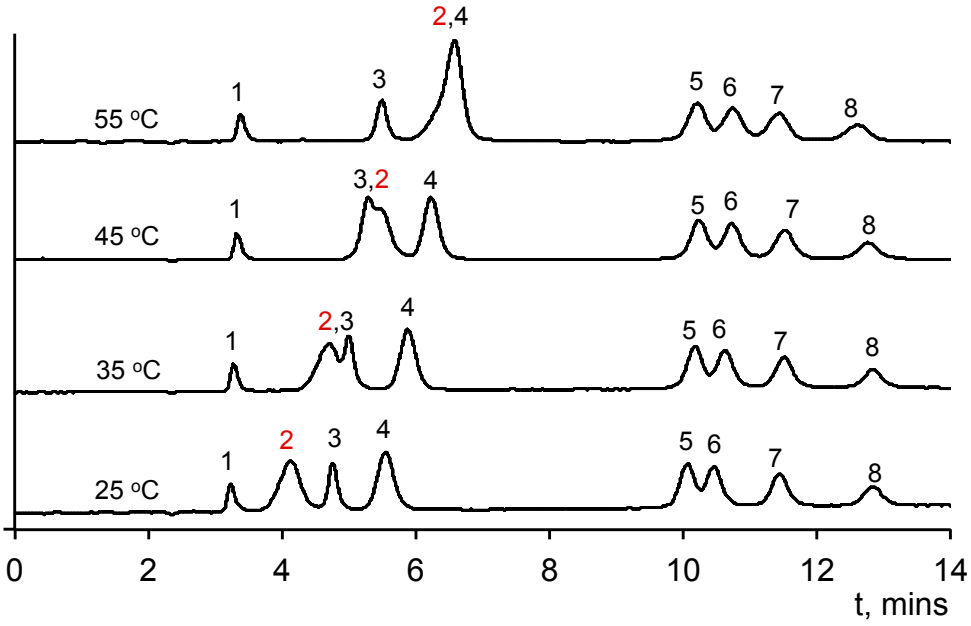

Fig. 3.8: Effect of column temperature (25 – 60 °C) on separation of alkaline earth, transition and heavy metal cations. Peaks: 1: 2.8 ppm Pb^{2+}, 2: 1.5 ppm Cu^{2+}, 3: 3.0 ppm Cd^{2+}, 4: 0.7 ppm Co^{2+}, 5: 0.9 ppm Mg^{2+}, 6: 1.25 ppm Ca^{2+}, 7: 1.75 ppm Sr^{2+}, and 8: 1.75 ppm Ba^{2+}. Eluent: 4 m*M* HNO_3/0.3 m*M* DPA, Flow rate: 0.8 mL/min, Injection volume: 20 µL, Detection: spectrophotometric at 540 nm after PCR with 0.2 m*M* ZnEDTA/0.12 m*M* PAR.

These results support those reported by Bashir and Paull [5], who carried out a similar temperature study on an IDA modified silica gel column, confirming the effect is independent of nature of the supporting silica substrate. The other notable effect is the closing of the elution window of the alkaline earth cations (and Mn^{2+}), as Ca^{2+}, Mn^{2+} (and to a lesser extent Mg^{2+}), each exhibit an increase in retention, whereas Sr^{2+} and Ba^{2+} exhibit the opposite trend.

3.3.4 Eluents selectivity

Within HPCIC it is known that increasing the ionic strength of the eluent via the addition of electrolytes (commonly KNO_3 at concentrations of 0.5–1.0 *M*), acts to suppress retention based upon electrostatic interactions, namely ion exchange, and thus ensure retention is dominated by complexation reactions [27]. To-date however, the effect upon system selectivity of the nature of the electrolyte added (specifically the cation) has not been achieved, with the exception of some limited observations upon the effects of adding either KCl or NaCl to the eluent, most notably in relation to the reduced retention of Cd^{2+} and Pb^{2+}, due to the formation of relatively stable chloro-complexes [5,22].

Therefore, here a series of eluents were prepared from various alkali and alkaline earth nitrate salts, together with an ethylenediamine based eluent. These eluents were then investigated for their effect upon the retention of transition metals cations, at concentrations of 0.165 *M* (for both alkali and alkaline earth salts) and 0.5 *M* (for alkali salts only), and at pH 2.0 and 2.5 (using HNO_3). Eluents produced using the alkaline earth salts could not be prepared at 0.5 *M* due to solubility limitations and a high baseline absorbance from post-column reaction absorbance detection with PAR. The resultant retention data is combined within Fig. 3.9 (a-f).

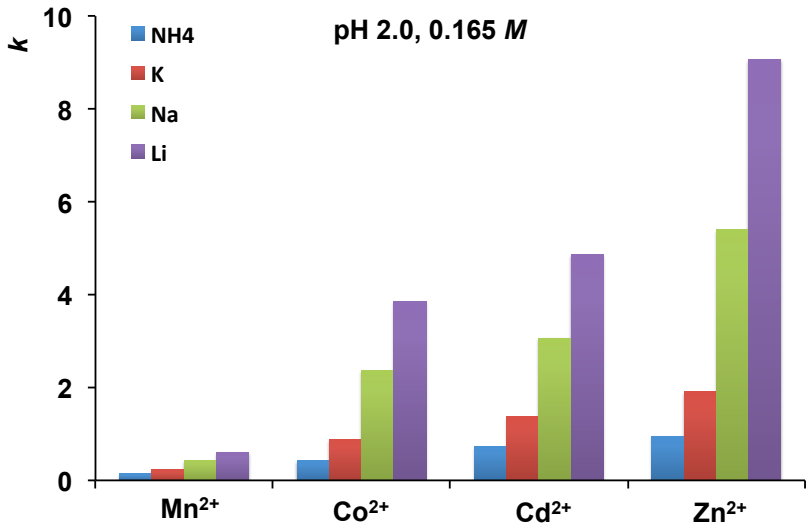

Fig. 3.9 (a): Effect of eluent cation (monovalent) upon retention of transition metal ions at concentration 0.165 *M*, at pH 2.0 (HNO_3). Flow rate: 0.8 mL/min, Column temperature: 25 °C, Injection volume: 20 µL, Detection: spectrophotometric at 510 nm after PCR with 0.15 m*M* PAR.

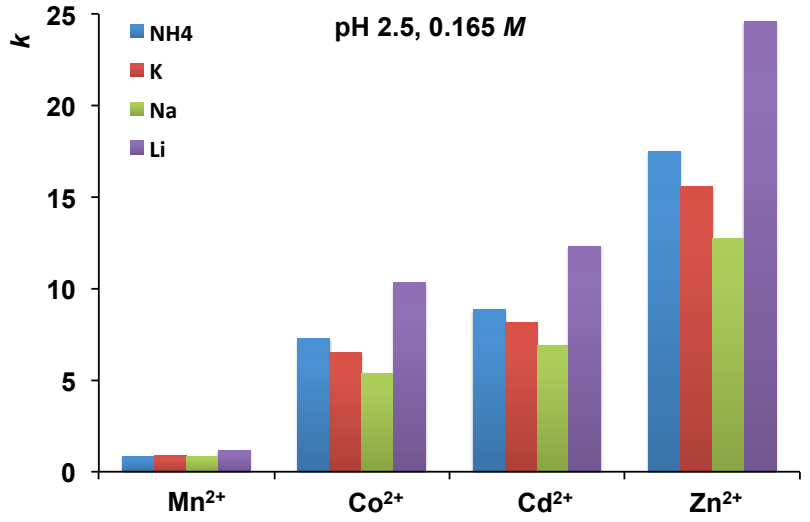

Fig. 3.9 (b): Effect of eluent cation (monovalent) upon retention of transition metal ions at concentration 0.165 *M*, at pH 2.5 (HNO_3). Flow rate: 0.8 mL/min, Column temperature: 25 °C, Injection volume: 20 µL, Detection: spectrophotometric at 510 nm after PCR with 0.15 m*M* PAR.

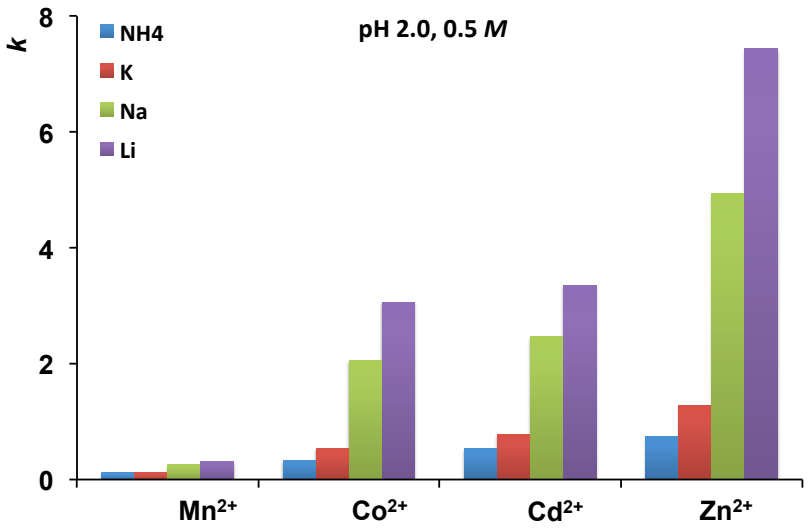

Fig. 3.9 (c): Effect of eluent cation (monovalent) upon retention of transition metal ions at concentration 0.5 *M*, at pH 2.0 (HNO_3). Column temperature: 25 °C, Flow rate: 0.8 mL/min, Column temperature: 25 °C, Injection volume: 20 µL, Detection: spectrophotometric at 510 nm after PCR with 0.15 m*M* PAR.

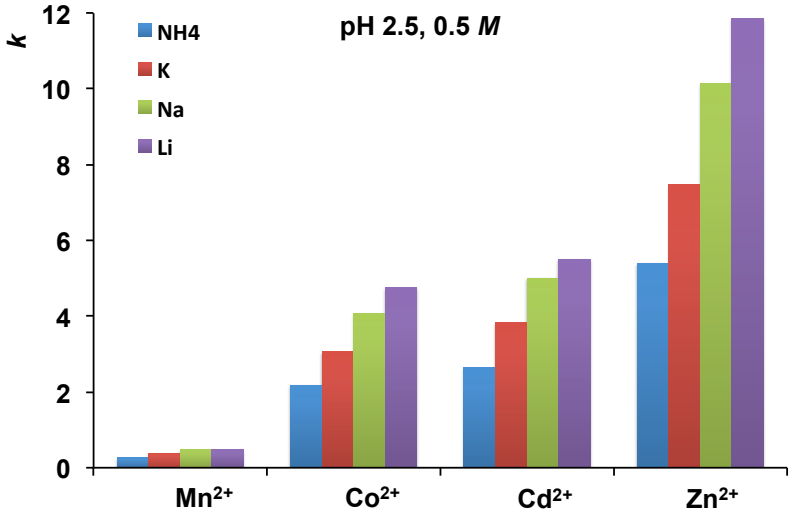

Fig. 3.9 (d): Effect of eluent cation (monovalent) upon retention of transition metal ions at concentration 0.5 *M*, at pH 2.5 (HNO_3). Column temperature: 25 °C, Flow rate: 0.8 mL/min, Column temperature: 25 °C, Injection volume: 20 µL, Detection: spectrophotometric at 510 nm after PCR with 0.15 m*M* PAR.

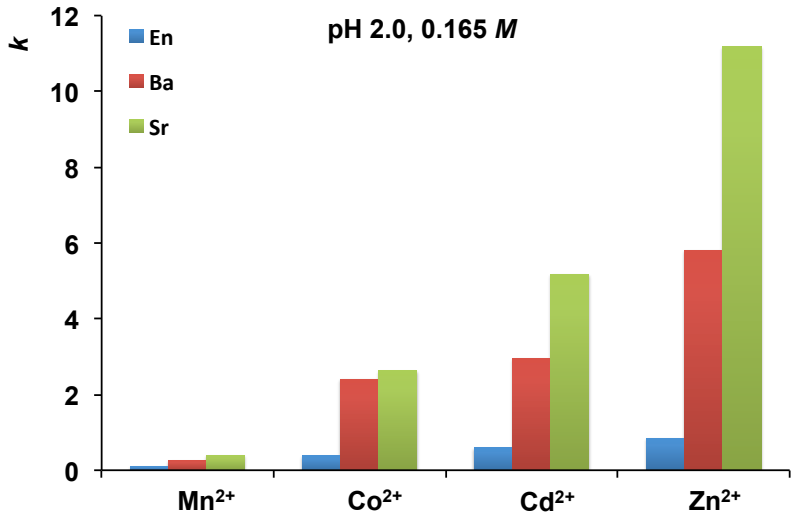

Fig. 3.9 (e): Effect of eluent cation (divalent) upon retention of transition metal ions at concentration 0.165 *M*, at pH 2.0 (HNO_3). Column temperature: 25 °C, Flow rate: 0.8 mL/min, Column temperature: 25 °C, Injection volume: 20 µL, Detection: spectrophotometric at 510 nm after PCR with 0.15 m*M* PAR.

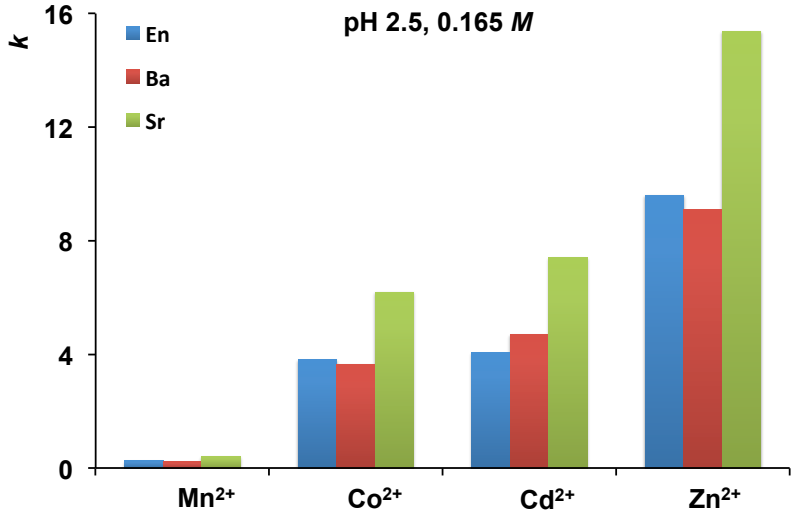

Fig. 3.9 (f): Effect of eluent cation (divalent) upon retention of transition metal ions at concentration 0.165 *M*, at pH 2.5 (HNO_3). Column temperature: 25 °C, Flow rate: 0.8 mL/min, Column temperature: 25 °C, Injection volume: 20 µL, Detection: spectrophotometric at 510 nm after PCR with 0.15 m*M* PAR.

Firstly, it should be noted that the change in eluent cation caused no change in elution order for the four transition metals, the order of retention remaining $Mn^{2+} < Co^{2+} < Cd^{2+} < Zn^{2+}$, which is the same as that seen with a simple dilute HNO_3 only eluent. Secondly, there was little obvious effect/trend in relation to peak efficiency determined across the majority of eluents investigated, although interestingly the three eluents resulting in the greatest average *N*/m values, were KNO_3, $LiNO_3$ and $NaNO_3$, each at 0.165 *M*, pH 2.5. These eluents averaged (for the above four metal ions) 42, 48 and 49 k *N*/m, compared to an average of <32 k *N*/m for all of the other eluent systems (Tables 3.1 and 3.2 show the full data for both retention and peak efficiency for each of the eluent conditions investigated).

What Fig. 3.6 (a-f) clearly shows is that the effect of the eluent cation upon selectivity is considerably more pronounced at lower pH. For alkali cation based eluents, at pH 2.0 the eluent strength increases in order from Li^+ (weakest), to Na^+, K^+, and NH_4^+ (strongest), with concentration having little impact. This eluent strength series corresponds closely to the retention order seen for these cations on carboxylated cation exchange resins, pointing clearly to ion exchange interactions playing a significant role in retention, despite the relatively high ionic strength of the eluent. As pH is increased, albeit relatively marginally, the effect upon column selectivity of the eluent cation is very much diminished, which would then support the case for complexation rapidly becoming the dominant retention mechanism. The same effect is evident with the divalent cation based eluents, with the nature of the eluent cation playing a greater role in the resultant selectivity at pH 2.0, than is evident at pH 2.5. The results suggest at pH 2.0 the ethylenediammonium cation (en^{2+}) acts as a much stronger eluent than either Ba^{2+} or Sr^{2+}, and that Ba^{2+} (being the more strongly retained cation in ion exchange), acts here as a stronger eluent cation than Sr^{2+}. Taken in entirety, the data demonstratively supports a mixed mode mechanism responsible for retention of the transition metal cations under the conditions investigated.

Table 3.1: Retention data for transition metal cations on various eluents.

Eluent Conc/pH	*k*'			
	Mn^{2+}	Co^{2+}	Cd^{2+}	Zn^{2+}
	Potassium Nitrate (KNO_3)			
0.165 *M*, pH 2.0	0.21	0.84	1.31	1.84
0.165 *M*, pH 2.5	0.78	6.19	7.76	14.88
0.5 *M*, pH 2.0	0.11	0.52	0.75	1.24
0.5 *M*, pH 2.5	0.30	2.82	3.53	6.94
	Lithium Nitrate ($LiNO_3$)			
0.165 *M*, pH 2.0	0.60	3.86	4.86	9.07
0.165 *M*, pH 2.5	1.08	9.92	11.87	23.73
0.5 *M*, pH 2.0	0.31	3.04	3.33	7.40
0.5 *M*, pH 2.5	0.38	4.36	5.06	11.00
	Sodium Nitrate ($NaNO_3$)			
0.165 *M*, pH 2.0	0.42	2.32	3.01	5.31
0.165 *M*, pH 2.5	0.76	5.14	6.61	12.21
0.5 *M*, pH 2.0	0.25	2.04	2.45	4.91
0.5 *M*, pH 2.5	0.37	3.71	4.58	9.36
	Ammonium Nitrate (NH_4NO_3)			
0.165 *M*, pH 2.0	0.12	0.40	0.69	0.90
0.165 *M*, pH 2.5	0.83	7.26	8.84	17.50
0.5 *M*, pH 2.0	0.10	0.31	0.50	0.72
0.5 *M*, pH 2.5	0.27	2.15	2.60	5.34
	Barium Nitrate ($Ba(NO_3)_2$)			
0.165 *M*, pH 2.0	0.15	2.07	2.57	5.15
0.165 *M*, pH 2.5	0.45	3.60	4.76	8.81
0.3 *M*, pH 2.5	0.10	3.21	4.15	8.11
	Strontium Nitrate ($Sr(NO_3)_2$)			
0.165 *M*, pH 2.0	0.29	2.36	4.71	10.28
0.165 *M*, pH 2.5	0.32	5.72	6.84	14.28
	Ethylenediamene (en)			
0.165 *M*, pH 2.0	0.08	0.34	0.55	0.79
0.165 *M*, pH 2.5	0.24	3.77	4.01	9.51

Table 3.2: Efficiency data for transition metal cations on various eluents.

Eluent Conc/pH	Efficiency (N/m)			
	Mn^{2+}	Co^{2+}	Cd^{2+}	Zn^{2+}
			KNO_3	
0.165 *M*, pH 2.0	31,500	12,000	22,000	35,000
0.165 *M*, pH 2.5	54,000	14,000	62,000	59,500
0.5 *M*, pH 2.0	28,500	14,000	29,500	14,500
0.5 *M*, pH 2.5	28,500	13,500	29,500	14,500
			$LiNO_3$	
0.165 *M*, pH 2.0	33,500	10,500	30,000	28,500
0.165 *M*, pH 2.5	60,000	17,500	64,000	54,000
0.5 *M*, pH 2.0	31,500	14,500	19,500	26,000
0.5 *M*, pH 2.5	35,500	10,000	41,500	47,500
			$NaNO_3$	
0.165 *M*, pH 2.0	31,000	18,000	26,000	24,500
0.165 *M*, pH 2.5	47,000	14,500	49,000	55,000
0.5 *M*, pH 2.0	26,000	8,000	22,500	20,500
0.5 *M*, pH 2.5	34,500	8,500	40,500	43,500
			NH_4NO_3	
0.165 *M*, pH 2.0	19,000	17,500	14,000	43,500
0.165 *M*, pH 2.5	14,000	10,000	25,500	18,500
0.5 *M*, pH 2.0	11,500	17,500	15,000	18,000
0.5 *M*, pH 2.5	7,000	7,500	15,000	23,500
			$Ba(NO_3)_2$	
0.165 *M*, pH 2.0	12,500	4,000	14,500	21,000
0.165 *M*, pH 2.5	46,000	5,000	34,000	34,500
0.3 *M*, pH 2.5	22,000	4,500	25,500	31,500
			$Sr(NO_3)_2$	
0.165 *M*, pH 2.0	5,190	1,400	19,000	7,000
0.165 *M*, pH 2.5	23,000	6,000	42,000	32,500
			en	
0.165 *M*, pH 2.0	36,500	17,500	18,500	29,000
0.165 *M*, pH 2.5	21,000	23,500	12,500	18,000

It should be noted that en^{2+}, either solely, or as an additive to the eluent, was often used in the early stages of the development of IC. For example, Sevenich and Fritz compared the elution power of 1 m*M* ethylenediammonium dichloride and 1 m*M* magnesium perchlorate at pH 2.5 for various metal ions separated on low capacity sulphonated PS-DVB cation exchangers [28]. The ethylenediammonium dichloride eluent demonstrated significantly stronger eluting power than magnesium perchlorate. The authors also reported the possibility of ethylenediammonium to coordinate Cu^{2+} even under such acidic conditions. However, from the comparison of the stability of metal complexes (ML) with ethylenediamine (log β_1 for Mn^{2+}, Co^{2+}, Cd^{2+}, Zn^{2+} and Cu^{2+} are 2.60; 5.5; 5.4; 5.7 and 10.5, respectively) it is difficult to expect complexation of investigated metal ions with ethylenediamine in the current system.

3.3.5 Column efficiency

One of the main advantages of monolithic phases is high flow- through permeability and low backpressure, which allow their use at elevated flow rates. Sugrue *et al.* [19] previously demonstrated the effect of flow rate on retention and peak efficiency of alkaline earth metal cations on the first generation HEIDA monolith. In a comparative study it was observed that peak efficiencies and resolution on the HEIDA functionalised silica monolith were slightly higher than that obtained using a 8 μm particle packed HEIDA-silica gel column, over the same flow rates, when using low ionic strength eluents. However, the HETP values were not too impressive when using eluents of higher ionic strength (1.0 *M* KCl), ranging from ~45 to >200 μm for Ca^{2+} and Mg^{2+} separated at flow rates ranging from 1.0 to 4.0 mL/min (although the use of post-column reaction detection, as is also the case within the current study, reduces the apparent column efficiency by ~15–20% [21]).

Here the effect of flow rate (from 0.6 to 1.8 mL/min) on retention factor, peak area, peak height and efficiency (HETP) was evaluated for a variety of transition metals (Mn^{2+}, Cd^{2+}, Co^{2+} and Zn^{2+}). The maximum flow rate was restricted in this instance by instrumental limitations, particularly in relation to delivery of the post-column reagent. For this investigation a 0.5 *M* KNO_3 eluent, pH 2.5, was used, (as KNO_3 is the most

common eluent used with such chelating columns to-date) and the temperature was kept constant at 25 °C. The concentration of the PCR solution of PAR was adjusted for each flow rate, such that the concentration reaching the detector was the same throughout the experiment (0.0465 m*M*).

Fig. 3.10 highlights how column efficiency decreased marginally for Mn^{2+}, Zn^{2+} and Cd^{2+} over the flow rate range studied, whereas for Co^{2+} a significant decrease of ~50% was observed (data shown based upon duplicate injections at each flow rate, the first of which was used to ensure column/eluent equilibrium, and with the second injection data plotted). As Co^{2+} and Zn^{2+} have very similar stability constants with HEIDA, the differences in efficiency are somewhat surprising, and unlike well known kinetically slow metal ions such as Ni^{2+}, has not been highlighted for IDA based phases previously. Unfortunately, studies on kinetics of complexation of metals with IDA its structural analogues has not received a great deal of attention in the past and therefore there is no reliable data on the kinetics of complexation of Co^{2+} with such ligands within the literature. However, as an approximation, the data on kinetics of metal complexation with a ligand such as glycine can be used. In this case the corresponding values show that the rate constant of 1.5×10^6 M^{-1} s^{-1} for Co^{2+} complexation with glycine is 30 times higher than seen for the so-called kinetically slow Ni^{2+} (namely 4.6×10^4 M^{-1} s^{-1}) [29]. However, this is significantly less than the corresponding values of 3.4×10^9 M^{-1} s^{-1} for Cu^{2+} and 7.0×10^7 M^{-1} s^{-1} for Zn^{2+} [30] (it should be noted that in the latter case the rate constant was measured at lower temperature 10 °C). These data would thus suggest that in fact Co^{2+} cannot be considered as a kinetically fast metal cation, as was previously assumed, and this may well be the cause of the relative peak shapes observed herein, in a similar way as commonly seen with chelating phases for peaks of Ni^{2+}. Similar conclusions can be also drawn from data on rate constants for the substitution of inner sphere water from various hydrated cations [21].

For Mn^{2+}, Zn^{2+} and Cd^{2+} the HETP ranged from an average of ~25 μm at a flow of 0.6 mL/min, to ~35 μm at a flow rate of 1.8 mL/min. As these values represent a significant improvement over those reported previously for the first generation of this time of HEIDA-silica monolith, which was found to be non-homogenously functionalised, the

indications are good that the new procedure for modification described herein results in improved surface coverage. Tailed peaks, particularly for Zn^{2+} reported previously as a result of secondary silanol interactions [18,19] are no longer evident with the new HEIDA-silica monolith.

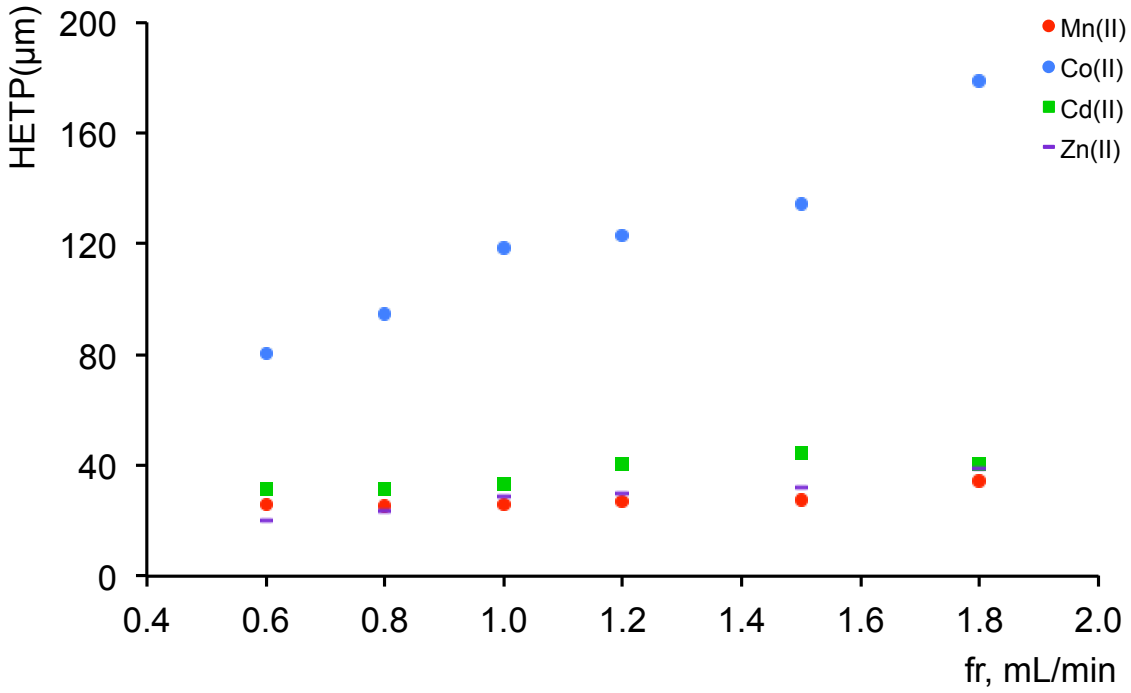

Fig. 3.10: Effect of eluent flow rate (mL/min) on peak efficiency (HETP) for transition metal cations (Mn^{2+}, Cd^{2+}, Co^{2+} and Zn^{2+}). Eluent: 0.5 *M* KNO_3 eluent, pH 2.5, Column temperature: 25 °C, Flow rate: 0.6–1.8 mL/min, Injection volume: 20 µL, Detection: spectrophotometric at 510 nm after PCR with 0.15 m*M* PAR.

Fig. 3.11 illustrates the above data chromatographically. The chromatograms illustrate how peak height is maintained whilst increasing flow rate, via adjustment of PCR concentration, although detector noise increases towards the higher flow rate. The difference in efficiency of the Co^{2+} peak compared to the immediately adjacent Cd^{2+} peak is very clear from the chromatograms shown.

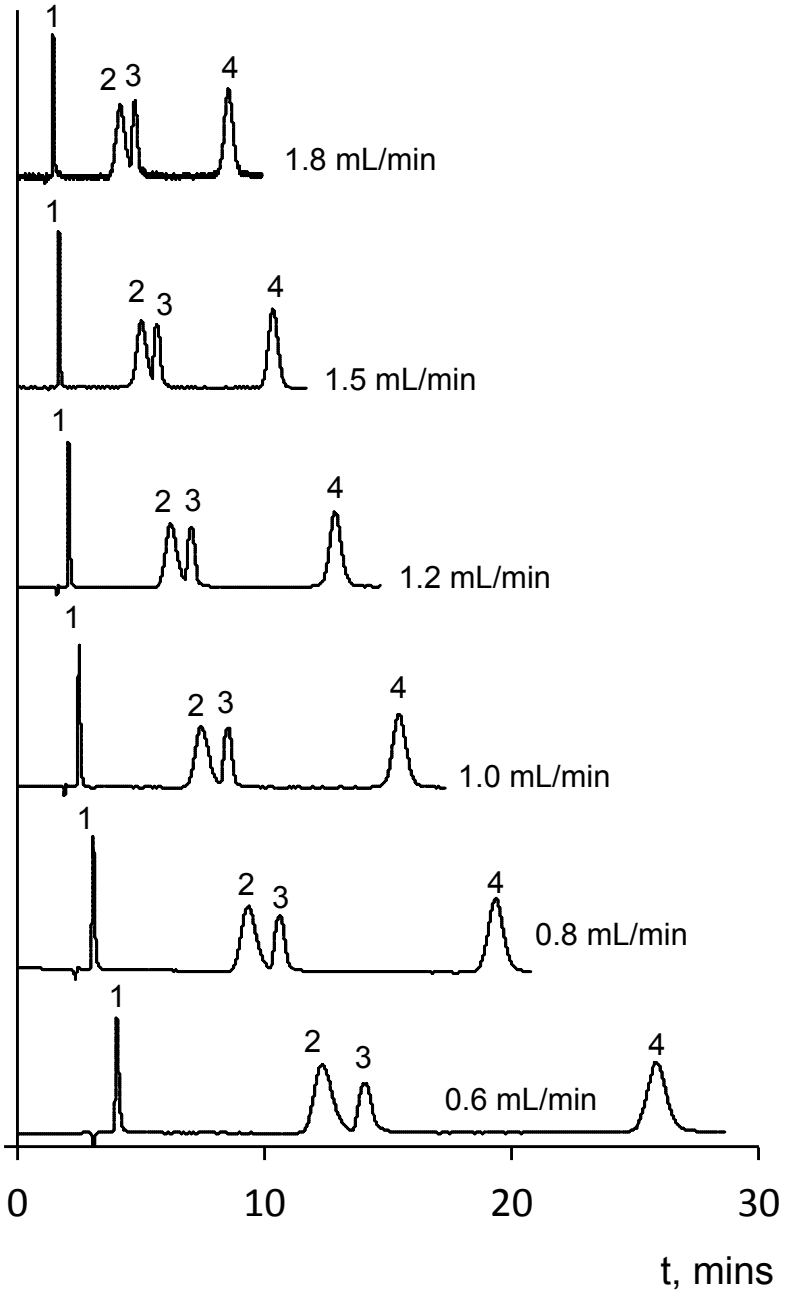

Fig. 3.11: Effect of eluent flow rate upon the separation of transition and heavy metal cations. Peaks: 1: 5 ppm Mn^{2+}, 2: 5 ppm Co^{2+}, 3: 5 ppm Cd^{2+}, 4: 5 ppm Zn^{2+}. Eluent: 0.5 *M* KNO_3, pH 2.5 (HNO_3), Flow rate: 0.6–1.8 mL/min, Column temperature: 25 °C, Injection volume: 20 µL, Detection: spectrophotometric at 510 nm after PCR with 0.15 m*M* PAR.

3.3.6. Separation of selected alkaline earth, transition and heavy metal cations with post-column reaction

Following the characterisation of the improved stationary phase, optimised chromatographic conditions were employed for the separation of selected transition, heavy and alkaline earth metals (see Fig. 3.12).

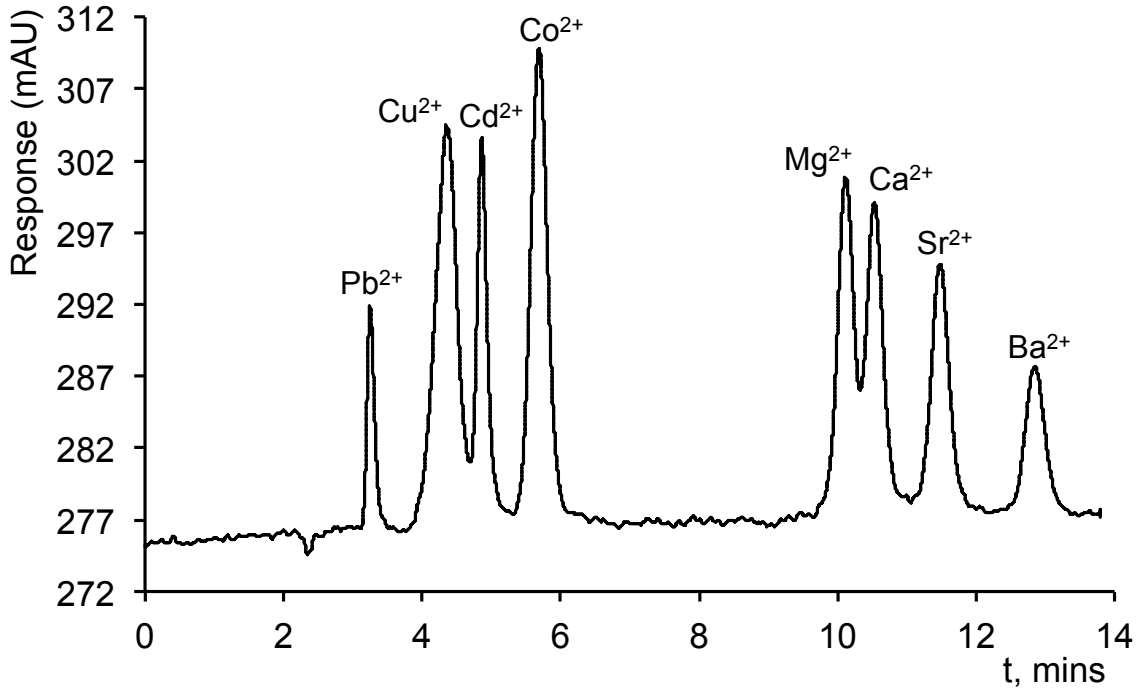

Fig. 3.12: Isocratic separation of eight alkaline earth, transition and heavy metal cations. Peaks: 2.8 ppm Pb^{2+}, 1.5 ppm Cu^{2+}, 3.0 ppm Cd^{2+}, 0.7 ppm Co^{2+}, 0.9 ppm Mg^{2+}, 1.25 ppm Ca^{2+}, 1.75 ppm Sr^{2+}, and 1.75 ppm Ba^{2+}. Eluent: 4 m*M* HNO_3/0.3 m*M* DPA, Flow rate: 0.8 mL/min, Column temperature: 25 °C, Injection volume: 20 μL, Detection: spectrophotometric at 510 nm after PCR with 0.2 m*M* ZnEDTA/0.12 m*M* PAR.

Using a 4 m*M* HNO_3 eluent, with 0.3 m*M* DPA, pH 2.4, the isocratic separation of a mixture of 8 metal cations was achieved, with post-column reaction detection using a 0.12 m*M* PAR/0.2 m*M* ZnEDTA solution. Under the conditions shown Mn^{2+} displayed similar retention to Ca^{2+} and Mg^{2+} and so resolution of these three cations was not possible. However, the selectivity shown, which is unique to the current stationary phase/eluent combination, is particularly well suited to the area of trace metal analysis in environmental samples, wherein levels of alkaline earth metals are present in excess concentrations compared to transition and heavy metal cations.

3.4 Conclusions

A full characterisation of a new HEIDA modified silica monolithic column was carried out. From the resultant column performance it would appear that improving the modification procedure of the stationary phase has resulted in an increased column capacity with a more homogenous surface modification, which provides better efficiency and separation of target metal cations. It was also shown that HEIDA-silica monoliths exhibit selectivity that can be readily manipulated, based upon a mixed ion exchange and chelation retention mechanism, to provide optimal separations of metal cations to suit a variety of potential applications. As a demonstration, here the separation of 8 metal cations was achieved isocratically in less than 14 min. The effect of eluent cation on column selectivity was also demonstrated, helping to elucidate the nature of the dual retention mechanism in play. From these results, it is clear that silica monoliths are a possible method for the determination of metal cations in complex samples at higher flow rates, which can present a problem for packed columns of a small particle size.

References

[1] P.N. Nesterenko, P. Jones, Journal of Chromatography A 770 (1997) 129.

[2] P.N. Nesterenko, P. Jones, Journal of Chromatography A 804 (1998) 223.

[3] W. Bashir, B. Paull, Journal of Chromatography A 907 (2001) 191.

[4] W. Bashir, B. Paull, Journal of Chromatography A 910 (2001) 301.

[5] W. Bashir, B. Paull, Journal of Chromatography A 942 (2002) 73.

[6] B.B. Paull, W.W. Bashir, Analyst 128 (2003) 335.

[7] J.C. Dias, L.T. Kubota, P.N. Nesterenko, G.W. Dicinoski, P.R. Haddad, Analytical Methods 2 (2010) 1565.

[8] L. Trojer, G. Stecher, I. Feuerstein, S. Lubbad, G.K. Bonn, Journal of Chromatography A 1079 (2005) 197.

[9] L. Trojer, G. Stecher, I. Feuerstein, G.K. Bonn, Rapid Communications in Mass Spectrometry 19 (2005) 3398.

[10] Q. Luo, H. Zou, X. Xiao, Z. Guo, L. Kong, X. Mao, Journal of Chromatography A 926 (2001) 255.

[11] S.-C. Chuang, C.-Y. Chang, C.-Y. Liu, Journal of Chromatography A 1044 (2004) 229.

[12] M.-Y. Ding, R. Zheng, H. Peng, Chinese Journal of Analytical Chemistry 37 (2009) 395.

[13] Á. Moyna, D. Connolly, E. Nesterenko, P.N. Nesterenko, B. Paull, Journal of Chromatography A 1249 (2012) 155.

[14] Á. Moyna, D. Connolly, E. Nesterenko, P.N. Nesterenko, B. Paull, Analytical and Bioanalytical Chemistry 405 (2012) 2207.

[15] B. Preinerstorfer, D. Lubda, W. Lindner, M. Lämmerhofer, Journal of Chromatography A 1106 (2006) 94.

[16] J. Scancar, R. Milacic, Trends in Analytical Chemistry 28 (2009) 9.

[17] S.D. Chambers, K.M. Glenn, C.A. Lucy, Journal of Separation Science 30 (2007) 1628.

[18] E. Sugrue, P. Nesterenko, B. Paull, Analyst 128 (2003) 417.

[19] E. Sugrue, P. Nesterenko, B. Paull, Journal of Separation Science 27 (2004) 921.

[20] N. Cardellicchio, S. Cavalli, P. Ragone, J.M. Riviello, Journal of Chromatography A 847 (1999) 251.

[21] B. Paull, P.N. Nesterenko, P. Jones, High Performance Chelation Ion Chromatography, RSC Chromatography Monographs, Royal Society of Chemistry Publishing, Cambridge, UK (2011).

[22] E.P. Nesterenko, P.N. Nesterenko, B. Paull, M. Meléndez, J.E. Corredor, Microchemical Journal 111 (2013) 8.

[23] https://sites.google.com/site/chemdiagr/

[24] NIST Standard Reference Database 46 - Version 8.0 for Windows, Critically selected 392 stability constants of metal complexes 2004.

[25] P. Jones, P.N. Nesterenko, Journal of Chromatography A 1213 (2008) 5.

[26] D. Connolly, L.P. Barron, E. Gillespie, B. Paull, Chromatographia 70 (2009) 915.

[27] P. Jones, P.N. Nesterenko, Journal of Chromatography A 789 (1997) 413.

[28] G. J Sevenich, J.S. Fritz, Journal of Chromatography A 371 (1986) 361.

[29] L.I. Budarin, K.B. Yatsimirskii, Russian Chemical Reviews 37 (1968) 209.

[30] M.W. Grant, Journal of the Chemistry Society, Faraday Trans. 1 69 (1973) 560.

4. Direct determination of transition metals in mussel tissue digests using high-performance chelation ion chromatography with monolithic silica based chelating ion exchangers

Abstract

A new high performance chelation ion chromatography method was developed for the direct separation and detection of selected transition metals in shellfish (mussel) tissue digest samples. Two different bonded silica monolithic chelating stationary phases, exhibiting differing selectivities for metals of interest, were applied within the method. The bonded chelating chemistries were HEIDA and *N*-(2-hydroxyethyl)-*N*-(2-[phosphonomethyl)amino]acetic (HEPMA) acids. Quantitative determination of Mn^{2+}, Cd^{2+} and Zn^{2+} concentrations within shellfish tissue (*Mytilus edulis*) was carried out, following microwave assisted acid digestion. Post-column detection was achieved using spectrophotometric detection at 510 nm after reaction with PAR. The eluents employed were 0.5 *M* KNO_3, pH 2.4, for the HEIDA-bonded stationary phase, and 0.1 *M* KNO_3, pH 2.6, for the HEPMA-bonded monolithic column. The HEPMA phase provided improved resolution between Mn^{2+} and interfering alkaline earth metal cations compared to the HEIDA-bonded phase. Concentrations of metals were determined using standard addition, and Cd^{2+}, Mn^{2+}, and Zn^{2+} cations were detected at < 10 µg/g, < 25 µg/g and < 700 µg/g, respectively. Sample analysis using sector field inductively coupled plasma-mass spectrometry (ICP-MS) was carried out to generate comparative data to that obtained using the chromatographic method. The results were comparable, further confirming HPCIC as a promising method for the determination of metal cations in complex samples.

Aims

The aim of this work was to apply the previously characterised HEIDA-silica monolith and an alternative chelating silica monolith column bonded with HEPMA to the separation and quantification of selected metal cations in a "real" complex sample, comparing the results of both stationary phases with the routinely used analytical technique ICP-MS.

4.1 Introduction

One of the main concerns surrounding metal contamination of the aquatic environment is the propensity of certain metals to undergo bioaccumulation, and the subsequent impact of this upon the exposed organisms, and within higher levels of the food-chain [1,2]. In particular, there has been long established concern into the environmental and health effects of trace metal contamination of the coastal marine environment, most notably with regard to elements such as Sn, Hg, Cd and Cu, and particularly in relation to potential contamination of certain seafoods [3-5]. The analysis of mussels and other bivalves for metal contamination is an important environmental analytical problem, as these organisms are typically accepted as bio- indicators of chemical pollution in coastal and estuarine waters, and of course in human foodstuff and aquaculture industry [6]. Dissolved metals and chemicals within the water can be inadvertently adsorbed and bioaccumulate within the soft tissues, and mussels can also adsorb species from the surface of particulates filtered from the water column. In relation to exposure studies, both the total concentration of metals within the tissue is of interest, and the effect of the size and age of the bivalve in relative to metal accumulation. Recently studies were carried out by Spann *et al.* [7], investigating the size- dependent effects of the exposure to low levels of Cd^{2+} and Zn^{2+}, both separately and in combination, on the Asian clam, *Corbicula fluminea*. The study was primarily focused upon observable effects upon the organism metabolome. However, interestingly the researchers observed that large and small clams could be differentiated by their metabolic composition, and that the two size classes showed opposite responses to the Cd^{2+} and Zn^{2+} spiked sediment. No effects of

Zn^{2+} alone on the metabolome were found and Cd^{2+} only influenced the smaller size class [7]. The determination of trace concentrations of transition metals and certain p-block elements (most commonly as Pb and Sn) within biological materials, and indeed other complex samples matrices, such as those of high ionic strength or containing excess concentrations of alkali and alkaline earth salts, remains a significant challenge. The presence of charged bio-molecules can significantly interfere with the determination of such metals in biological tissues and fluids, with the issue of matrix interferences when dealing with such samples, a recurring problem for many established analytical (e.g. spectrophotometric or electroanalytical) techniques [8,9]. Commonly used atomic spectroscopic methods, such as AAS, AES and inductively coupled plasma based methods, ICP-AES and quadrupole based mass spectrometry (ICP-MS), often require significant dilution of the samples, and can suffer significant polyatomic interferences (particularly for low resolution instruments) originating from the sample matrix or from within the plasma itself. Sample preparation solutions to such interferences can involve the use of releasing/suppressing reagent additives to samples, or typically matrix removal and solute preconcentration, both of which can compromise sensitivity and accuracy of the resultant data. In the case of ICP-MS, instrumental solutions to overcome spectral interferences include the use of reaction cell or high resolution instrumentation, albeit at higher cost and with greater operational complexity.

The use of standard IC with such samples is also problematic, due to limited selectivity between matrix and solute (divalent) cations, together with the so-called "self elution" effect, where the ion exchange sites can become swamped with excess matrix alkali and alkaline earth metal ions [10]. However, chelating ion exchange stationary phases, which replace standard ion exchange groups with chelating functionalities, exhibit better group selectivity and are generally more suited to the analysis of these types of complex matrices [11].

Iminodiacetic acid (Fig. 4.1 (a)) functionalised chelating exchangers have demonstrated excellent selectivity for transition metals in HPCIC [12,13], and silica IDA stationary phases have previously been applied to the separation and determination of metal cations in various complex sample types [10,12-17]. Nesterenko and Jones [14] developed a

single column method for the pre-concentration and separation of trace transition metals in highly saline waters on a 250 x 4.0 mm I.D. particle packed Diasorb IDA silica column, and Dias *et al*. [13] developed an isocratic method for the determination of trace transition metals in fuel ethanol, using an IDA functionalised silica column (150 x 4.0 mm I.D.) with spectrophotometric detection at 495 nm following post-column reaction (PCR) with PAR).

More recently attention has also been focused on porous monolithic chelating stationary phases [18], and their application to the determination of alkaline earth metals in water samples [19,20].

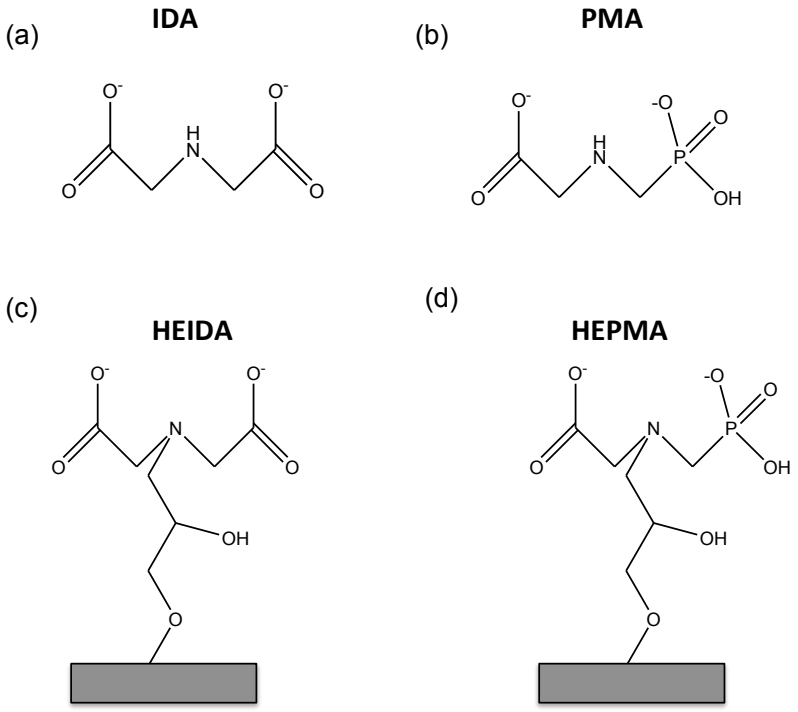

Fig. 4.1: Structures of (a) iminodiacetic acid, (b) 2-[(phosphonomethyl)amino]- acetic acid, (c) *N*-hydroxyethyliminodiacetic and (d) *N*-(2-hydroxyethyl)-N-(2-[phosphonomethyl)amino]acetic acid.

However, although IDA is a commonly used chelating functionality in HPCIC, the determination of Mn^{2+} can present a problem, due to weak retention relative to other transition metals, with Mn^{2+} having been shown to exhibit similar behaviour to alkaline earth metals (as discussed in Chapter 3). The introduction of alternative chelating groups onto the surface of stationary phase will of course drastically change the resultant separation selectivity. Caldarola *et al.* [21] very recently modified a commercially available 100 x 4.6 mm I.D. silica monolithic column with 2-[(phosphonomethyl)amino]acetic acid (PMA), also known as the herbicide, glyphosate (Fig. 4.1(b)). In comparison with IDA, PMA contains both carboxylic and phosphonic acid groups, with the later resulting in alternative selectivity to that shown by IDA.

In the work presented herein, the monolithic silica stationary phases, functionalised with either HEIDA or HEPMA acid, were applied within HPCIC to the separation and determination of Mn^{2+}, Cd^{2+} and Zn^{2+} in mussel tissue digests, obtained from size fractionated mussels (*Mytilus edulis*), collected from a estuarine location close to a large zinc refinery (Derwent River, Hobart, Tasmania) [22]. The stationary phases were compared for their selectivity towards the metals of interest in this complex sample matrix, and separation conditions were optimised for the quantitation of the trace metal content. Results were compared to those obtained using sector field inductively coupled plasma-mass spectrometry, as ICP-MS represents the current preferred approach to the analysis of such sample matrices [22-24].

4.2 Experimental

4.2.1 Instrumentation

The IC systems used were as described in Section 3.2.1. A JPP Chromatography Signal Extraction System 201 (JPP Chromatography Ltd, Devon, UK) was used in conjunction with a Metrohm IC system for noise reduction during data acquisition. Samples were freeze dried using a Breda Scientific Model LY-5-FM model freeze drier. Microwave digestion of samples was performed using a Milestone MLS 1200 high performance

microwave digestion unit with MLS Mega 240 terminal (Milestone Microwave Lab Systems, USA).

4.2.2 Reagents

Analytical or higher grade reagents and Milli-Q water (Millipore, Bedford, MA, USA) were used for the preparation of all solutions. Eluents were prepared from KNO_3 from BDH Ltd., (Poole, UK) and acidified using dilute HNO_3 sourced from 70% HNO_3, Chem-Supply Pty. Ltd., (Gillman, Australia). 4-(2-Pyridylazo) resorcinol, was purchased from Kodak (Rochester, NY, USA). Aqueous ammonia solution (28%) for the preparation of the PCR solution was supplied by Fluka (Glossop, UK). Hydrogen peroxide and HNO_3, used for the microwave digestion of samples were from Sigma Aldrich (Sydney, Australia). Spectrosol atomic absorption standard solutions containing Mn^{2+}, Co^{2+}, Cd^{2+} and Zn^{2+}, with concentrations 1.00 g/L were purchased from BDH Chemicals (Poole, UK). Metal stock solutions were prepared from atomic absorption standards in acidified DW, and stored in polypropylene bottles. Working standards were prepared on the day of use unless stated otherwise. All eluents were filtered before use through a 0.22 µm nylon membrane filter and degassed through sonication.

4.2.3 Preparation of chelating silica monolithic stationary phases

The HEIDA modified silica monolithic column (100 x 4.6 mm I.D.) was prepared as described in Section 3.2.4.

For the production of the HEPMA modified monolithic column, the reaction mixture for the modification process consisted of 5 g PMA (isolated from commercially available 360 g/L solution of glyphosate isopropylammonium salt) (Multicrop, Australia), 5 mL of 3-glycidoxypropyltrimethoxy-silane (Sigma-Aldrich, Sydney, Australia) and 20 mL of 1 *M* NaOH. The mixture was stirred at 70 ºC for 1 h to allow the PMA to react with the epoxy group of the silane, and the pH was then adjusted to 5.0 with acetic acid in order to avoid compatibility problems with the silica monolith. The resulting mixture was recycled for 24 h in the column flow direction, following which the column was then turned and flushed with modification solution from outlet to inlet [21]. The column was

washed as with the HEIDA column prior to use. Figs. 4.1 (c) and 4.1 (d) illustrate the resultant stationary phase chemistries from the above modification processes.

4.2.4 Sample pre-treatment

Approximately 60 mussels (*Mytilus edulis*) were randomly selected from an estuarine site within the Derwent river system, Hobart, approximately 3 km downstream from a large zinc refinery (Derwent River, Hobart, Tasmania). The shellfish were divided according to size (0–5 cm, 5–8 cm, 8–10 cm) and stored within a -80 °C freezer. Prior to analysis the soft tissues were removed from their shells, and representative samples from each size group were then freeze dried at -30 °C for 24 h before being ground using mortar and pestle. Microwave digestion was then performed on each sample (1 g each), using 6 mL concentrated HNO_3 and 1 mL concentrated H_2O_2 to digest the tissue samples. Sample digestion was carried out in close accordance with guidelines and procedures laid out within USEPA Method 3051A [25] and manufacturers operating recommendations (Milestone Microwave Lab systems). Sample pH was adjusted to 2.0 with 50% NaOH, and diluted to 50 mL volume with DW. Immediately prior to analysis, samples were diluted 1:4 with DW for determination of Mn^{2+} and Zn^{2+}, and undiluted for the determination of Cd^{2+}. All samples were filtered with 0.45 μm syringe filters.

4.2.5 ICP-MS analysis

Total elemental concentrations were determined using a sector field inductively coupled plasma mass spectrometer (Thermo Fisher Element 2, Bremen, Germany). Indium (High Purity Standards, Charleston, USA) was added to prepared samples (diluted as necessary) as an internal standard (100 mg/L) along with UHP nitric acid (Seastar Chemicals, BC, Canada) to a final concentration of 1%. Samples were introduced to the ICP-MS via an autosampler (CETAC ASX-500, Ohmaha, USA). Quantitation was via the method of external calibration performed using a series of standards prepared from premixed standard solutions (QCD Analysts, Environmental Science Solutions, Spring Lake, USA). All standard solutions were prepared daily prior to use, with calibration accuracy verified by the analysis of independent NIST 1640 "Trace Elements in Natural Water" SRM (Gaithersburg, MD, USA). Multiple blank solutions and quality control

samples were regularly analysed to monitor instrument performance during each analytical sequence. The same original sample digests were simultaneously analysed by both ICP-MS and HPCIC. Using ICP-MS a total of 5 repeat analyses of each size fractioned sample was completed, following a further minimum 100 fold procedural dilution of each 50 mL digest solution, equal to a total dilution of 5000 in relation to the original solid freeze dried tissue samples.

4.3 Results and discussion

4.3.1 High performance chelation ion chromatography of mussel digest using HEIDA column

A HEIDA-silica monolithic stationary phase was previously chromatographically characterised in detail (Chapter 3). Based on the obtained results, an eluent consisting of 0.5 *M* KNO_3, adjusted to pH 2.4 using dilute HNO_3, was selected, which was optimal for the isocratic separation of the transition metal ions, Mn^{2+}, Co^{2+}, Cd^{2+} and Zn^{2+}. The use of this high ionic strength eluent also minimises retention of any excess alkali and alkaline earth metal cations present within the sample matrix. Fig. 4.2 shows a typical separation of the selected metals obtained under the above conditions. The separation shown was achieved with a flow rate of 0.8 mL/min for the eluent pump, and with the peristaltic pump for delivery of PCR set to 0.36 mL/min. Column temperature was set to 25 ºC.

The separation shown in Fig. 4.2 provides excellent selectivity for the four metal ions in standard solutions. However, the retention of Mn^{2+} is rather limited, and co-elution with weakly retained Mg^{2+} and Ca^{2+} occurs for samples which contain these common ions, under such eluent conditions. This selectivity can be explained with reference to Table 4.1 [26-28], which list the stability constants (albeit solution based) for IDA, and shows the relative strength of complexation between alkaline earth metals, Mn^{2+} and other transition metals of interest, specifically in the case of the mussel digest samples, Cd^{2+} and Zn^{2+}. The above chromatographic conditions were applied within the analysis of each of three samples of the microwave assisted acid digests of size classified freeze dried mussel tissue.

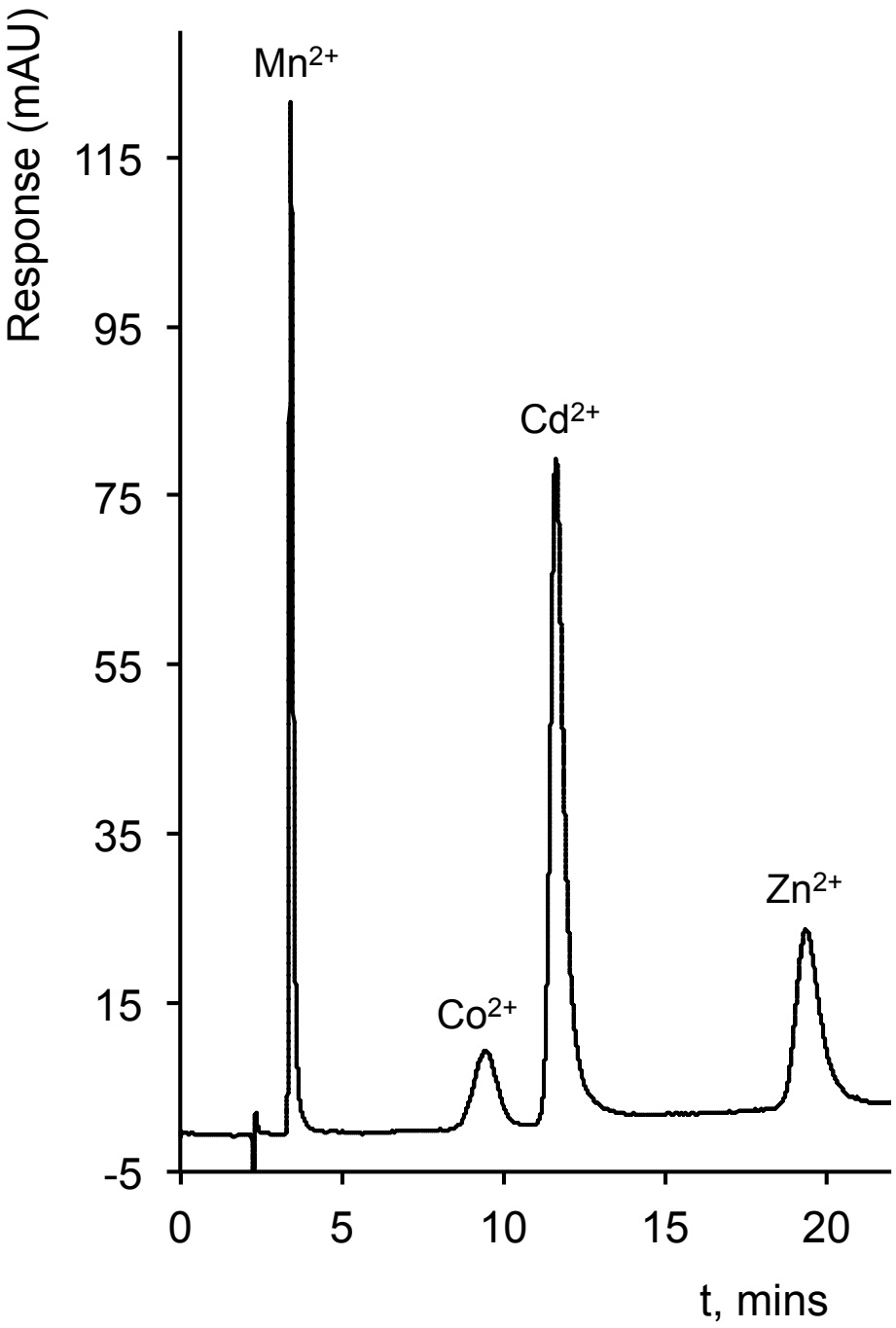

Fig. 4.2: Isocratic separation of transition metals (Mn^{2+}, Co^{2+}, Cd^{2+}, Zn^{2+}), on HEIDA modified silica monolith. Eluent: 0.5 *M* KNO_3, pH 2.4, Flow rate: 0.8 mL/min, Column temperature: 25 ºC, Injection volume: 20 µL, Detection: spectrophotometric at 510 nm after PCR with 0.15 m*M* PAR.

Table 4.1: Stability constants of complexes of metal ions with IDA and PMA (glyphosate) in aqueous solution at 25 ºC [26-28].

	IDA, (pK_{a1} = 1.77, pK_{a2} = 2.98)		PMA (pK_{a1} = 0.78, pK_{a2} = 2.09, pK_{a3} = 5.69)	
Metal ion	$\log \beta_1$	$\log \beta_2$	$\log \beta_1$	$\log \beta_2$
Na^{+}	0.36	-	1.4	-
Mg^{2+}	2.98	4.85	3.28	5.47
Ca^{2+}	2.60	5.90	3.29	5.87
Mn^{2+}	4.72	7.82	5.50	7.80
Cd^{2+}	5.71	10.10	7.29	10.91
Fe^{2+}	5.80	10.10	6.87	11.18
Co^{2+}	6.97	12.22	7.23	11.12
Zn^{2+}	7.15	12.40	8.74	11.69
Ni^{2+}	8.30	14.60	7.90	12.30
Cu^{2+}	10.56	16.30	11.86	15.94
Fe^{2+}	10.72	19.15	16.09	23.0
La^{3+}	5.88	9.97	6.7	10.1
VO^{2+}	9.0	-	10.69	15.9
Al^{3+}	8.18	15.33	13.7	16.2

The resultant sample chromatogram for the 0–5 cm sample is shown (Fig. 4.3 (a)). As expected quantitation of Mn^{2+} in the sample solutions was not possible due to the peak co-elution. Reduction of eluent strength in this case lead to excessive retention of Zn^{2+} and the use of gradient elution was not ideal due to PCR based detection.

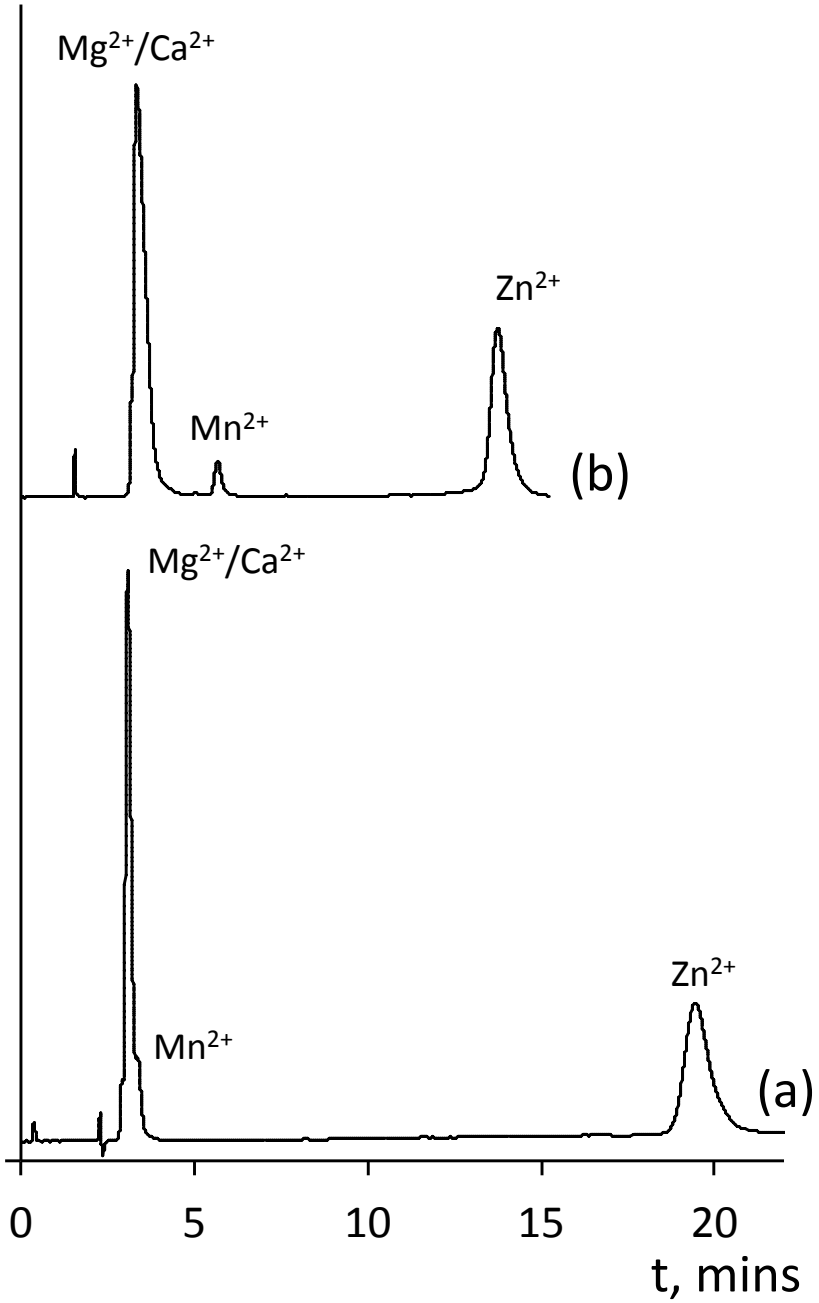

Fig. 4.3: Overlay (offset) of the isocratic separation of mussel tissue digest sample (0–5 cm) on chelating (a) HEIDA and (b) HEPMA-silica monoliths, 100 x 4.6 mm I.D. Eluent: (a) 0.5 *M* KNO_3, pH 2.4; (b) 0.1 *M* KNO_3, pH 2.6, Flow rate: (a) 0.8 mL/min, (b) 1.2 mL/min, Column temperature: 25 ^{o}C, Injection volume: 20 µL, Detection: spectrophotometric at 510 nm after PCR with 0.15 m*M* PAR.

However, using the HEIDA column, quantitation of the Zn^{2+} present within the sample digests was carried out, with the injected sample diluted ~1:200 from original dry mass. Quantitation was carried out using standard addition, the results of which are included within Table 4.2.

Table 4.2: Quantitative data for determination of Zn^{2+} in shellfish using high performance chelation ion chromatography (HEIDA).

Sample size (cm)	Zn^{2+} HPCIC (HEIDA), µg/g	Standard addition (+ 0 to 3.0 mg/L, duplicate injections)		
		Slope	Intercept	R^2
0 to 5	581.3	1485.6	4410.2	0.998 (n = 13)
5 to 8	230.2	1329.6	1477.4	0.998 (n = 6)
8 to 10	294.2	1235.0	1802.5	0.994 (n = 5)
Average	368.6	1350.1	2563.4	0.997

The method provided an average value for all sizes of ~370 µg per g dry weight, with the highest concentration present in the smallest mussel size category. This pattern was also seen within the ICP-MS data (Table 4.3 (c)), which correlated closely to the HPCIC values with an average concentration for all samples of ~430 µg/g, and again highest Zn^{2+} concentrations in the smallest class of mussels. On a size classified basis, relative agreement ($[Zn]_{HEIDA}/[Zn]_{ICP-MS}$) between the HPCIC data and the ICP-MS data was 0.76, 0.96 and 1.02 for 0 to 5 cm, 5 to 8 cm and 8 to 10 cm samples, respectively.

Table 4.3: Quantitative data for shellfish analysis using high performance chelation ion chromatography (HEPMA) and ICP-MS. Determination of (a) Zn^{2+}, (b) Mn^{2+} and (c) Cd^{2+}.

(a) Sample size (cm)	Cd^{2+} HPCIC (HEPMA), µg/g	Standard addition (+ 0 to 250 µg/L, duplicate injections)			Cd^{2+} ICP-MS (Average of n = 5)	
		Slope	Intercept	R^2	µg/g	% RSD
0 to 5	4.3	0.381	32.419	0.997 (n=6)	7.5	17.2
5 to 8	7.2	0.372	55.519	0.995 (n=6)	9.7	22.1
8 to 10	6.7	0.377	49.415	0.997 (n=6)	10.3	15.5
Average	6.1	0.377	45.8	0.996	9.2	18.3
(a) Sample size (cm)	Mn^{2+} HPCIC (HEPMA), µg/g	Standard addition (+ 0 to 0.5 mg/L, duplicate injections)			Mn^{2+} ICP-MS (Average of n = 5)	
		Slope	Intercept	R^2	µg/g	% RSD
0 to 5	12.8	1732.9	225.81	0.997 (n = 5)	55.8	13.1
5 to 8	28.3	1271.0	77.06	0.995 (n = 5)	6.4	44.3
8 to 10	45.6	1159.0	255.68	0.997 (n = 5)	48.3	10.3
Average	28.9	1387.6	186.18	0.996	36.8	22.6
(c) Sample size (cm)	Zn^{2+} HPCIC (HEPMA), µg/g	Standard addition (+ 0 to 4.0 mg/L, duplicate injections)			Zn^{2+} ICP-MS (Average of n = 5)	
		Slope	Intercept	R^2	µg/g	% RSD
0 to 5	685.5	932.7	3253.9	0.996 (n = 5)	766.6	6.9
5 to 8	188.2	1011.2	956.1	1.000 (n = 5)	239.0	19.5
8 to 10	312.6	864.5	1383.5	0.998 (n = 5)	289.6	15.2
Average	395.4	936.1	1864.3	0.998	431.7	13.9

4.3.2 High performance chelation ion chromatography of mussel digest using HEPMA column

The data within Table 4.1 for PMA complexation of metal ions suggested a HEPMA modified monolithic phase would overall provide a slightly higher strength chelating column, with greater selectivity between the alkaline earth metal ions and Mn^{2+}.

The prepared HEPMA column was first evaluated chromatographically for alkaline earth and transition metal selectivity, and indeed found to provide very similar (to HEIDA), yet slightly greater retention of target metal ions. Most importantly the HEPMA phase did indeed provide significantly improved selectivity for the crucial Ca^{2+}/Mg^{2+} and Mn^{2+} peaks. Following a concise investigation of the column selectivity, an eluent of 0.1 *M* KNO_3, pH 2.6, was found optimum, and delivered at a flow rate of 1.2 mL/min. At higher pH values, PMA is known to form insoluble complexes with certain metal cations, so acidic eluents must be used with this particular phase. All other chromatographic conditions were identical to the HEIDA-bonded column. Fig. 4.4 shows overlaid chromatograms of a sample digest, before and after the standard addition of Mn^{2+} (+0.1 mg/L). Despite the complexity of the sample matrix, Fig. 4.4 shows how the chelating column provided very acceptable peak efficiency for Mn^{2+}, equal to N = 3543 (~35K *N*/m).

Fig. 4.3 (b) shows the full chromatogram of the digest sample in direct comparison with that obtained using the HEIDA column. The comparison shows not only the improved resolution of Mn^{2+} and alkaline earth cations, but a reduced selectivity between $Mn^{2+}$and Zn^{2+}, resulting in a significant reduction in overall analysis time for this particular sample. However, this reduced selectivity is not reflected in the log β_1 stability constant data shown in Table 4.1, although for the log β_2 data the difference in constants between the two cations (Mn^{2+} and Zn^{2+}) is greater for IDA than PMA. As retention here is dominantly stationary phase complexation, it is unlikely 2:1 complexes are possible, which points to additional factors affecting selectivity, including the impact of the linker chemistry upon the final stationary phase selectivity and/or additional secondary retention mechanisms, such as simple ion exchange [29].

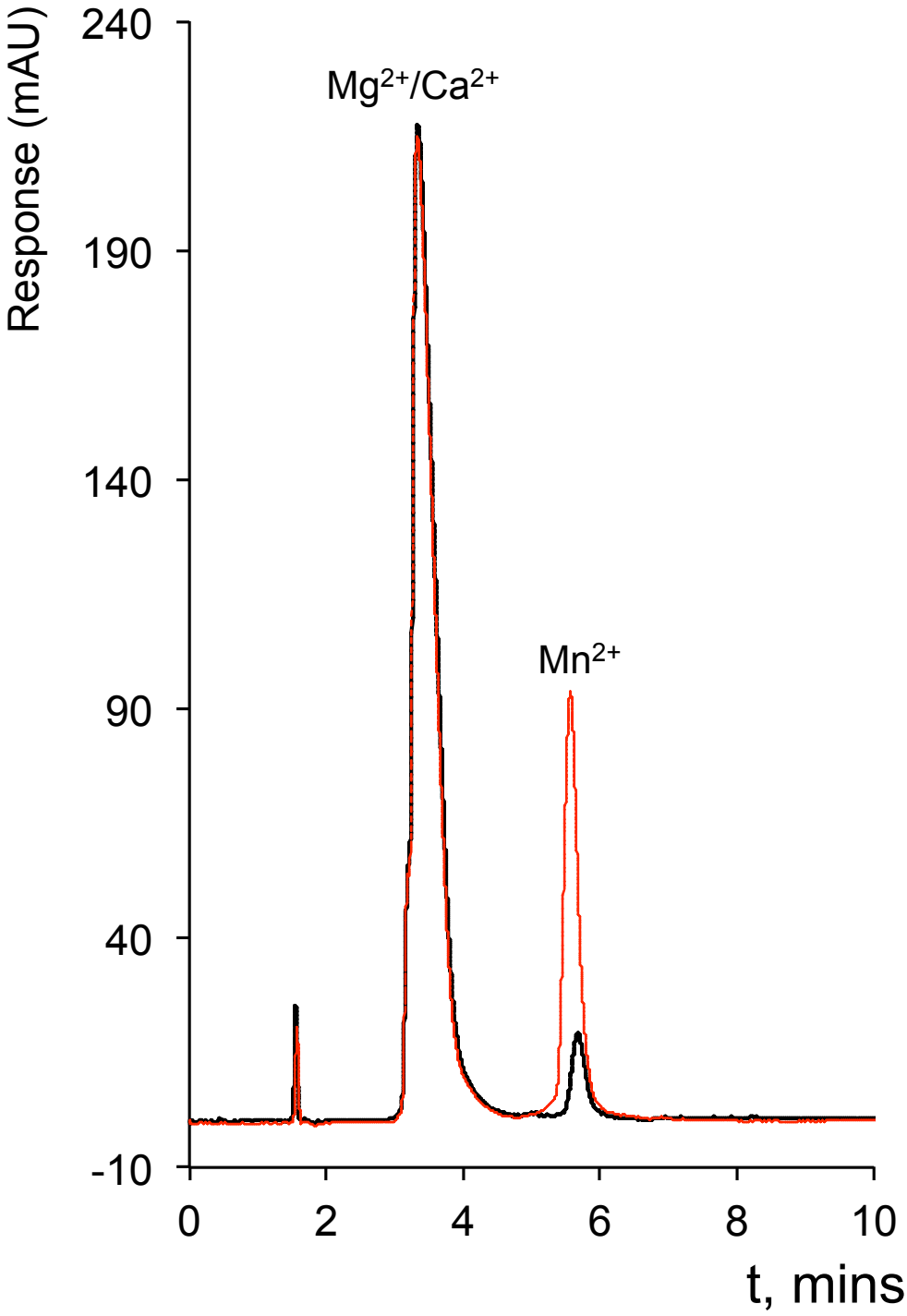

Fig. 4.4: Overlay of mussel tissue digests (0–5 cm) chromatograms, obtained upon the HEPMA column, before and after standard addition of Mn^{2+} at 0.1 mg/L. Chromatographic conditions as Fig. 4.3 (b).

The HEPMA column was applied within HPCIC to the quantitation of Zn^{2+}, Mn^{2+} and Cd^{2+} within each of the size fractioned shellfish digest samples, the results of which can be seen in Table 4.3 (a)–(c). For Zn^{2+} the HEPMA method provided excellent corroboration of the HEIDA data, with relative values ($[Zn]_{HEIDA}/[Zn]_{HEPMA}$) of 0.85, 1.22 and 0.94 for 0 to 5 cm, 5 to 8 cm and 8 to 10 cm samples, respectively, and 0.93 for the averaged data for all sample sizes. The average concentration determined using the HEPMA method was 0.92 of that determined using ICP-MS, and on a size classified basis, ($[Zn]_{HEPMA}/[Zn]_{ICP-MS}$) was 0.89, 0.79 and 1.08 for 0 to 5 cm, 5 to 8 cm and 8 to 10 cm samples, respectively. However, once again the trend of highest Zn^{2+} concentrations within the smallest/youngest mussel class was confirmed. The data obtained for Mn^{2+} using HEPMA ranged between 13 and 46 μg/g, with an average concentration of ~29 μg /g. The averaged data corresponded relatively well with averaged ICP-MS data at 37 μg/g ($[Mn]_{HEPMA}/[Mn]_{ICP-MS}$ = 0.78), although individual size fractioned data was less satisfactory, bar the 8–10 cm sample set (8–10 cm, $[Mn]_{HEPMA}/[Mn]_{ICP-MS}$ = 0.94).

The reason for discrepancies between methods for the sample size samples is unclear, although in the case of the 5 to 8 cm sample set, % RSD of up to 44% using ICP-MS (based upon repeat analyses), is higher than normally expected. Differences in sample dilution for the two methods may be a factor to consider in such comparisons, with the HPCIC method limited to 200 fold dilution from solid sample, compared to a total 5000 fold dilution within the ICP-MS method used.

Table 4.3 (a) shows the data for Cd^{2+} determination using both the HEPMA method and comparison data from ICP-MS. In this case sample dilution was restricted to 50 fold from solid within the HPCIC method, as Cd^{2+} concentrations were close to the method quantitation limit (see below). Table 4.4 shows ICP-MS results for the typical matrix composition of the sample digests at this dilution.

Despite this matrix complexity, averaged data for the three sized fractioned samples for Cd^{2+} concentration was in reasonable agreement with ICP-MS, being ~9 and 14 μg/g, respectively ($[Cd]_{HEPMA}/[Cd]_{ICP-MS}$ = 0.67), with both analyses confirming a general increase in concentration with size/age of the mussel, which was also seen with the above Mn^{2+} data (when using HPCIC). On a size classified basis, relative

agreement ($[Cd]_{HEPMA}/[Cd]_{ICP-MS}$) between the HPCIC data and the ICP-MS data was 0.57, 0.74 and 0.65 for 0 to 5 cm, 5 to 8 cm and 8 to 10 cm samples, respectively.

Table 4.4: Matrix composition of shellfish digest as determined using ICP-MS.

Mussel tissue digest matrix[a] cations ICP-MS		
Average of n = 3 analyses		
Cation	Mg/L	Range
Na^{+}	57,135	48,790-62,780
K^{+}	252	233-264
Ca^{2+}	517	88-1,310[b]
Mg^{2+}	66	62-70
Ba^{2+}	1.2	0.3-1.7
Sr^{2+}	3.0	1.0-6.6
P^{3+}	181	149-225
S^{2+}	313	284-330
Fe^{2+}	1.8	1.6-2.0
Co^{2+}	<0.1	<0.1
Ni^{2+}	0.3	0.2-0.4
Cu^{2+}	0.2	0.2-0.2

[a] ~ 1 g dried tissue in 50 mL volume.

[b] Probable shell contamination of sample

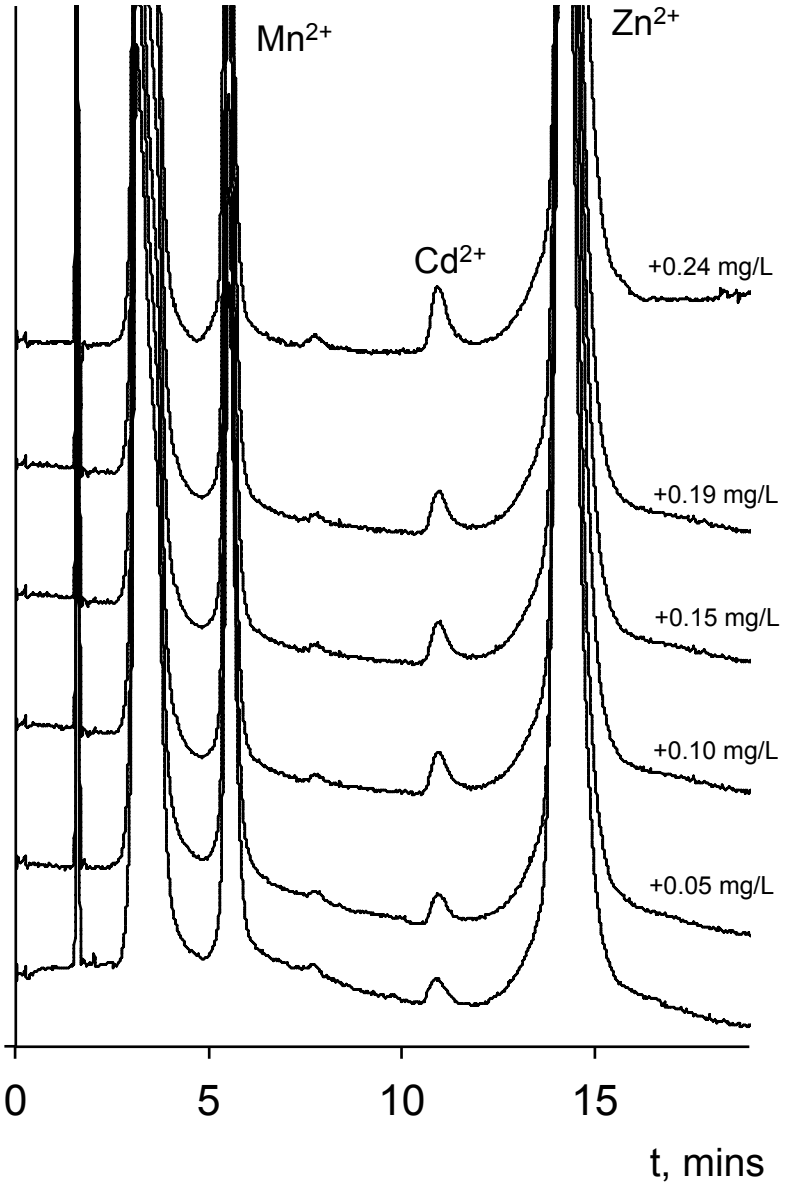

Fig. 4.5: Overlaid HPCIC sample chromatograms showing standard addition of Cd^{2+} to mussel tissue digest sample using HEPMA chelating column. Chromatographic conditions as Fig. 4.3 (b).

An unspiked sample was injected 10 times to confirm retention time precision, with average retention times of 5.65 ± 0.03 min (0.55% RSD), 10.67 ± 0.03 min (0.28% RSD), and 13.67 ± 0.07 min (0.5% RSD), for Mn^{2+}, $Cd^{2+}$and Zn^{2+}, respectively. Peak height precision (n = 6) for Mn^{2+} and Zn^{2+} within the Cd^{2+} spiked chromatograms shown in Fig. 4.5 was measured as 1.7% RSD for Mn^{2+} and 2.4% RSD for Zn^{2+} (see Fig. 4.6 for full scale version of overlaid chromatograms demonstrating peak height precision for Mn^{2+} and Zn^{2+}).

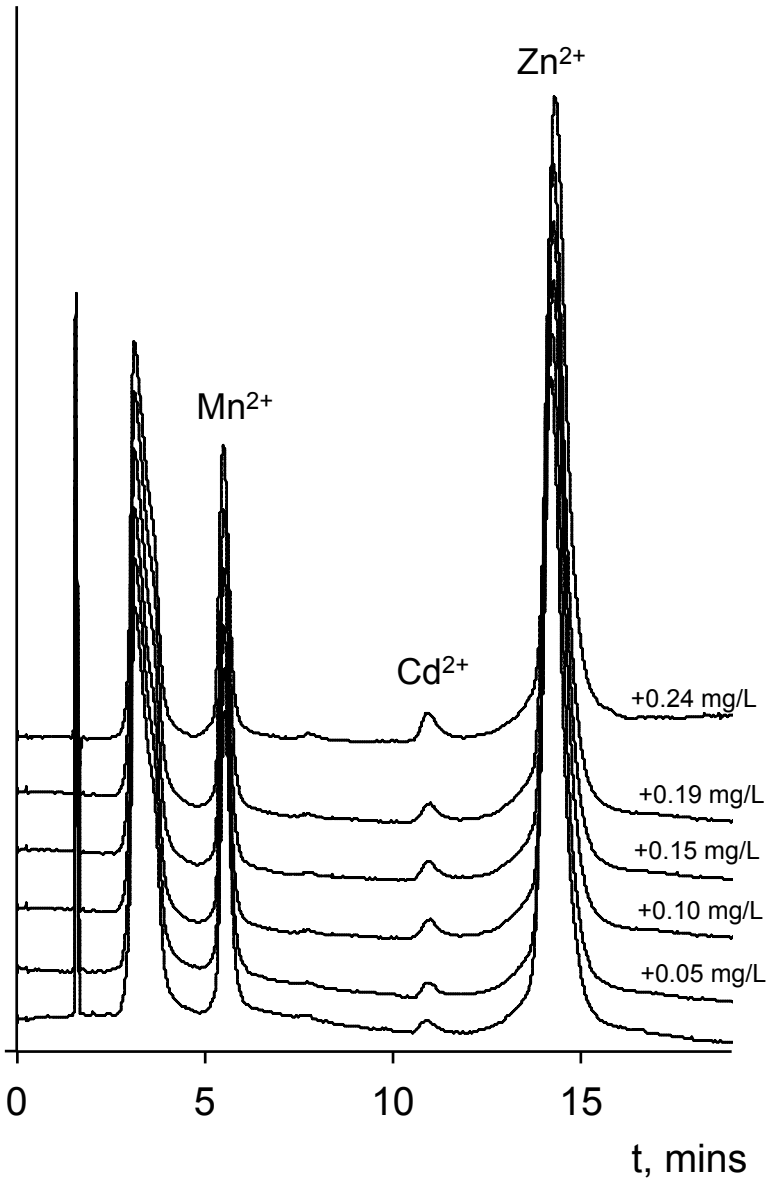

Fig. 4.6: Full scale overlaid HPCIC sample chromatograms showing standard addition of Cd^{2+} to mussel tissue digest sample using HEPMA chelating column. Chromatographic conditions as Fig. 4.3 (b).

Long-term column retention time stability was observed over a period of 20 days, with ~10 hours a day usage, equal to an estimated 12,000 column eluent volumes. No measurable degradation in peak shapes or significant changes in retention times were noted over this period. The method LLOQ calculated for Cd^{2+} was determined as 3.3 µg/g of dry mussel tissue, based upon 10 times the baseline noise of 0.1 mAU (from Fig. 4.6 measured at 6, 8 and 12 min).

The sample chromatograms show how trace Cd^{2+} is well resolved from both the relatively large Mn^{2+} and Zn^{2+} peaks, and also from a small unidentified peak eluting at approximately 7.5 min. As the chromatogram was recorded using the PAR PCR detection method, this small peak should be a trace metal present within the sample, however, the retention time does not correspond to Co^{2+}, Ni^{2+}, Pb^{2+}, Cu^{2+} or Fe^{3+} under the eluent conditions used, which apart from Co^{2+} would all elute after Zn^{2+}. From Table 4.1 selectivity and ICP-MS data, it is possible this small peak could indicate traces of Fe^{2+}, which were present within the sample blanks.

To summarise the size related metal concentrations, it can be stated that no overall quantitative pattern was observed between the size of the mussel and the quantities determined, with Zn^{2+} behaving differently than Cd^{2+} and Mn^{2+} in age/size-concentration dependence. However, the results were determined to be significantly different between sample sizes, using analysis of variance (ANOVA) testing at a 95% confidence level. To confirm these observations a larger sample set from multiple locations is currently being investigated.

4.4 Conclusions

HPCIC was successfully developed and applied to the detection and quantification of selected transition metal cations directly in mussel tissue acid digests. The results confirmed HPCIC as a useful analytical approach to the determination of metal ions in high ionic strength and complex samples, with which conventional chromatographic and spectroscopic techniques can experience significant matrix effects. The HEIDA and HEPMA phases employed provided complimentary selectivity, with the HEPMA phase particularly suited to the mussel digest sample. Resultant data for metals determined compared very well overall with ICP-MS data, despite very large differences in the dilution factors involved between the two approaches. As both phases were shown to have high tolerance to high ionic strength samples, HPCIC employing these columns can therefore be used as a cheap and versatile analytical technique for the determination of transition metals in such samples (i.e. seawater and biological tissues).

References

[1] J.R. Shaw, T.D. Dempsey, C.Y. Chen, J.W. Hamilton, C.L. Folt, Environmental Toxicology and Chemistry 25 (2006) 182.

[2] M.G. Macklin, K.A. Hudson-Edwards, E.J. Dawson, Science of the Total Environment 194-195 (1997) 391.

[3] B. Paull, M. Foulkes, P. Jones, Analyst 119 (1994) 937.

[4] H. Lu, X. Yin, S. Mou, J.M. Riviello, Journal of Liquid Chromatography & Related Technologies 23 (2000) 2033.

[5] D. Joksimovic, I. Tomic, A.R. Stankovic, M. Jovic, S. Stankovic, Food Chemistry 127 (2011) 632.

[6] L.L. Bartolomé, N.N. Etxebarria, I.I. Martínez-Arkarazo, J.C.J. Raposo, A.A. Usobiaga, O.O. Zuloaga, D.D. Raingeard, M.M. Ortiz-Zarragoitia, M.P.M. Cajaraville, Archives of Environmental Contamination and Toxicology 59 (2010) 244.

[7] N.N. Spann, D.C.D. Aldridge, J.L.J. Griffin, O.A.H.O. Jones, Aquatic Toxicology 105 (2011) 11.

[8] C.Y. Liu, N. Lee, T.H. Wang, Analytica Chimica Acta 337 (1997) 173.

[9] B. Paull, P.N. Nesterenko, P. Jones, High Performance Chelation Ion Chromatography, RSC Chromatography Monographs, Royal Society of Chemistry Publishing, Cambridge, UK (2011).

[10] W. Bashir, B. Paull, Journal of Chromatography A 907 (2001) 191.

[11] P. Jones, P.N. Nesterenko, Journal of Chromatography A 789 (1997) 413.

[12] L. Barron, M. O'Toole, D. Diamond, P.N. Nesterenko, B. Paull, Journal of Chromatography A 1213 (2008) 31.

[13] J.C. Dias, L.T. Kubota, P.N. Nesterenko, G.W. Dicinoski, P.R. Haddad, Analytical Methods 2 (2010) 1565.

[14] P.N. Nesterenko, P. Jones, Journal of Chromatography A 770 (1997) 129.

[15] P.N. Nesterenko, P. Jones, Journal of Chromatography A 804 (1998) 223.

[16] P.N. Nesterenko, O.A. Shpigun, Russian Journal of Coordination Chemistry 28 (2002) 726.

[17] W. Bashir, B. Paull, Journal of Chromatography A 942 (2002) 73.

[18] E. Sugrue, P. Nesterenko, B. Paull, Analyst 128 (2003) 417.

[19] J. Scancar, R. Milacic, Trends in Analytical Chemistry 28 (2009) 9.

[20] E. Sugrue, P. Nesterenko, B. Paull, Journal of Separation Science 27 (2004) 921.

[21] D. Caldarola, P.N. Nesterenko, B. Onida, Surface Modification of Silica Based Monolith with Glyphosate for Fast Ion Chromatography, Poster 214, Proceedings of HPLC2012, Anaheim, USA, 16 June 2012.

[22] A.T. Townsend, A.J. Seen, Science of the Total Environment 424 (2012) 153.

[23] P.L. Brown, V.J. Carolan, D.J. Hafey, M. Iko, S.J. Markich, R.J. Morrison, Wetlands Australia 21 (2006) 228.

[24] C. Copat, G. Arena, M. Fiore, C. Ledda, R. Fallico, S. Sciacca, M. Ferrante, Food and Chemical Toxicology 53 (2013) 33.

[25] US Environmental Protection Agency Method 3051A, Microwave assisted acid digestion of sediments, sludges, soils, and oils (February 2007).

[26] K. Popov, H. Rönkkömäki, L.H.J. Lajunen, Pure and Applied Chemistry 73 (2001) 1641.

[27] R. Smith, A. Martell, NIST critically selected stability constants of metal complexes database (1998).

[28] R.M. Smith, A.E. Martell, Science of the Total Environment 64 (1987) 125.

[29] E.P. Nesterenko, P.N. Nesterenko, B. Paull, M. Meléndez, J.E. Corredor, Microchemical Journal 111 (2013) 8.

5. A new N-hydroxyethyliminodiacetic acid modified core-shell silica phase for chelation ion chromatography of alkaline earth, transition and rare earth elements

Abstract

Core shell stationary phases have become increasingly popular in recent years, as they provide excellent efficiencies due to their unique morphology. To date, there has been no reported instance of a core shell stationary phase with a chelating ligand attached to the surface. In this work, sub-2-μm (1.7 μm) bare core shell silica has been modified with iminodiacetic acid functional groups by silane chemistry, forming a new HEIDA stationary phase and used to pack a 50 mm x 4.6 mm I.D. stainless steel column. The retention of alkaline earth, transition and heavy metal cations was investigated on the prepared stationary phase. The influence of nitric acid concentration, addition of complexing agent dipicolinic acid, eluent pH and column temperature on the column performance was investigated. It was shown that alkaline earth metals did not retain well on the core shell column under the eluent conditions investigated, and displayed a standard ion exchange retention mechanism, whilst transition and heavy metals were more strongly retained due to the secondary chelation mechanism. The efficiencies obtained for transition and heavy metal cations were comparable or higher than those previously obtained for silica based chelation stationary phases, with a short elution time (~5 mins) using a nitric acid eluent (10 m*M*). Increasing the ionic strength of the eluent with the addition KNO_3 (0.12 m*M*) and increasing the column temperature (70 °C) allowed the separation of a mixture of 14 lanthanides and yttrium in under 10 minutes. Excellent efficiencies of up to 200,000 *N*/m (for Ce^{3+}) were shown.

Aims

The aim of this work was to characterise the novel HEIDA core-shell stationary phase for the chromatographic behaviour of various metal cations and compare selectivity and efficiency to previously characterised HEIDA-silica phases of different morphologies, namely the HEIDA-silica monolith.

5.1 Introduction

Core shell particle (or superficially porous particle) columns have long been used for fast separations in LC [1-3]. However, in recent years their development has been rapidly advancing since the introduction of ultra high-performance liquid chromatography (UHPLC), to meet the demand for faster analyses without compromised efficiency [4]. UHPLC refers to the advances in columns and instrumentation designed to withstand higher pressure, for increased resolution, speed and sensitivity. Guiochon *et al.* have published a large volume of work regarding the performance of core shell particles [5-9], including a comprehensive review on their history, evolution and modern properties [10]. Core-shell particles are composed of a dense solid core surrounded by a layer of porous silica [5]. The morphology of such particles is shown in Fig. 5.1 and leads to an increase in column permeability and subsequently a reduced analysis column pressure drop, compared to similarly sized entirely porous particles.

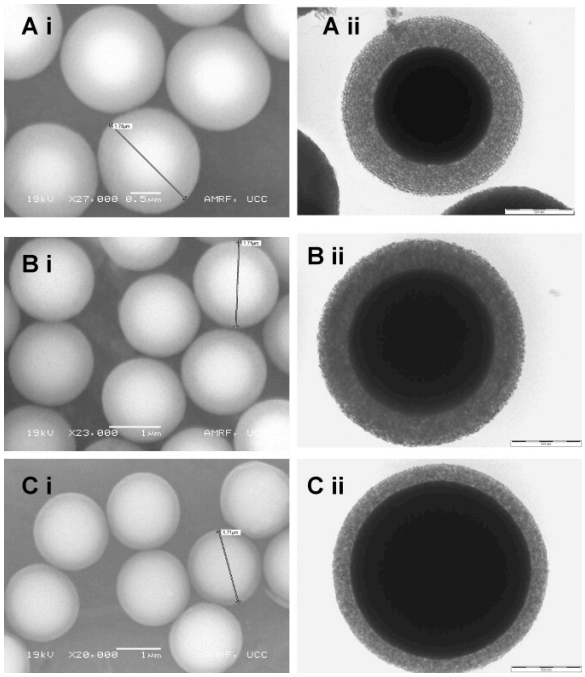

Fig. 5.1: Electron micrograph of three core shell "EIROSHELL™" 1.7 µm particles with different shell thickness: (Ai) SEM of EiS-350 and (Aii) TEM of EiS-350; (Bi) SEM of EiS-250 and (Bii) TEM of EiS-250; (Ci) SEM of EiS-150 and (Cii) TEM of EiS-150. [11].

Also observed are reduced band broadening and improved peak capacities due to the reduction of all terms of the van Deemter equation [12],

$$H_{(HETP)} = A + \frac{B}{u} + c_p u + c_f u$$

where A and B are the coefficients of eddy diffusion and longitudinal diffusion respectively, and $c_p u$ and $c_f u$ are the transparticle and film mass transfer resistance coefficients respectively.

The use of thin skin or "pellicular" particles dates back to the late 1960's when Horvath and Lipinski pioneered the use of shell particles consisting of 30-50 µm, nonporous solid glass spheres, coated with a 1-2 µm thick layer of porous organic polymer used for ion exchange chromatography [3,13]. The idea behind these stationary phases was that a higher efficiency would occur in comparison to fully porous particles due to the faster diffusion time through a thin layer compared to

diffusion through the entire particle [10]. Resistance to mass transfer through the stationary phase is then reduced. This approach however, was restricted, as the porous layer had poor uniformity and mechanical stability. In addition, these sorbents had limited surface area and therefore low loading capacity, and only a small number of compounds could be analysed. Consequently, although some core-shell sorbents were commercialised, this type of stationary phase did not remain popular.

Around the same time, the development of fully porous particles of increasingly smaller sizes that could be used to obtain higher efficiencies was taking place [14]. However the use of smaller particles presented the problem of increased pressure, and LC systems did not meet the requirements of these particles. This changed with the introduction of UHPLC, and in 2004 the emergence of particles with a sub-2- μm diameter marked a new phase for chromatographic performance. In the late 2000's, core-shell particles were reintroduced following a number of advances in sol-gel technology that resulted in increased surface area and narrow particle size distribution [15]. These advances in particle technologies have resulted in an improvement of the main physiochemical properties that affect mass transfer kinetics and thus contribute to the performance of core shell columns, including the surface area size, thickness of the shell, the surface roughness and the particle-size distribution and column packing [16]. Sub-3-μm core shell silica stationary phases in particular have received increasing attention due to the reduced plate heights that they can generate (below HETP ~3.5 μm for small molecules [17,18]) compared with columns packed with fully porous sub-2-μm particles [4]. It has been shown that only the second generation of monolithic columns (Chromolith^{TM}) displays similar column performance. However, they still cannot be operated at high back pressures (> 200 bar) [19], compared with columns packed with sub-3-μm core–shell which can be used up to 600 bar [6]. In 2009 Phenomenex produced the Kinetex 1.7 μm core-shell sorbent, the only commercially available sub-2-μm core–shell column, which has generated the lowest reported HETP of any UHPLC column (< 1.5 μm), and has been applied to the separation of both small and large molecules such as peptides and proteins [15].

The most common functionality used for the production of core shell stationary phases is C_{18}, which has been used for the majority of commercially available shell columns, and has been characterised in detail in recent years [4]. To date, there has been no reported instance of the application of a chelating functionality to a core shell silica based stationary phase for the chromatographic separation of metal cations using HPCIC.

In the work presented herein, a novel sub-2-µm HEIDA-bonded silica core shell stationary phase was prepared and characterised for alkaline earth and transition metals, and compared with a HEIDA functionalised silica monolith for chromatographic performance. The iminodiacetic based functionality was chosen as one of the most successful chelating ion exchange chemistries. The effects of nitric acid eluent concentration, dipicolinic acid concentration, column temperature and eluent flow rate have been studied and discussed. Finally, the stationary phase was applied to the fast separation of a mixture of lanthanide cations, where excellent peak efficiencies were achieved.

5.2. Experimental

5.2.1. Instrumentation

For the packing of the column, a constant pressure electrically driven pump from SSI LabAlliance (PA, USA) was used. The packing was controlled using the Quickset pump control software V.1.2, also from SSI LabAlliance. All chromatographic details are described in Section 2.2.1.

5.2.2. Reagents

Analytical or higher grade reagents and Milli-Q water (Millipore, Bedford, MA, USA) were used for the preparation of all solutions. Nitric acid eluents were prepared from 70% nitric acid (Sigma Aldrich, Dublin, Ireland). Pyridine-2,6-dicarboxylic acid, 99% (DPA) and potassium nitrate for eluent preparation were obtained from Sigma–Aldrich (Dublin, Ireland). Post-column reagents PAR, *o*-cresolphthalein complexone (*o*-CPC), arsenazo III and reagents for their preparation (ammonium hydroxide (28%), acetic acid, ethylenediaminetetraacetate (ZnEDTA),

and boric acid were purchased from Sigma Aldrich (Dublin, Ireland).

Metal standard solutions in their salt form were purchased from BDH Chemicals (Poole, UK) (Ba^{2+}, Mn^{2+}, Cd^{2+}, La^{3+}, Ce^{3+}) or Sigma Aldrich (Dublin, Ireland) (Ca^{2+}, Sr^{2+}, Mg^{2+}, Mn^{2+}, Co^{2+}, Zn^{2+}). An ICP (1000 ppm) Y^{3+} standard was from Sigma Aldrich (Dublin, Ireland). Stock metal standard solutions were prepared at concentration of 1000 ppm in acidified (5% (v/v)) Milli-Q water, and stored in polypropylene bottles. Working standards were prepared on each day of use unless stated otherwise. For the separation of rare earth metals, a mixture of 100 ppm 16 rare earth elements (13 lanthanides, lanthanum, yttrium and scandium) in 5% (v / v) nitric acid was obtained from Johnson Matthey (Karlsruhe, Germany). All eluents were filtered before use through 0.22 µm nylon membrane filters and degassed using sonication.

5.2.3. Detection

For characterisation of the HEIDA bonded silica core shell stationary phase, various post-column reagents were employed depending on the analyte(s) of interest. The PCR used for the detection of transition and heavy metal ions Mn^{2+}, Co^{2+}, Cd^{2+} and Zn^{2+} was composed of 0.15 m*M* PAR, 2.0 *M* NH_4OH, pH 10.5 and detection was performed at wavelength 510 nm [20]. For the detection of alkaline earth metals only, 0.4 m*M* *o*-CPC was prepared in 0.25 *M* boric acid adjusted to pH 10.5 with 2 *M* NaOH solution. The detection was performed at 570 nm [21]. For all work related to the determination of lanthanides and Y^{3+}, 1.5 x 10^{-4} *M* arsenazo III in 0.5 *M* acetic acid was employed and detection wavelength was 650 nm [22].

5.2.4 Preparation of core shell stationary phase

For the production of the HEIDA monolithic columns, PEEK housed bare monolithic silica columns (Onyx Monolithic Si) of 100×4.6 mm I.D. were purchased from Phenomenex (Cheshire, UK). According to the manufacturer, the silica monolith had a surface area of 300 m2/ g with a bimodal porous structure (porosity 81%), comprising macropores of 2 µm diameter, and mesopores of 13 nm diameter. The functionalisation of silica monoliths was performed as described by Nesterenko *et al*. [22]. The synthesis of the 1.7 µm superficially porous silica particles (with a 1.45 µm

solid core and 0.25 μm porous shell thickness, surface area 90 m2/g and pore size 10 nm) was as per the registered patent [28]. Surface modification of the core-shell silica particles was achieved using a similar approach to that developed earlier for the modification of HEIDA modified silica monolith columns [22]. Briefly, the modification of 1.5 g of silica particles was performed under controlled reflux of water suspension of the particles for 6 hours with 30-fold excess of the modifier acidified to pH 6.0 with concentrated acetic acid. The modifier was prepared by the reaction of 3-glycidoxypropyltrimethoxysilane with 3-fold excess of IDA under alkaline conditions (pH 12) by stirring for 30 min at 60 °C. Potassium carbonate was used as a buffer. All reagents were dissolved in deionised water. The chemically bonded, epoxylated mesoporous silica sample was washed with both water and acetone, then packed into a stainless steel column (as above).

5.3 Results and discussion

HEIDA-silica stationary phases have been well characterised, most recently for an HEIDA modified silica monolith (Chapter 3). However it was necessary to characterise this new chelating core-shell stationary phase for its retention and selectivity properties and to compare its performance to HEIDA-silica columns of different morphologies. Any differences in selectivity could be due to the nature of the core shell particles, which as mentioned above had not yet been applied to the separation of metal cations for chelation chromatography.

5.3.1 Selectivity

As discussed in Chapter 3, the selectivity of metal cations can be manipulated by altering various mobile phase parameters. The details of the mechanisms of mobile phase parameters are discussed in detail in Chapter 3. Accordingly, they will not be not be considered here and the following Section will focus on the results on the HEIDA-silica core-shell column.

5.3.1.1 Effect of HNO_3 concentration/pH

Using dilute HNO_3 eluent in the range 2 to 10 m*M* for alkaline earth metals and 4 to 10 m*M* for transition metals, the effect on selectivity and retention of metal ions was observed. As demonstrated in Fig. 5.2, the relationship between log *k* and HNO_3 concentration for all metal cations was linear, with slopes in the range of 1.89 to 2.11 (absolute value) for alkaline earth metals, and from 2.10 to 2.23 for transition metals. The elution order (at constant flow rate (0.8 mL/min) and constant temperature (30 ^{o}C)) was $Mg^{2+} < Sr^{2+} \leq Ca^{2+} < Ba^{2+} < Mn^{2+} < Co^{2+} < Cd^{2+} < Zn^{2+}$. The elution order of transition metals was in agreement with that of previously determined fully porous HEIDA-silica data, likely due to the higher formation constants for transition metal-IDA complexes [23]. There was a slight change in the elution order of all alkaline earth and transition metals compared to the HEIDA-monolith (Section 3.3.1), where Mn^{2+} was retained for slightly longer than Ba^{2+}.

The effect of HNO_3 concentration was also carried out on the more strongly retained lanthanide cations. In an unsuppressed electrostatic interaction system one would expect that the elution order of the lanthanide series would be reversed. However, the results suggest a chelation dominant mechanism, likely due to the high column temperature (Section 1.4.2). The plot of log concentration HNO_3 vs log *k* was linear as expected (Fig. 5.3) [23], with slopes proportional to the number of electrons replaced by each metal coordinated to the immobilised ligands (1.3 for La^{3+} to 2.2 for Lu^{3+}).

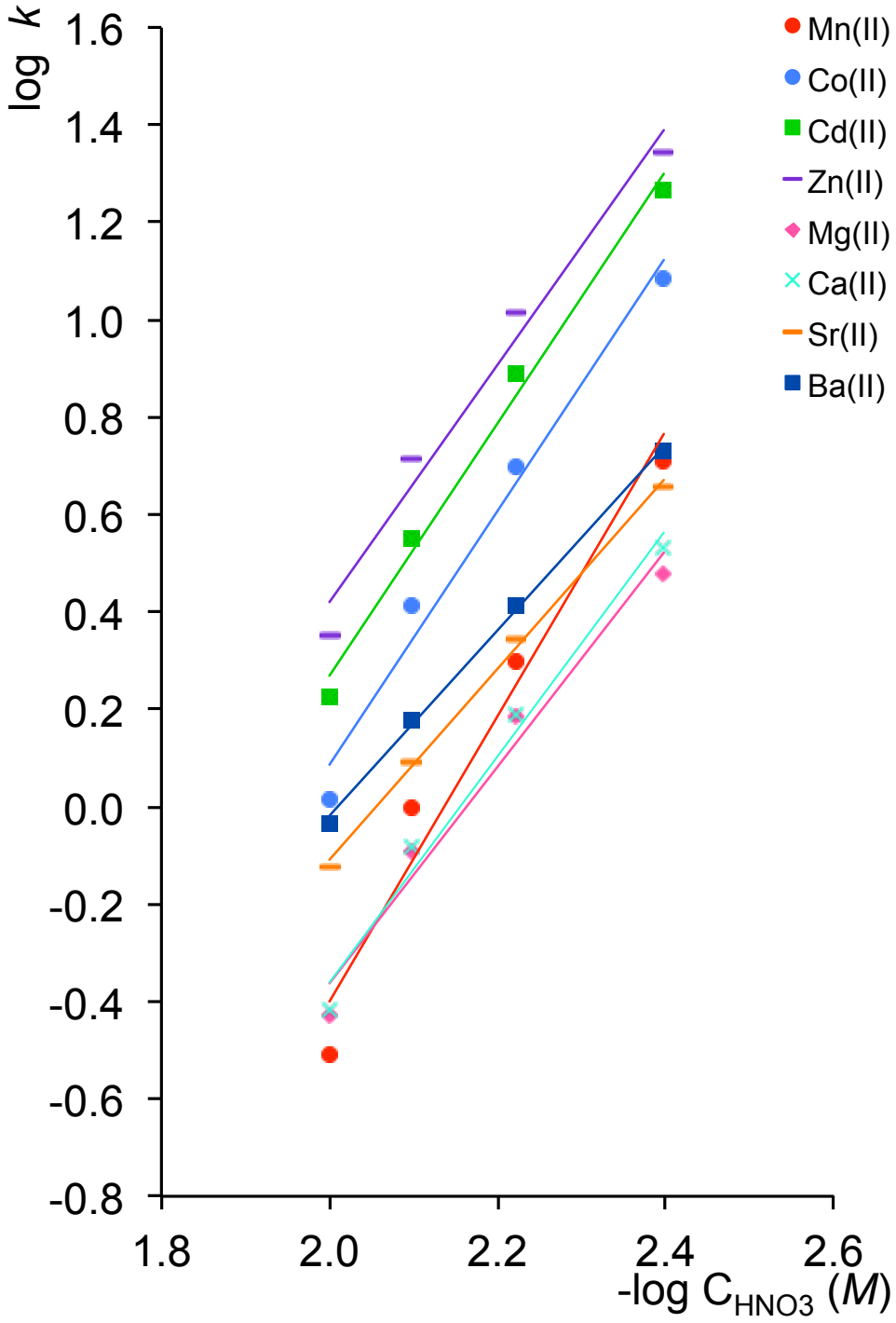

Fig. 5.2: Effect of HNO_3 eluent concentration on retention of alkaline earth and transition metal cations on HEIDA-silica core-shell column. Eluent: HNO_3, Flow rate: 0.8 mL/min, Column temperature: 30 ^{o}C, Injection volume: 20 µL, Analyte concentration: 10 ppm, Detection: spectrophotometric at 510 nm after PCR with 0.2 m*M* ZnEDTA/0.12 m*M* PAR or 570 nm with 0.4 m*M* *o*-CPC at 0.4 mL/min.

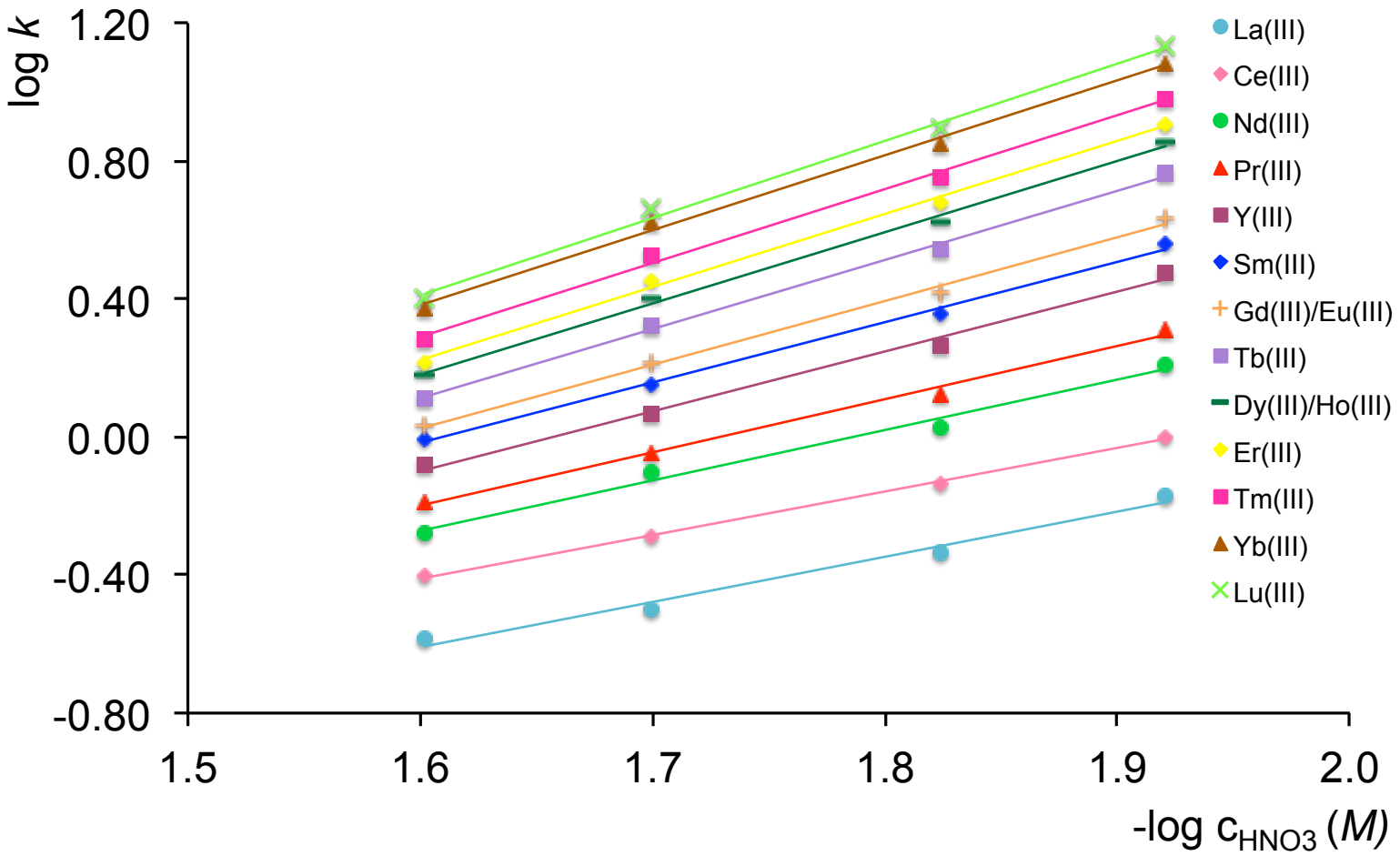

Fig. 5.3: Effect of HNO_3 eluent concentration on retention of lanthanide and yttrium metal cations on HEIDA-silica core-shell column. Eluent: 6 m*M* HNO_3, 0.3 m*M* DPA, Flow rate: 0.8 mL/min, Column temperature: 30 ^{o}C. Injection volume: 10 µL, Analyte concentration: 10 ppm, Detection: spectrophotometric at 650 nm after PCR with 1.5 x 10^{-4} *M* arsenazo III at 0.4 mL/min.

5.3.1.2 Addition of complexing agent to the eluent

The addition of a complexing agent such as dipicolinic acid can drastically change the selectivity of metal cations. Fig. 5.4 shows the effect that the addition of DPA to the eluent has on the retention of metal cations and how retention can be manipulated to achieve a faster separation.

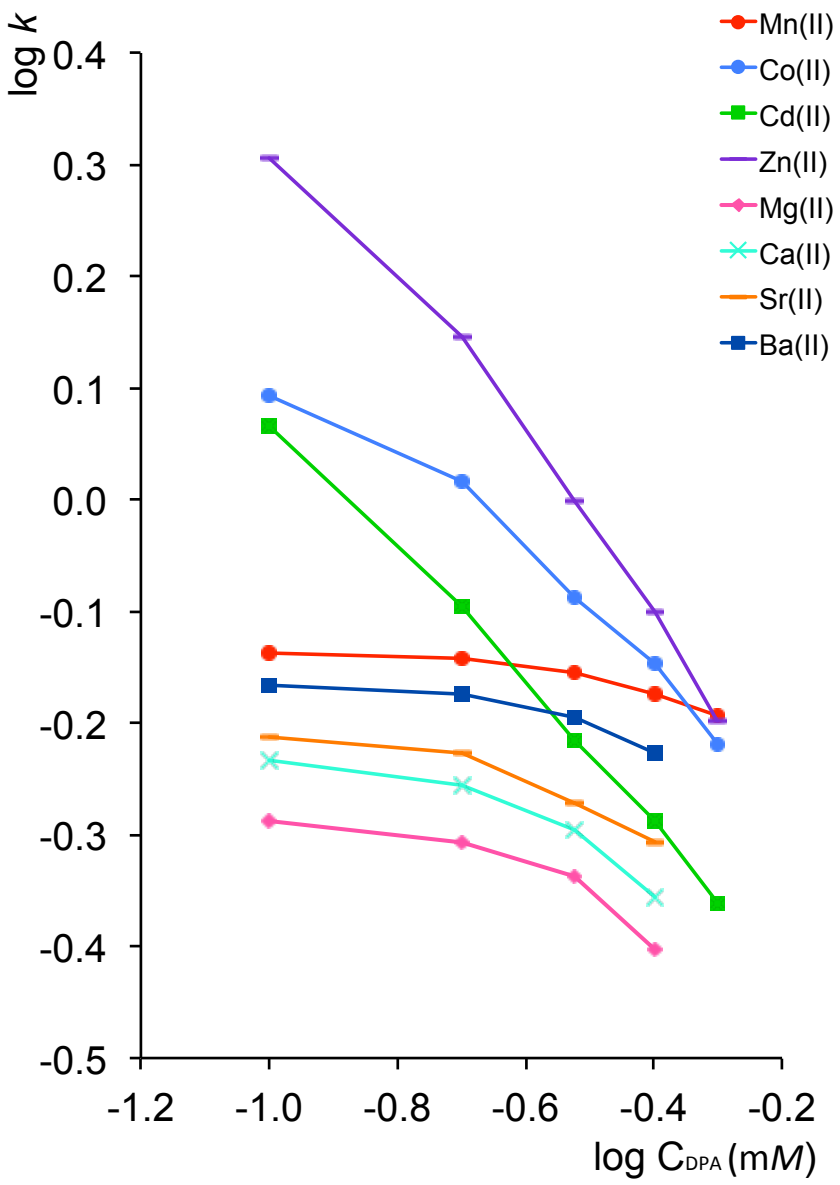

Fig. 5.4: Effect of DPA eluent concentration (0.1 to 0.5 m*M*) on retention of metal cations using HEIDA-silica core-shell column. Eluent: 6 m*M* HNO_3, other chromatographic details as Fig. 5.2.

As expected, the effect of the addition of DPA on transition metals was greater than on alkaline earth metals due to the higher stability constants and therefore complexes formed. Mn^{2+} displayed behaviour similar to that of alkaline earth metals due to the similar stability constants, with little change in retention. However, a slight increase in retention of the alkaline earth metals suggests a chelation dominant mechanism is present. As with the HEIDA-silica monolith (Section 3.3.2), the use of DPA as a complexing agent in the eluent can be used to manipulate selectivity of metal cations.

5.3.1.3 The effect of ionic strength on the separation of lanthanides

As IDA is a moderate cation exchanger, unwanted electrostatic interactions occur between the functional group and the metal cations. To suppress these interactions and ensure chelation is the dominant retention mechanism, strong electrolytes such as sodium or potassium nitrate can be added to the eluent. The retention order of transition and heavy metals typically does not change between suppressed and unsuppressed ion exchange elution systems on HEIDA-silica, although the main effect will be a difference in resolution due to an increase in *k* values. This is not, however, the case with lanthanide metal cations, where previous work on HEIDA-silica had shown changes in the order of retention between suppressed and unsuppressed systems [22,24]. If there is no suppression of the electrostatic interactions then retention is a combination of ion exchange and chelation mechanisms [25] and shows poor separation selectivity, which worsens with the more strongly retained (heavier) lanthanides, due to a decreased chelation affinity. This is clearly demonstrated in Fig. 5.5 (a), where the separation of a mixture of 14 lanthanides was attempted on a nitric acid only (25 m*M*) eluent. It is obvious that a dual retention mechanism of simple ion exchange and chelation is present. The addition of 0.75 *M* potassium nitrate to the nitric acid eluent (Fig. 5.5 (b)) had a drastic effect on the retention and peak shape of the lanthanides, as a result of the suppression of electrostatic interactions between the HEIDA groups and the trivalent metal cations.

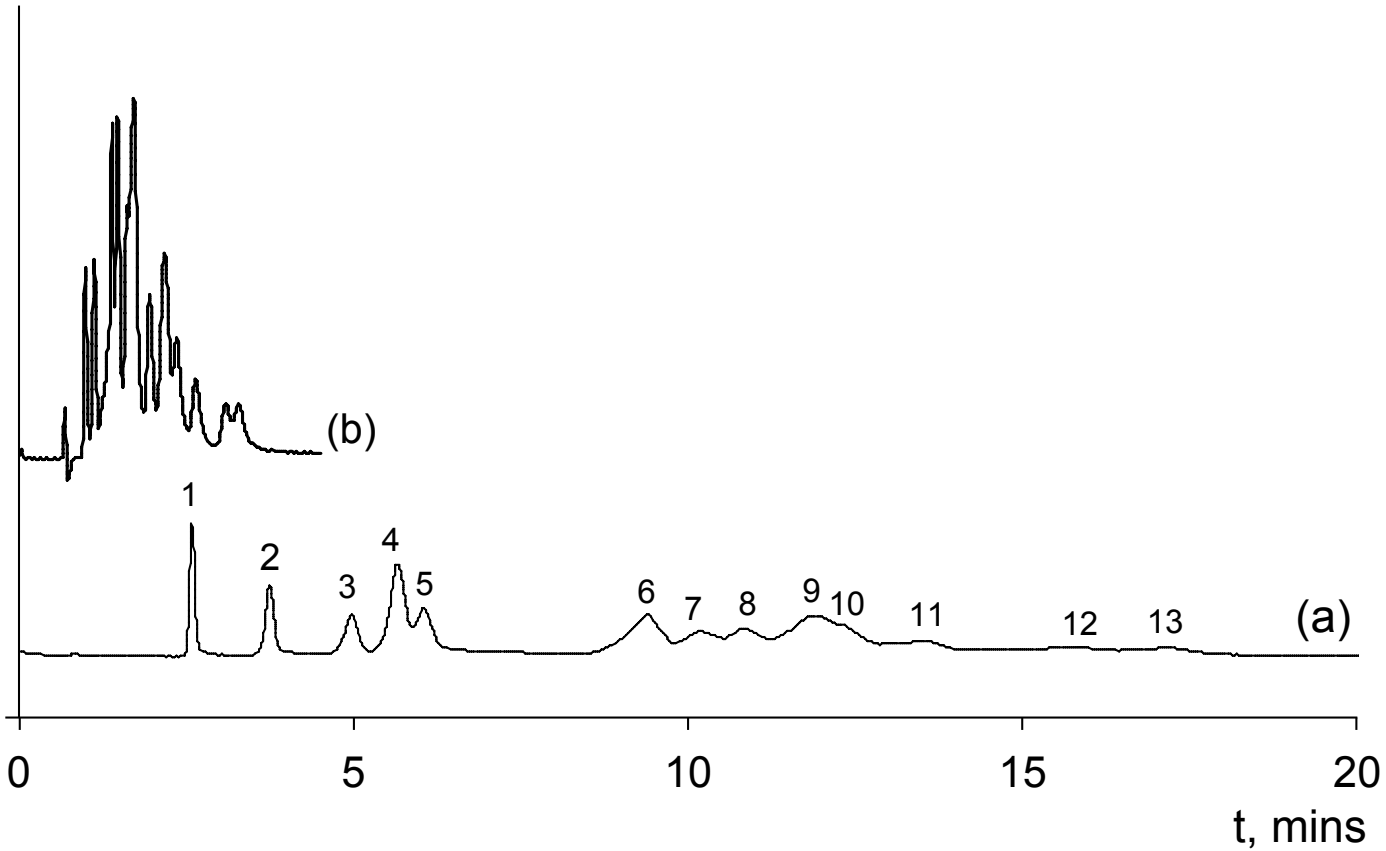

Fig. 5.5**:** The effect of the addition of KNO_3 in the eluent on the isocratic separation of rare earth metals HEIDA-silica core shell column. Analytes in order of elution (which did not change): 1: La^{3+}, 2: Ce^{3+}, 3: Pr^{3+}, 4: Nd^{3+}, 5: Y^{3+}, 6: Sm^{3+}, 7: Gd^{3+}/Eu^{3+}, 8: Tb^{3+}, 9: Dy^{3+}/Ho^{3+}, 10: Er^{3+}, 11: Tm^{3+}, 12: Yb^{3+}, 13: Lu^{3+}. Eluent: (a) 25 m*M* HNO_3 only, (b) 25 m*M* HNO_3/0.75 *M* KNO_3, Flow rate: 0.8 mL/min, Column temperature: 70 ^{o}C, Injection volume: 10 µL, Detection: spectrophotometric at 650 nm after PCR with 1.5 x10^{-4} *M* arsenazo III at 0.4 mL/min.

The order of elution is in good agreement with the stability constant values of the metals with HEIDA [23], which is a strong indicator that chelation is the dominant system. In order to improve peak resolution, the concentration of nitric acid was reduced (keeping the concentration of potassium nitrate constant at 0.75 *M*) until resolution improved, (Fig. 5.6).

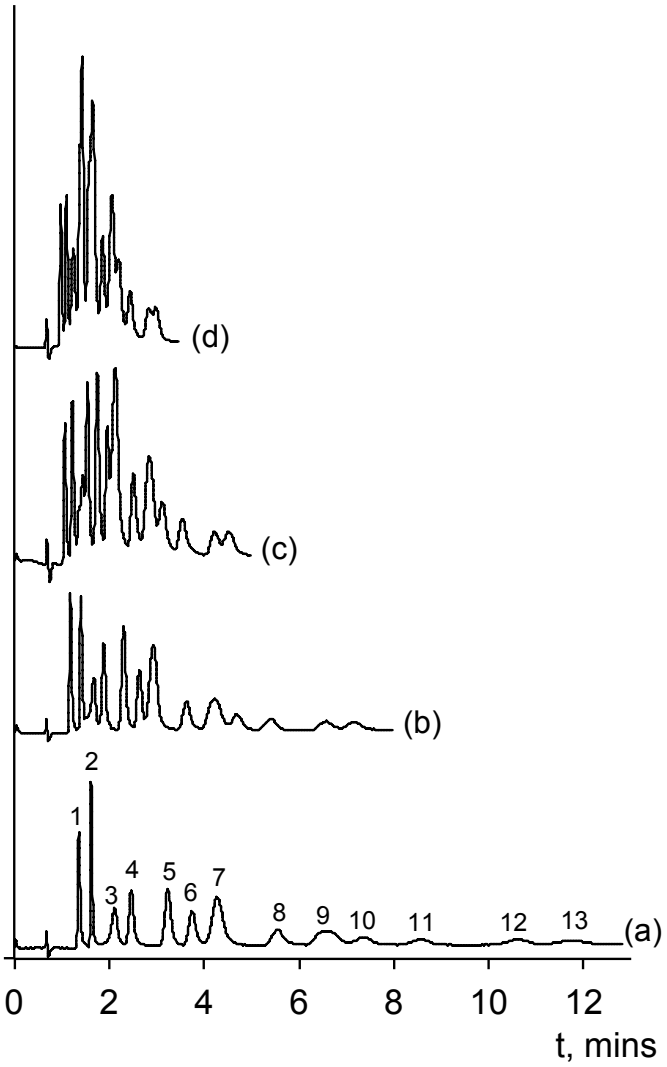

Fig. 5.6: Chromatographic separation of lanthanides using varying concentrations of HNO_3 in the eluent. Analytes in order of elution (which did not change): 1: La^{3+}, 2: Ce^{3+}, 3: Pr^{3+}, 4: Nd^{3+}, 5: Y^{3+}, 6: Sm^{3+}, 7: Gd^{3+}/Eu^{3+}, 8: Tb^{3+}, 9: Dy^{3+}/Ho^{3+}, 10: Er^{3+}, 11: Tm^{3+}, 12: Yb^{3+}, 13: Lu^{3+}, Eluent: 0.75 *M* KNO_3 with (a) 12, (b) 15, (c) 18, (d) 20 m*M* HNO_3, Flow rate: 0.8 mL/min, Column temperature: 70 ºC, Injection volume: 10 µL, Detection: spectrophotometric at 650 nm after PCR with 1.5 x10^{-4} *M* arsenazo III at 0.4 mL/min.

5.3.2 Efficiency

Column efficiency depends strongly on both the particle size and the particle structure [28]. As discussed in Section 5.1, the greatest advantage of the morphology of core-shell stationary phases is the reduction of all terms of the van Deemter equation [12], resulting in improved efficiency. Here, the efficiency of the core-shell column was evaluated and compared to the HEIDA-silica monolith.

5.3.2.1 Comparison with HEIDA-silica monolith

In order to fully and accurately compare the selectivity and efficiency of the HEIDA-silica core-shell stationary phase to the previously characterised HEIDA-silica monolith, a mixture of transition metals Mn^{2+}, Co^{2+}, Cd^{2+} and Zn^{2+} was analysed on both columns at identical conditions. Tables 5.1 and 5.2 highlight the higher efficiencies that the core-shell sorbent provide compared to the HEIDA-monolith.

Table 5.1: Chromatographic data for transition metal cations on HEIDA-silica core-shell column. Eluent: 10 m*M* HNO_3, Column temperature: 30 ^oC.

Cation	*N*/m	HETP (μm)	*k*'	Resolution	Asymmetry
Mn^{2+}	66,000	62.5	1.0	4.56	1.4
Co^{2+}	18,000	91.0	1.83	4.03	1.25
Cd^{2+}	67,000	58.8	3.16	1.66	1.35
Zn^{2+}	46,000	50.0	3.83	N/A	1.21

Table 5.2: Retention and efficiency data for transition metal cations on HEIDA-silica monolith. Eluent: 10 m*M* HNO_3, Column temperature: 30 ^oC.

Cation	*N*/m	HETP (μm)	*k*'	Resolution	Asymmetry
Mn^{2+}	16,000	15.2	0.54	3.18	1.12
Co^{2+}	11,000	55.6	2.24	4.03	1.26
Cd^{2+}	17,000	14.9	3.13	3.59	1.37
Zn^{2+}	20,000	21.7	2.90	N/A	1.29

The efficiency (*N*/m) values obtained for Co^{2+} on the core shell column were significantly lower than the other metal cations, which is in good agreement with the

results obtained on the HEIDA-silica monolith, where this trend was also observed. The lower efficiency is illustrated in Figs. 5.7 and 5.8 where it can be clearly seen that the peak shape for Co^{2+} is broader than the later eluting Cd^{2+} and Zn^{2+}. This is likely due to the fact that Co^{2+} is not a kinetically fast metal cation, although further work on this subject is necessary to confirm this theory.

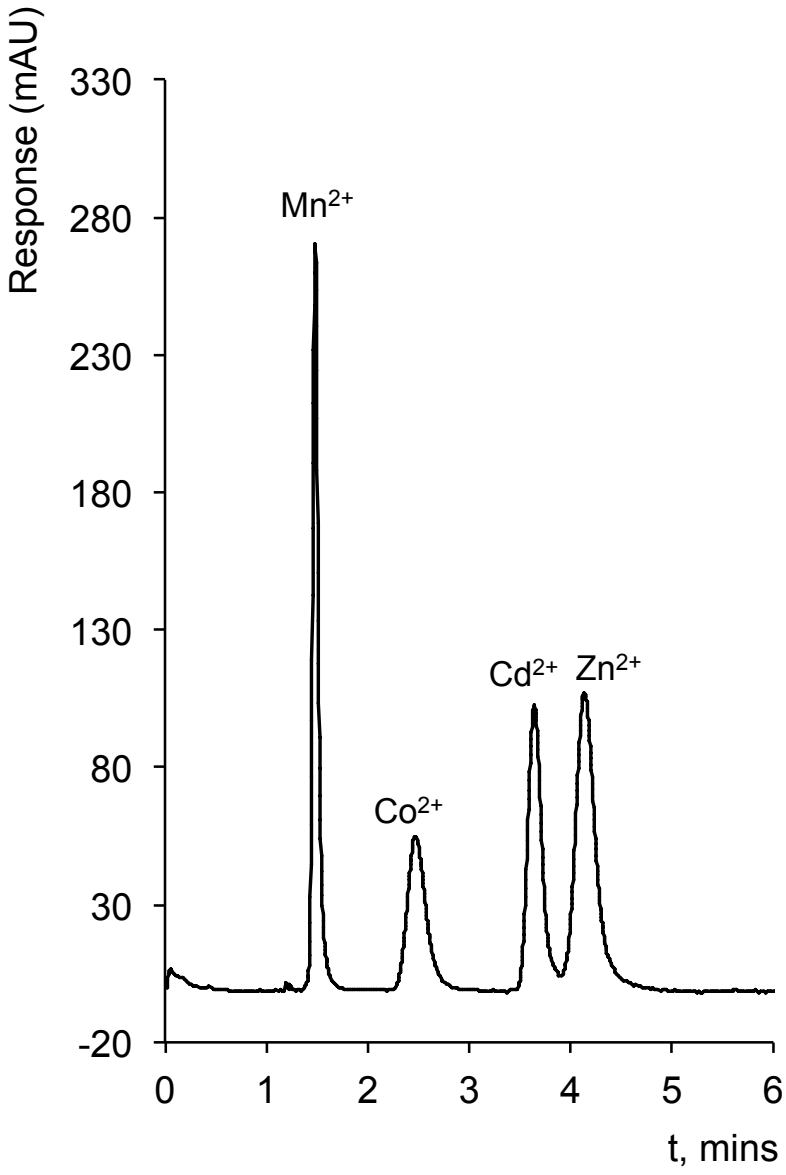

Fig. 5.7: Isocratic separation of transition metal cations Mn^{2+}, Co^{2+}, Cd^{2+} and Zn^{2+} on HEIDA-silica core-shell column. Eluent: 10 m*M* HNO_3, Flow rate: 0.8 mL/min, Column temperature: 30 ^{o}C, Injection volume: 10 µL, Analyte concentration: 10 ppm, Detection: spectrophotometric at 510 nm after PCR with 0.15 m*M* PAR, at 0.4 mL/min.

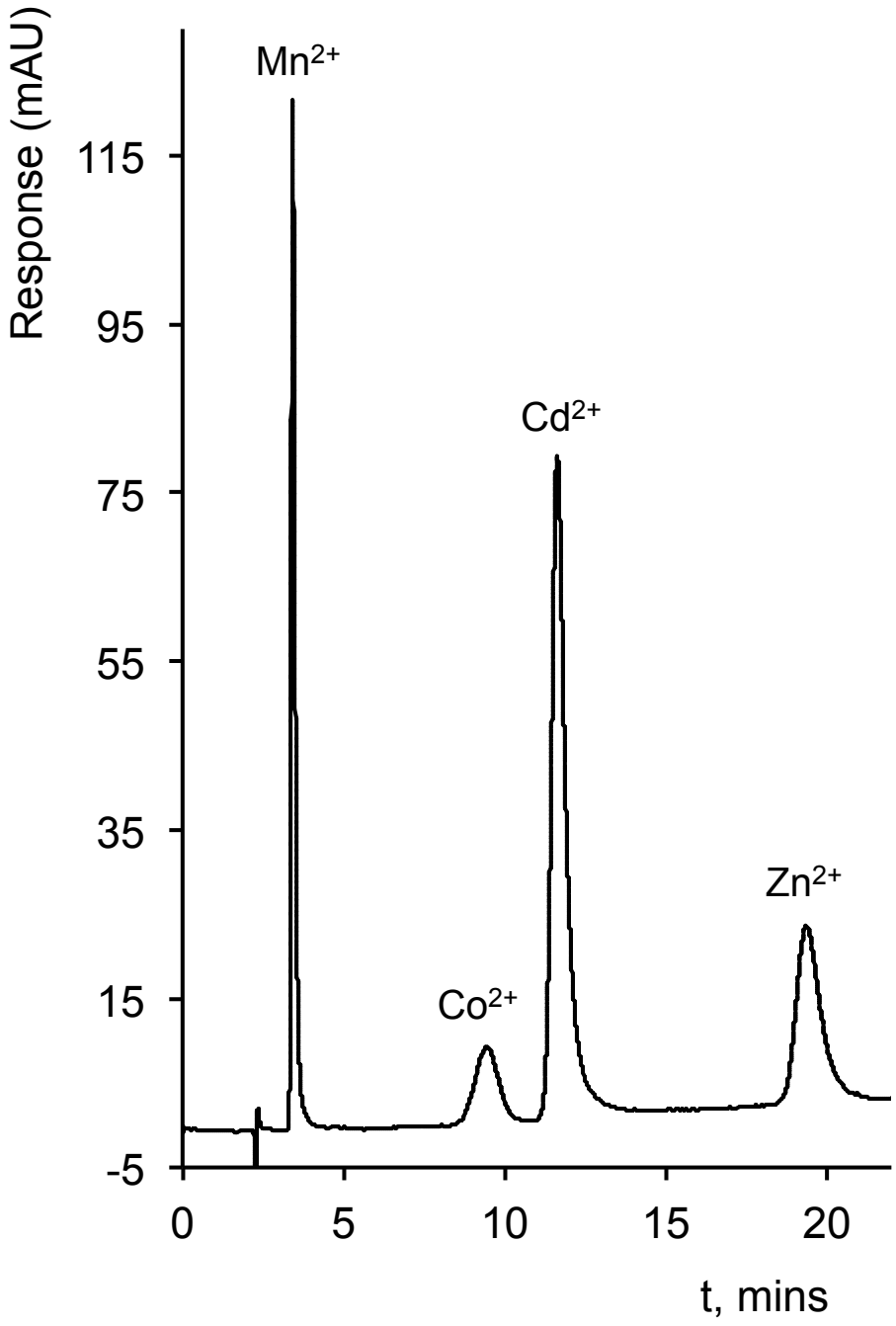

Fig. 5.8: Isocratic separation of transition and heavy metal cations Mn^{2+}, Co^{2+}, Cd^{2+} and Zn^{2+} on HEIDA-silica monolith column. Eluent: 10 m*M* HNO_3, Flow rate: 0.8 mL/min, Column temperature: 30 ^{o}C. Injection volume: 10 µL, Analyte concentration: 10 ppm, Detection: spectrophotometric at 510 nm after PCR with 0.15 m*M* PAR at 0.4 mL/min.

The order of elution of transition metal cations is identical to that of the HEIDA-monolith, corresponding to the HEIDA-metal stability constants. There is a slight difference in selectivity observed, as seen in Figs. 5.7 and 5.8, which is likely due to the nature of the core shell particles compared to the HEIDA monolith. The selectivity displayed on the core shell column is also slightly different to that observed on a fully porous bare silica column (150 x 4.0 mm I.D., 5 μm) with 8 m*M* HNO_3 eluent [26]. The core shell stationary phase shows better resolution of Co^{2+} and Cd^{2+} compared to the bare HEIDA-silica and HEIDA-silica monolith, but Cd^{2+} and Zn^{2+} are slightly less resolved. The elution times on the core shell are comparable to the bare silica column and significantly faster than the silica monolith. Using a 10 m*M* HNO_3 eluent, retention for Mn^{2+}, Co^{2+}, Cd^{2+} and Zn^{2+} was reduced by 34.9%, 32.7%, 39.1% and 33.3% respectively. There is also a noticeable difference in the resolution of Cd^{2+} and Zn^{2+}, again likely due to the difference in column morphology and rate at which the cations form complexes on the surfaces of the particular stationary phase. Peak asymmetry was comparable for all peaks, with the exception of a slightly higher value Mn^{2+} than determined on the silica monolith.

5.3.2.2 Column loading capacity

It was necessary to evaluate how the column worked together with the system. Small particle columns typically need to be run on systems with high pressure capabilities, and core shell sorbents can become overloaded more easily than their fully porous counterparts, causing band broadening and a decrease in efficiency [27]. Mn^{2+}, Cd^{2+} and Zn^{2+} were injected at different sample injection volumes (10, 15, 20, 30, 40 and 50 μL). It is clear from Fig. 5.9 (sample injection volume vs *N*/m) that peak efficiency decreases with increased sample volume (29, 35 and 20% for Mn^{2+}, Cd^{2+} and Zn^{2+} respectively, from 10 to 50 μL), therefore sample injection volume was kept relatively low (~10 μL) for all further analysis on the HEIDA-core shell column.

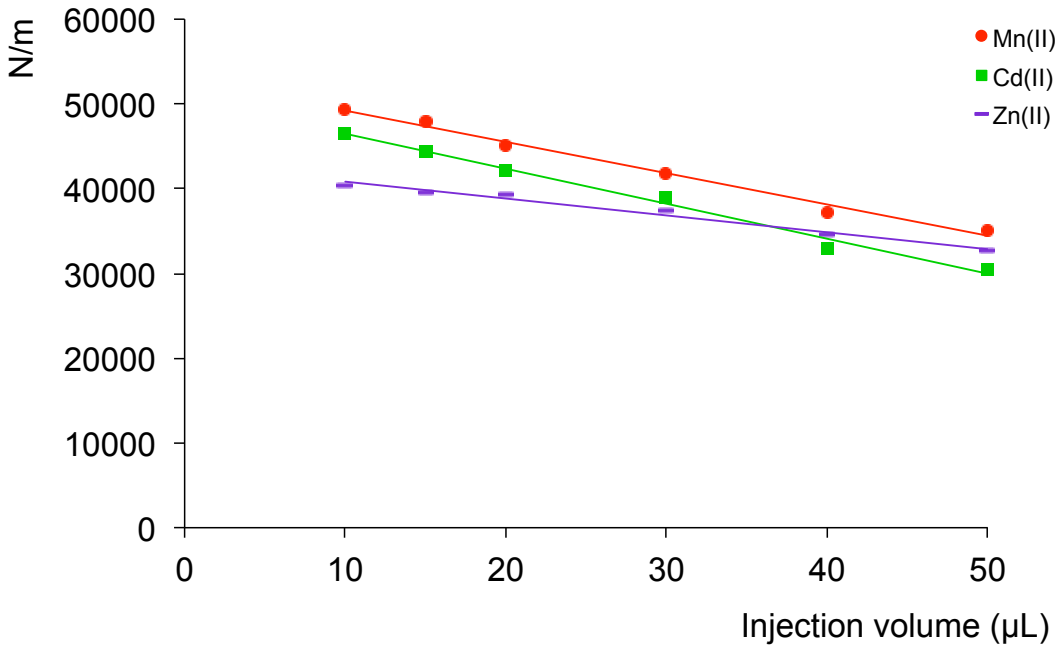

Fig. 5.9: Effect of sample loop size (µL) on efficiency of Mn^{2+}, Cd^{2+} and Zn^{2+}. Eluent: 6 m*M* nitric acid, Flow rate: 0.8 mL/min, Column temperature: 30 ^{o}C. Analyte concentration: 10 ppm, Detection: spectrophotometric at 510 nm after PCR with 0.15 m*M* PAR at 0.4 mL/min.

5.3.2.3 Flow rates

The effect of flow rate on retention, selectivity and efficiency of transition metals was recorded and the results reported. The pressure limitations of the IC system allowed for the analysis of metals over a range of 0.1-1.4 mL/min, in 0.05 mL increments. For all analysis the post-column reagent was set to a flow rate of ½ of the eluent flow rate. All injections were carried out in triplicate with the mean result reported. The van Deemter curve generated (Fig. 5.10) shows that for transition metals the optimum flow rate was ~0.6 mL/min, with the exception of Co^{2+} where the lowest HETP value was generated at 0.5 mL/min. For direct comparison to the HEIDA-silica monolith (Fig. 3.10), efficiency values over the range of 0.6 to 1.2 mL/min (3.61 to 7.23 cm/min linear velocity) were compared.

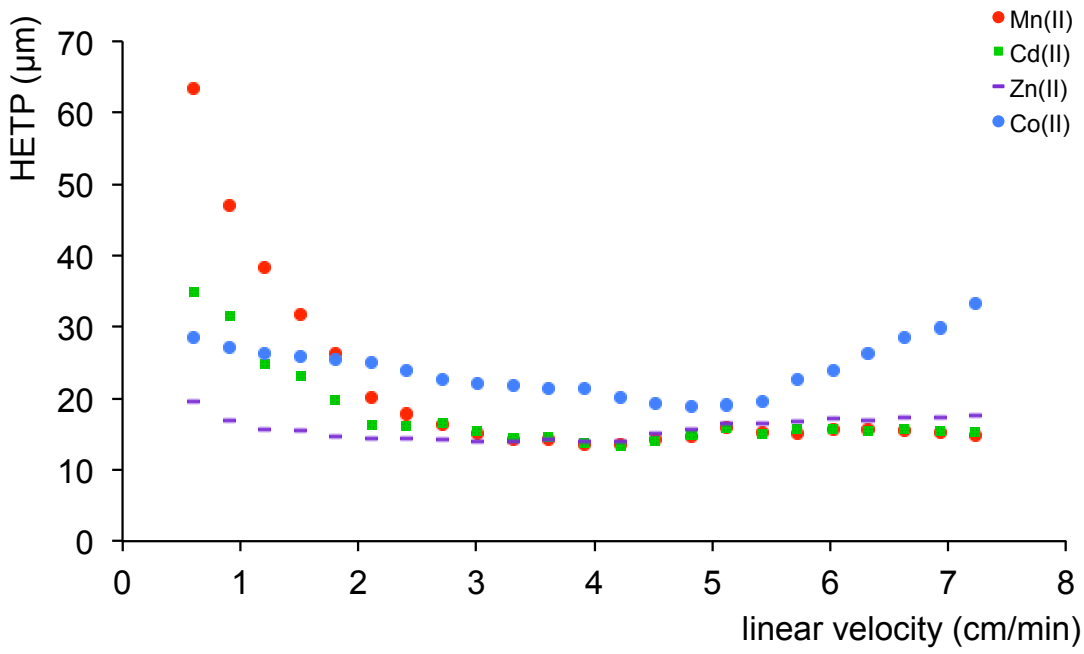

Fig. 5.10: HETP for transition metals Mn^{2+}, Co^{2+}, Cd^{2+} and Zn^{2+} for HEIDA-silica core-shell column: Eluent: 6 m*M* HNO_3, Column temperature: 40 ºC, Injection volume: 10 µL, Detection: spectrophotometric at 510 nm after PCR with 0.15 m*M* PAR, PCR flow rate: set to ½ eluent flow rate.

For both columns the relationship between flow rate and retention was linear over the range of 0.6 to 1.2 mL/min. There is a noticeable difference in the effect of increasing the flow rate between stationary phases. The HEIDA-silica core-shell column shows a significantly smaller reduction in HETP values from 0.6 to 1.2 mL/min compared to the monolith (5.1, 29.1, 6.2 and 19.1% reduction compared to 3.6, 35.0, 22.3 and 31.3% for Mn^{2+}, Co^{2+}, Cd^{2+} and Zn^{2+} respectively). The large effect of flow rate on efficiency for Co^{2+} is similar to that observed on the HEIDA-silica monolith (Section 3.3.5), although the eluent here does not contain potassium nitrate. The retention of all transition metal cations steadily decreases with increased flow rate, as seen in Fig. 5.11.

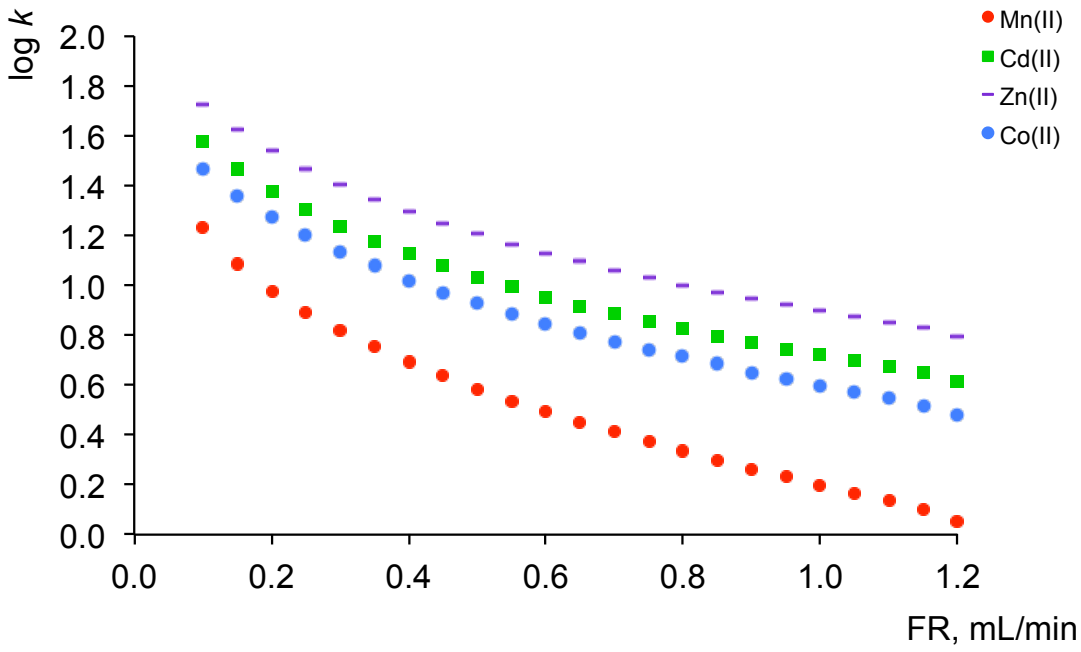

Fig. 5.11: *k*' as a function of flow rate for HEIDA-silica core-shell column: Eluent: 6 m*M* HNO_3, Column temperature: 40 °C, Injection volume: 10 µL, Detection: spectrophotometric at 510 nm after PCR with 0.15 m*M* PAR, PCR flow rate set to ½ of eluent flow rate.

The effect of flow rate on retention and efficiency was also observed on a mixture of lanthanides and yttrium, using an eluent of 0.75 *M* KNO_3/12 m*M* HNO_3. Here, the effect of flow rate on efficiency was determined over the range 0.6 to 1.2 mL/min, as below these flow rates the lanthanides were not well resolved and efficiency values could not be accurately calculated. As seen in Fig. 5.12, over this range the effect of flow rate on retention was linear, and there was a larger difference in elution time on the more strongly retained lanthanides. A van Deemter plot (Fig. 5.13) was generated and the optimum flow rate was determined to be 0.6 mL/min where the HETP values were the lowest for most cations (< 5.0 µm for Ce^{3+}) (Tables 5.3 (a) and (b) for full efficiency data). However, at this flow rate the run time increases by ~50%. This is seen from the chromatograms presented in Fig. 5.14.

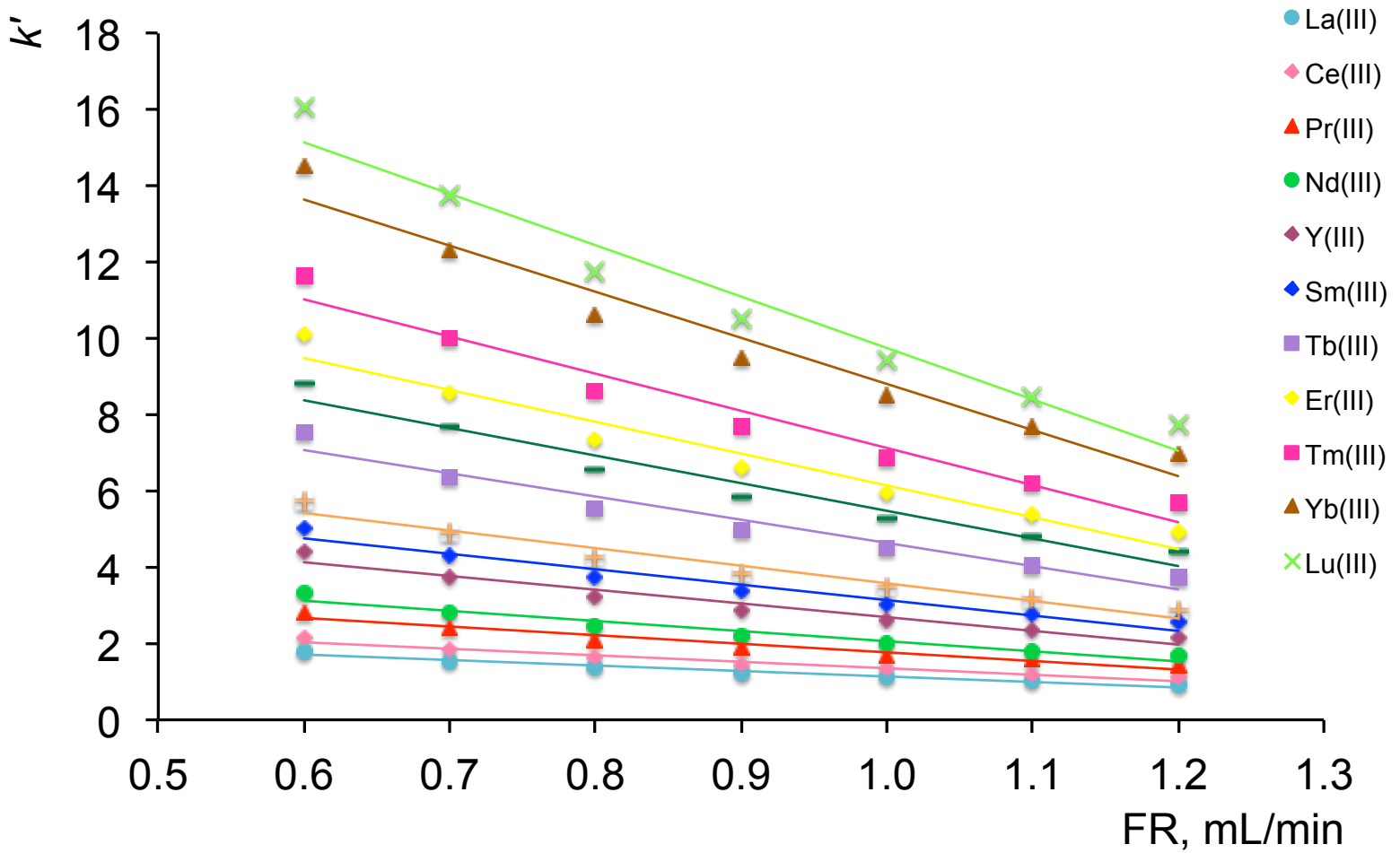

Fig. 5.12: *k'* as a function of flow rate of lanthanides on HEIDA-silica core-shell column: Eluent: 0.75 *M* KNO_3/12 m*M* HNO_3, Column temperature: 40 °C, Injection volume: 10 µL, Detection: spectrophotometric at 650 nm after PCR with 1.5 x10^{-4} *M* arsenazo III, PCR flow rate set to ½ eluent flow rate (mL/min).

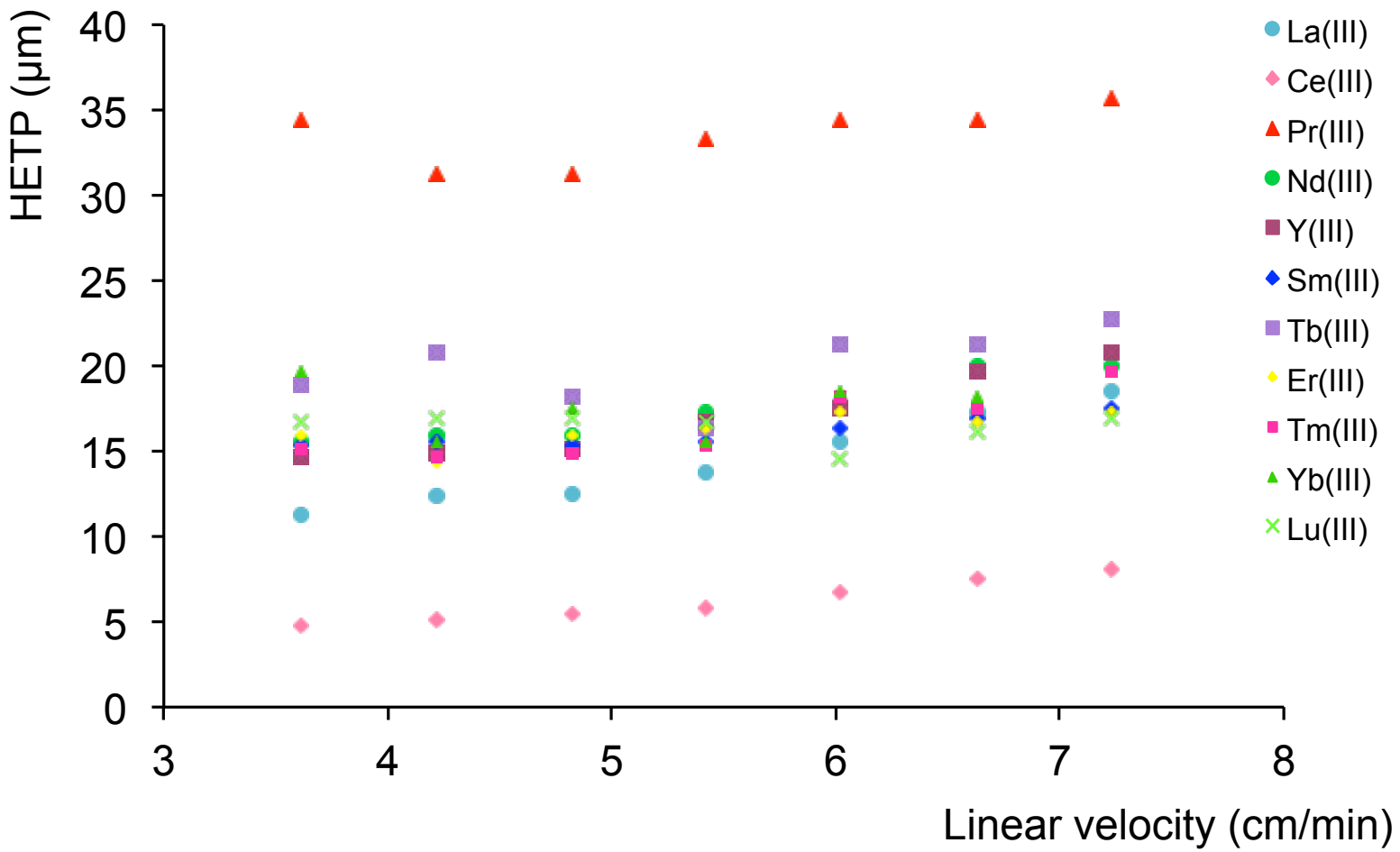

Fig. 5.13**:** Effect of flow rate on efficiency of selected rare earth metal cations on HEIDA-silica core-shell column: Eluent: 0.75 *M* KNO_3/12 m*M* HNO_3, Column temperature: 40 ºC, Injection volume: 10 µL, Detection: spectrophotometric at 650 nm after PCR with 1.5 x10^{-4} *M* arsenazo III, PCR flow rate set to ½ eluent flow rate (mL/min).

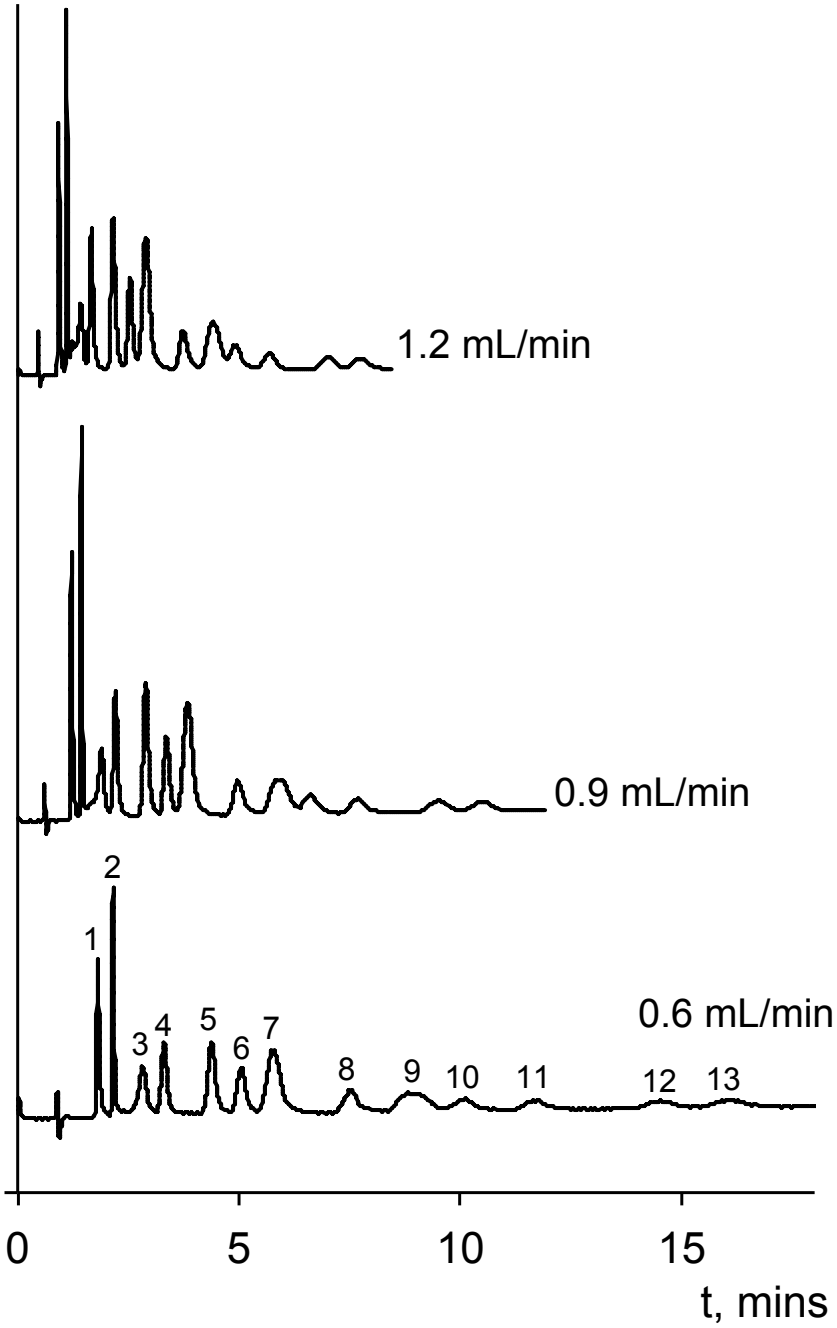

Fig. 5.14: Overlaid chromatograms showing the effect of increasing flow rate on 14 lanthanides and yttrium on HEIDA-silica core-shell column. Analytes in order of elution (which did not change): 1: La^{3+}, 2: Ce^{3+}, 3: Pr^{3+}, 4: Nd^{3+}, 5: Y^{3+}, 6: Sm^{3+}, 7: Gd^{3+}/Eu^{3+}, 8: Tb^{3+}, 9: Dy^{3+}/Ho^{3+}, 10: Er^{3+}, 11: Tm^{3+}, 12: Yb^{3+}, 13: Lu^{3+}, Eluent: 0.75 *M* KNO_3 with 12 m*M* HNO_3, Column temperature: 70 ºC, Injection volume: 10 µL, Detection: spectrophotometric at 650 nm after PCR with 1.5 x10^{-4} *M* arsenazo III at ½ eluent flow rate (mL/min).

Table 5.3: Effect of flow rate on lanthanide metal cations, (a) *N*/m and (b) HETP values.

FR (mL/min)	(a) *N*/m										
	La^{3+}	Ce^{3+}	Pr^{3+}	Nd^{3+}	Y^{3+}	Sm^{3+}	Tb^{3+}	Er^{3+}	Tm^{3+}	Yb^{3+}	Lu^{3+}
0.6	89,000	208,000	29,000	64,000	68,000	65,000	53,000	63,000	66,000	68,000	60,000
0.7	81,000	194,000	32,000	63,000	67,000	64,000	48,000	70,000	68,000	51,000	59,000
0.8	80,000	182,000	32,000	63,000	66,000	65,000	55,000	63,000	67,000	64,000	59,000
0.9	73,000	171,000	30,000	58,000	60,000	64,000	61,000	61,000	65,000	57,000	60,000
1.0	64,000	150,000	29,000	56,000	57,000	61,000	47,000	58,000	55,000	64,000	69,000
1.1	58,000	134,000	29,000	50,000	51,000	59,000	47,000	60,000	57,000	54,000	62,000
1.2	54,000	124,000	28,000	50,000	48,000	57,000	28,000	63,000	66,000	68,000	60,000

FR (mL/min)	(b) HETP (μm)										
	La^{3+}	Ce^{3+}	Pr^{3+}	Nd^{3+}	Y^{3+}	Sm^{3+}	Tb^{3+}	Er^{3+}	Tm^{3+}	Yb^{3+}	Lu^{3+}
0.6	11.2	4.8	34.5	15.6	14.7	15.4	18.9	15.9	15.1	14.7	16.7
0.7	12.4	5.2	31.3	15.9	14.9	15.6	20.8	14.3	14.7	19.6	17.0
0.8	12.5	5.5	31.3	15.9	15.2	15.4	18.2	15.9	14.9	15.6	17.0
0.9	13.7	5.9	33.3	17.2	16.7	15.6	16.4	16.4	15.4	17.5	16.7
1.0	15.6	6.7	34.5	17.9	17.5	16.4	21.3	17.2	18.2	15.6	14.5
1.1	17.2	7.5	34.5	20.0	19.6	17.0	21.3	16.7	17.5	18.5	16.1
1.2	18.5	8.06	35.7	20.0	20.8	17.5	22.7	17.2	19.6	18.2	17.0

At higher flow rates Pr^{3+} starts to split and interfere with Ce^{3+}. At a flow rate of 1.0 mL/min, all peaks are eluted in < 10 minutes, which is significantly faster than the elution times previously achieved for rare earth metals on any previous IDA type silica stationary phases at the same flow rate [22]. Here, (with slightly different eluent conditions) an isocratic separation of the rare earth metals had only been possible in run times of ~70 [22] and later ~40 minutes [26].

5.3.3 Column temperature

The effect of column temperature in HPCIC has been discussed in detail in Sections 1.4.2 and 3.3.3. Here, the effect of temperature on retention and efficiency was investigated for selected alkaline earth, transition and rare earth metals. For a chromatographic system based upon chelation, an increase in column temperature should lead to an increase in retention due to improved kinetics and an increase in the equilibrium constant [29]. Fig. 5.15 shows a van't Hoff plot for alkaline earth and transition metals on the HEIDA core-shell stationary phase, where the results are similar to those obtained on the HEIDA-silica monolith.

Using a 25 m*M* nitric acid / 0.1 *M* potassium nitrate eluent, the effect of column temperature on a mixture of La^{3+}, Ce^{3+} and Y^{3+} was also investigated, and the increase in retention at increased temperature for all metals is clearly shown in the van't Hoff plot (Fig. 5.16). As expected, there is a significant increase in retention of all metals with elevated column temperature, due to the chelation dominant retention mechanism. A significant improvement in the chromatographic separation of Ce^{3+} and Y^{3+} was observed, where co-elute occurs at lower column temperatures. This is shown chromatographically in Fig. 5.17. The more profound increase in retention of Y^{3+} compared to other cations has previously been observed on a fully porous 5 µm IDA type silica gel column [22], and demonstrates how altering the column temperature can be used to manipulate the selectivity of Y^{3+} and improve the separation of a mixture of rare earth metals. Furthermore, increasing the column temperature reduces the viscosity of the eluent, allowing elevated flow rates.

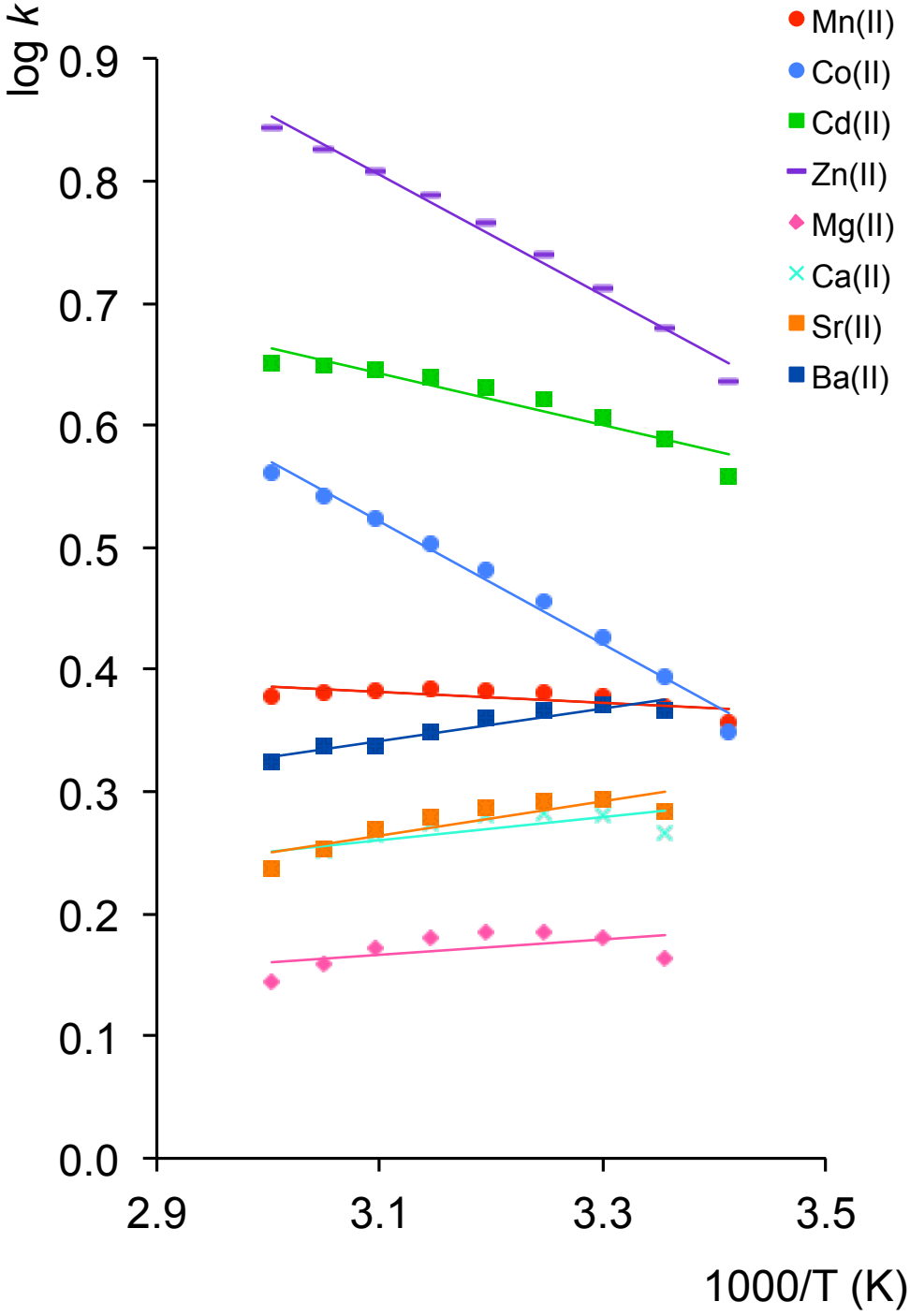

Fig. 5.15: Van't Hoff plot metal cations for alkaline earth and transition metal cations on HEIDA-silica core-shell column. Eluent: 6 m*M* HNO_3, Flow rate: 0.8 mL/min, Injection volume: 10 µL, Analyte concentration: 10 ppm, Detection: spectrophotometric at 510 nm after PCR with 0.15 m*M* PAR or 570 nm with *o*-CPC at 0.4 mL/min.

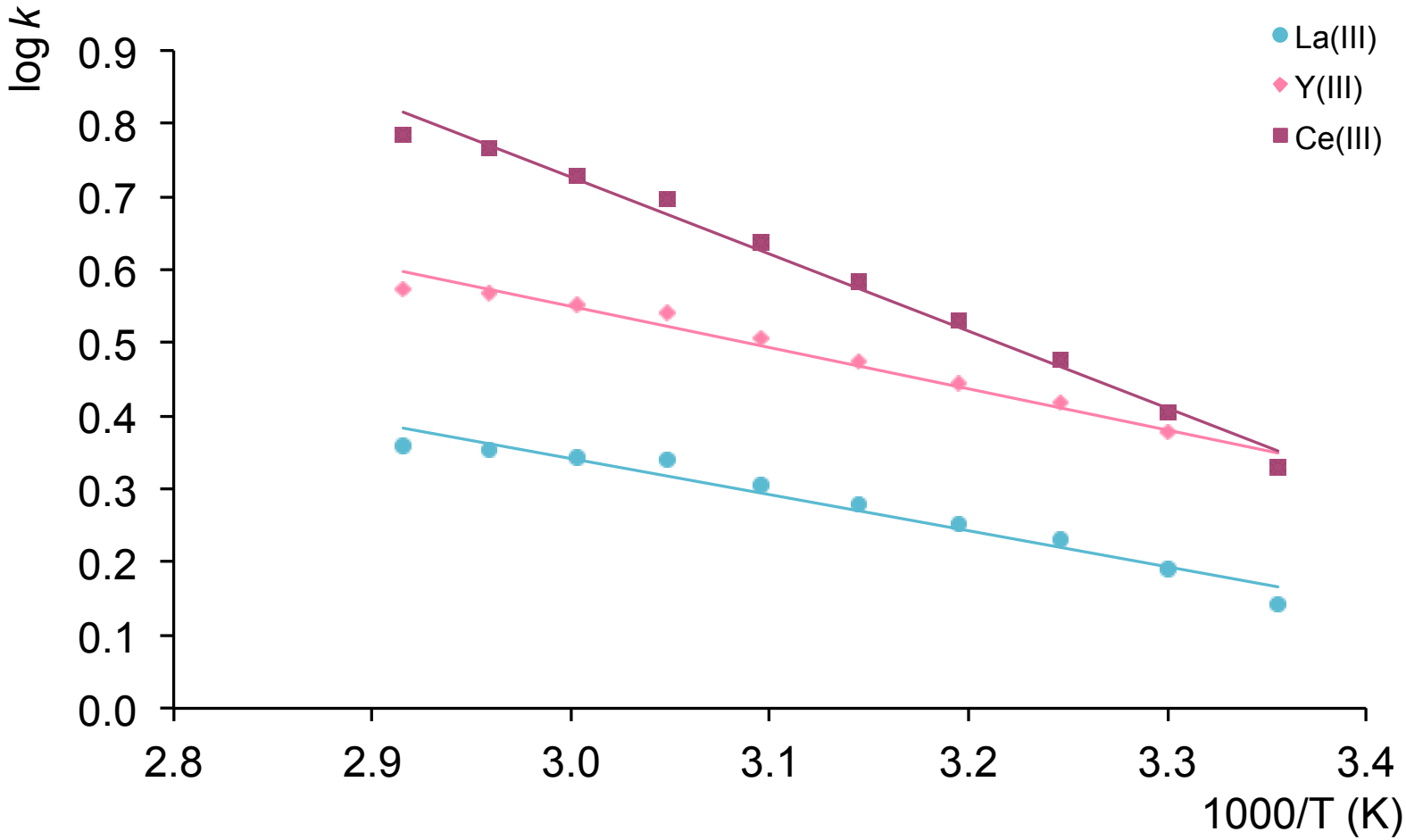

Fig. 5.16: Van't Hoff plot for La^{3+}, Ce^{3+} and Y^{3+} on HEIDA-silica core-shell column. Eluent: 25 m*M* HNO_3/0. 1 *M* KNO_3, Flow rate: 0.8 mL/min, Injection volume: 10 µL, Detection: spectrophotometric at 650 nm after PCR with 1.5 x10^{-4} *M* arsenazo III at 0.4 mL/min.

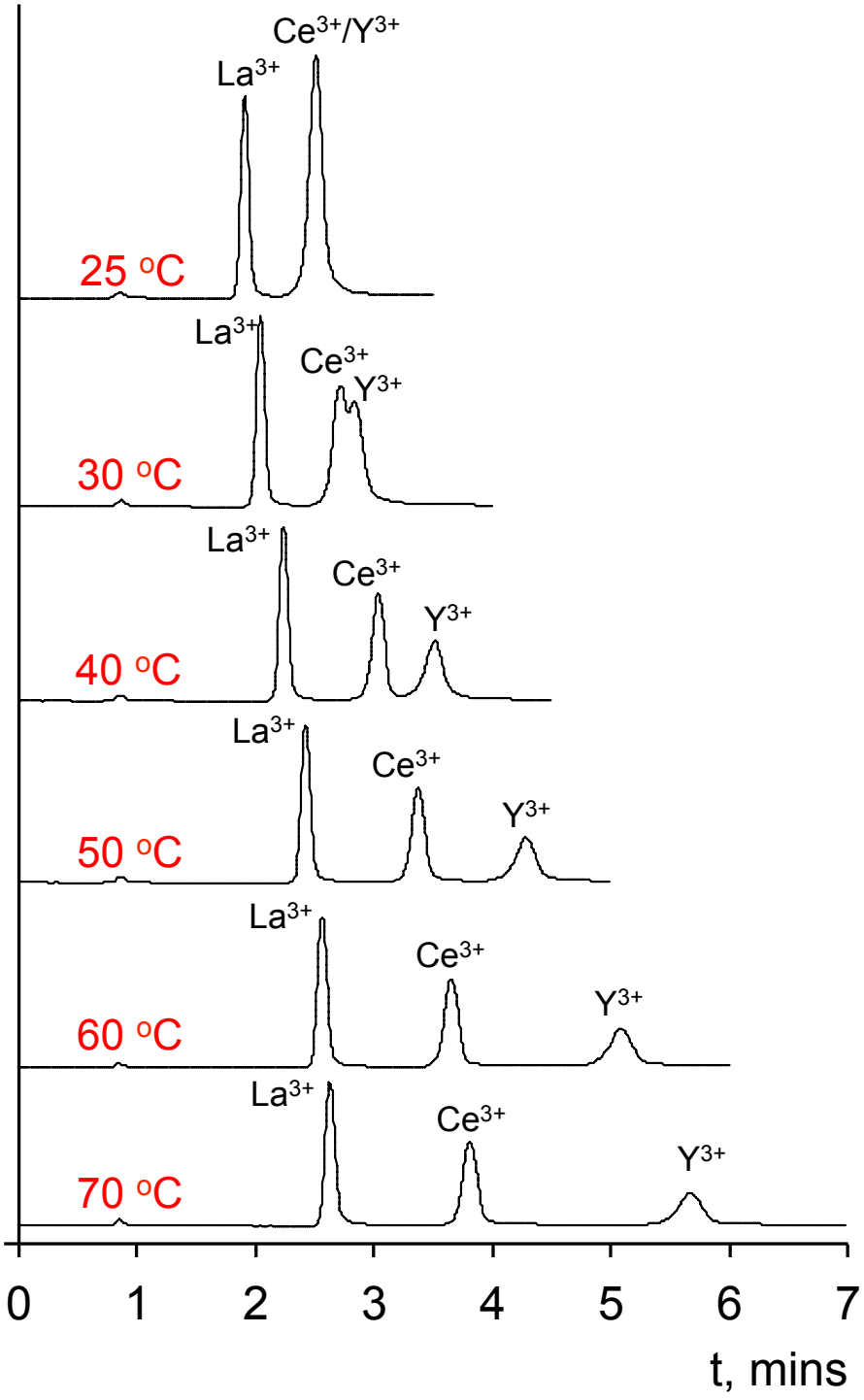

Fig. 5.17: Overlaid chromatograms showing the effect of column temperature (25 – 70 ºC) on La^{3+}, Ce^{3+} and Y^{3+} on HEIDA-silica core-shell column. Eluent: 25 m*M* HNO_3/0.1 *M* KNO_3, Flow rate: 0.8 mL/min, Injection volume: 10 µL, Detection: spectrophotometric at 650 nm after PCR with 1.5 x10^{-4} *M* arsenazo III at 0.4 mL/min.

The instrument limitations allowed a column temperature of no higher than 70 ºC, therefore a water bath was constructed using a large beaker of water placed a hot plate to further increase the column temperature to 75 ºC. The difference in retention and selectivity between 70 ºC and 75 ºC is clearly demonstrated in Figs. 5.18 and 5.19, and the comparative data can be seen in Table 5.4 (a) and (b). There is a significant increase in retention when column temperature was increased to 75 ºC, with all metals showing an increase of > 35%. At identical chromatographic conditions, peak efficiencies increased for nearly all peaks at higher column temperature, with the exception of Ce^{3+}, which can be explained by the splitting of Pr^{3+}. Resolution also improved for most peak pairings, noticeably for Dy^{3+} and Ho^{3+}, however there was a negative effect on the separation of the Y^{3+} and Sm^{3+} where resolution worsened. The effect of the "gadolimium break" where Gd^{3+} elutes before Eu^{3+} due to the smaller stability constant [22] was not observed at either temperature due to co-elution of the peak pairs. Possible drawbacks of heating the column in this way are reduced detector response and the presence of a noisier baseline. There was a significant decrease in peak height after the increase in temperature. Furthermore, at high temperatures the column stability may also be affected with extended use.

Table 5.4: Retention data for lanthanides on core shell column at column temperature (a) 70 ºC and (b) 75 ºC. Eluent: 0.75 *M* KNO_3 with 12 m*M* HNO_3, Injection volume: 10 µL, Detection: spectrophotometric at 650 nm with post-column reagent: 1.5 x10^{-4} *M* arsenazo III at ½ eluent flow rate (mL/min).

(a)	70 ºC retention data					
Cation	RT (Min)	Resolution	Asymmetry(EP)	*N*/m	HETP	*k'*
La^{3+}	1.10	3.00	1.61	64,000	15.63	0.36
Ce^{3+}	1.31	3.03	1.59	150,000	6.67	0.61
Pr^{3+}	1.71	1.74	0.92	29,000	34.48	1.11
Nd^{3+}	2.00	3.51	1.19	56,000	17.86	1.47
Y^{3+}	2.60	2.11	1.20	57,000	17.54	2.21
Sm^{3+}	3.04	1.53	1.11	61,000	16.39	2.75
Gd^{3+}	3.47	N/A	N/A	N/A	N/A	3.28
Eu^{3+}	3.47	N/A	N/A	N/A	N/A	3.28
Tb^{3+}	4.49	1.56	1.24	47,000	21.28	4.55
Dy^{3+}	5.30	N/A	N/A	N/A	N/A	5.54
Ho^{3+}	5.30	N/A	N/A	N/A	N/A	5.54
Er^{3+}	5.96	1.95	1.10	58,000	17.24	6.35
Tm^{3+}	6.90	2.86	0.93	55,000	18.18	7.51
Yb^{3+}	8.50	1.47	0.98	64,000	15.63	9.50
Lu^{3+}	9.42	N/A	1.10	69,000	14.49	10.63

(b)	75 ºC retention data					
Cation	RT (Min)	Resolution	Asymmetry (EP)	*N*/m	HETP	*k*'
La^{3+}	1.22	2.13	1.67	66,000	15.15	0.71
Ce^{3+}	1.38	4.40	1.69	130,000	7.69	0.94
Pr^{3+}	2.05	1.88	0.99	44,000	22.73	1.89
Nd^{3+}	2.42	4.58	1.24	39,000	25.64	2.41
Y^{3+}	3.50	1.45	1.23	62,000	16.13	3.93
Sm^{3+}	3.88	1.98	1.41	65,000	15.38	4.47
Gd^{3+}	4.55	N/A	N/A	N/A	N/A	5.40
Eu^{3+}	4.55	N/A	N/A	N/A	N/A	5.40
Tb^{3+}	6.09	2.75	1.35	64,000	15.63	7.58
Dy^{3+}	7.24	0.90	0.93	N/A	N/A	9.19
Ho^{3+}	7.61	1.82	1.28	N/A	N/A	9.72
Er^{3+}	8.53	2.78	1.13	71,000	14.08	11.01
Tm^{3+}	10.13	4.18	1.04	97,000	10.31	13.27
Yb^{3+}	12.80	2.15	0.91	108,000	9.26	17.02
Lu^{3+}	14.48	N/A	1.00	88,000	11.36	19.39

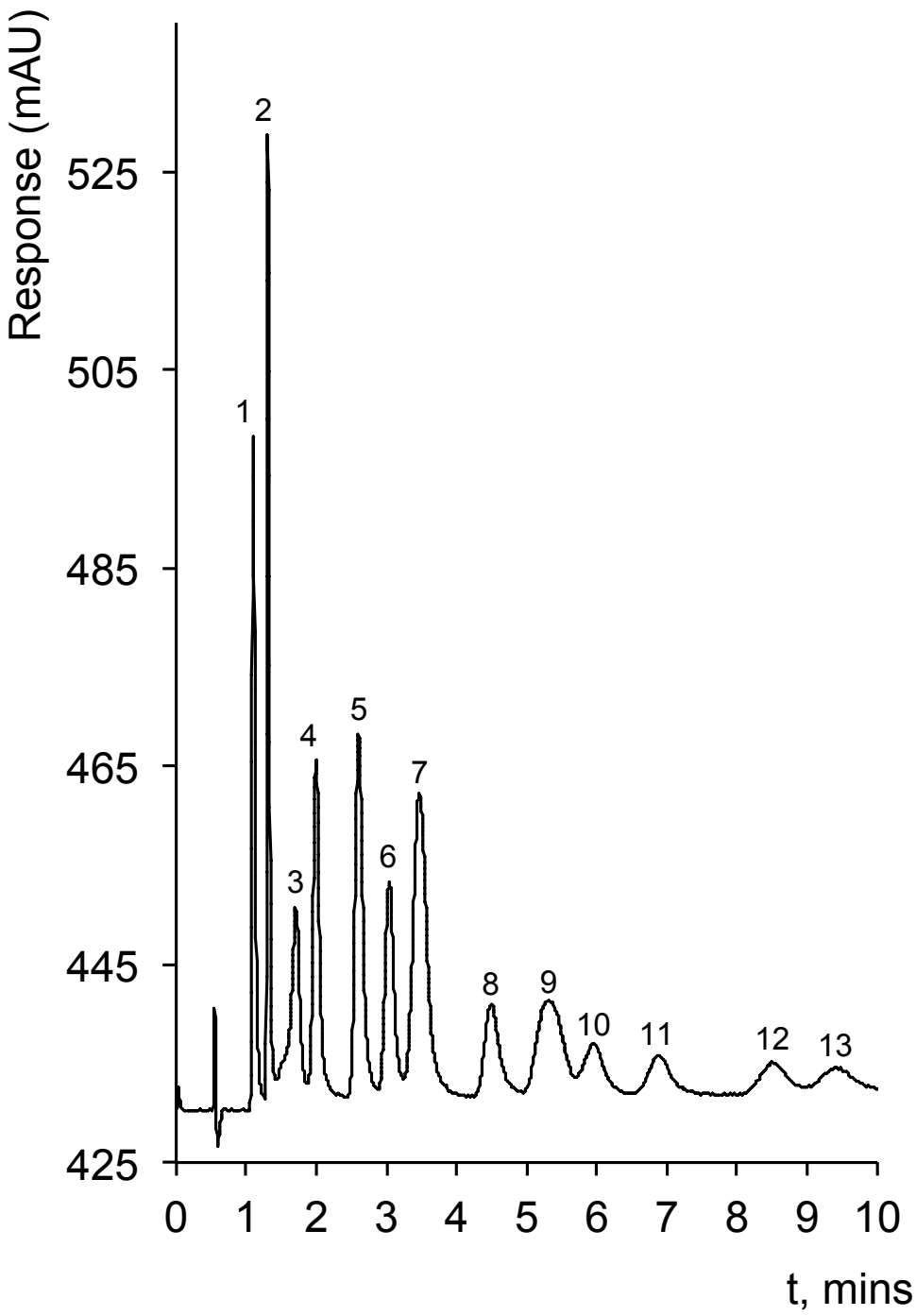

Fig. 5.18: Separation of lanthanides on HEIDA-silica core-shell column at column temperature 70 ºC. Peaks: 1: La^{3+}, 2: Ce^{3+}, 3: Pr^{3+}, 4: Nd^{3+}, 5: Y^{3+}, 6: Sm^{3+}, 7: Gd^{3+}/Eu^{3+}, 8: Tb^{3+}, 9: Dy^{3+}/Ho^{3+}, 10: Er^{3+}, 11: Tm^{3+}, 12: Yb^{3+}, 13: Lu^{3+}. Eluent: 0.75 *M* KNO_3/12 m*M* HNO_3, Flow rate: 1.0 mL/min, Injection volume: 10 µL, Detection: spectrophotometric at 650 nm after PCR with 1.5 x10^{-4} *M* arsenazo III at 0.5 mL/min.

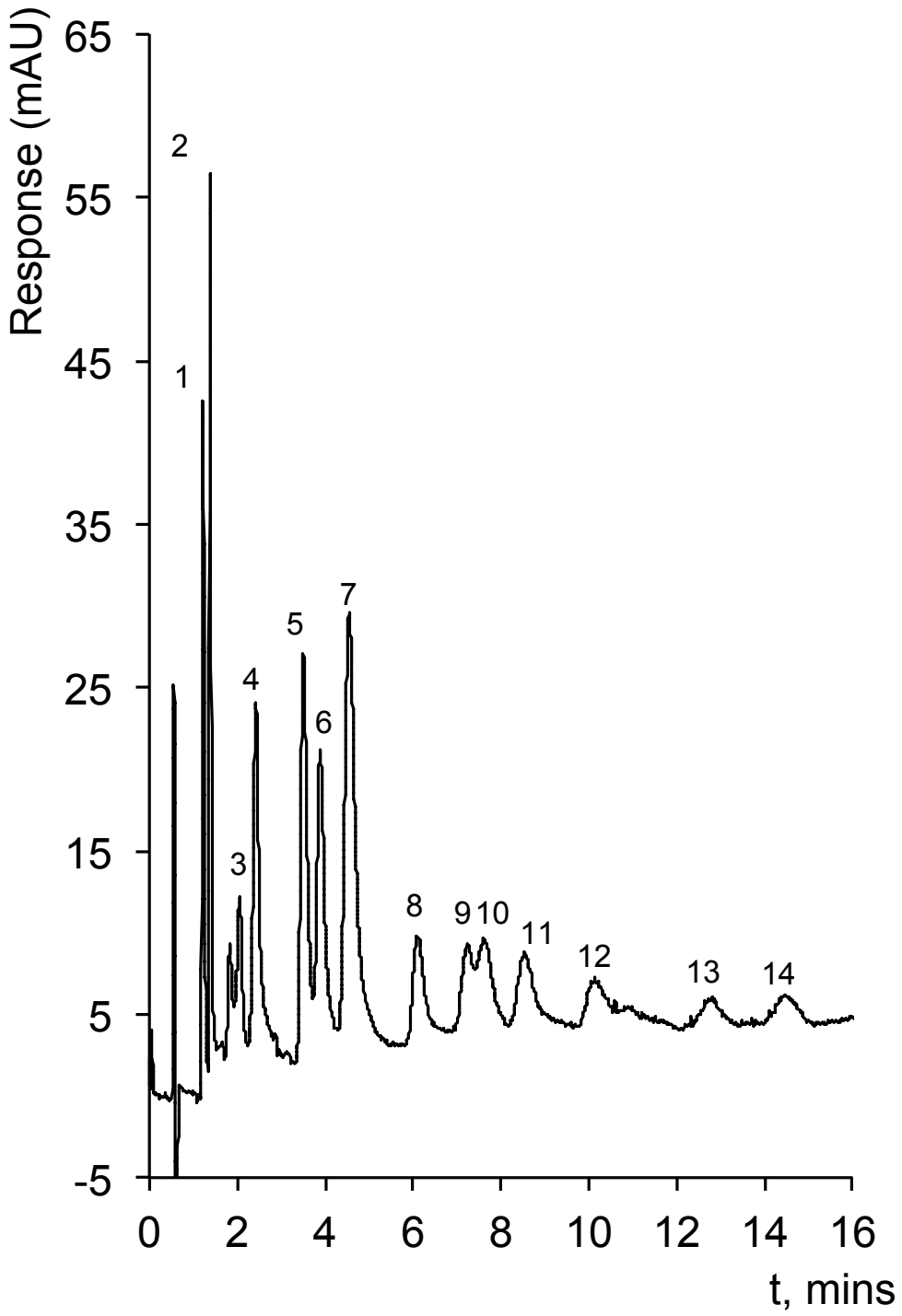

Fig. 5.19: Separation of lanthanides on HEIDA-silica core-shell column at column temperature 75 ºC. Peaks: 1: La^{3+}, 2: Ce^{3+}, 3: Pr^{3+}, 4: Nd^{3+}, 5: Y^{3+}, 6: Sm^{3+}, 7: Gd^{3+}/Eu^{3+}, 8: Tb^{3+}, 9: Dy^{3+}, 10: Ho^{3+}, 11: Er^{3+}, 12: Tm^{3+}, 13: Yb^{3+}, 14: Lu^{3+}. Eluent: 0.75 *M* KNO_3/12 m*M* HNO_3, Flow rate: 1.0 mL/min, Injection volume: 10 µL, Detection: spectrophotometric at 650 nm after PCR with 1.5 x10^{-4} *M* arsenazo III at 0.5 mL/min.

5.3.4 Optimisation of separation of rare earth metal cations

As discussed in Section 2.3.1.2, HEIDA-type bonded silica has been applied to the chromatographic separation of the lanthanide series due to their high affinity for cation exchangers. The high HEIDA-complex stability constants allow the elution order of the lanthanide series to be predicted. From the previous characterisation of the core-shell stationary phase, the chromatographic conditions were selected in order to achieve a separation in the fastest time possible with the maximum efficiency.

As previously seen (Section 5.3.1.3), the use of an eluent with the addition of potassium nitrate to suppress electrostatic separations improves resolution and separation selectivity; therefore the eluent selected was 12 m*M* HNO_3 with 0.75 *M* KNO_3. The choice of eluent, coupled with increasing the column temperature (to 70 ^{o}C) ensured that chelation was the dominant mechanism, and separation selectivity was optimised. At these conditions, a flow rate of 0.8 mL/min was selected, as all peaks were eluted in ~ 12 minutes and Pr^{3+} does not split (see Fig. 5.20). Unfortunately the two peak pairings of Gd^{3+}-Eu^{3+} and Dy^{3+}-Ho^{3+} were unresolved, therefore further optimisation for the isocratic separation of all rare earth cations may be required.

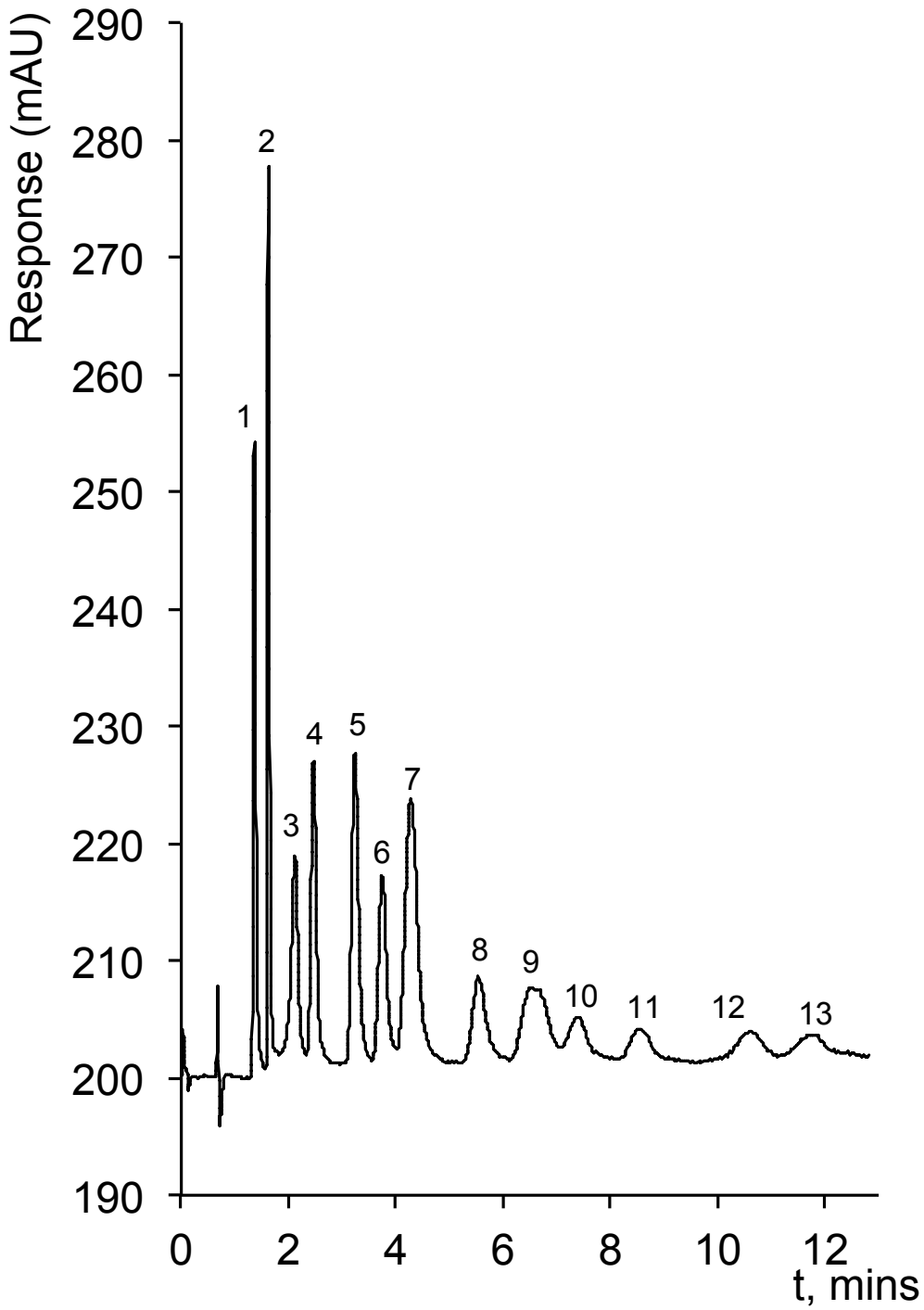

Fig. 5.20: Optimised separation of lanthanides on HEIDA-silica core-shell column. Peaks: 1: La^{3+}, 2: Ce^{3+}, 3: Pr^{3+}, 4: Nd^{3+}, 5: Y^{3+}, 6: Sm^{3+}, 7: Gd^{3+}/Eu^{3+}, 8: Tb^{3+}, 9: Dy^{3+}/Ho^{3+}, 10: Er^{3+}, 11: Tm^{3+}, 12: Yb^{3+}, 13: Lu^{3+}. Eluent: 0.75 *M* KNO_3/12 m*M* HNO_3, Flow rate: 0.8 mL/min, Column temperature: 70 ^oC, Injection volume: 10 µL, Detection: spectrophotometric at 650 nm after PCR with 1.5 x10^{-4} *M* arsenazo III at 0.4 mL/min.

5.4 Conclusions

A full characterisation of a new IDA modified core-shell silica column was completed. The data presented highlights the column performance, where the efficiencies generated are significantly higher than those of other silica IDA based stationary phases, including a recently investigated HEIDA-silica monolith column. It was shown that the retention of transition and alkaline earth metals can be manipulated by altering mobile phase parameters such as eluent pH, temperature and addition of complexing agent dipicolinic acid to the eluent. The behaviour of the aforementioned metal cations was typically similar to other previously characterised IDA type silica phases, and no difference in selectivity was observed. The column was subsequently applied to the detection and separation of a mixture of lanthanide cations. By optimising eluent conditions and ensuring a chelation dominant retention mechanism through the addition of potassium nitrate to the eluent, the isocratic separation of a mixture of lanthanide cations was achieved in under 10 minutes, significantly less time that previously achieved on an IDA based silica column. Excellent efficiencies were demonstrated, including > 200,000 *N*/m for Ce^{3+}, also significantly higher than those previously reported on an IDA based silica stationary phase. As the column demonstrated excellent performance towards lanthanide separations, it could find an application in the nuclear energy industry (e.g. the control of coolant water purity).

References

[1] J.J. Kirkland, Analytical Chemistry 37 (1965) 1458.

[2] J.J. Kirkland, Analytical Chemistry 41 (1969) 218.

[3] C.G. Horvath, B.A. Preiss, S.R. Lipsky, Analytical Chemistry 39 (1967) 1422.

[4] F. Gritti, A. Cavazzini, N. Marchetti, G. Guiochon, Journal of Chromatography A 1157 (2007) 289.

[5] F. Gritti, N. Tanaka, G. Guiochon, Journal of Chromatography A 1236 (2012) 28.

[6] F. Gritti, G. Guiochon, Journal of Chromatography A 1280 (2013) 35.

[7] F. Gritti, G. Guiochon, Journal of Chromatography A 1217 (2010) 8167.

[8] F. Gritti, C.A. Sanchez, T. Farkas, G. Guiochon, Journal of Chromatography A 1217 (2010) 3000.

[9] F. Gritti, G. Guiochon, Journal of Chromatography A 1236 (2012) 105.

[10] G. Guiochon, F. Gritti, Journal of Chromatography A 1218 (2011) 1915.

[11] J.O. Omamogho, J.P. Hanrahan, J. Tobin, J.D. Glennon, Journal of Chromatography A 1218 (2011) 1942.

[12] J.O. Omamogho, E. Nesterenko, D. Connolly, J. Glennon, LC-GC Europe, Recent Developments in LC Column Technology (October 2012) 31.

[13] C. Horvath, S.R. Lipsky, Analytical Chemistry 41 (1969) 1227.

[14] J.J. Kirkland, Analytical Chemistry 64 (1992) 1239.

[15] S. Fekete, K. Ganzler, J. Fekete, Journal of Pharmaceutical and Biomedical Analysis 54 (2011) 482.

[16] http://www.phenomenex.com/Kinetex/CoreShellTechnology.

[17] F. Gritti, I. Leonardis, D. Shock, P. Stevenson, A. Shalliker, G. Guiochon, Journal of Chromatography A 1217 (2010) 1589.

[18] F. Gritti, I. Leonardis, J. Abia, G. Guiochon, Journal of Chromatography A 1217 (2010) 3819.

[19] F. Gritti, G. Guiochon, Journal of Chromatography A 1225 (2012) 79.

[20] N. Cardellicchio, S. Cavalli, P. Ragone, J.M. Riviello, Journal of Chromatography A 847 (1999) 251.

[21] E.P. Nesterenko, P.N. Nesterenko, B. Paull, M. Meléndez, J.E. Corredor, Microchemical Journal 111 (2013) 8.

[22] P.N. Nesterenko, P. Jones, Journal of Chromatography A 804 (1998) 223.

[23] B. Paull, P.N. Nesterenko, P. Jones, High Performance Chelation Ion Chromatography, RSC Chromatography Monographs, Royal Society of Chemistry Publishing, Cambridge, UK (2011).

[24] P.N. Nesterenko, P. Jones, Analytical Communications 34 (1997) 7.

[25] P. Nesterenko, P. Jones, Journal of Liquid Chromatography & Related Technologies 19 (1996) 1033.

[26] P.N. Nesterenko, P. Jones, Journal of Separation Science 30 (2007) 1773.

[27] F. Gritti, G. Guiochon, Journal of Chromatography A 1254 (2012) 30.

[28] L. Barron, M. O'Toole, D. Diamond, P.N. Nesterenko, B. Paull, Journal of Chromatography A 1213 (2008) 31.

[29] A.I. Elefterov, M.G. Kolpachnikova, P.N. Nesterenko, O.A. Shpigun, Journal of Chromatography A 769 (1997) 179.

6. Final conclusions and future work

This reasearch thesis described the development and characterisation of novel stationary phases for HPCIC. HPCIC has become an increasingly popular method for the analysis of metal cations in complex samples due to the advantages outlined in Section 1.1. Due to the unique selectivity that each chelating ligand has for a particular metal cation, there are numerous possibilities for the development of potential chelating stationary phases, dependent on the analytes of interest. Therefore number of different chelating columns with different morphologies were fabricated and/or characterised for selected metal cations. Retention, selectivity and peak efficiencies were compared for various elution parameters which affect the behaviour of each metal. The results allowed further understanding of the retention mechanism in HPCIC compared to standard ion exchange chromatography.

For the first time, RFIC-ER was applied to the detection of metal cations for HPCIC (Chapter 2). Suppressed conductivity was employed as the detection method in place of the commonly used method of post-column reaction. The use of a reagent free chromatography system removes the need for eluent preparation, reducing analysis time and the possibility of eluent contamination. Here, RFIC-ER was used to investigate the chromatographic behaviour of IDA bonded polymer and silica based stationary phases. Silica based stationary phases, in particular silica-IDA have become increasingly popular in recent years due to the excellent efficiencies that they provide when compared to their polymeric counterparts. Furthermore, the belief that silica based stationary phases have poor hydrolytic stability has been disproved.

Therefore, the retention and selectivity of selected alkali, alkaline earth, transition and rare earth metals on Poly-IDA and HEIDA-silica columns were evaluated, where a mixed mode retention mechanism of standard ion exchange and chelation chromatography occurred. A mixture of seven rare earth metals was successfully separated isocratically on both columns employing RFIC-ER. Retention was weaker on the Poly-IDA column, suggesting a lower degree of chelation due to the absence of an OH group in close proximity to IDA on the polymeric stationary phase. Furthermore, the efficiency values were significantly lower than those obtained on the HEIDA-silica column, suggesting that the method of attachment of the IDA groups to the surface of the stationary phase has a significant effect on the behaviour of metal cations. Thus, for the remaining work (Chapters 3 to 5) the chelating

stationary phses were silica-based. Although the separation of lanthanides was achieved using RFIC-ER with suppressed conductivity detection, precipitation of the more strongly retained metal ions occurred. Spectrophotometric detection with post-column reaction is clearly the more suitable method for detection in HPCIC, although it is more time consuming and costly.

One of the column morphologies selected for application in HPCIC was a silica monolith (Chapter 3), which are characterised by their high efficiency values and relatively low column pressures at higher flow rates. A commercially available (Onyx Monolithic Si, 100 × 4.6 mm I.D.) was 'in-column' covalently functionalised with 2-HEIDA groups, and applied to the simultaneous and rapid separation of alkaline earth and transition metal ions, using HPCIC. This column had previously been modified with IDA and partially characterised [1,2], however band broadening occurred as a result of heterogeneous distribution of functional groups along the surface of the stationary phase. The modification procedure was changed to include flushing the IDA/silane modification solution in both directions. There was a clear improvement in peak shape, particularly for Zn^{2+}, confirming that the new modification procedure resulted in a more homogenous distribution of HEIDA groups. The stationary phase was fully characterised to explore its capabilities and the possibility of a separation of a number of metal cations. The effect of a number of elution parameters on retention and selectivity were investigated, including eluent pH, addition of a complexing agent, column temperature, eluent selectivity and flow rate. This also allowed a greater understanding of the behaviour of metal cations belonging to different groups in HPCIC. Manipulating these parameters allowed the separation of a mixture of 8 selected metals in less than 14 minutes using a 4 m*M* HNO_3 eluent, with 0.3 m*M* DPA, pH 2.4 with post-column reaction detection using a 0.12 m*M* PAR/0.2 m*M* ZnEDTA solution.

As HPCIC is generally used for the analysis of complex matrices, it was necessary to apply the HEIDA-silica monolith to such a sample. In this case (Chapter 4), a new method was developed for the direct separation, detection and quantitative determination of Mn^{2+}, Cd^{2+} and Zn^{2+} concentrations in shellfish (mussel) tissue digest samples. In order to suppress any simple ion exchange interactions and ensure retention was through chelation only, the eluent employed was 0.5 *M* KNO_3,

adjusted to pH 2.4 using dilute HNO_3, which was optimal for the isocratic separation of the transition metal ions, Mn^{2+}, Co^{2+}, Cd^{2+} and Zn^{2+}. Post-column detection was achieved using spectrophotometric detection at 510 nm after reaction with 4-(2-pyridylazo) resorcinol. Quantitation of Cd^{2+} and Zn^{2+} was successfully achieved using the HEIDA-silica monolith, however quantitation of Mn^{2+} in the sample solutions was not possible due to the lack of resolution from interfering alkaline earth metal cations present in the sample matrix. This was due to fact that Mn^{2+} has similar stability constants for IDA-metal complexes to the alkaline earth metals. Reduction of eluent strength in this case resulted in excessive retention of Zn^{2+}, therefore for the analysis of Mn^{2+} an identical silica monolith modified with HEPMA was employed. This chelating ligand contains carboxylic and phosphonic acid groups, with the latter resulting in alternative selectivity to that shown by IDA, particularly for Mn^{2+}. Using a 0.1 *M* KNO_3 eluent, resolution between Mn^{2+} and interfering alkaline earth metal cations was achieved using the HEPMA phase, and the determination of Cd^{2+}, Mn^{2+}, and Zn^{2+} cations was carried out successfully in less than 15 minutes. Using the method of standard addition, concentrations determined for Cd^{2+}, Mn^{2+}, and Zn^{2+} were < 10 µg/g, < 25 µg/g and < 700 µg/g respectively. The determination of Zn^{2+} in the samples was carried out on both the HEIDA and HEPMA silica monoliths for direct comparison, and the results were comparable with ICP-MS analysis data, proving that the correct choice of chelating ligand for the metal analyte of choice is an alternative method to standard spectroscopic methods which often require sample dilution and/or preconcentration.

The final chelating stationary phase to be characterised was a HEIDA-bonded core shell silica column. Core shell particle columns have become increasingly popular in recent years for the excellent efficiencies they provide due to their morphology, which allows increased column permeability, and subsequently elevated peak efficiencies and reduced run times. Bare core-shell silica (1.7 µm) was modified with IDA under reflux and used to pack a short (50 x 4.6 mm I.D.) column, which was then characterised for selected metal cations in the same way as the HEIDA-monolith. The peak efficiencies generated were significantly higher than those of other silica IDA stationary phases. The behaviour of alkaline earth, transition and heavy metal cations was similar to that observed on other previously characterised IDA-silica phases, and a slight difference in selectivity compared to the HEIDA-

silica monolith was observed , further proving that the method of attachment of the chelating ligand plays a role in the retention mechanism. The column was subsequently applied to the detection and separation of a mixture of lanthanide cations, and the separation of a mixture of lanthanide cations was achieved in less than 10 minutes by optimising eluent conditions and ensuring a chelation dominant retention mechanism. This was the first instance of a core-shell column with a chelating functionality, which is a possible platform for a variety of chelating ligands, depending on the metal cation of interest.

One of the main advantages of HPCIC is the wide number of chelating ligands available, each with their own unique selectivity towards particular metal cations. A number of different chelating stationary phases with different morphologies were investigated throughout this thesis; therefore there are numerous possibilities for novel columns with various bonded chelating ligands.

One possible chelating ligand that has not been investigated is iminodipropionic acid (IDPA) (Fig. 6.1), which has a slightly different structure to IDA (Fig. 6.3). The use of IDPA in separation science applications has not previously been examined, with only preliminary work carried out on dissociation and stability constants of transition and heavy metals [3]. Therefore, IDPA modified columns would be possible novel stationary phases for HPCIC.

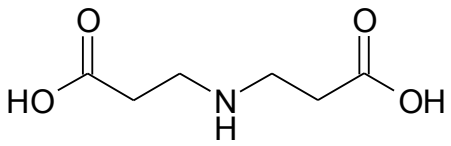

Fig. 6.1: Structure of iminodipropionic acid

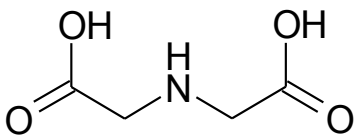

Fig. 6.2: Structure of iminodiacetic acid

The IDA core-shell column provided higher peak efficiencies than any other reported values for IDA-silica columns. Thus, there are numerous possibilities for the use of chelating core-shell stationary phases, employing various ligands. Possible chelators include the aforementioned IDPA, and HEPMA, which was successfully applied to the determination of transition metal cations (Chapter 4).

The work described in this thesis successfully developed next stationary phases for HPCIC, exploiting different column morphologies and chelating ligands for the determination of metal cations of interest. Taking into account the unique selectivity of chelating ligands, fast run times and excellent peak efficiencies observed on these chelating columns, it is clear that HPCIC is a suitable and promising method for the analysis of complex samples where interference from alkali metal salts can present problems. The different column morphologies investigated opened new possibilities depending on the applications. For example, monolithic stationary phases can be used for very fast separations (e.g. rapid direct seawater analysis in the field), and core shell columns provide exceptional peak efficiencies and peak capacities and permit the simultaneous separation of a large number of cations. The findings in the area of reagent free CIC will facilitate its integration into deployable and portable systems.

References

[1] E. Sugrue, P. Nesterenko, B. Paull, Analyst 128 (2003) 417.

[2] E. Sugrue, P. Nesterenko, B. Paull, Journal of Separation Science 27 (2004) 921.

[3] S. Chaberek, A.E. Martell, Journal of the American Chemical Society 74 (1952) 5052.